Strathclyde Institute of Pharmacy and Biomedical Sciences

Synthesis and Evaluation of Targeted Dendrisomes as Novel Gene and Drug Delivery Systems for Cancer Therapy

By

Joan Onyebuchi Erebor

A thesis presented in fulfilment of the requirements for the degree of

Doctor of Philosophy

2018

This thesis is the result of the author's original research. It has been composed by the author and has not been previously submitted for examination which has led to the award of a degree.

Signed:

Date:

DEDICATION

This work is dedicated to two great men who mentored me, Late Rev. Prof E.T. Ehiametalor and Late Dr J.K. Ojimba.

ACKNOWLEDGEMENTS

First and foremost, I want to say thank you Heavenly Father, my Lord Jesus Christ and the Holy Spirit my teacher, the maker of heaven and earth, who gave me the opportunity, privilege, provision, grace, wisdom and strength to obtain a doctorate degree against the odds.

My gratitude also goes to my primary supervisor Dr Christine Dufès. Thank you for accepting me as your student, for your guidance, direction and support during my PhD program. Thank you for introducing me to gene delivery and for your technical aid with the *in vivo* experiments. My second supervisor, Prof Gavin Halbert, thank you so much for accepting me as your student as well, for your support, encouragement and guidance. I am extremely grateful to the Tertiary Education Trust Fund (TETFUND) Nigeria who via my beneficiary Institution, University of Benin, funded a major part of this project. I want to appreciate my current Vice Chancellor Prof F. F Orunmwense and former Vice Chancellor Prof O. G. Oshodin, as well as my mentors Prof M. A. Iwuagwu, Prof C Usifoh and Dr M. Elliott. I also want to appreciate Prof A. O. Okhamafe, Prof C. F Mafiana, Prof J. A. Okhuoya, Prof O. Okojie, Prof and Mrs B. Sanni, Mr T. Maduabum, Mr Fregene, Mr Odigie, Prof J. O. Igoli, Prof M. Uhumwangho and Dr M. I. Arhewoh for their ensuring that necessary documentation was approved, for their encouragement and support towards completion of this project.

Technical assistance was provided for some experiments carried out in this project. Thus, I want to specially thank Magaret Mullin, Dr R. J. Tate, Anne Goudie and Monika Warzecha for their technical assistance with the TEM imaging, the agarose gel assay, the DSC and AFM imaging respectively. I also want to appreciate Dr S Somani for technical help with the Fluorescence microscopy and part of the bio distribution assay, and Najla for some of the plasmid DNA preparation. Michael McGlone (IT), Dufès Lab, my colleagues and other members of room RW 501p, Partha and Sajad. My appreciation also goes to LOCCAF family, Winners Chapel International Glasgow, Tron Church Glasgow, Gift of Life Ministries Nigeria, Church of God Mission International, Brightmoor Christian Church, Rev. Mrs L. Ehiametalor, Mr and Mrs Leo Nwobi, Pastor and Pastor (Mrs) C. Ode, Pastor and Mrs Y Ajayi,

Pastor and Barr (Mrs) D. Adetoro, Dr and Mrs B. Olusina, Pastor and Mrs S Effiong, Rev B. Mathias, Rev.Fr. C Akue, Rev. Fr. A Obiyan, Pastor Segun, Chief. Dr. I. Kachikwu, Dr and Dr Mrs Idaewo, Mrs Pat Opeyemi, Sylvester, Nkechi, Dr and Mrs G. Eze, Dr and Dr Mrs U. D. Oboh, Yetunde, Mr and Dr (Mrs) Iyawe, Mercy, Dr L. Kachikwu, Emma, Rosemary, Ndidi, Irene, John, Katie, Amit, Susan, Lynn, Nicola, Mariam, Lina, Stephen, Tar, Mr and Mrs B Omojimite, Mr and Mrs Asemwota; thank you all for your acquaintance, advice, prayers, and your support financially and otherwise.

My darling husband Peter Omoruyi Erebor, words are not enough to express how much I appreciated your support and prayers from the beginning to the end of this program. Thank you for being a backbone of strength to me. My lovely children Daniella, Ethan and Kadmiel, thanks for being patient with me, the sacrifices you made in adjusting to new environments, making me smile and cheering me on, I love you all. My dear parents Chief. Engr. and Mrs F. N Mafiana thank you very much for believing in me, praying for me and supporting me financially and otherwise. My siblings Zelonye, Ugo and Onyinye, my in-laws, The E.N.O Erebor family, Mrs K Anarado, Mr K Omesiete, Mr O. Omesiete, friends and well-wishers I appreciate you all.

Great have you been O Lord my God in my life and greatly to be praised. Without you I would not be here, because of you Lord I live.

Quote: "Faithful is he that calls you, who also will do it" 1 Thess 5:24 (KJV 2000).

Table of Contents

List of Figures

List of Tables

ABBREVIATIONS

AFM	Atomic force microscopy
Arg	Arginine
AIDS	Acquired immunodeficiency syndrome
BCNU	Carmustine (bis-chloroethylnitrosourea)
Conc	Concentration
CLSM	Confocal laser scanning microscopy
CLSPEGMal	Cholesterol -PEG- Maleimide
DAB	Diaminobutane core
DAB-Am-16	Polypropylenimine hexadecaamine Dendrimer, Generation 3.0
DAPI	4‟,6-diamidino-2-phenylindole
DDAO	7-hydroxy-9H-(1,3-dichloro-9,9-dimethylacridin-2-one)
DDAO-G	9H-(1,3-dichloro-9,9-dimethylacridin-2-one-7-yl)-D Galactopyranoside
DHP	Dihexadecyl phosphate
DMEM	Dulbecco's Modified Eagle Medium
DMSO	Dimethyl sulfoxide
DNA	Deoxyribonucleic acid
DOPE	L-α-Phosphatidylethanolamine, dioleoyl
DOX	Doxorubicin
DSC	Differential scanning calorimetry
E. coli	*Escherichia coli*
EDTA	Ethylenediaminetetraacetic acid
EGCG	Epigallocatechin-3-gallate
EPR	Enhanced permeability and retention effect
FBS	Foetal Bovine Serum
HA/PPNPs	hyaluronic acid (HA)-decorated polyethylenimine-poly (D, L-lactide-co-glycolide)
IC_{50}	Growth inhibitory concentration

ILP	Isolated limb perfusion
IL-12	interleukin-12
IV	Intravenous
KDa	Kilodalton
Leu	leucine
LOD	Limit of Detection
LOQ	Limit of Quantification
Lys	lysine
MDR	Multidrug resistance
MLV	Multilamellar vesicles
MPS	Mononuclear Phagocytic System
MTT	3-(4,5-dimethylthiazol-2-yl)-2,5-diphenyl-tetrazolium bromide
MTD	Maximum tolerated dose
N/A	Not applicable
NGR-hTNF	Asparagine-glycine-arginine-human tumour necrosis factor
NR	Not reported in the study
NCI	National Cancer Institute
ONPG	O-nitrophenyl- β-D-galactosidase
ORR	Objective response rate
PAMAM	Polyamidoamines
PBS	Phosphate buffered saline
pCMV β-Gal	Plasmid DNA encoding β-galactosidase
PDI	Polydispersity index
p (DNA)	Plasmid DNA
PEG	Polyethylene glycol
PEI	Polyethylenimine
PIC	Protease Inhibitor Cocktail

P-gp	P-glycoprotein
PLB	Passive lysis buffer
PMSF	Phenylmethylsulfonyl fluoride
PPI	Poly (propylene imine) dendrimer
PTX	Paclitaxel
RES	Reticuloendothelial system
rTNF	Recombinant TNF
rhTNFα	Recombinant human TNF-alpha
RPMI	Roswell Park Memorial Institute
SCID	Severe combined immunodeficient
Solulan C24	Cholesteryl poly (24) oxyethylene ether
Span 60®	Sorbitan monostearate
UV	Ultraviolet
TBE	Tris-Borate-EDTA
TEM	Transmission electron microscopy
Tf	Transferrin
Tfcj	Transferrin conjugation process of non-PEGylated dendrisomes
TfcjP	Transferrin conjugation process of PEGylated dendrisomes
TfR	Transferrin receptor
TPGS	d-α-tocopheryl polyethylene glycol 1000 succinate
TNFα	Tumour necrosis factor
Tf-bearing	Transferrin-bearing
TRAIL	Human tumor necrosis factor α-related apoptosis-inducing ligand

ABSTRACT

Introduction: The co-delivery of cancer therapeutics in hybrid nanocarriers is currently being investigated in order to achieve an additive or synergistic effect in cancer therapy. The aim of this study was to synthesize and evaluate novel transferrin-bearing dendrisomes to co-deliver therapeutic DNA encoding TNF-α and doxorubicin. Dendrisomes were thus investigated in this project *in vitro* and *in vivo* for their DNA carrying abilities as well as their ability to co-deliver therapeutic DNA and an anticancer drug. The targeted dendrisomes in this project are thus aimed at ensuring a higher selective uptake intracellularly using targeting ligand transferrin. Transferrin receptors have been found to be overexpressed on most cancer cells and are thus attractive as target sites for selective receptor-mediated tumour targeting.

Methods: The dendrisomes were formulated with a combination of a lipid blend incorporating non-ionic surfactants and a dendrimer via heating and probe sonication. Doxorubicin was encapsulated in the dendrisomes through probe sonication. Conjugation of transferrin to the dendrisomes was done using bifunctional cross-linking. Characterization of the dendrisomes was then carried out through techniques including, size and zeta potential measurements, TEM, DNA condensation assays, AFM. *In vitro* studies were also carried out using fluorescence microscopy, confocal laser scanning microscopy, gene transfection assays and anti-proliferative assay. Biodistribution and antitumour efficacy studies were also carried out using xenograft models.

Results: Dendrisomes were successfully formulated that were in the nanometer range (less than 500 nm). Some were neutral, and some were positively charged as obtained

from zeta potential readings. TEM pictures showed that these novel dendrisomes were spherical. DNA condensation and doxorubicin encapsulation efficiency were respectively above 75% and 95% and demonstrated the ability of the dendrisomes to carry both DNA and drug. DNA encoding β-galactosidase was successfully expressed in A431, B16F10-Luc-G5 and T98G cancer cells. Cellular uptake experiments demonstrated that the novel dendrisomes caused increase in doxorubicin and DNA intracellular uptake. Anti-proliferative efficacy was improved following treatment with dendrisomes co-delivering DNA encoding TNF-α and doxorubicin, compared to that observed with doxorubicin alone or DNA encoding TNF-α alone with synergism observed in B16F10-Luc-G5 cells that were treated with transferrin bearing, doxorubicin encapsulated DSOLm dendrisomplexes.

Conclusion: In conclusion, this project is the first demonstration of transferrin-targeted novel dendrisomes being complexed to therapeutic plasmid DNA encoding TNF-α for gene delivery while concurrently entrapping anticancer drug doxorubicin for cancer therapy. The novel targeted dendrisomes were shown to have the capacity to co-deliver therapeutic plasmid DNA encoding TNF- α and anticancer drug doxorubicin to cancer cells *in vitro* and *in vivo*, thus leading to increased anti-proliferative effect *in vitro* and slightly increased therapeutic efficacy at the doses used *in vivo* in selected cancer cell lines and solid tumours overexpressing transferrin respectively.

CHAPTER 1: INTRODUCTION

1.1 Cancer therapy

Cancer refers to a group of diseases in which there is abnormal, uncontrolled division and multiplication of cells that are able to invade other tissues (National Cancer Institute 2014). Cancer cells have been shown to cause a deregulated imbalance between cell death and cell proliferation, through gene mutation, amplification, deletion, irregular gene transcription or translation (Ruddon 2007). It was estimated that there were almost 14.1 million new cases of cancer globally in 2012, with 488,632 and 1,685,210 diagnosis being made respectively in the UK in 2014 (Cancer Research UK, 2016) and in the USA in 2016 (Cancer Facts and Figures, 2016). In 2013, cancer caused approximately 8.2 million deaths worldwide (International Agency for Research on Cancer, 2013). The figures obtained on incidence of cancer worldwide thus necessitates the urgent need for effective but safe therapeutic agents to cure or successfully manage these patients.

The most common classification of cancer is based on the site of origin of the disease and covers over 100 types of cancer (Almeida and Barry, 2010; National Cancer Institute, 2015). Cancer types can be broadly grouped as carcinomas, sarcomas, leukaemias, lymphomas, multiple myelomas and melanomas. Carcinomas originate from epithelial cells, such as those in the breast and prostate. Sarcomas originate within bone and soft tissues, such as muscle fat, vascular and lymph vessels, and any fibrous tissue cells. Leukaemias are formed in the bone marrow while lymphomas develop in leucocyte cells, namely T cells and B cells. Multiple myelomas are cancers that are formed by malignant plasma cells and then cause tumours in bones throughout the

body (Almeida and Barry 2010; National Cancer Institute, 2015; American Cancer Society 2017).

Cancer therapy is currently carried out through chemotherapy, radiotherapy and surgery (Moorthi *et al.*, 2011). Over the years, efficacious cancer treatment with low side effects on normal tissues has been difficult to achieve. This has resulted in poor prognosis in some types of cancer like exocrine pancreatic cancer and liver cancer with a relative survival rate of 5% and 17% respectively after 5 years (American Cancer Society 2016), despite the wide range of cancer treatments currently available. The factors influencing the therapeutic outcome are multiple, including the nature of the disease, stage of the disease, multidrug resistance, physiological makeup of the human body and individual human idiosyncrasies. These factors thus cause the same type of cancer to have a good prognosis in some cancer patients and a poor prognosis in others. This situation has led to an area of a cancer therapy called individualised therapy which is hoped will increase the survival rates of cancer patients (Bleeker *et al.*, 2012)

Cancer has been shown to exhibit some unique intrinsic and cellular characteristics that distinguishes it from any other pathologies. These unique characteristics have been highlighted as the cause for the high mortality and morbidity rate of cancer. They include sustained proliferative signalling, ability to evade growth suppressors, activation of invasion and metastasis, replicative immortality, induction of angiogenesis and resistance to cell death, deregulation of cellular energetics and avoidance of immune destruction (Hanahan and Weinberg, 2000; Hanahan and Weinberg, 2011).

The major challenge encountered over the years with cancer chemotherapy is the non-selectivity of anticancer drugs, leading to severe adverse effects in patients. In addition, multidrug resistance also causes treatment failure in cancer chemotherapy (Persidis 1999). These problems could be attributed to several factors, such as poor aqueous solubility of the drugs, low cell membrane permeability (Svenson 2009), as well as insufficient uptake of the anticancer drugs into the cancer cells (Frank *et al.*, 2014). The immune system response to anticancer drugs through the reticuloendothelial system (RES) is also a limiting factor in the delivery of antineoplastic agents. Due to these challenges, the need for further research to achieve safe and efficacious cancer therapy is necessary. Therefore, targeted drug delivery has been developed to remediate this issue.

1.2 Gene therapy and gene delivery systems

DNA is referred to as a long polymer of repeating units called nucleotides. The existence of DNA and its function was first discovered by Swiss chemist Friedrich Miescherin in 1869 (Maderspacher, 2004; Dahm, 2005). DNA is a long double stranded helical structure that consists of two strands linked via hydrogen bonds. These strands are made up of units called nucleotides (Pray, 2008). Nucleotides consist of three main constituents: a phosphate group, a deoxyribose sugar group and one of four types of nitrogen-containing bases (adenine (A), thymine (T), guanine (G) and cytosine (C)). Adenine (A) and guanine (G) are purines while cytosine (C) and thymine (T) are pyrimidines (Figure 1.1) (Wolpert, 1984; Semenza, 2003; Gerstein *et al.*, 2007; Genome.gov, 2015).

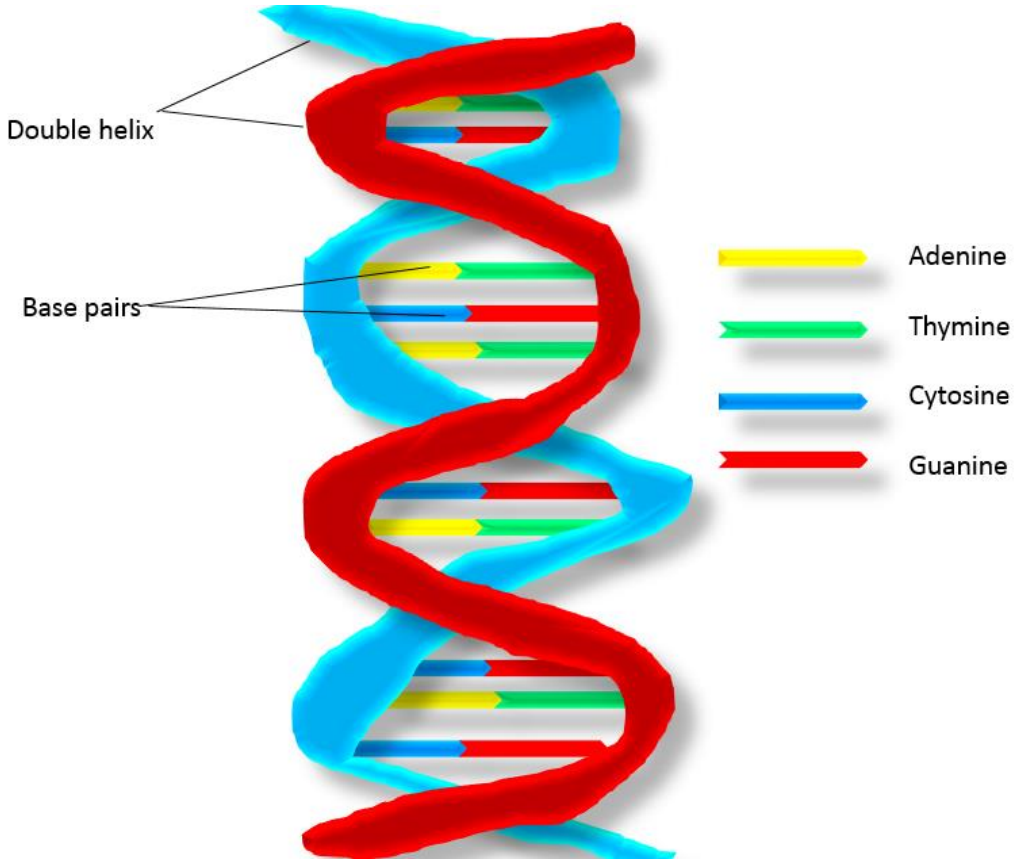

Figure 1.1: Schematic Structure of DNA

Plasmids are circular, extrachromosomal double-stranded DNA (dsDNA) molecules that are present in the cells of bacteria, yeast, and some higher eukaryotic cells. Their existence is distinct from the chromosomal DNA of the host cell (Lodish *et al.*, 2000). Plasmid DNA used in gene therapy are usually formed recombinant DNA technology and contain human or non-human genes that are usually being between 5 and 20 kb in length ($3.3x10^6$ – $13.2x10^6$ Da) (Prazeres *et al.*, 1999).

A Genes is defined as a deoxyribonucleic acid (DNA) segment that contributes to phenotype/ function of the cells (Wain *et al.*, 2002). A human cell contains about 20

000-25 000 genes present in the chromosomes. Any abnormality in a gene or set of genes can lead to dysfunctionality of the whole cell, tissues and eventually the organ (Almeida and Barry, 2010).

Gene therapy involves the introduction of genetic material into a person's somatic cells to treat (or to prevent) a disease. The main approaches being used are: (i) substituting a mutated gene that is causing the disease with a healthy gene, (ii) knocking out the malfunctioning gene, (iii) inserting a new gene into the host to prevent the occurrence of the disease in an individual that is at risk of developing a genetic diseases (Park *et al.,* 2006). Gene therapy has successfully been used in the treatment of patients suffering from severe combined immunodeficiency syndromes and Adenosine deaminase deficiency (X-SCID and ADA-deficiency) (Bordignon *et al.,* 1995) and haemophilia (Skinner, 2013). It is currently investigated for the treatment or prevention of inherited and acquired terminal/life threatening diseases, such as cancer (El-Aneed 2004), cardiovascular diseases and acquired immune deficiency syndrome (AIDS) (Ginn *et al.,* 2013; Jin *et al.,* 2014).

Gene therapy can be classified into two main groups: germ line gene therapy and somatic gene therapy. Germ line therapy involves the manipulation of germ cells that leads to a change that is transferred to the next generation of the individuals' progeny. Somatic gene therapy, on the other hand, involves the insertion of genes to somatic cells, but the change achieved is not inherited by the individuals' progeny and hence does not affect the genetic structure of the next generation (Wirth *et al.,* 2013; Ibraheem *et al.,* 2014).

Gene expression, also called transfection, involves the insertion of foreign nucleic acids into cells in order to change the genetic characteristic of the cell (Kim and Eberwine, 2010). There are two main types of transfection: stable transfection and transient transfection. Genetic materials that have undergone stable transfection tend to persist in the host genome even after replication, while genetic materials that have gone through transient transfection can be easily lost.

Instruments, such as gene gun, ultrasound and electroporation (also called electro-permeabilisation) have been used to deliver therapeutic genes into patients (Ibraheem *et al.*, 2014). However the main challenge with gene delivery is the fact that free plasmid DNA administered intravenously is subjected to degradation in the systemic circulation of the body (Niven *et al.,* 1998). As a result, DNA carriers have been used to protect and deliver plasmid DNA to the desired site of action. These systems face the challenge of achieving high efficiency, targeted gene expression, longer period of gene expression (Lundstrom 2003). They can be classified as viral and non-viral (synthetic) systems (Dufès *et al.,* 2005).

1.2.1 Viral delivery systems

Viral drug delivery systems are carriers that utilize viruses as the vector of gene products (Robbins and Ghivizzani, 1998; Lundstrom, 2003). They were the first type of vectors used for gene delivery, because of their innate capability of entry into mammalian cells, enabling them to take over DNA replication, transcription and translation of the host mammalian cell. Some viruses have been modified to enable them to transfer genetic material to change the gene sequence in the host. The main

viruses that are being utilized for gene delivery are adenovirus, adeno-associated virus (AAV), Herpes Simplex virus, lentivirus and retrovirus (Figure 1.2) (Ratko *et al.,* 2003).

The adenovirus has long been the chosen vector for gene delivery. In 2003, in China, Shenzhen-based SiBiono GenTech launched the first gene therapy Gendicine™ (a recombinant adenovirus containing the tumour-suppressor gene p53) into the market for the treatment of head and neck squamous cell carcinoma. It has so far been successful in the patients receiving it in conjunction with radiotherapy, with minimal side effects such as common cold and fever (Peng 2005; Jia 2006). Another gene therapy product, Oncorine™, has also received approval by the Chinese SFDA in 2005. Oncorine™ is used alongside chemotherapy for the management of late-stage refractory nasopharyngeal cancer (Wirth *et al.,* 2013).

Glybera ™ (alipogene tiparvovec) is an adeno-associated viral vector that was the first gene therapy to be registered in the European Union in 2012, for the treatment of lipoprotein lipase deficiency (Ylä-Herttuala 2012).

Viral vectors have the advantages of: high transfection efficiency, intrinsic cell surface binding selectivity; enabling them to transduce several cell types as seen in the adenovirus, prolonged gene expression; as observed with the AAV (Ratko *et al.*, 2003; Park *et al.,* 2006), some degree of stability for a period.

Viral gene delivery systems also present several disadvantages: acute immune responses in some patients, viral insertional mutagenicity; as seen in adeno-associated viruses, no targeting specificity for some viruses, such as the adenovirus, herpes simplex virus and retrovirus, cytotoxicity; as observed in herpes simplex virus, systemic viral infections and viral protein immunogenicity, difficulty with the production of viral vectors, handling and scale-up, limitation of the length of genes that could be carried; as observed with Adenovirus and Lentivirus, long term instability, require special storage facilities, challenge of maintaining high quality assurance (Ratko *et al.*, 2003; Jin *et al.*, 2014; Wang *et al.*, 2014; Ibraheem *et al.*, 2014).

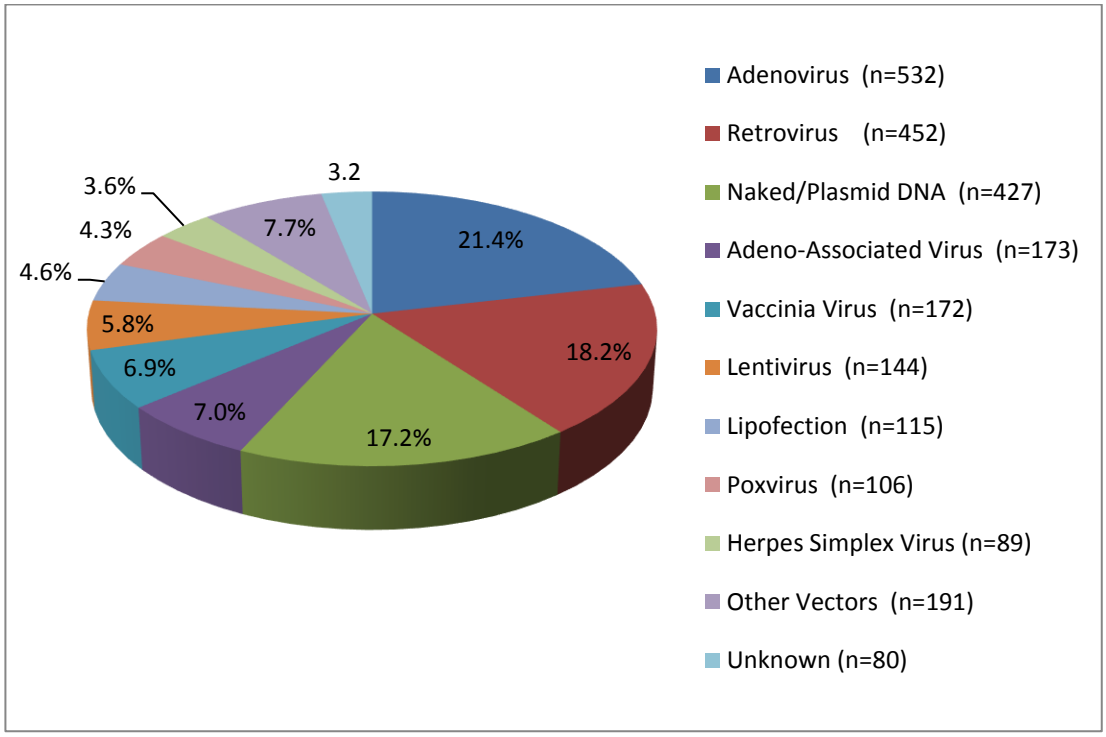

Figure 1.2: Viral vectors used in gene therapy clinical trials (Adapted from The Journal of Gene Medicine www.abedia.com/wiley/vectors.php acessed 250417)

.

1.2.2 Non-viral delivery systems

Non-viral methods of gene transfer include the use synthetic gene vectors/ carriers, such as lipid-based nanocarriers like liposomes (Ruponen *et al.*, 2003), polymer-based delivery systems which include dendrimers such as Polyamidoamine (PAMAM) and diaminobutyric poly (propylene imine) (DAB-Am-x or PPI) dendrimers (Park *et al.*, 2006; Wyrozumska *et al.*, 2006). Non-viral gene transfer using synthetic gene vectors/ carriers, occurs through endocytosis. After endosomal uptake, the synthetic gene vectors/ carriers then undergo endosomal escape. Nuclear localization of the DNA complexes into the nucleus of the cell then occurs which leads to transgene expression.

This occurs by the internalized DNA within the nucleus of the cell undergoing transcription to form RNA. The RNA formed then undergoes translation leading to the formation of the required proteins (Figure 1.3) (Khalil *et al.*, 2006; Wyrozumska *et al.*, 2006).

The use of gene therapy for the prevention and treatment of tumours is an area of research that has been attracting a lot of interest for a very long time. Nevertheless, no non-viral formulation has been able to reach the clinical commercialization stage so far, due to challenges with delivery and site specificity. However, research into the use of dendrimers as gene delivery systems is currently being carried out (Dufès *et al.*, 2005; Schatzlein *et al.*, 2005).

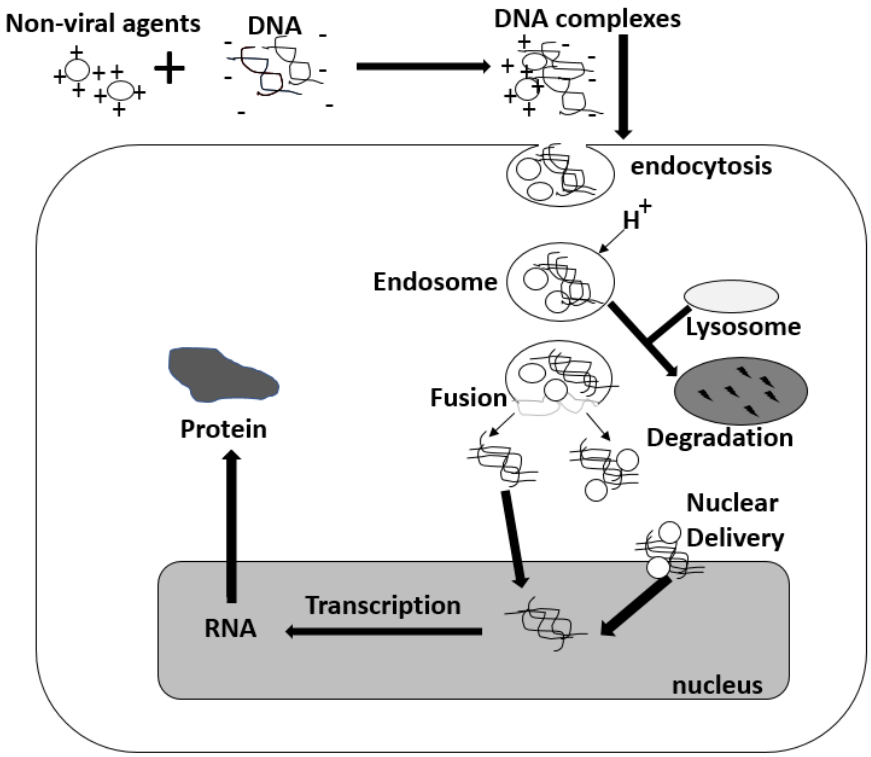

Figure 1.3: Schematic representation of endosomal uptake of DNA with the aid of non-viral agents (Adapted from Khalil *et al.*, 2006)

Non-viral delivery systems have some advantages over viral delivery systems (Ratko *et al.*, 2003; Ruponen *et al.,* 2003): transport of larger-sized DNA, as compared to the challenge of limited DNA sizes that can be carried in viral vectors, low immunogenicity, which is still a major source of concern with viral vectors, higher safety profile than viral vectors, easier manufacturing and scale-up process, maintenance of Good Manufacturing Practice and quality assurance is easier, less complicated storage targeted delivery is feasible.

However non- viral delivery systems also have disadvantages (Santander-Ortega *et al.*, 2014): low transfection, transient expression which reduces their efficiency, the

complexes formed with DNA have low colloidal stability, require DNA complexation immediately before treatment which would require expertise.

1.2.2.1 Liposomes

Liposomes are synthetically prepared spherical lipid bi- or multilayered vesicles made of lipidic bi- or multilayers delimitating an aqueous phase/ compartment, allowing the entrapment of both hydrophilic and hydrophobic drugs, nutrients or imaging enhancing agents (Figure 1.4) (Laouini *et al.,* 2012). They are made from phospholipids, such as dipalmitoylphosphatidylcholine (DPPC), dimyristoylphosphatidylcholine (DMPC), N- [1-(2, 3-dioleyloxy) and propyl]-N, N, N-trimethylammonium chloride (DOTMA).

There are various types of liposomes. These are based on different classifications. Classification based on size and number of layers: Small unilamellar vesicles (SUV)- single bilayer- size range: 20-100 nm, Large unilamellar vesicles (LUV)- single bilayer- size range: up to 1000 nm oligolamellar (OLV) 100-500nm, Multilamellar vesicles (MLV) - number of concentric bilayers - size range 200-1000 nm (Wagner and Vorauer-Uhl, 2011; Laouini *et al.,* 2012).

Classification based on their composition and their mechanism of circulation duration: Long-circulating liposomes, Conventional liposomes, pH-sensitive liposomes, Cationic liposomes, Immunoliposomes (Sharma and Sharma, 1997).

The first anticancer drug to be encapsulated in liposomal suspensions that received clinical approval was Doxorubicin HCl liposomal injection (Slingerland *et al.*, 2012). Liposomes have also been used in gene delivery for transporting DNA. However, they present the inconvenience of having large sizes of cationic lipid-DNA complexes and high surface charge, resulting in their fast clearance from the blood circulation (Allen and Cullis, 2013).

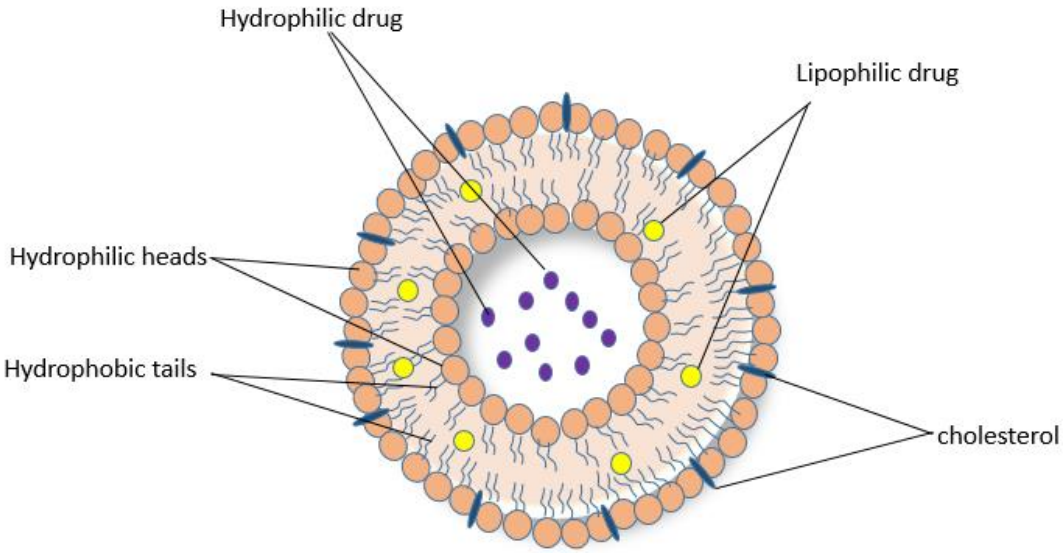

Figure 1.4: Schematic representation of a liposome

1.2.2.2 Niosomes

Niosomes are non-ionic surfactant vesicles formed by non-ionic hydration of surfactants and cholesterol, without incorporation of natural phospholipids (Mahale *et al.*, 2012). They are used as carriers for lipophilic, hydrophilic and amphiphilic drugs. Their non-ionic nature reduces the toxicity and limits their reaction with cells. This, in turn, helps improve the therapeutic index of drugs (Sankhyan and Pawar, 2012). The

structure of niosomes structure is like that of liposomes except that they are formulated from non-ionic surfactants. Individual non-ionic surfactants molecules have different geometrical structures which when known help in predicting the self- assembling structures that they will form. This structural, geometrical parameter of a non-ionic surfactant is called its critical packing parameter (CPP). A CPP less than 0.5 point towards a great influence from the hydrophilic head group area of the molecule, thus supporting the formation of spherical micelles. Whereas surfactants with a CPP value between 0.5 and 1 would form bilayer vesicles, and a CPP larger than 1 would form inverted micelles due to the impact of a large hydrophobic group volume (Uchegbu and Vyas 1998; Wilkhu *et al.*, 2014).

The presence of cholesterol, an important component of the cell membrane, increases the rigidity, fluidity and permeability of the bilayer of niosomes. Niosomes protect the carried drug molecules from degradation and inactivation (Marianecci *et al.,* 2014). Encapsulation of doxorubicin (DOX) in niosomes was shown to cause apoptosis of A431 cancer cells with reduced toxicity *in vivo* (Dufès *et al.*, 2004). In another study, the intravenous injection of niosomes loaded with doxorubicin showed a significant increase in the amount of doxorubicin in the plasma as compared with the free drug, with no lung toxicity observed in the AKR mice used (Uchegbu *et al.*, 1994).

Niosomes have been successfully used in gene delivery for the transfection of DNA pEGFP-C2 in human cervical carcinoma cell line (HeLa cells) (Paecharoenchai *et al.*, 2014) and in the delivery of pCMS-EGFP plasmid to HEK-293, ARPE-19 and MSC-D1 cell lines (Ojeda et al. 2015).

Niosomes are classified based on their number of bilayers and their size. Classification according to their lamellarity is as follows: Multilamellar vesicles (MLV) (1-5 μm), Large unilamellar vesicles (LUV) (0.1 – 1μm), Small unilamellar vesicles (SUV) (25 – 500 nm) (Biju. *et al.,* 2006). Classification according to their size: Small niosomes (100 nm – 200 nm), Large niosomes (800 nm – 900 nm), Giant niosomes (2 μm – 4 μm).

Niosomes present the following advantages and disadvantages: entrapment of drug molecules in niosomes is similar in manner to that observed in liposomes, more stable than liposomes (phospholipids involved in liposome formulation are easily oxidized), and hence have a longer storage time than liposomes, high biocompatibility, biodegradability, non-immunogenicity and low toxicity *in vivo*, chemically stable (Biju, 2006), improvement of oral bioavailability of poorly absorbed drugs (Moghassemi and Hadjizadeh, 2014). Niosomes also have the advantage of accommodating of drug molecules with a wide range of solubilities, because of the presence of both hydrophilic and hydrophobic moieties in their structure (Biju *et al.,* 2006; Sankhyan and Pawar, 2012; Kamboj *et al.,* 2013).

As with all nanoparticles, the main challenge of niosomes is their possible toxicity following long-term use and their degradation by bile salts when orally administered.

1.2.2.3 Dendrimers

The name dendrimer is derived from the Greek word “dendron” that literally means “tree”. Dendrimers are nanoscale, spherically shaped, well-defined, regularly branched polymers. They consist of three main parts: an inner core, the interior layer (from which generations emerge through radially attached repeating units to the central core) and an exterior layer (conferring terminal group functionality) which is attached to the outermost generation of the interior layer (Figure 1.5) (Tomalia *et al.,* 1986; Jain *et al.,* 2010). Dendrimers are structurally different from hyper branched polymers that exhibit non-defined branching characteristics. They have a narrow polydispersity and a multifunctional surface which makes their surface chemistry easy to modify (Duncan and Izzo 2005; Li *et al.,* 2013; Kesharwani *et al.,* 2014)**.** They have the capacity to encapsulate drugs, either in their core or at their surface through covalent linking (Bei *et al.,* 2010). The use of dendrimers in gene delivery is linked to their ability to bind to negatively charged nucleic acid molecules (Chaplot and Rupenthal 2014).

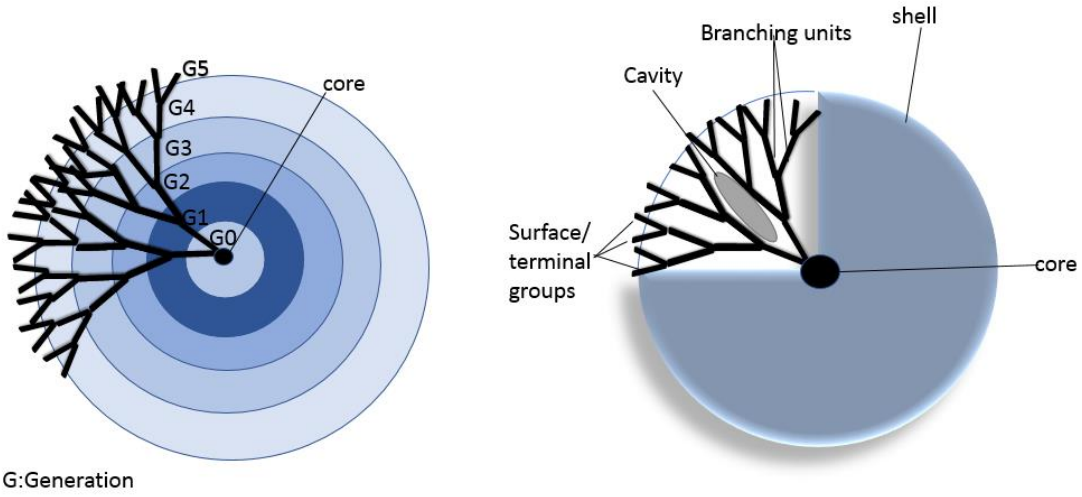

Figure 1.5: Structure of Dendrimers (Adapted from Dufès *et al.*, 2005)

There are two main approaches for their synthesis: the convergent and divergent approaches. The divergent approach involves building the structure of the dendrimer from the core outwards (bottom-top) by attaching branches through chemical reactions. The convergent approach was designed by Hawker and Fréchet. This involves building the dendrimers from the outer layer towards the interior core via the connecting of surface active molecules together ("top-bottom"). Polyamidoamine (PAMAM) and diaminobutyric poly (propylene imine) (DAB-Am-x or PPI) dendrimers are the most extensively used dendrimers to date (Hawker and Frechet 1990). They are formulated through the divergent approach (Malik *et al.*, 2000).

Poly (propyleneimine) dendrimers have been successfully used for gene delivery (Svenson 2009). Dendriplexes formulated with generation 3 (G3-) diaminobutyric polypropylenimine (DAB-Am-16) dendrimers conjugated with transferrin have been shown to cause a substantial increase in the anti-proliferative activity against A431

cells when compared to the DAB-Am-16 dendriplexes formulated without transferrin *in vitro* and *in vivo* (Lemarié *et al.*, 2012).

In past research work, it has been demonstrated that poly (propyleneimine) dendrimers had the ability to target the liver and avoid the lung for the delivery of genes (Schatzlein *et al.*, 2005). In addition, intravenously administered transferrin-bearing generation 3- DAB-Am-16 complexed with DNA encoding Tumour Necrosis Factor (TNF)- α, led to tumour regression in murine models bearing subcutaneous PC-3 and DU145 tumours, with excellent long-term response (Al Robaian *et al.*, 2014). The Al Robaian *et al.*, project made the use of generation 3- DAB-Am-16 dendrimer the choice dendrimer delivery system to be included in the formation of dendrisomes for this project.

1.2.2.4 Hybrid nanocarrier systems

Hybrid systems for drug/gene combinations as non-viral gene transfection vectors have been attracting a growing interest in achieving safe and efficacious drug and gene delivery (Torchilin 2008). This can be attributed to the fact that, though non-viral vectors have several advantages over viral vectors, though they still exhibit lower gene transfer efficiencies than viral vectors (Sun and Zhang, 2010). Hybrid nanocarriers have also been generating a lot of interest due to the postulation that they have the capacity to co-deliver more than one anticancer therapeutic agent and hence cause an additive or a synergistic effect. This proposition is being based on the concept that nanocarriers that have the capacity to deliver a combination of anticancer therapies with different mechanisms of action would provide a solution to the challenge that the

heterogeneity, unique microenvironment and physiological structure that solid tumours possess (He *et al.*, 2015). Various groups have been had been able to successfully make hybrid nanocarrier systems that can co-deliver chemotherapeutic drugs and genes. Examples of these hybrid nanocarrier systems are mentioned in the following paragraphs.

A research work by Han *et al.* showed that transferrin-modified doxorubicin and enhanced green fluorescence protein plasmid (pEGFP) co-encapsulated in nanostructured lipid carriers (T-NLC) significantly increased anti-tumour activity in C57BL/6 mice bearing A549 solid tumours when compared to the doxorubicin and enhanced green fluorescence protein plasmid (pEGFP) co-encapsulated in nanostructured lipid carriers (NLC) that were not bearing transferrin. It was observed that after 15 days of administration of T-NLC, transferrin-modified DOX- and pEGFP co-encapsulated Solid lipid nanoparticles (T-SLN), NLC, free doxorubicin the tumor weight in the treated mice were inhibited by 66%, 39%, 47% and 17% respectively as compared with the control *in vivo*. This showed that the unique formulation of the formulation of the NLC (as compared to the Solid lipid nanoparticles SLN) as well as the addition of transferrin to the NLC made a difference in antitumour efficacy for codelivery of enhanced green fluorescence protein plasmid (pEGFP) and doxorubicin (DOX) (Han *et al.*, 2014).

Another research work successfully used targeted multifunctional PEI-PEG based nanoparticles for the co-delivery of plasmid EGFP and doxorubicin to human liver carcinoma cell line (HepG2) and human breast adenocarcinoma cell line (MCF-7) *in vitro* (Liu *et al.*, 2013). A research work by Wang *et al.*, showed how hyaluronic acid

decorated PEI-PLGA nano carriers that encapsulated doxorubicin and were bearing miR-542-3p (DOX/ miR-542-3p -HA/ PPNPs), led to increased cellular uptake in MDA-MB-231 cells compared to MCF-7 cells in a study focused on for triple negative breast cancer (TNBC) therapy. MTT assays of MDA-MB-231 cells treated with hyaluronic acid decorated PEI-PLGA nano carriers that encapsulated doxorubicin (DOX-HA/PPNPs) showed cell viability of only 35.5%, while MDA-MB-231 cells treated with PEI-PLGA nano carriers that encapsulated doxorubicin (DOX-PPNPs) showed a viability of 50.3%. On the other hand, the co-delivery of DOX and miR-542-3p by HA/PPNPs (DOX/ miR-542-3p -HA/ PPNPs) demonstrated a significantly higher cytotoxicity (27.0% survival) than the (DOX-HA/ PPNPs) and miR-542-3p-HA/PPNPs alone in MDA-MB-231cells. This showed that there was significant synergetic efficacy achieved for the combination of miR-542-3p and DOX. However, there was a sharp contrast observed in the MCF-7 cells treated with the DOX-PPNPs and DOX-HA/PPNPs that exhibited a similar decrease in cell viability. This suggests that the cancer cell lines used for studies are very important because different cell lines can produce varied results (Wang *et al.,* 2016). Based on the foregoing, the utilization of hybrid nanocarriers for co-delivery of chemotherapeutic drugs and genes using non-viral delivery systems gives credence for further investigation.

1.3 Nanomedicine for Cancer targeting using nanocarriers

Nanomedicine, in a broad sense, is the application of nanotechnology to the practice of medicine, for prevention, diagnosis and treatment of disease, and to gain an increased understanding of the complex underlying mechanisms of the disease (Frank *et al.,* 2014). It may also be defined as the monitoring, repair and control of human

biological systems at the molecular level, using engineered nanodevices and nanostructures (Freitas 2006). The prefix "nano" in the word nanotechnology is coined from the Greek word "nano" which means dwarf (Sahoo *et al.,* 2007). Nanotechnology is a rapidly growing aspect of science and technology that involves the formation, application and manipulation of particles, devices or systems at the nanoscale level; the level of atoms, molecules, and supramolecular structures. A nanometre is a billionth of a metre (Jain, 2014). The late Nobel physicist Richard P. Feynman is referred to as "the father of nanotechnology" (Feynman 1960). The use of nanotechnology in medicines and medical devices was aimed at ensuring better outcomes at nanoscale at very low doses. It has been discovered that at nanoscale, the intrinsic properties of drug have been shown to exhibit unique properties such as higher penetration ability into living cells/tissues (Etheridge *et al.,* 2013).

Drug delivery systems refer to drug formulations that deliver therapeutic substances to a specific sites in the body at a particular rate and/or time (Jain, 2008). The main purposes of using drug delivery systems are to improve bioavailability, increase therapeutic indexes, and ensure desirable rates of drug release from formulations at specific sites of action, without negatively affecting normal tissues. This leads to an improved patient compliance and an increase in positive therapeutic outcomes (Paolino *et al.,* 2006; Singh *et al.,* 2011). In drug delivery, nanomedicines have been shown to improve the physico-chemical characteristics of drugs following administration (Uchegbu and Siew, 2013).

Various types of nanocarriers, such as liposomes (Çağdaş *et al.,* 2014), niosomes (Bayindir and Yuksel, 2010), dendrimers, solid lipid nanoparticles (Acevedo-Morantes *et al.,* 2013) and other nanoparticles (Dobrovolskaia and McNeil, 2007) are currently being investigated for drug delivery, as earlier described in this thesis. Some of these carriers are already available commercially, such as the liposomal vincristine marketed as Mariqbo® (Chang and Yeh, 2012) and liposomal cytarabine (DepoCyt®) (Chamberlain 2012). Nanocarriers have been found to increase the efficacy and therapeutic index of chemotherapeutic agents, and reduce their side effects when compared to conventional drugs (Plapied *et al.,* 2011; Chang and Yeh, 2012). A study by Kim and colleagues (2011) showed that there was improved selectivity for cancer cells *in vitro* when a liposomal formulation encapsulating a combination of cytarabine and daunorubicin. There was a much higher accumulation of daunorubicin in the acute myeloid leukaemia cells than in normal cells (Kim *et al.,* 2011). Nanocarriers have also been shown to have prolonged circulation times in the blood stream without being detected and destroyed by the macrophage system (Maherani *et al.,* 2011). Though a lot of research is ongoing in the area of nanomedicine, the issue of long term safety and efficacy is still an underlying challenge, as well as the cost of production of these nanomedicines (Skotland *et al.,* 2014). The need for more research to try and resolve these problems becomes even more critical in the area of cancer targeting.

Targeting in drug delivery is an area of huge interest in modern pharmaceutical research. It refers to the ability of a therapeutic agent to act on the site of action with little or no activity on non-target tissue. Nanocarriers used in cancer targeting are aimed at efficaciously selectively targeting cancer cells, thereby leaving the healthy

cells undamaged (Fanciullino *et al.,* 2013). The ability of selectively increasing the concentration of the drug at the site of action desired while concurrently reducing the occurrence of side effects on normal tissues, makes targeted nanomedicines very desirable as compared to non-targeted drug delivery systems, especially in cancer treatment (Kleinstreuer *et al.,* 2014). At present, this is achieved by using delivery systems via passive or active targeting of therapeutic substances to tumours (Peer *et al.,* 2007; Torchilin 2010; Li *et al.,* 2015).

1.3.1 Passive targeting

Passive targeting can be referred to the phenomena in which drug carriers preferentially accumulate in a region or organ due to an ongoing pathological state *in vivo* (Fahmy *et al.,* 2005; Perrie and Rades 2012). Passive targeting has been observed to occur in various situations: by the (Mononuclear Phagocytic System) MPS combined with the blood and lymphatic vessels in the body, secondly effect through changes in local physiological conditions in the body such as a reduction or an increase in pH or increased levels of enzymes, or thirdly via the enhanced permeability retention (EPR) effect. Passive targeting via the MPS system has been used to treat macrophage intracellular microbial diseases such as visceral Leishmaniasis (Perrie and Rades 2012). Liposomal amphotericin B which is currently being used for treating visceral leishmaniasis, has been found to preferentially accumulate in the liver and spleen. The great number of macrophages in these organs and as well as nanometer size and unique lipid composition of the liposomal amphotericin B the has been deduced as the cause of this occurrence (Stone *et al.,* 2016). A reduction in pH; which is a local physiological condition in the body, has been successfully used for passive

targeting with 1-palmitoyl-2-oleoyl-sn-glycero3-phosphocholine (POPC) pH sensitive liposomes in triggering the release of doxorubicin in cellular lysosomes of PANC-1 pancreatic cancer cells (Nahire *et al.,* 2014). The most commonly reported form of passive targeting is via the EPR effect.

The EPR effect has been successfully utilized to achieve passive targeting *in vivo* in solid tumours (Fang *et al.,* 2011; Maeda *et al.,* Yin *et al.,* 2014). It has been observed in drug delivery that nanocarriers preferentially accumulate inside the interstitial space of tumours (Torchilin, 2010). This has been attributed to the abnormally high porosity in the vasculature in solid tumours due to the excessive production of various vascular mediators and cytokines, such as bradykinin and vascular endothelial growth factor (VEGF) in cancer cells. This has been attributed to tumours triggering uncontrolled angiogenesis in order to obtain an increased supply of oxygen and nutrients to grow and sustain themselves (Hanahan and Weinberg, 2011). Thus this porous vasculature in tumours, enables nanoparticles and macromolecular anticancer agents to preferentially accumulate in cancer cells than normal cells and hence exert their cytotoxic effect with higher specificity (Figure 1.6) (Nakamura and Maeda, 2013; Yhee *et al.,* 2013). This mechanism is referred to as the enhanced permeability and retention (EPR) effect. The antitumour drug Doxil® is an example of an anticancer nanocarrier that utilizes passive targeting via the EPR effect in exerting it's antitumour effect as one of the mechanism of action (Barenholz 2012).

PEGylation of nanocarriers has been shown to modify the structure of the surface membrane of nanocarriers thereby leading to an increase in the retention of the

PEGylated nanocarriers systemically, thus there is a prolongation in the circulation of the PEGylated nanocarriers *in vivo* (Barenholz, 2012). The prolongation in circulation of PEGylated nanocarriers presents the advantage of being taken up into the tumour vasculature in a higher concentration via passive targeting based on the EPR effect. PEGylated gold nanoparticle conjugates utilizing passive targeting were shown to preferentially accumulate in cancer cells *in vivo* in nude mice due to the exploitation of this effect (Cheng *et al.,* 2008). Studies using multifunctional nanoparticle quantum dots probes also showed that these nanoparticles accumulated at prostate cancer sites in nude mice via the EPR effect (Gao *et al.,* 2004). However, it has been demonstrated that passive targeting presents the disadvantage of having uneven therapeutic concentrations in different parts of the tumour and in some macromolecules inaccessibility to some pharmacological targets (Nichols and Bae, 2013; Bertrand *et al.,* 2015). This can be explained by the fact that passive targeting is a very slow process and that the EPR effect may not occur homogeneously even within individual tumours (Kraft *et al.,* 2014; Khawar *et al.,* 2015).

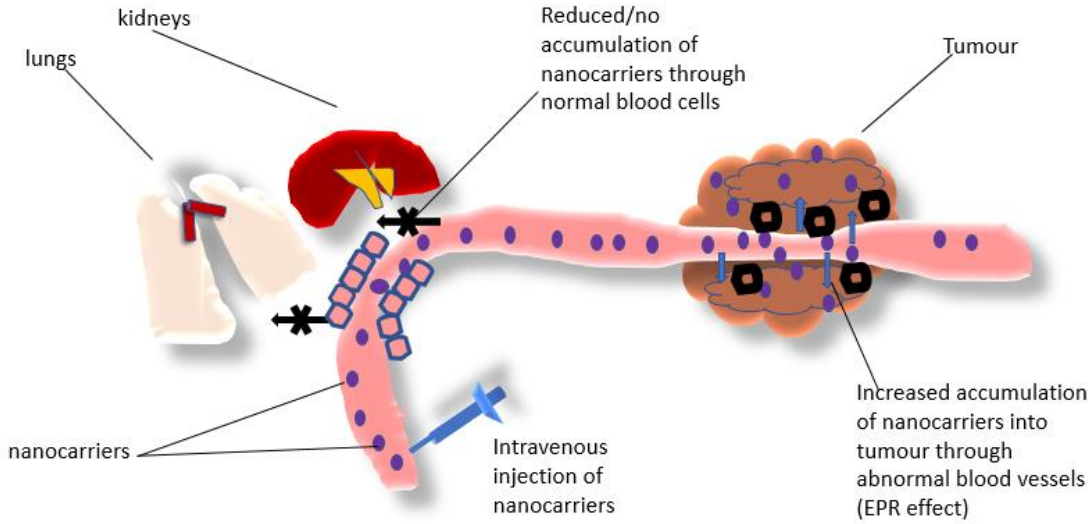

Figure 1.6: Passive targeting of cancer cells via the Enhanced Permeability and Retention effect (Adapted from Yhee *et al.*, 2013)

1.3.2 Active targeting

The concept of active targeting was first conceptualized by Paul Ehrlich with his idea of the "magic bullet"(Kulve 2010). "The magic bullet" ideology gives the hypothesis that on administration, a drug entity should go directly to the required site of action without causing damage to normal cells, tissues or organs. Active targeting involves the use of a targeting ligand/ moiety, conjugated to carrier and the drug or therapeutic agent to be released (Singh *et al.,* 2011), with the capacity to recognize specific antigens or cell membrane receptors and bind to them.

The use of ligands, such as transferrin, conjugated to dendriplexes DNA encoding TNFα to target transferrin receptors on prostate carcinomas is an example of active targeting (Al Robaian *et al.,* 2014). The selective drug delivery to the target tissue increases the therapeutic efficiency of the drug and decreases its undesirable effect on

non-target tissue. A suitable drug delivery system for the delivery of anticancer drugs and genes should be able to improve the efficacy of cancer treatment, as well as to ensure selective accumulation of the drug in the cancer cells or/and deliver the genes to the appropriate site for gene expression. This will ensure reduced toxicity of the anticancer treatment (Nichols and Bae, 2013).

Several ligands are currently in use for targeting nanocarriers, such as transferrin (Somani *et al.,* 2014), folic acid (Vaitilingam *et al.*, 2012) and hyaluronic acid (Han *et al.,* 2015). Among these ligands, transferrin and folic acid are most commonly used.

1.3.2.1 Transferrin

Transferrin is an iron-binding glycoprotein that transports iron throughout the blood to the liver, spleen and bone marrow (Dufès *et al.,* 2013). The use of transferrin as a targeting ligand is based on the fact that iron is essential for tumour cell growth and can be effectively carried to tumours that overexpress transferrin receptors (Lemarié *et al.,* 2012). Transferrin receptor 1 (TFR1), also known as CD71, is an attractive target for selective receptor-mediated gene delivery to tumours because it is overexpressed in a high percentage of human cancers, including ovarian, breast, colon cancers and glioblastoma cell lines. (Calzolari *et al.,* 2007; Xu *et al.,* 2013). Due to the fact that transferrin receptors are also expressed in some rapidly dividing healthy tissues, transferrin is hence used as a ligand in active targeting (Dufès *et al.,* 2013). This well-studied ligand has been used as a tumour-targeting ligand for several drug delivery systems, for example in the co-delivery of DNA and doxorubicin using nanostructured lipid carriers (Han *et al.,* 2014) and in the delivery of genes to the brain using targeted

polypropylenimine dendrimer (Somani *et al.,* 2014). Comparative studies using transferrin-targeted and non-targeted polymeric chitosan vesicles encapsulating doxorubicin, showed that the transferrin-targeted vesicles resulted in a greater tumoricidal activity against doxorubicin-resistant A2780AD and A431 cell lines (Dufès *et al.,* 2004).

1.3.2.2 Folic Acid

Folic acid is a synthetic compound that has been used as targeting agent to cancer cells that overexpress folate receptors FRα, FRβ, and FRγ (Vaitilingam *et al.,* 2012; Chen *et al.,* 2013). *In vivo* folate is involved in purine and thymidine synthesis. Purine and thymidine are constituents involved in nucleic acid synthesis and hence are involved in cell growth. It has been observed that, although some normal cells express folate receptors naturally (Kane *et al.,* 1988), there is overexpression of folate receptors on cancer cells due to the high need of folate by cancer cells for their rapid growth. Overexpression of folate receptors in cancer cells is thus makes folic acid a potential targeting ligand in nanomedicine.

1.4 Plasmid DNA encoding Tumour Necrosis Factor alpha (TNF-α)

Plasmid DNA encoding Tumour Necrosis Factor alpha (TNF- α) is a therapeutic, pleiotropic cytokine, with antitumoral activity composed of 3 non-covalently linked TNF- α monomers, each of about 17.5 KDa. DNA encoding TNF- α is mainly secreted by macrophages. DNA encoding TNF- α has also been found to be highly expressed on tumours. DNA encoding TNF- α exerts its effects in tumours mainly by the destruction of the endothelial cells of the tumour-associated vasculature. It binds to

TNFR-1 receptors, and thus exerts it's activity through these receptors (Figure 1.7) (Nikoletopoulou *et al.,* 2013). DNA encoding TNF- α induces cellular apoptosis by causing an increase in the permeability of tumour cells, up-regulation of tissue factor, fibrin deposition and thrombosis, thereby leading to the destruction of the endothelial cells and thus cell death of tumour cells at high doses (Wang and Lin 2008; Burton and Libutti 2009).

It will be observed in Figure 1.8A that the healthy endothelial lining has a lower permeability than the tumour endothelial lining. In Figure 1.8B, on treatment with DNA encoding TNF-α, it is observed that the healthy endothelial lining remains undamaged. This could be attributed to the lack of TNFR-1 expression on the cell membrane thus not allowing for binding of DNA encoding TNF-α hence no effect is exhibited. However, in the case of the tumour endothelial, it is observed that upon treatment with DNA encoding TNF-α, that rupture of the tumour endothelial lining occurs. This is because DNA encoding TNF-α is able to bind to the TNFR-1 receptors thus allowing for the apoptotic effect of DNA encoding TNF-α to be initiated. Another group has also proposed that the hyper permeability and destruction of the vascular lining of the tumour vasculature, allows for the selective accumulation of anticancer drugs in the tumour vasculature, thereby giving a synergistic effect (van Horssen *et al.,* 2006).

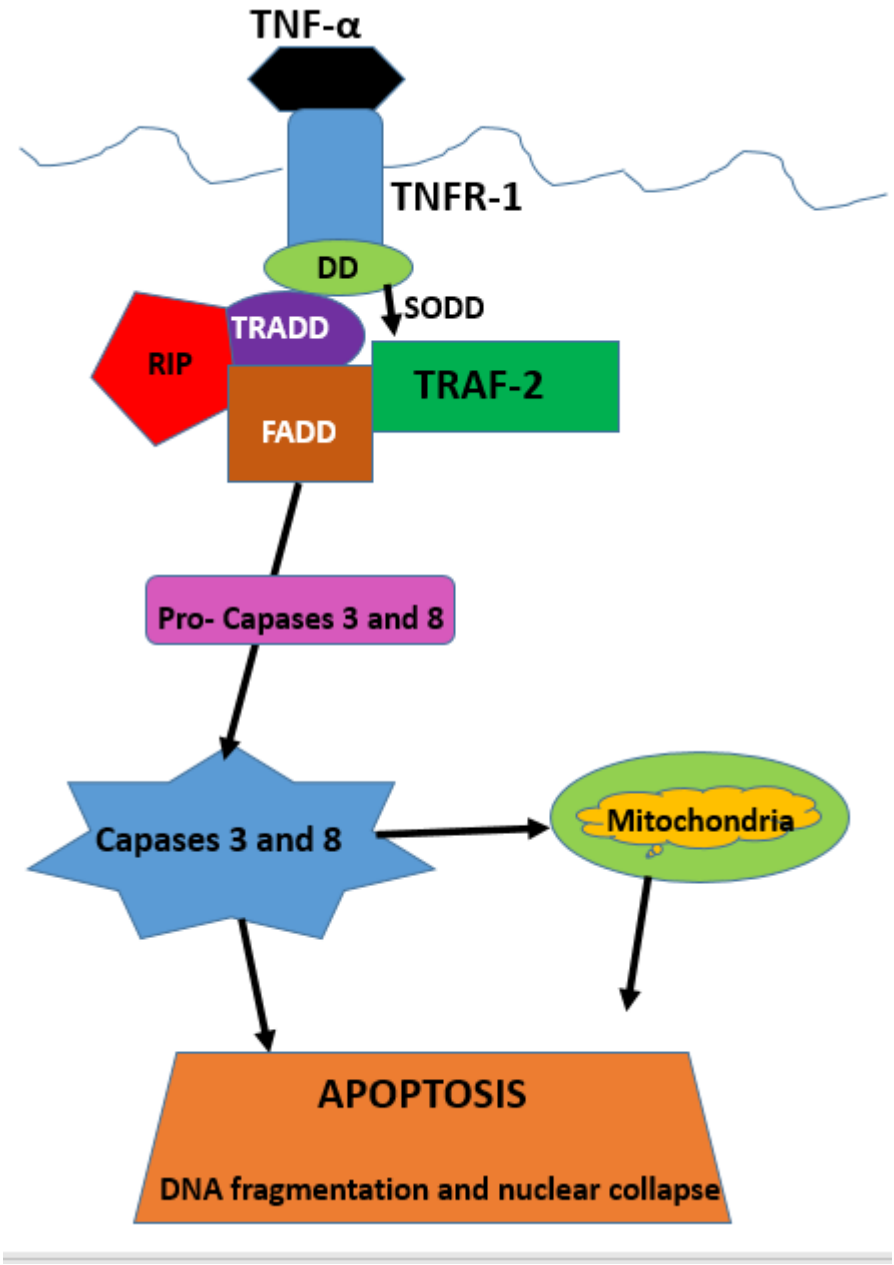

TNF-α: Tumour necrosis factor alpha, TNFR-1: Tumour necrosis factor receptor-1

TRADD: TNFR-associated death domain TRAF-2: TNFR-associated factor,

DD: Death Domain, SODD: Silencer of death domain protein

FADD: Fas-associated death domain, RIP: Receptor interacting protein

Figure 1.7: TNFR1 mediated cell death signaling pathway
(Adapted from Horssen *et al.*, 2006 and Nikoletopoulou *et al.*, 2013)

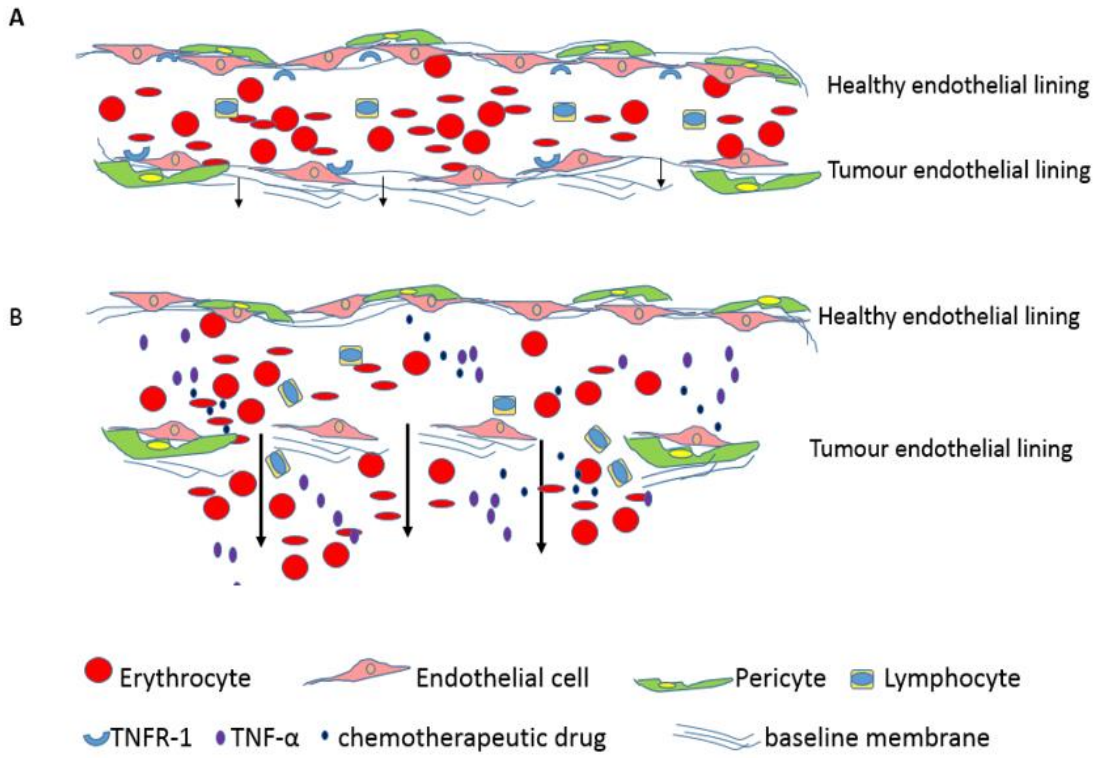

Figure 1.8: A schematic representation of the differences in the effect of DNA encoding tumour necrosis factor α (TNF-α) on healthy and tumour endothelium with (A) as a vessel with healthy endothelial lining (upper layer) and tumour endothelial lining (lower) before DNA encoding TNF-α treatment. While (B) represents a vessel with healthy endothelial lining (upper layer) and tumour endothelial lining (lower) after DNA encoding TNF-α treatment. (Adapted from van Horssen *et al.*, 2006).

Though DNA encoding TNF- α has high therapeutic potential in cancer therapy, the use of DNA encoding TNF-α in patients is currently being limited due to severe side effects such as hypotension hepatotoxicity, thrombocytopenia and neurotoxicity (Roberts *et al.*, 2011) caused by high systemic toxicity. Localized therapy (isolated limb perfusion) is currently in use in combination with melphalan for patients with metastatic melanoma cells that are in transition, but this use is limited in the case of already metastasized cancer cells (Borsi *et al.*, 2003). Clinical studies utilizing Recombinant human DNA encoding TNF-α as a single therapeutic and in combination

with chemotherapy have been carried out. The indications, doses and method of administration of DNA encoding TNF-α have been included in the proceeding tables. (Table1.1 and Table1.2).

Table 1.1: Recombinant human TNF-α (rhTNF-α) Phase II clinical studies as a single agent for cancer therapy (Adapted from Roberts *et al.*, 2011)

Study	Total number of patients	Tumor Type	Dose TNF-α[a]	Schedule	Maximum Number of Cycles	ORR	Major Reported Toxicities
Heim *et al.*, 1990	15	Advanced colorectal cancer	3 x 10^5 U/m^2/day	Daily for days 1-3 every 2 weeks	4	9%	Dyspnea, Fever and Leucopenia.
Kemeny *et al.*, 1990	16	Advanced colorectal cancer	100-150 µg/m^2/day	100 µg/m^2/day twice daily on day 1. 150 µg/m^2/day Twice daily for days 2-5. This was repeated every other week.	4	NR	Neurotoxicity, Leukopenia Gastrointestinal toxicity, Chills, Pain, Hypotension, Hypertension, Hepatotoxicity and Vascular thrombosis.
Whitehead *et al.*, 1990	25	Metastatic colorectal cancer	150 µg/m^2/day	Daily for 5 days every 2 weeks	4	0%	Chills, Nausea, Vomiting, Anemia, Hepatoxicity.
Brown *et al.*, 1991	26	Pancreatic adenocarcinoma	150 µg/m^2/day	Daily for 5 days every 2 weeks	7	NR	Fever, Rigor, Nausea, Vomiting, Anorexia, Hypotension, Hyperglycemia, Anemia, Dyspnea, Hepatotoxicity Coagulopathy and Tachycardia
Budd *et al.*, 1991	22	Metastatic breast cancer	150 µg/m^2/day	Daily for 5 days every 2 weeks	4	0%	Hypotension. Diarrhea. Leukopenia. Hepatotoxicity. Intracranial hemorrhage
Feldman *et al.*, 1992	21	Malignant melanoma	150 µg/m^2/day	Daily for 5 days every 2 weeks for 4 cycles, then every three weeks	4+	5%	Fever, Chills, Nausea, Vomiting, Hypotension, Hepatotoxicity and Constitutive symptoms.

[a] - Intravenous infusion was used for delivery of TNF-α for all studies. ORR - objective response rate. N/A - not applicable. NR - not reported in study

Table 1.2: Recombinant human TNF-α Clinical studies in combination with chemotherapy for cancer therapy (Adapted from Roberts *et al.*, 2011)

Study	Total Number of Patients	Tumor Type	Study Design	Chemotherapy	Dose of Chemotherapy/ TNF-α[a]	Regimen	Maximum Number of Cycles	ORR	MTD	Major Reported Toxicities
Jones *et al.*, 1992	41	Advanced melanoma	Phase II	BCNU	BCNU 200 mg/m^2 rhTNF-α ± 88 µg/m^2	Daily for 5 days every 48-days	2	BCNU + rhTNF-α - 10.5% BCNU - 20%	N/A	Hepatotoxicity, Leukopenia, Hematological toxicity and Rigor.
Sella *et al.*, 1995	21	Metastatic prostate cancer	Phase I	Actinomycin D	Actinomycin 1300-400 µg/m^2; rTNF-α starting at 5-60 µg/m^2	IV Actinomycin D followed by rTNF daily for 5-days every 4 weeks	NR	0%	400 µg/m^2 Actinomycin D and 40 µg/m^2 rTNF-α	Fatigue, Neutropenia, Thrombocytopenia, Respiratory toxicity, Neurotoxicity, Nausea and Vomiting.
Yamamoto *et al.*, 2002	10	Recurrent malignant astrocytomas	Phase II	Carboplatin and Etoposide	Carboplatin 400 mg/m^2 (day 1). Etoposide 100 mg/m^2 (days 1-3). TNF-SAM2 80x10^4 U/m^2 (day 7)	Maximum 5 doses over 2 weeks every 8-12 weeks	4	33%	N/A	Leukopenia
Meany *et al.*, 2008	21	Recurrent or refractory Wilms tumor	Phase II	Dactinomycin	Dactinomycin 15 µg/kg/d and rTNF 200 µg/kg/d	Daily for 5-day s every 3 weeks	10	16%	0.8µg/m^2 NGR-hTNF and 75mg/m^2	Thrombocytopenia, Hepatopathy, Neutropenia, Leucopenia, Anemia, Myalgia, Lymphopenia, Hypotension, Nausea, Hematuria, Stomatitis, Neurologic, Bronchospasm and Peripheral capillary leak.
Gregorc *et al.*, 2009	15	Solid tumors	Phase I	Doxorubicin	NGR-hTNF (0.2-0.4-0.8-1.6 µg/m2) and doxorubicin (60-75 mg/m2)	Every 3 weeks	15	7%	N/A (low dose NGR-hTNF therapy)	No dose limiting toxicities observed. Neutropenia, Anemia, Leukopenia, Thrombocytopenia, Leukopenia, Lymphopenia, Neutropenic fever, pain, committing, cough, anorexia, hepatopathy, acute myocardial infarction and pulmonary embolism.

[a] - Intravenous infusion was used for delivery of TNF-α for all studies. ORR - objective response rate. MTD - maximum tolerated dose. NR - not reported in study. N/A - not applicable

This project proposes to formulate a nano carrier that can carry DNA encoding TNF-α TNF-α alone or co-deliver it with the chemotherapeutic agent doxorubicin, to maximise its therapeutic efficacy, while simultaneously reducing/eradicating the challenge of systemic toxicity in a single formulation. A research work using transferrin targeted generation 3 DAB-Am-16 dendrimers complexed with DNA encoding TNF-α has shown the potential for the use of DNA encoding TNF- α for prostate tumour therapy (Al Robaian *et al.,* 2014). Thus, we are expecting that we will be able to achieve therapeutic efficacy in melanoma tumour therapy.

1.5 Doxorubicin

Doxorubicin (Adriamycin®) is a potent anthracycline antineoplastic agent that acts by DNA intercalation leading to cell apoptosis (Figure 1.9). Anthracyclines are anti-tumour drugs that interfere with enzymes involved in DNA replication. These drugs work in all phases of the cell cycle (Chen *et al.,* 2012; Yang *et al.,* 2013; Yang *et al.,* 2014). Other examples of anthracyclines include Daunorubicin , Epirubicin, Idarubicin (Chen *et al.,* 2012). They are widely used for a variety of cancers.

Doxorubicin (DOX) is used in the treatment of leukaemia, Hodgkin's lymphoma, cancers of the bladder, breast, lung, ovaries, stomach, thyroid, soft tissue sarcoma and multiple myeloma (Svenson 2009). Though doxorubicin has a very broad spectrum of activity, its use is limited by its severe side effects which are dose related such as cardiotoxicity (Zhang *et al.,* 2012), hepatotoxicity and nephrotoxicity (Lahoti *et al.,* 2012) due to its non-selectivity (Han *et al.,* 2014). To overcome this issue, tumour-targeting nanocarriers are being investigated to enhance tumour cell-specific delivery

and reduce adverse effects to normal cells (Szwed and Jozwiak 2014; Xu *et al.*, 2014; Wang *et al.*, 2016). Doxorubicin was also chosen because its absorbance and fluorescence characteristics make it easy to detect and quantify in various experiments like drug release (Barenholz, 2012). These factors made doxorubicin the anticancer drug selected for this project.

The exact antitumour mechanism of action of doxorubicin is unclear. There are several proposed mechanisms; but the most widely proposed and accepted mechanism of action is via intercalation with DNA and inhibition of mammalian DNA topoisomerase II leading to DNA damage and thus cell death (Tewey *et al.*, 1984; Bodley *et al.*, 1989).

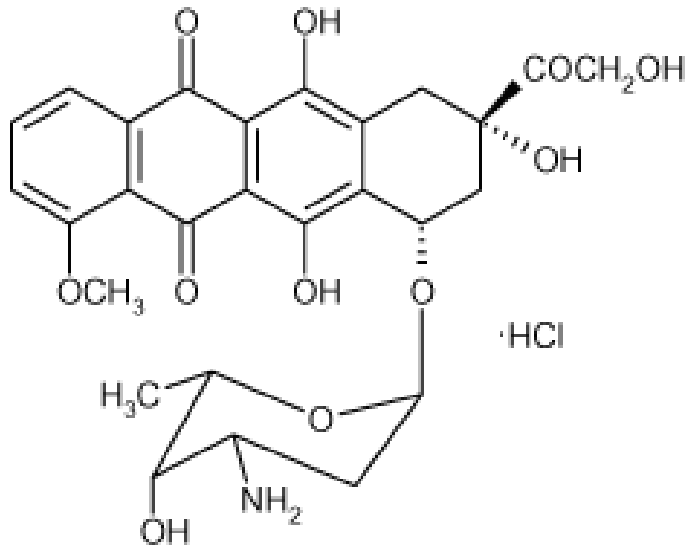

Figure 1.9: Chemical structure of doxorubicin

1.6 Aims and Objectives

The aim of this research project was to investigate if novel transferrin-targeted dendrisomes carrying a therapeutic plasmid DNA and the anti-cancer drug

doxorubicin could improve the therapeutic efficacy on cancer cells *in vitro* and on xenograft models after intravenous administration.

Specifically, the key objectives of this project are:

1. Preparation and characterization of novel transferrin-bearing dendrisomes with the capability to encapsulating doxorubicin and complex them with plasmid DNA encoding β-galactosidase.
2. Evaluation of their gene expression capability when complexed with plasmid DNA encoding β-galactosidase on cancer cells overexpressing transferrin receptors, *in vitro.*
3. Evaluation of their cancer inhibitory effect when encapsulating doxorubicin alongside complexation with therapeutic plasmid DNA encoding TNF α, *in vitro.*
4. Evaluation of their targeted efficacy *in vivo,* following intravenous injection on mice bearing subcutaneous tumours.

In Chapter 2, the focus is on the preparation and characterisation of various dendrisome formulations using the non-ionic surfactant Span 60®, DAB-Am-16 dendrimer and Solulan C24 or d-α-tocopheryl polyethylene glycol 1000 succinate (TPGS). These formulations were characterised for their size, targeting a size less than 500 nm. Zeta potential measurements were carried out to determine the surface charge of the dendrisomes formed. Transmission electron microscopy (TEM) showed the morphology of the nanocarriers formulated. Investigation of DNA condensation abilities of the dendrisomes was done to know if the dendrisomes could carry DNA,

while doxorubicin entrapment studies were done to confirm drug encapsulation efficiency and show drug release.

The emphasis of Chapter 3 is to show the activity of dendrisome formulations *in vitro* via transfection, anti-proliferative assay and cellular uptake experiments. Transfection experiments carried out with plasmid β-Galactosidase were done to show the gene expression capability of the various dendrisomes. Anti-proliferative studies were also carried out to establish the half maximal inhibitory concentration IC_{50} of the dendrisomes. Cellular uptake experiments were done using confocal laser scanning microscopy for qualitative analysis of the uptake of fluorescent DNA in order visualise the DNA uptake into the cell cytoplasm.

Chapter 4 involves investigating the activities of the PEGylated Solulan C24 dendrisomes chosen to quantify β-galactosidase activity in tumours and the antitumour activity *in vivo* using xenograft models. Quantification of β-galactosidase activity in tumours was carried out using fluorescent dye DDAO galactoside (DDAO-G). Balb/c mice were the mice used for all the *in vivo* experiments.

Chapter 5 contains the concluding remarks of the investigative work carried out in this project. Suggestions on future works that could be done using the contribution to knowledge that this project has made were also given in the concluding chapter.

CHAPTER 2: PREPARATION AND CHARACTERIZATION OF DENDRISOMES

2.1 Introduction

Dendrisomes as defined by Al-Jamal *et al.,* 2003 are supramolecular aggregates made from cationic lipidic dendron vesicular assemblies. Florence *et al.,* 2005 on the other hand, defined dendrisomes as dendrimer –based vesicles. Based on the current research ongoing with hybrid nanocarriers, dendrisomes could also be defined as vesicular hybrid nanocarriers formulated from a combination of dendrimers/ dendrons and lipid blends.

A research question was raised in the concluding portion of Al-Jamal *et al.,* 2005 a; and that was that the self-assembled dendrisomes discussed in the publication gave rise to the need for further investigation into the *in vitro* and in *vivo* characterisation of dendrisomes for drug delivery. This project is thus aimed at providing an answer to this research question using dendrimers and not dendrons.

The formulations made in this project have never been prepared before. The closest formulations to these dendrisomes before now were lysine-derived amphiphilic dendron aggregates with cholesterol, (Al-Jamal *et al.,* 2003; Al-Jamal *et al.,* 2005a and b, Florence *et al.,* 2005), PEGylated G5 PAMAM Dendrimer Modified soybean lecithin and cholesterol nanoliposomes (Ma *et al.,* 2015) and the co-assembly of amphiphilic dendrimers with palmitoyloleoylphosphocholine (POPC) forming hybrid nanocarriers (Hinman *et al.,* 2017).

The dendrisomes formulated in this project are composed of non-ionic surfactants, DAB-Am-16 dendrimers, cholesterol, including a phospholipid in one of the

dendrisome formulations. Their synthesis was done using heating and probe sonication. Evaluation of their characteristics was done using various techniques and experiments such as DLS for size measurement, TEM and AFM for their morphology, Picogreen assay and agarose gel assay to ascertain their DNA condensation capabilities, encapsulation efficiency studies and drug release studies to ascertain their drug delivery capabilities were also carried out. A dendrisome is a hybrid nanocarrier formulated from a combination of dendrimers and lipid blends (Parimi *et al.*, 2008; Akesson *et al.*, 2010). The dendrisomes to be developed in this project are novel hybrid, multifunctional, nano-sized non- PEGylated and PEGylated drug delivery systems that will have the capacity to entrap drugs, carry plasmid DNA on their periphery, and targeted with the targeting ligand transferrin.

Dendrisomes combine the advantages of the abilities of dendrimers to form strong DNA complexes because of their amine groups, while also addressing the challenge of safety and biocompatibility feature with the addition of lipids in their composition. It is hypothesized that an additive or synergistic effect might be observed in these novel nanostructures, when transferrin decorated dendrisomes co-deliver an anticancer drug and therapeutic gene to cancer cells. The dendrisomes formulated in this project all had the basic ingredients of Span 60®, cholesterol and DAB-Am-16 dendrimer. Various other lipids were included to formulate different structures. The lipids included were either Solulan 24, or d-α-tocopheryl polyethylene glycol 1000 succinate (TPGS), or TPGS and L-α-Phosphatidylethanolamine, dioleoyl (DOPE), or Dihexadecyl phosphate (DHP). Tests on the formulations with or without

encapsulating doxorubicin were carried out. The proposed general structure of the dendrisomes formulated is seen below (Figure 2.1).

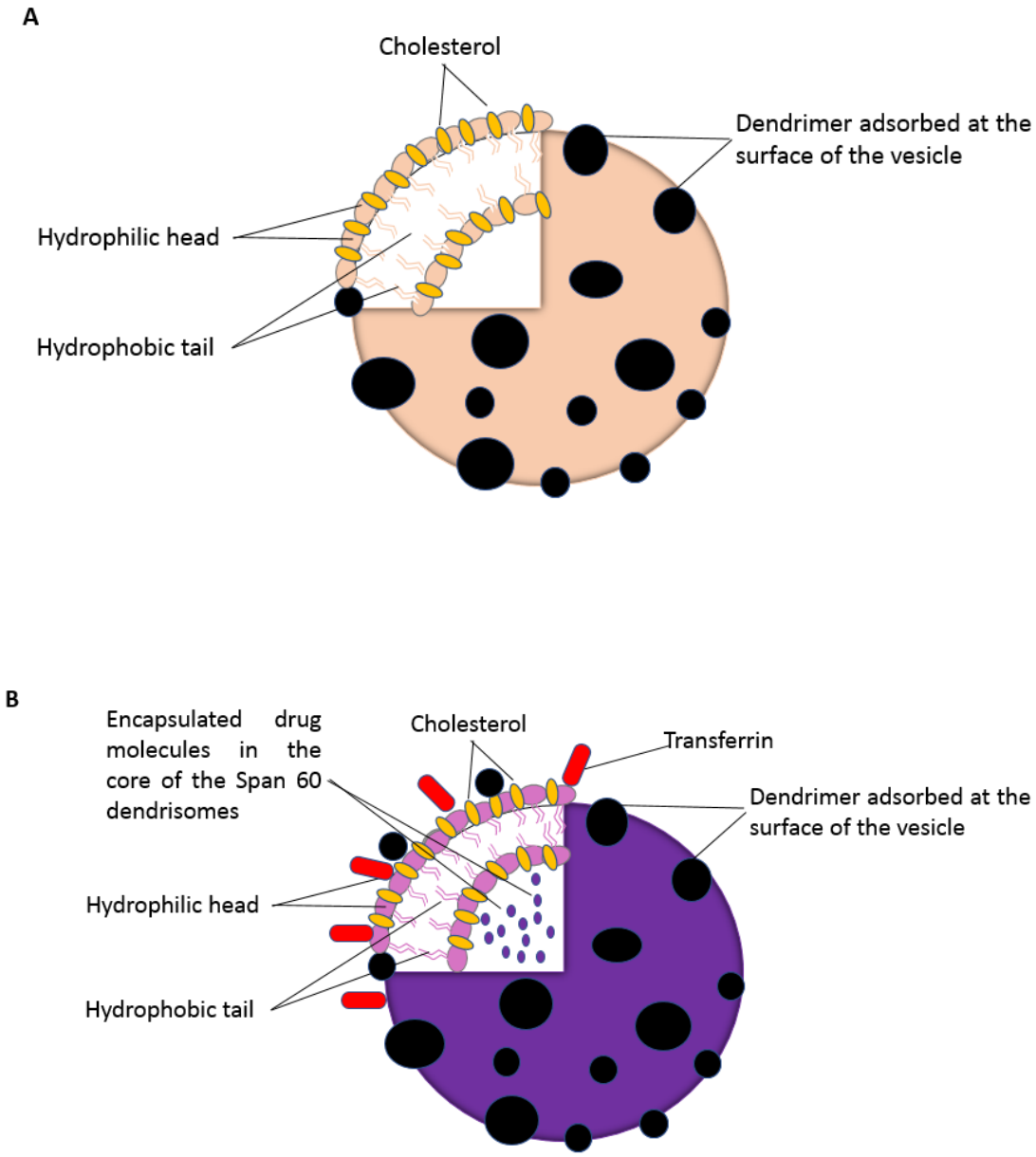

Figure 2.1: Hypothesized surface structure of a blank dendrisome (A) and hypothesized structure of a dendrisome encapsulating doxorubicin and conjugated with transferrin (B).

A research work by Wang *et al.,* showed how MDA-MB-231 cells treated with hyaluronic acid decoration of PEI-PLGA nano carriers encapsulating of doxorubicin and bearing miR-542-3p (DOX/ miR-542-3p- HA/PPNPs) led to increased cellular uptake and higher cytotoxicity in triple negative breast cancer (TNBC) therapy, when compared to the other treatments: hyaluronic acid decorated PEI-PLGA nano carriers encapsulating of doxorubicin (DOX- HA/PPNPs), PEI-PLGA nano carriers encapsulating of doxorubicin (DOX- PPNPs), hyaluronic acid decorated PEI-PLGA nano carriers with miR-542-3p (HA/PPNPs) and free DOX. This study is demonstrating that: targeting through decoration of a formulated a novel hybrid nanocarrier dendrisome, with a targeting ligand, as well co-delivering a chemotherapeutic agent with a therapeutic gene should a cause synergistic or at least an additive effect in cancer therapy.

To develop dendrisomes with anticancer delivery efficacy and specificity, the strategy would be:

1) target this delivery system to cancer cells overexpressing specific cell surface receptors and 2) to combine the delivery of the therapeutic DNA with another therapeutic DNA / drug having complementary therapeutic effects, carried by the same system.

Tumour-targeted dendrisomes will be used in delivering genes and/or anticancer drugs to ensure that cancer cells are specifically targeted after systemic administration without being widely distributed in other cells in the body.

2.1.1 Formulation of dendrisomes

2.1.1.1 Sorbitan monostearate (Span® 60)

Span® 60 is a hydrophobic non-ionic surfactant with long alkyl chain length (C18) that belongs to a group of non-ionic surfactants called Sorbitan fatty acid esters (Figure 2.2). It is a derivative of polyoxyethylene esters that has a gel transition temperature of 56–58 ºC (Kumar and Rajeshwarrao, 2011). The high phase transition temperature of Span 60®, has been shown to aid the prevention of the leakage of encapsulated drugs in niosomes which helps improve the stability of these formulations (Uchegbu and Florence 1995). It has been shown that Span 60® had a higher entrapment efficiency of entrapped drugs when it was compared to other Spans like Span 20 (Kumbhar *et al.,* 2013). A study done using several Spans to formulate niosomes encapsulating colchicine, showed that the niosomes formulated with Span 60® and cholesterol had a high encapsulation efficiency of 99 ± 0.2 % and demonstrated a sustained release profile (Hao *et al.,* 2002).

When Span 60® was used with cholesterol to form Tf-bearing niosomes entrapping tocotrienol, it was found to cause tumour regression for 40% of B16-F10 murine melanoma tumours and 20% of A431 human epidermoid carcinoma tumours (Fu *et al.,* 2011). A research work done on non-ionic surfactant vesicles formulated with Span 60® or Span 80 entrapping an anti-inflammatory drug celecoxib demonstrated that the vesicles that had Span 60® incorporated in them, had a higher encapsulation efficiency at 80.35 % than the Span 40 (Auda *et al.,* 2016).

A lot of research work has been done using Span 60® that demonstrates its ability to the increase vesicular stability, give high entrapment efficiency and prolonged release ability of entrapped drugs in the formulations it is incorporated into. This formed the basis for which Span 60® was chosen to be incorporated in the formulation of the new dendrisome structures formed, in this project.

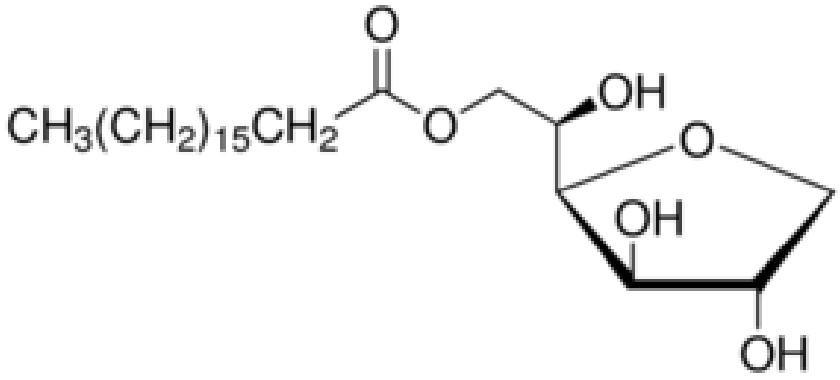

Figure 2.2: Structure of Span 60® Sorbitan monostearate

2.1.1.2 Generation 3- diaminobutyric poly (propyleneimine) dendrimer (DAB-Am-16)

Generation 3- diaminobutyric poly (propyleneimine) dendrimer ((with a 1,4-diaminobutane core (4-carbon core) (DAB) also known as Polypropylenimine hexadecaamine Dendrimer, Generation 3.0, is a poly (propyleneimine) (PPI) dendrimer with a 1,4-diaminobutane core (4-carbon core), with 16 amino propyl surface groups that gives rise to the high reactive capacity of this dendrimer (Figure 2.3) (Sigma-Aldrich, 2016). Polypropylenimine dendrimers were first synthesized by

de Brabander-van den Berg and Meijer in 1993 (de Brabander-van den Berg and Meijer, 1993). It has been found to be more biocompatible than PAMAM dendrimers. This characteristic has been attributed to the fact that it has aliphatic spacers that separates the trifurcate sites thereby reducing its toxicity (Chai and Niu 2001). A research work proved that cell cytotoxicity of Polypropylenimine dendrimers was mainly dependent on the generation of the Polypropylenimine being used. It was observed that cytotoxicity increased with increase in generations: DAB-Am- 8 < DAB-Am- 4 < DAB-Am-16 < DAB-Am-32 < DAB-Am-64. However, it was observed that it was the reverse in terms of transfection efficacy, with DAB-Am-8 and DAB-Am-16 having the highest transfection efficacy and DAB-Am-32 and DAB-Am-64 exhibiting the lowest transfection efficacy in A431 cancer cell line. Nevertheless, it was discovered that the particle size of the DAB-Am-8 dendriplex was large with a mean particle size of 518 nm while DAB-Am-16 dendriplex had a mean particle size of 180 nm (Zinselmeyer *et al.,* 2002). Based on this, DAB-Am-16 was the dendrimer chosen to be used in the dendrisome formulations for this project.

As earlier mentioned generation 3- diaminobutyric polypropylenimine dendrimer is a dendrimer that has proven to be efficacious when targeted with transferrin. Studies carried out with transferrin-bearing DAB-Am-16 dendrimer complexed to plasmid DNA encoding p73, demonstrated up to 120-fold enhanced anti-proliferative activity *in vitro* in A431 cancer cell lines, as compared to the non-targeted DAB-Am-16 dendriplexes. When administered intravenously *in vivo*, the p73-encoding DAB-Am-16 dendriplex caused a fast and continued inhibition of tumour growth over a period of one month, thereby leading to full tumour suppression in 10% of A431 and B16-

F10 tumours in female immunodeficient BALB/c mice, this resulted in long-term survival of the animals (Lemarié *et al.*, 2012). In another research work carried out, treatment of A431 tumours in mice with Tf-bearing DAB-Am-16 complexed with TNFα expression plasmid, led to fast and unremitting tumour regression over the month. There was long-term survival of 100% of the animals. At the conclusion of the *in vivo* experiment, 90% of the tumours treated with Tf-bearing DAB-Am-16 dendriplexes had completely disappeared, while the remaining 10% of the tumours, presented a partial response to the treatment (Koppu *et al.*, 2010).

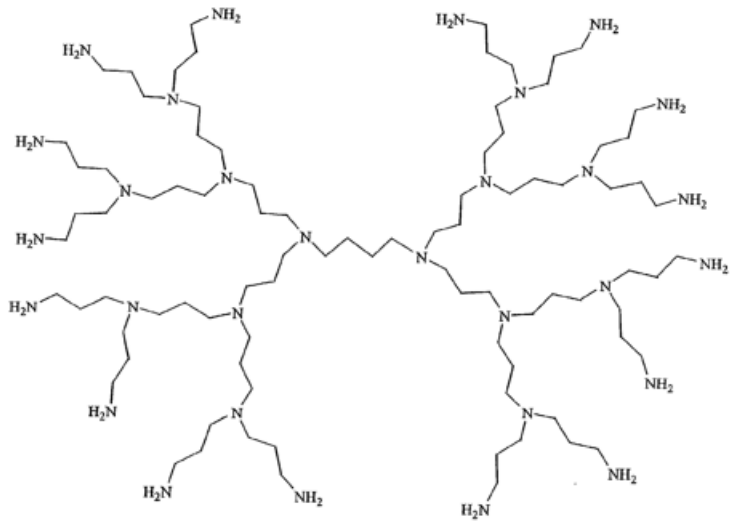

Figure 2.3: Schematic representation of the structure of Polypropylenimine dendrimer Gen 3.0 DAB-Am-16

2.1.1.3 Cholesterol

Cholesterol is a compound that belongs to a group of compounds called steroids. It has a steroid nucleus which consists of four rings, with a hydrocarbon side chain, and a

hydroxyl group attached to the steroid nucleus (Figure 2.4). It is found in the body tissues (and blood plasma) of vertebrate animals. Cholesterol is found in large amounts within the liver, spinal cord, and brain of the body and it gives stability to the membranes of cells (The Merck Index, 2001; Encyclopaedia Britannica, 2016).

In self- assembled bilayer vesicles, it has been found that cholesterol has the capacity to modify the fluidity of the chains in the membrane, thereby causing an increment in the spatial, organisational, arrangement of the structures, thus leading to a reduction in the permeability of the bilayer membrane (Bayindir and Yuksel 2010). Cholesterol was found to increase the encapsulation efficiency of niosomes encapsulating doxorubicin and also to stabilize the membranes of niosomes thereby aiding prolonged release of the entrapped doxorubicin (Uchegbu and Florence 1995). A study carried out by Ritwiset *et al.,* showed that the addition of cholesterol to Span 60® niosomes caused an increase in the bilayer stability. The suggested mechanism of action for this, was that the addition of cholesterol to the Span 60® fluid bilayer caused an increase in the hydrogen bond number of Span60/cholesterol and concurrently reduced the hydrogen bond number of the Span60®/Span60®. Wilkhu *et al.,* deduced that the addition cholesterol into vesicular formulations containing non-ionic surfactants caused the self- assembling of the non-ionic surfactants into bilayer vesicles by amplifying the total critical packing parameter (CPP), of the surfactant mix. Both investigations proved the fact that the inclusion of cholesterol into vesicular formulations, lead to the support of the formation of non-ionic surfactants into more stable bilayered, self-assembled structures, within a shorter period of time (Wilkhu *et al.,* 2014; Ritwiset *et al.,* 2016). Being that stability is an important factor in lipid

vesicular formulations, the inclusion of cholesterol into the formulation of dendrisomes became necessary.

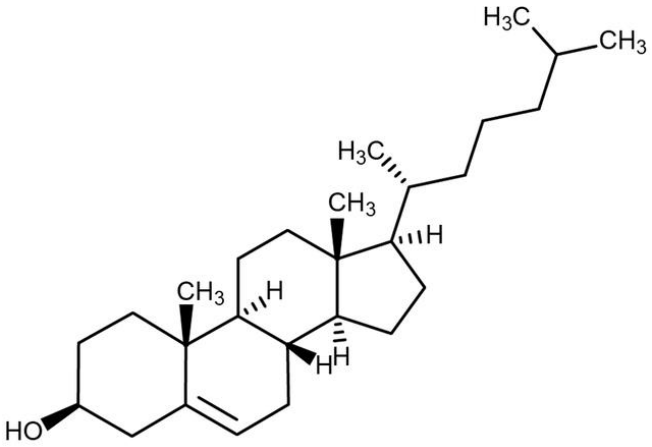

Figure 2.4: Chemical structure of cholesterol

2.1.1.4 Polyoxyethylene-24-cholesteryl ether (Solulan C24)

Solulan™ C-24 lanolin derivative is a complex of ethoxylated cholesterol and ethoxylated vegetable fatty alcohol (Figure 2.5) (Lubrizol, 2005). It is a non-ionic surfactant that has been successfully used in the formulation of niosomes (Dimitrijevic *et al.,* 1997; Dufès *et al.,* 2000; Fu and Dufès, 2014; Fu *et al.,* 2011; Fu *et al.,* Dufès, 2009). Solulan C24 has been shown to cause steric stabilisation in niosomes encapsulating doxorubicin when 10 mole % Solulan C24 replaced 5 mole % dicetylphosphate in the niosome formulations (Uchegbu and Florence 1995). In a study done utilizing Solulan C24 in a formulation for amphotericin B, it was discovered that the Solulan C24 formulation of Amphotericin B was found to be more effective than that of the commercial formulation Fungizone® which is used for the treatment of systemic candidiasis, when tested and compared intraperitoneally.

Although intravenously it was found to be without significant difference, the cause of this was unclear. However, this study still showed that Solulan C24 is a viable non-ionic surfactant that should be investigated further (Tasset and Roland 1992). Another research work done showed that Solulan C24 caused an increase in absorption of encapsulated metformin into monolayers of human intestinal epithelial (Caco-2) cells by penetrating and solubilising the membranes of the cells (Dimitrijevic *et al.*, 2000). As the hybrid dendrisomes entrapping doxorubicin and simultaneously complexed with plasmid encoding TNF-α will need to be efficiently taken up intracellularly in order to exert their therapeutic effect, the characteristic of being a good absorption enhancer (Junyaprasert *et al.*, 2013) made Solulan C24 a key choice in being included in the formulation of some of the dendrisomes.

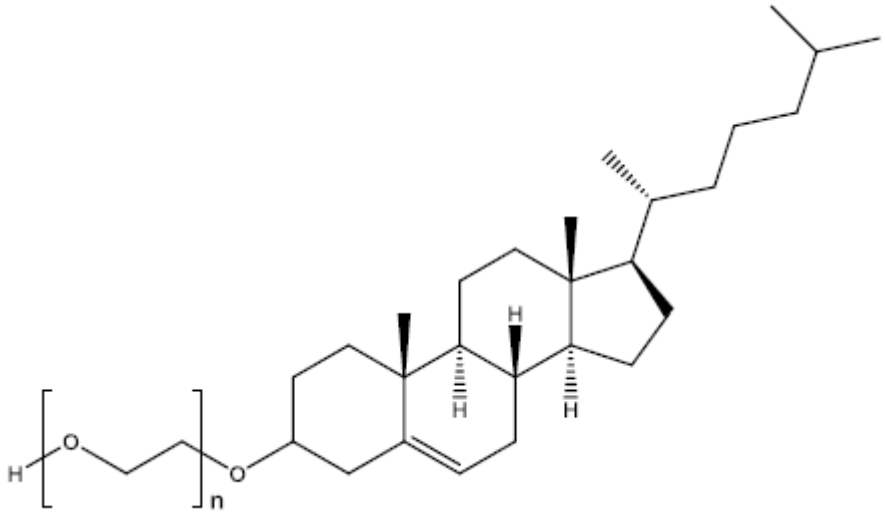

Figure 2.5: Structure of Polyoxyethylene-24-cholesteryl ether (Solulan C24)

2.1.1.5 d-α-tocopheryl polyethylene glycol 1000 succinate (TPGS)

The non-ionic surfactant d-α-tocopheryl polyethylene glycol 1000 succinate (TPGS) is a water-soluble derivative of natural vitamin E, consisting of a lipophilic alkyl tail and hydrophilic polar head portion (Figure 2.6) (Wang *et al.*, 2013). It is formed by the esterification of vitamin E succinate with PEG 1000. Used as an absorption enhancer, TPGS has been successfully used as a solubilizer and emulsifier in lipid based drug delivery formulations (Wempe *et al.*, 2009; Turk *et al.*, 2014). TPGS is known to enhance the cellular uptake of drugs (Zhang *et al.*, 2012). As cellular uptake is a major issue in the effectiveness of chemotherapeutic agents currently available, this feature made it a plausible ingredient in the formulation of some dendrisome formulated in this project. TPGS has been approved by the US FDA as a safe pharmaceutical adjuvant for use in drug formulation. On investigation by Dintaman and Silverman, TPGS was discovered to cause the reversal of P-glycoprotein (P-gp) mediated multidrug resistance and also inhibit P-glycoprotein mediated drug transport (Dintaman and Silverman, 1999). This attribute makes TPGS a very valuable excipient in anticancer drug/ gene formulations as multidrug resistance as mentioned earlier is one of the challenges facing cancer therapy today.

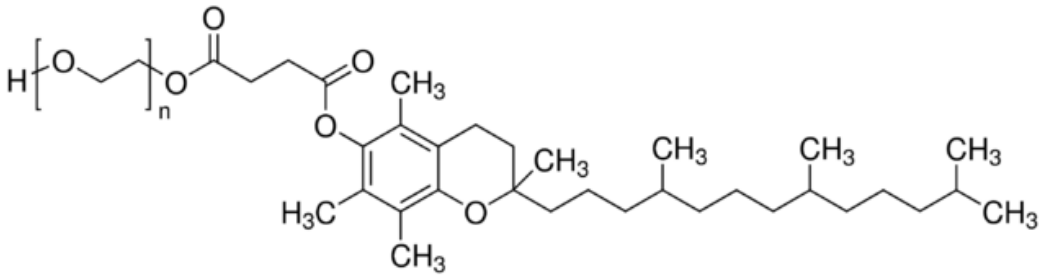

Figure 2.6: Structure of D-α-Tocopherol polyethylene glycol 1000 succinate (TPGS)

2.1.1.6 Dihexadecyl Phosphate (DHP)

Dihexadecyl phosphate (DHP) also commonly known as Dicetyl phosphate (DCP) is a negatively charged lipid (Figure 2.7) that has been extensively used in formulating liposomes and niosomes (Hood & Devoe 2015; Carugo *et al.*, 2016; Sezgin-Bayindir *et al.*, 2015). It is widely used as an additive to vesicle formulations as a negative surface charge inducing agent that prevents aggregation of vesicles (Khan *et al.*, 2016). It also has the capacity to form vesicles in the presence of excess aqueous solvent upon sonication, extrusion or organic solvent injection methods (Feitosa 2008). Investigations into the ability of Polypropylenimine dendrimers to translocate into mixed anionic liposomes consisting of dihexadecyl phosphate, phosphatidylcholine and cholesterol have been successfully carried out (Tsogas *et al.*, 2006). This gave more credence to the feasibility of dendrisomes incorporating DHP being successfully formulated.

A novel synthesized DHP conjugate; Dicetyl phosphate-tetraethylenepentamine (DCP-TEPA) was used to formulate DCP-TEPA-based polycation liposomes (TEPA-PCL). Studies on the capacity of this DCP-TEPA-based polycation liposomes (TEPA-PCL) to carry siRNA showed that TEPA-PCL complexed with cholesterol-conjugated siRNA exhibited a high knockdown efficiency in stable luciferase-transfected B16-F10 murine melanoma cells (Asai *et al.*, 2011). In another study involving non-viral gene delivery, a different DHP conjugate; PEI(1800)-DCP conjugate successfully showed gene transfection when assessed using β- galactosidase transfection assay (Dewa *et al.*, 2004). These gene delivery studies were a good indicator that DHP dendrisomes if successfully formulated might have the potential to carry DNA.

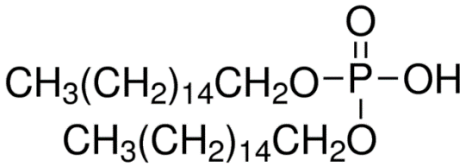

Figure 2.7: Chemical Structure of Dihexadecyl phosphate

2.1.1.7 Cholesterol -PEG- Maleimide5000 (CLS-PEG-Mal, MW 5000)

Cholesterol-poly (ethylene glycol) when conjugated with conjugated maleimide forms a compound called Cholesterol-PEG-maleimide$_{5000}$ (CLS-PEG-Mal$_{5000}$). Cholesterol-PEG-MAL5000 is a lipophilic lipid PEG conjugate that is soluble in water (Figure 2.8) (NANOCS.net 2016). Cholesterol-PEG-MAL5000 has been proposed to be able to formulate targeted liposomes that can increase circulation time for entrapped drugs as well as for non-viral transfection reagents. PEGylation of nanocarriers has also been found to cause increase in circulation of the nanocarriers thereby leading to increased efficacy *in vivo*. The coating of PEGylated liposomal doxorubicin HCl injection (Doxil®) has been proven to cause a reduction in the extent of uptake of the doxorubicin liposomal formulation by eluding recognition and elimination by the RES (Janssen 2015). Another proposed mechanism for this effect has been given as the attachment of the methoxy poly (ethylene glycol) polymers to lipid anchors *in vivo* (Gabizon *et al.,* 2003). Studies done by Qi *et al.,* and Tang *et al.,* displayed that PEGylation PAMAM dendrimer generation 5, caused a significant increase in gene delivery efficacy (Qi *et al.,* 2009; Tang *et al.,* 2012).

Cholesterol-PEG-MAL_{5000} has the capability to form heterobifunctional linkages because of the presence of the maleimide group. On modification of proteins with Traut's reagent (2-Iminothiolane hydrochloride), Traut's reagent causes the introduction of thiol groups into proteins by reacting with the amino groups of the proteins that have been modified, in the case of this project targeting ligand transferrin (Singh *et al.*, 1996; Huang *et al.*, 2007; Yu *et al.*, 2012). The maleimide group on the surface of the dendrisomes reacts with the thiol-containing moieties of targeting ligand transferrin to form heterobifunctional linkages to form stable thioether bonds, at the same time the primary amine groups on the other end react with amine reactive molecules supplied by the dendrimer portion of the dendrisome formulations (Figure 2.9) (Hermanson 2013). This became necessary to ensure that the transferrin ligand could efficiently target transferrin receptors *in vivo*. Based on the above facts and deductions, cholesterol-PEG-mal_{5000} was added to the initial dendrisome formulations successfully formed in this project to increase therapeutic efficacy of the targeted dendrisomes *in vivo*.

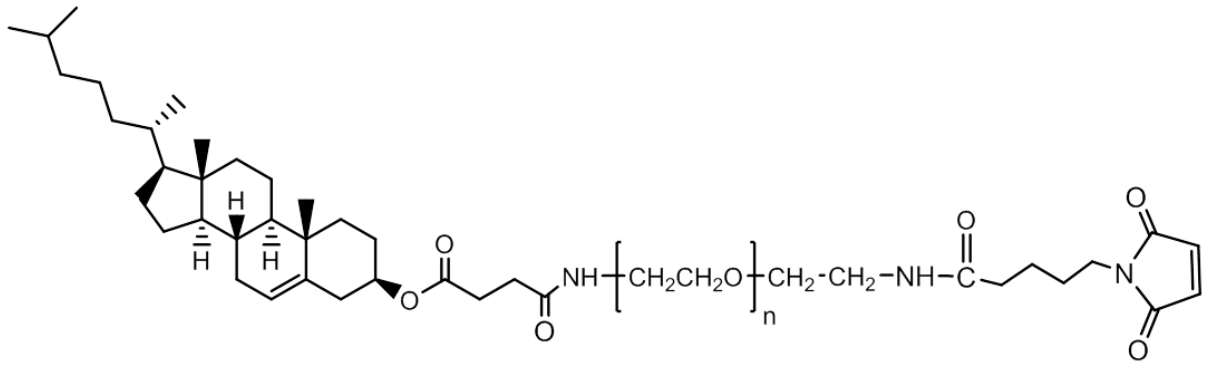

Figure 2.8: Structure of Cholesterol-PEG-Maleimide

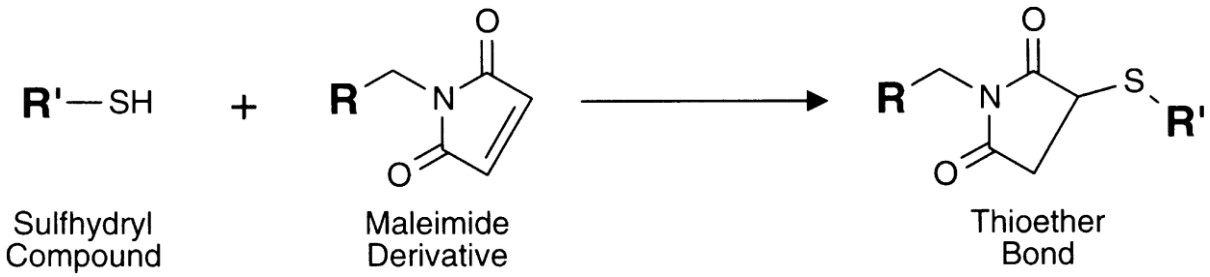

Figure 2.9: Schematic representation of the reaction between a maleimide derivative and a thiolated compound (adapted from Hermanson 2013)

2.1.1.8 Dimethylsuberimidate (DMSI)

Dimethylsuberimidate (DMSI) is a homobifunctional imidoester cross-linker that has been successfully using in conjugating transferrin to nanocarriers via covalent bonding. The imido ester group of dimethylsuberimidate reacts with primary amine groups of nanocarriers to form at pH7-10 imido amides bound (amidine). It has a molecular weight of 273.21 (Interchim 2017). Examples of DMSI crosslinking transferrin with nanocarriers are as follows: transferrin (Tf) conjugation using DMSI to doxorubicin loaded palmitoylated glycol chitosan (GCP) vesicles (Dufès *et al.,* 2004), generation 3-diaminobutyric polypropylenimine dendrimer (DAB-Am-16) (Koppu *et al.,* 2010; Lemarié *et al.,* 2012 and Al Robaian *et al.,* 2014), and vesicles entrapping Tocotrienol (Fu *et al.,* 2014). This informed its choice as the first crosslinker used.

2.1.2 Dynamic light scattering (DLS) for size measurement

Dynamic light scattering (DLS) also known as photon correlation spectroscopy (PCS) as well as quasi-elastic light scattering (QELS), is a non-invasive analytical technique commonly used in measuring the size of particles and molecules. This technique is measures the diffusion particles undergoing Brownian motion. Brownian motion simply refers to the random motion of particles suspended in a fluid (a liquid or a gas) resulting from their collision with the quick atoms or molecules in a gas or liquid. The measurements obtained are then translated by the machine into size and size distribution measurements. The size is given as Stoke's radius or hydrodynamic radius of the particle being measured. This size measurements obtained are extrapolated by the DLS machine based on the Stokes-Einstein equation seen in the equation below (equation 2.1) (Brar and Verma 2011; Minton 2016). The measurement of the size of the particles in a sample is very important as this is the first analytical step taken to ascertain if a nano particle has been formed.

Equation 2.1:

$$D = \frac{k_B T}{6\pi\eta r}$$

Where D = diffusion coefficient constant, k_B = Boltzmann's constant, T = absolute temperature, η = viscosity of the suspending medium, and r = radius of a spherical particle.

The DLS technique measures the size of the particles as well as their polydispersity index. Poly dispersity (*Đ*) now called dispersity in IUPAC classification, refers to a measure of the width of molecular weight distributions (MWD) (Rogošić *et al.*, 1996). It has also been defined as the measure of dispersion or spread as well as the ratio of the weight-average (Mw) and number-average (Mn) molecular weights of a test sample suspended in medium (Gilbert *et al.,* 2009; Gentekos *et al.,* 2016). It provides information on the non-uniformity of the size distribution of the particles being measured. Polydispersity values that are less than -0.05 will hardly be seen while values larger than 0.7 are an indication that the sample being measured has a size distribution that is too broad (Malvern, 2011). A low polydispersity index is preferred in the formulation of targeted drug and/or gene moieties because it ensures a more uniform cellular uptake.

Currently the Non-Invasive Back Scatter technology (NIBS) is the technology being used in the Malvern Zetasizer Nano ZS, instead of the 90 degree scattering optics technology due to increased sensitivity it provides in the readings obtained from small and highly diluted samples. DLS for this project was used to measure the sizes of the dendrisomes formulated with a Zetasizer Nano ZS.

2.1.3 Phase analysis light scattering (PALS) for measuring zeta potential

Phase analysis light scattering (PALS) is an analytical tool used for the measurement of electrophoretic motilities which are interpreted as zeta potential (surface charge of particles) (McNeil-Watson *et al.,* 1998). It is based on the principles of the

conventional laser Doppler electrophoresis instrument alongside a digital phase analysis system. In the machine, an electric field is sent through the dispersion of particles being measured, thus generating an electric field that causes the particles to scatter beams of light thereby causing the particles to move at a velocity that is proportional to the surface charge that they carry (Miller *et al.,* 1991). The frequency of the scattered light by the Doppler Effect and mixing with the light beam causes a shift which produces a positive or negative frequency shift depending on the surface charge of the particles being measured. Since the direction of the electric field that was sent through the instrument is a known value, the charge, magnitude as well as scale of the electrophoretic mobility is then interpreted by the machine. Thus, the laser interferometric technique M3-PALS (Phase analysis Light Scattering) of the Zetasizer Nano ZS Malvern translates the velocity of the particles into the zeta potential of the sample being tested.

2.1.4 Transmission Electron Microscopy (TEM)

Transmission Electron Microscopy is an investigative microscopy technique used in characterising the structure and morphology of nanostructures through visualization in pictures. It has the added capacity of measuring and showing the various dimensions of the particles in the sample (Harris 2015). The Transmission Electron Microscope is an advanced microscope that uses the interaction of the high energy beam of electrons that it produces, and the electrons of the sample being visualised to produce pictures showing the surface morphology and shape of a stained sample. A TEM microscope consists of three major components: an electron gun and the condenser system,

secondly the image-producing system and thirdly the image-recording system (Joy *et al.*, 2016).

The specimens to be investigated must be prepared by coating them with a transparent thin foil that is resistant to damage by the electron beam. TEM images are produced by a fixed transmitted beam of electrons being transmitted through the thin dried specimen (Michler 2008). Emission of electrons in a TEM microscope is initiated from a thermionic or a field-emission source. These emitted electrons are then accelerated in the gun by a high-voltage generator. The electron beam is then formed with the aid of a series of lenses; condenser lenses and sometimes a condenser mini-lens, a condenser lens aperture, a condenser lens stigmator and beam tilt. The electron beam then passes through the objective lens and strikes the specimen being investigated. After passing through the specimen, the electrons produce an image through the action of the objective lens and an objective aperture in the back focal plane of the lens. Focussing of the image is done by an objective stigmator and enlarged by an image-forming system consisting of a series of intermediate and projector lenses and alignment units. The final highly magnified image becomes visible on the viewing screen or is captured by a camera or an electron-sensitive film (Michler 2008).

2.1.5 Fluorescence spectrophotometry

Fluorescence spectroscopy is a highly sensitive, analytical technique that is used in identifying, confirming the existence and studying the behaviour of coloured

compounds that have the ability to emit light when excited by light or other electromagnetic radiation in a sample. This light produced is called fluorescence. (Lakowicz 2011; Sauer *et al.,* 2011). There are three basic components of a fluorescence spectrophotometer: a light source that provides incident radiation, a sample holder and a detector that is capable of precise interpretation of the emission signal generated and present it in a readable form. However for more complex fluorescence spectrophotometers, monochromators are included in the instrument for the selection of the excitation wavelength and the emission wavelength of the incident light for the sample being investigated (PerkinElmer 2000). When a sample is excited by a light source such as electromagnetic light, the electrons of the sample in absorb the energy; the excited electrons on returning to the ground-state orbital thereby leading to the emission of a photon which produces the emission spectra detected. The emission can be measured as wavelength with the unit as nanometres, and wavenumbers with units of cm^{-1}. Some coloured compounds are also known fluorophores and fluorescent probes produce fluorescence on excitation by incident light. The commonly known stable and bright fluorophores absorb and emit light within the range of wavelength 300 and 700 nm (Lakowicz, 2011).

2.1.6 Plasmid DNA preparation process

The rigorous processes for plasmid DNA preparation and purification are required because the quality of the plasmid produced for gene therapy needs to high, free from bacterial proteins, toxins, genomic DNA or RNA (Prazeres *et al.,* 1999). The process of plasmid DNA preparation involves six main stages: fermentation of the host microbe in a growth medium, harvesting the bacteria cells through centrifugation or

microfiltration, cell lysis through mechanical or chemical methods, clarification and concentration through microfiltration or ultrafiltration, purification is via size exclusion methodologies, after which elution is done (Ferreira *et al.,* 2000; Sun *et al.,* 2013).

Plasmids for gene therapy are usually formed in a bacteria culture of *Escherichia coli* with the bacteria cells as the host via fermentation (Prazeres *et al.,* 1998). After the required period of incubation, the host cells are harvested through centrifugation of the culture medium in which they were grown. There are different kits currently available for the preparation of plasmid DNA from the harvested bacteria cells. The QIAGEN Giga preparation kit was used for this project. It has the advantage of providing a fast, simple, and economical plasmid preparation method for use in laboratory experiments (Dhaliwal 2013). The process of cell lysis is mainly done through alkaline lysis using sodium dodecyl sulfate (SDS) in order to release the plasmid DNA from the bacteria cytoplasm (Birnboim and Doly, 1979). Purification for removal of RNA impurities from the DNA solution is done via size exclusion methodologies (B. Sun et al. 2013). Elution of the plasmid DNA is done using slightly alkaline buffer. DNA precipitation is done using isopropanol (Caramelo-Nunes *et al.,* 2012; Dhaliwal 2013).

2.1.7 DNA Complexation Experiments

2.1.7.1 Gel Retardation assay

Gel retardation assay also known as Electrophoretic Mobility Shift Assay (EMSA) or band shift assay (Lane *et al.,* 1992), is an investigative analysis that is based on the interactions between nucleic acids and proteins. It analyses the movement of free or

complexed DNA molecules on a non-denaturing polyacrylamide gel matrix. Previous studies using DAB-Am-16 dendrimer complexed with DNA as well as free DNA have been carried out and the results obtained correlated with the PicoGreen® assay which is also a DNA complexation assay that shows the degree of DNA complexation as well as its stability (Aldawsari *et al.,* 2011). Gel retardation studies in this project were used to visualise the degree of complexation of DNA with the dendrisomes formulated through photographs obtained using Ultraviolet (UV) light (Lane *et al.,* 1992; Scott *et al.,* 1994; Hellman and Fried 2007; Alves and Cunha 2012). The DNA condensation capability of the dendrisomplexes formulated in this project were investigated using agarose gel retardation assay.

2.7.1.2 PicoGreen® assay

PicoGreen® is a fluorescent probe that increases in fluorescence emission when it interacts with double stranded DNA. The purpose of the PicoGreen® intercalation assay was to show the degree of complexation that had occurred between plasmid DNA and dendrisomes and the stability of the dendrisomplexes formed over a 24-hour period. This complexation was detected by the amount of fluorescence produced by PicoGreen® molecules via spectrofluorimetry. If there was successful complexation of the DNA to the dendrisomes, there would be decreased fluorescence when compared with the fluorescence obtained with the free double stranded DNA samples (Dragan *et al.,* 2010). If there was no complexation of the DNA to the nanocarriers, the free double-stranded DNA would be able to interact with PicoGreen®, leading to high fluorescence (Koppu *et al.,* 2010).

2.1.8 Aims and Objectives

The aim of this chapter is to formulate dendrisomes and characterise the dendrisomes formed. Various techniques will be used to ascertain the successful formation of these structures. Size and zeta potential measurements will first be carried out to ensure that the structures obtained are within the size range and of the surface charge desired. Sizes below 500nm with low polydispersity are required due to the need for the dendrisomes to be able to passively enter the cancer cell vasculature and not be destroyed by macrophages (Torchilin, 2010 ; Etheridge *et al.*, 2013). Secondly, TEM microscopy will be carried out to visualise the morphology of the dendrisomes formed. Thirdly the ability and degree of the dendrisomes formed to condense DNA will be tested to ensure that the dendrisomes have the capability to carry therapeutic genes. Fourthly the capacity of the dendrisomes formed to entrap as well as release the anticancer doxorubicin, will also be tested. The dendrisomes to be formed are being postulated to be able to carry drugs and gene and target transferrin receptors. Hence full characterization is required to ensure that the dendrisomes formed have these capabilities. Once successfully formed, their efficacy *in vitro* will then be tested in the proceeding chapter.

2.2 Material and Methods

Table 2.1 Materials and reagents

Materials/reagents	Supplier/source
Ampicillin	Sigma Aldrich (Poole, UK)
Expression plasmid encoding β-galactosidase (pCMVsport β-galactosidase)	Invitrogen, ThermoFisher Scientific (Paisley, UK)
DAB-Am-16, Polypropylenimine hexadecaamine Dendrimer, Generation 3.0	Sigma Aldrich (Poole, UK)
Doxorubicin	Enzo (Colorado, US)
L-α-Phosphatidylethanolamine, dioleoyl (DOPE)	Sigma-Aldrich (Poole, UK)
Lysogeny broth (L-broth)	Sigma-Aldrich (Poole, UK)
Human holo-transferrin	Sigma-Aldrich (Poole, UK)
Isopropanol	Sigma-Aldrich, UK
NanoVan	Nanoprobes, (New York, USA)
Phosphate buffered saline (PBS) tablets	Sigma Aldrich (Poole, UK)
Quanti-iT™ PicoGreen® dsDNA reagent	Invitrogen, ThermoFisher Scientific (Paisley, UK)
Cholesteryl poly-24-oxyethylene ether (Solulan C24)	Ansted, West Virginia, USA.
Sorbitan monostearate (Span 60®)	Sigma Aldrich, (Poole, UK)
D-α-tocopheryl polyethylene glycol 1000 succinate (TPGS)	Eastman Chemical Company (Tennessee, USA)

Table 2.2: Transition Temperature of lipids

Lipid	Transition Temperature (T_m)
Sorbitan monostearate (Span 60®)	56–58 °C (Kumar and Rajeshwarrao, 2011)
Cholesterol	147-149 °C (Wilkhu *et al.*,2014)
Solulan C24	43-45 °C (Uchegbu and Schatzlein, 2006)
d-α-tocopheryl polyethylene glycol 1000 succinate (TPGS)	37-41 °C (pmcisochem, 2008)
Dihexadecyl phosphate (DHP)	74-75 °C (Sigma, 2016)

Table 2.3 The Composition of dendrisome formulations

Formulation	Span 60 (mg)	DAB-Am-16 (mg)	Chol (mg)	Solulan C24 (mg)	TPGS (mg)	DOPE (mg)	DHP (mg)	Dox 10mg/mL (µL)	Tf (mg)	DMSI (mg)	CLS-PEG-Mal_{5000} (mg)
DEN-SOL	65	50	58	54	-	-	-	-	-	-	-
DEN-SOL-Tf	65	50	58	54	-	-	-	-	12	-	-
DEN-SOL-DOX-C	65	50	58	54	-	-	-	300	-	-	-
DEN-SOL- DOX-Tf	65	50	58	54	-	-	-	300	12	24	-
DSOLm Control	65	50	48	54	-	-	-	-	-	-	10
DSOLm Tf	65	50	48	54	-	-	-	-	12	-	10
DSOLmDox Control	65	50	48	54	-	-	-	-	-	-	10
DSOLmDox Tf	65	50	48	54	-	-	-	300	12	-	10
DEN-TPGS1	65	50	58	-	54	-	-	-	-		-
DEN-TPGS2	65	50	58	-	57	6	-	-	-		-
DTPGSmd control	65	50	48	-	57	6	-	-	-	-	10
DTPGSmdTf	65	50	48	-	57	6	-	-	12	-	10
DTPGSmdDOX Control	65	50	48	-	57	6	-	300	-	-	10
DTPGSmdDOXTf	65	50	48	-	57	6	-	300	12	-	10
DEN-DHP	65	50	58	-	-	-	18	-	-	-	-

2.2.1 Preparation of Solulan C24 dendrisomes

Solulan C24 dendrisomes (DEN-SOL) were formed by probe sonication (Fu *et al.,* 2009) which is a modification of a method used in formulating niosomes (Dufès *et al.,* 2000). Solulan 24, Span 60®, cholesterol and DAB-Am-16 were used at molar ratio (4:5:5:1). Solulan 24 (54 mg), Span 60® (65mg), cholesterol (58mg), DAB-Am-16 (50 mg), in 2 mL PBS buffer was stirred for 1 h at 60 °C. This was followed by probe sonication (Sonics Vibracell™, Newton, CT) for a total of 4 min, with 2 min interval between 2 min probe sonication sessions. The instrument was set at 75% of its maximal capacity. This process formed DEN-SOL dendrisomes.

2.2.2 Preparation of Transferrin-bearing Solulan C24 dendrisomes

Transferrin-bearing Solulan C24 (DEN-SOL-Tf) dendrisomes were prepared by mixing the with cross-linker dimethylsuberimidate (DMSI) (24 mg) and holo-transferrin (12 mg) in 0.2 M triethanolamine buffer (2 mL) using a previously described method (Dufès *et al.,* 2000). The reaction occurred for 2 h at room temperature, under constant magnetic stirring.

2.2.3 Formulation of Solulan C24 dendrisomes encapsulating doxorubicin

Tf-bearing DEN-SOL and control DEN-SOL dendrisomes encapsulating doxorubicin (DEN-SOL-DOX-Tf and DEN-SOL-DOX-C) were prepared using a modification of an earlier described method (Dufès *et al.,* 2000). Formulation of the dendrisomes for the encapsulation of doxorubicin were done using Solulan 24 (54 mg), Span 60® (65mg), cholesterol (58mg), DAB-Am-16 (50 mg), in 1.7 mL PBS buffer at pH 7.4 after which the mixture was vortexed and heated with a magnetic stirrer for 1 h at

60 °C. Doxorubicin solution (300 µL) at a concentration of 10 mg/mL was added to the mixture, which was then vortexed again. This was followed by probe sonication (Sonics Vibracell™, Newton, CT) for a total of 4 min, with 2 min interval between 2 min probe sonication sessions. The instrument was set at 75% of its maximal capacity. The formulation of Tf- bearing DEN-SOL dendrisomes encapsulating doxorubicin (DEN-SOL-DOX-Tf) was done by first making control DEN-SOL dendrisomes encapsulating doxorubicin (DEN-SOL-DOX-C) as described above and then conjugating the control (DEN-SOL-DOX-C) dendrisomes (DEN-SOL-DOX) with transferrin as earlier described in section 2.2.2. (Figure 2.10).

2.2.4 Preparation of D-α-tocopheryl polyethylene glycol 1000 succinate (TPGS) dendrisomes

DEN-TPGS1 dendrisomes were prepared following the same procedure as DEN-SOL dendrisomes, but the component Solulan 24 was substituted with TPGS (54 mg). The formulation mix of DEN-TPGS1 was therefore: TPGS, Span 60®, cholesterol and DAB-Am-16 were used at molar ratio (1:5:5:1). TPGS (54 mg), Span 60® (65mg), cholesterol (58mg), DAB-Am-16 (50 mg), in 2 mL PBS buffer was stirred for 1 h at 60 °C. This was followed by probe sonication (Sonics Vibracell™, Newton, CT) for a total of 4 min, with 2 min interval between 2 min probe sonication sessions. The instrument was set at 75% of its maximal capacity. This process formed DEN-TPGS1 dendrisomes. DEN-TPGS2 dendrisomes were also prepared using probe sonication, there was a modification in the amount of TPGS used (57 mg) and in the method of preparation. DEN-TPGS2 dendrisomes were formulated with TPGS, Span 60®, cholesterol, L-α-Phosphatidylethanolamine, dioleoyl (DOPE) and DAB-Am-16 at molar ratio (5:19:19:1:4). TPGS (57 mg) was added to 2 mL distilled water and

allowed to dissolve for 5minutes. The resulting mixture was then probe sonicated (Sonics Vibracell™, Newton, CT) for 2 minutes. The dispersion formed was then added to the glass container containing Span® 60 (65 mg), cholesterol (58 mg), L-α-Phosphatidylethanolamine, dioleoyl (DOPE) (6 mg) and DAB-Am-16 (50 mg). The mixture was slightly vortexed and stirred on a magnetic stirrer for 1 hour at 65°C. This was followed by probe sonication (Sonics Vibracell™, Newton, CT) for a total of 4 min, with 2 min interval between 2 min probe sonication sessions. The instrument was set at 75% of its maximal capacity. This process formed DEN-TPGS2 dendrisomes (Figure 2.11).

2.2.5 Purification of Solulan C24 and TPGS dendrisomes

Purification (and concurrent removal of unbound transferrin for the transferrin-bearing Solulan dendrisomes) was done using a size exclusion chromatography technique with Sephadex G50. This was immediately followed by concentration of the Solulan C24 dendrisomes with dialysis technique, using a dialysis tubing with molecular weight cut-off of 3500 Da ThermoFisher Scientific (Paisley, UK) immersed in polyethylene glycol 8000 (PEG 8000) powder. Whenever the PEG 8000 powder surrounding the dialysis tubing containing the dendrisomes became very damp, the PEG 8000 powder surrounding the dialysis tube was replaced with dry PEG 8000 powder. This process was repeated until the dendrisomes dispersion was approximately 2 cm in length in the dialysis tubing (Figure 2.12) (Dufès *et al.,* 2004). The concentrated dispersion was collected and made up to 2 mL with PBS in a 10 mL glass bottle and stored in the store at 2-8°C. The same process was repeated for TPGS dendrisomes (Figure 2.10, 2.11 and 2.12).

2.2.5.1 Purification of Solulan dendrisomes encapsulating doxorubicin

Purification and concurrent removal (also removal of excess doxorubicin, unbound transferrin of the transferrin-bearing Solulan dendrisomes) was done using a size exclusion chromatography technique with Sephadex G50. This was immediately followed by concentration of the dendrisomes with dialysis technique, using a dialysis tubing with molecular weight cut-off of 3500 Da ThermoFisher Scientific (Paisley, UK) immersed in polyethylene glycol 8000 (PEG 8000) powder. Whenever the PEG 8000 powder surrounding the dialysis tubing containing the dendrisomes became very damp, the PEG 8000 powder surrounding the dialysis tube was replaced with dry PEG 8000 powder. This process was repeated until the dendrisomes dispersion was approximately 2 cm in length in the dialysis tubing (Dufès *et al.,* 2004). The concentrated dispersion was collected and made up to 2 mL with PBS in a glass vial and stored in the store at 2-8°C (Figure 2.10).

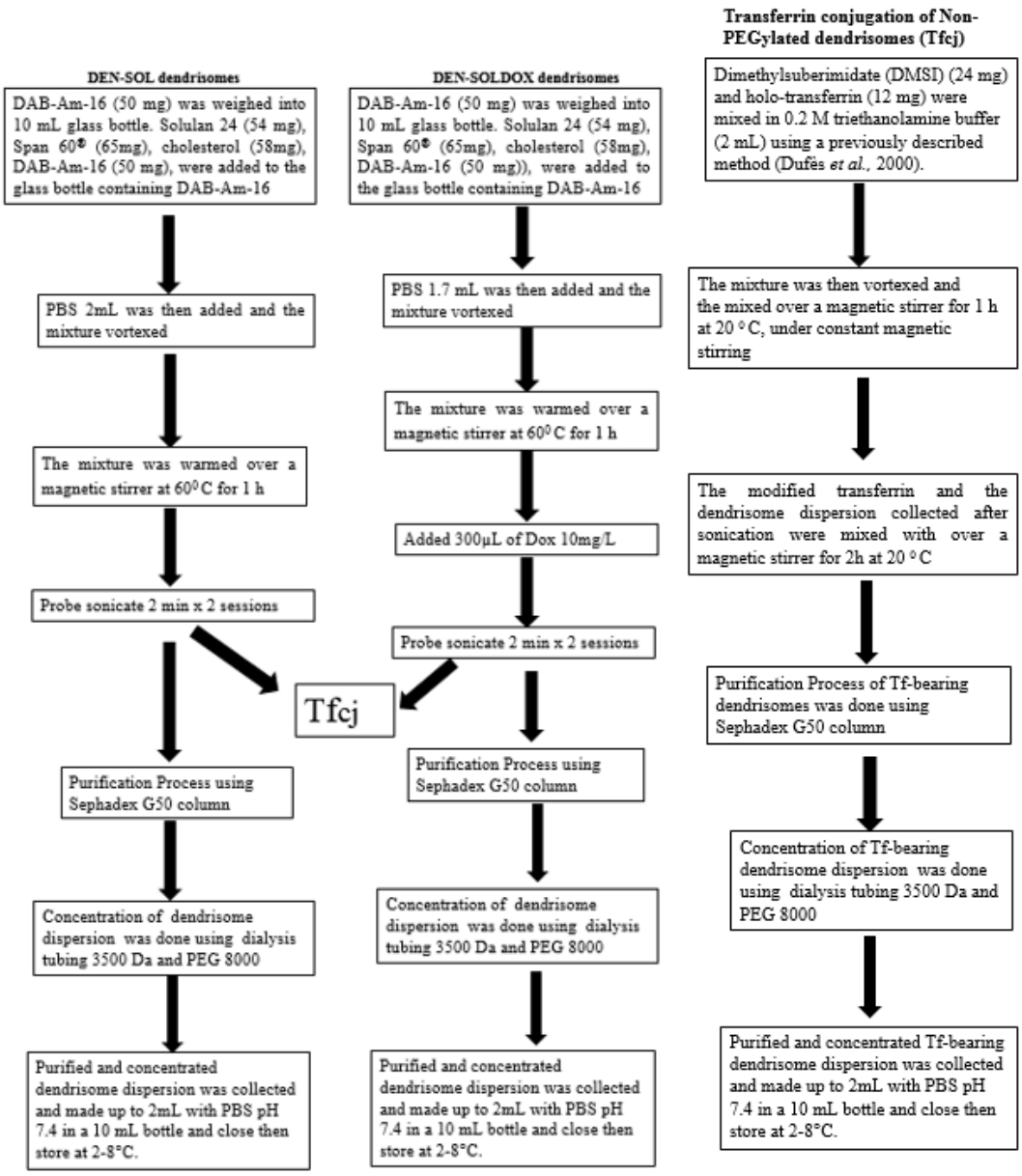

Tfcj: Transferrin conjugation process of non-PEGylated dendrisomes

Figure 2.10: Work Flow Scheme of formulation of Solulan C24 (DEN-SOL) dendrisomes.

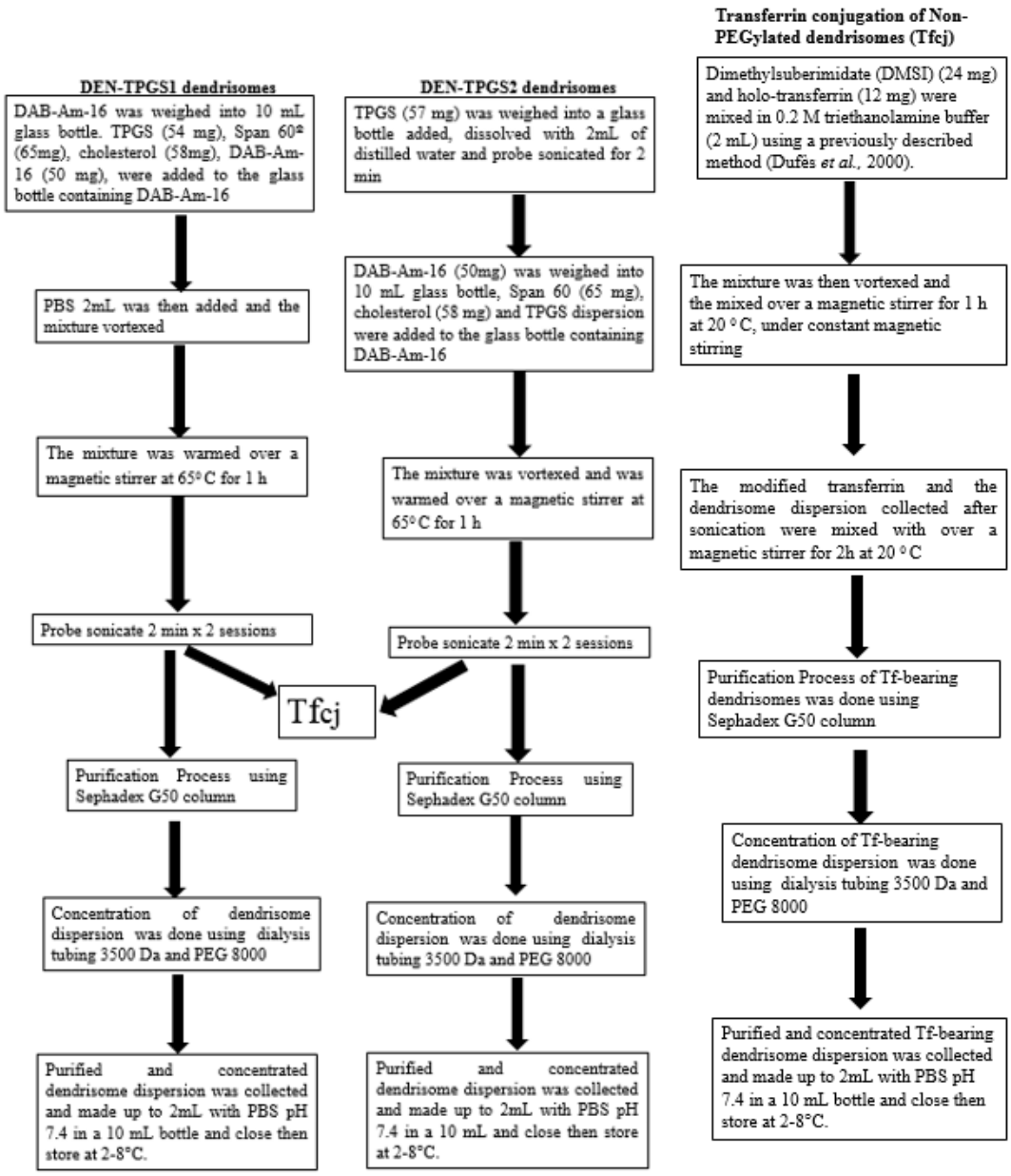

Tfcj: Transferrin conjugation process of non-PEGylated dendrisomes

Figure 2.11: Work Flow Scheme of formulation of TPGS (DEN-TPGS) dendrisomes.

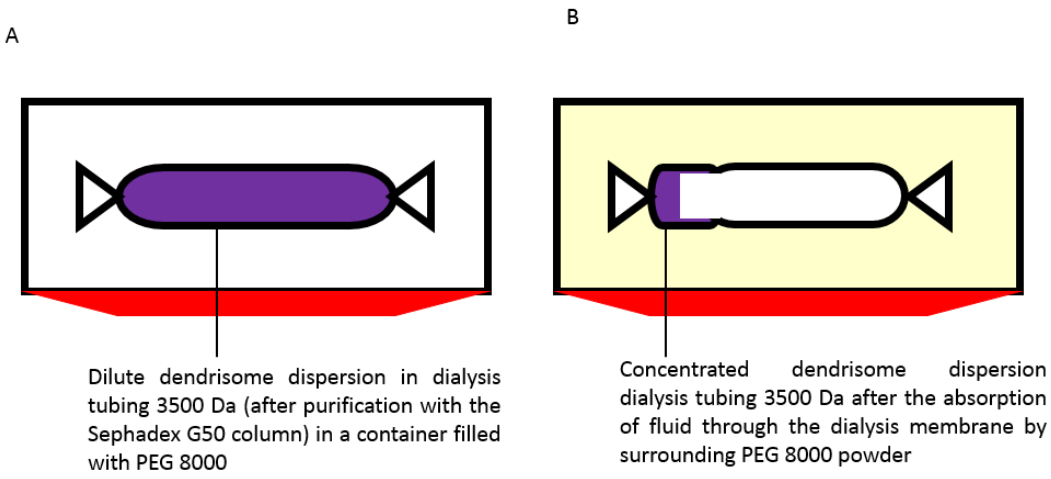

Figure 2.12: Schematic representation of the concentration of the dendrisome dispersions purified via Sephadex 50 column. After purification, the dilute dispersion is transferred into a dialysis 3500 Da and then placed in a container prefilled with PEG 8000 (A). Concentration of the dispersion takes place via the absorption through the dialysis membrane (B).

2.2.6 Preparation of Dihexadecyl phosphate (DHP) dendrisomes

Several formulations of Dihexadecyl phosphate dendrisomes (DEN-DHP) were attempted using probe sonication as with a modification of a method used to make niosomes (Fu *et al.*, 2009; Dufès *et al.*, 2000). DEN-DHP dendrisomes formulations were formulated with either (8 mg) or (18 mg) of Dihexadecyl phosphate, (65mg), cholesterol (48mg), cholesterol-PEG_{5000}- maleimide (10 mg) and DAB-Am-16 (50 mg), in 2 mL PBS buffer and the mixture was mixed over a magnetic stirrer for 1 h at 60 °C. This was followed by probe sonication (Sonics Vibracell™, Newton, CT) for a total of 6 min, with 2 min interval between 2 min probe sonication sessions. The instrument was set at 75% of its maximal capacity. Purification of the formulation was done using Vivaspin 6 centrifugal concentrator tubes with a molecular weight cut off of 100,000 Daltons in a swing bucket centrifuge (Beckman coulter, UK) at 7500 rpm

(6,600 x g) at 20°C for 15 minutes. The concentrated dispersion was then collected and made up to 4 mL with pH 7.4 PBS and stored in the store at 2-8°C.

2.2.7 Preparation of PEGylated Solulan C24 dendrisomes

PEGylated Solulan C24 (DSOLm) dendrisomes were formed using probe sonication as with a modification of a method used to make niosomes (Fu *et al.,* 2009; Dufès *et al.,* 2000). PEGylated Solulan C24 dendrisomes were formulated by probe sonication through a modification of a method previously used in formulating vesicles (Dufès *et al.,* 2000; Fu *et al.,* 2011). Solulan 24, Span 60®, cholesterol, cholesterol-PEG-maleimide5000, DAB-Am-16 were used at molar ratio (65:75:60:1:15). Solulan 24 (54 mg), Span 60 (65mg), cholesterol (48mg), cholesterol-PEG_{5000}- maleimide (10 mg) and DAB-Am-16 (50 mg), in 2 mL PBS pH 7.4 buffer were mixed over a magnetic stirrer for 1 h at 60 °C. This was followed by probe sonication Sonics Vibracell™ (Newton, CT) for a total of 6 min, with 2 min interval between 3 min probe sonication sessions. The instrument was set at 75% of its maximal capacity. The PEGylated Solulan C24 control dendrisomes were thus formed.

2.2.8 Preparation of Transferrin- bearing PEGylated Solulan C24 dendrisomes

PEGylated Tf-bearing Solulan C24 dendrisomes (DSOLmTf) were prepared Transferrin- bearing PEGylated Solulan C24 dendrisomes were prepared by cross-linking transferrin (12 mg) with the control dendrisomes. This was done by first modifying the transferrin with Traut's reagent. Transferrin (12 mg) was first dissolved in 1.2 mL sodium phosphate buffer containing sodium chloride (50 mM sodium

phosphate buffer, 150 mM NaCl, pH 8.0) to make a 10 mg/mL solution. The Traut's reagent (106 µL of stock solution 2mg/mL in distilled water) was added to the transferrin solution (1.2 mL, 10mg/mL), to make it ten-fold molar excess of the molarity of transferrin. The reaction was then carried out for 1 h at 20^{o}C , under constant magnetic stirring (Hermanson 2013b).

Purification of the thiolated transferrin from unreacted Traut's reagent was then done through centrifugation in Vivaspin 6 centrifugal concentrator tubes (Sartorius® Göttingen, Germany) with molecular weight cut off of 5000 Daltons, at 9,500 rpm (10,500 x g) at 20°C for 15 minutes. The transferrin conjugation step was done immediately after purifying the thiolated transferrin to prevent the recyclization of the free thiol in the thiolated transferrin which could lead to a simultaneous decrease in thiol availability for linking with the maleimide group in the control dendrisomes. Transferrin conjugation (12 mg) with control dendrisomes (2 mL) was done by mixing over a magnetic stirrer for 2 h at 20^{o}C.

Purification of the transferrin-bearing (Tf-dendrisomes) and control PEGylated Solulan C24 dendrisomes were then carried out using Vivaspin 6 centrifugal concentrator tubes (Sartorius® Göttingen, Germany) with a molecular weight cut off of 100,000 Daltons in a swing bucket centrifuge (HermLe® Z323K Wehingen, Germany) at 7,500 rpm (6,600 x g) for 15 minutes. The concentrated dispersions were individually collected, made up to 4 mL with PBS pH 7.4 and stored in the store at 2-8°C (Figure 2.13).

2.2.9 Formulation of PEGylated Solulan C24 dendrisomes encapsulating doxorubicin

Tf-bearing DSOLm (DSOLmDoxTf) and control (DSOLmDoxC) dendrisomes encapsulating doxorubicin were prepared using a modification of an earlier method used to formulate niosomes (Dufès *et al.,* 2000). Formulation of the dendrisomes for the encapsulation of doxorubicin were achieved by mixing Solulan C24 (54 mg), Span 60® (65 mg), cholesterol (48 mg), cholesterol-PEG- maleimide5000 (10 mg), DAB-Am-16 (50 mg) at molar ratio (65:75:60:1:15) in 1.7 mL PBS buffer were mixed over a magnetic stirrer for 1 h at 60 °C. The mixture was vortexed and heated with a magnetic stirrer for 1 h at 60 °C. Doxorubicin (3mg) was added by (300 µL of doxorubicin 10 mg/mL solution) was added to the mixture, which was then vortexed again. This was followed by probe sonication Sonics Vibracell™ (Newton, CT) for a total of 6 min, with 2 min interval between 2 min probe sonication sessions. The instrument was set at 75% of its maximal capacity. The formulation of Tf-bearing dendrisomes encapsulating doxorubicin was done by first making control dendrisomes as described above. Transferrin Conjugation of the control dendrisomes encapsulating doxorubicin was then carried out as described in section 2.28 (Figure 2.13).

2.2.9.1 Purification of PEGylated Solulan C24 dendrisomes encapsulating doxorubicin

The removal of excess doxorubicin, (as well as any unbound transferrin for transferrin-bearing dendrisomes) concurrently with the purification and concentration of the transferrin-bearing (Tf-dendrisomes) and control PEGylated Solulan C24 dendrisomes encapsulating doxorubicin were then carried out using Vivaspin 6 centrifugal concentrator tubes (Sartorius® Göttingen, Germany) with a molecular weight cut off

of 100,000 Daltons in a swing bucket centrifuge (HermLe® Z323K Wehingen, Germany) at 7,500 rpm (6,600 x g) for 15 minutes. The concentrated dispersions were individually collected, made up to 4 mL with PBS pH 7.4 and stored in the store at 2-8°C (Figure 2.13).

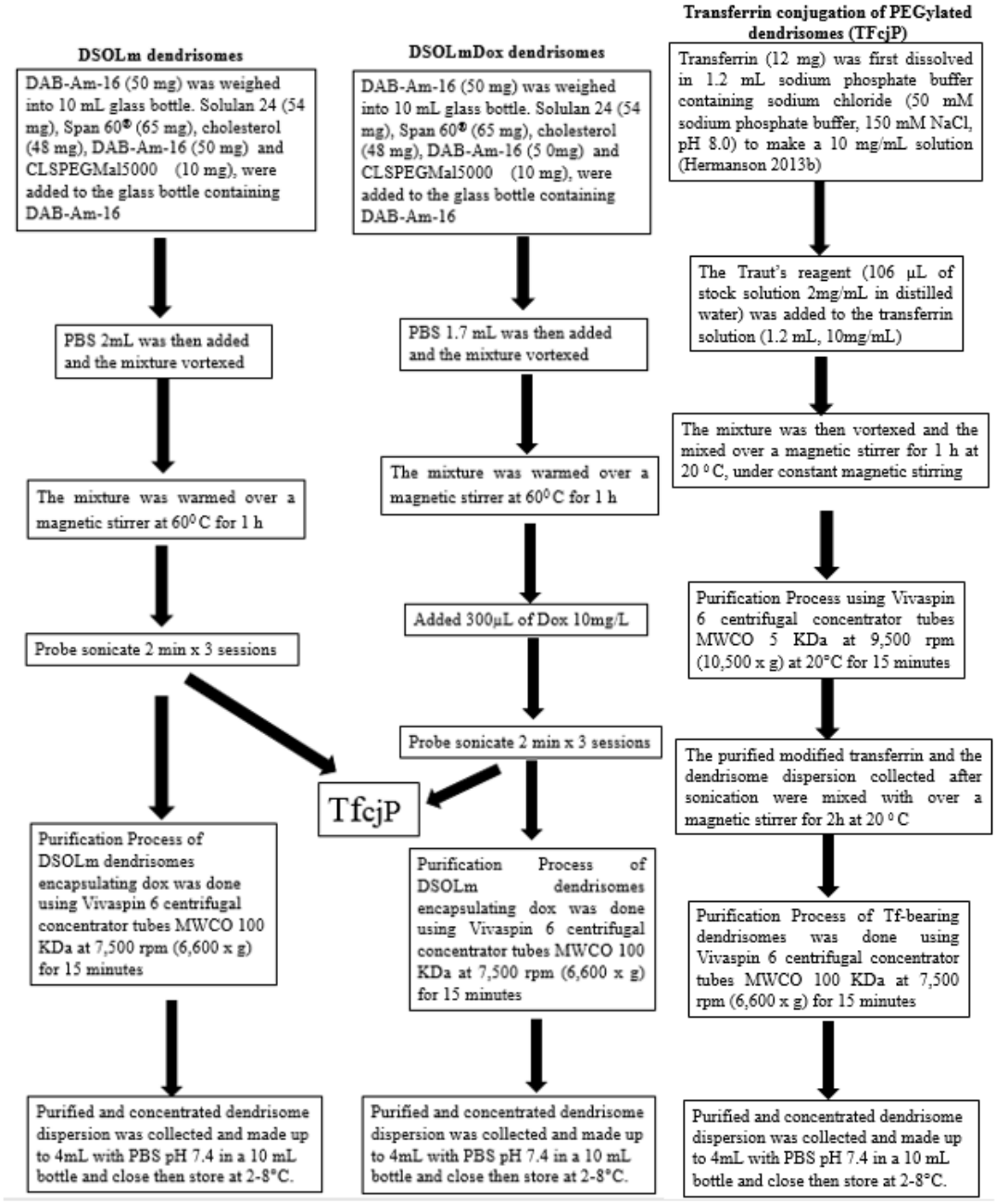

TfcjP: Transferrin conjugation process of PEGylated dendrisomes

Figure 2.13: Work Flow of Formulation of PEGylated Solulan C24 (DSOLm) dendrisomes.

2.2.10 Preparation of PEGylated D-α-tocopheryl polyethylene glycol 1000 succinate (TPGS) dendrisomes

PEGylated TPGS dendrisomes (DTPGSmd) were formed using probe sonication with a modification of a method used to make niosomes (Fu *et al.*, 2009). DTPGSmd dendrisomes were formulated with TPGS, Span 60®, cholesterol, cholesterol-PEG-maleimide, L-α-Phosphatidylethanolamine, dioleoyl (DOPE) and DAB-Am-16 were used at molar ratio (20:75:60:1:4:15). TPGS (57 mg), Span 60® (65mg), cholesterol (48mg), cholesterol-PEG- maleimide (10 mg), L-α-Phosphatidylethanolamine, dioleoyl (DOPE) (6 mg) and DAB-Am-16 (50 mg) were weighed into individual containers. TPGS (57 mg) was added to 2 mL distilled water and allowed to dissolve for 10 minutes. The resulting mixture was then probe sonicated (Sonics Vibracell™, Newton, CT) for 2 minutes. The dispersion formed was then added to the glass container containing Span® 60 (65 mg), cholesterol (48 mg), cholesterol-PEG-maleimide (10 mg), L-α-Phosphatidylethanolamine, dioleoyl (DOPE) (6 mg) and DAB-Am-16 (50 mg). The mixture was slightly vortexed and stirred on a magnetic stirrer for 1 hour at 65°C.

This was followed by probe sonication (Sonics Vibracell™, Newton, CT) for a total of 6 min, with 2 min interval in between 2 min probe sonication sessions, to obtain PEGylated TPGS targeted dendrisomes (DTPGSmd) control vesicles. The instrument was set at 75% of its maximal capacity. This process formed DTPGSmd dendrisomes. Purification of the dendrisomes was done using Vivaspin 6 centrifugal concentrator tubes with a molecular weight cut off of 100,000 Daltons in a swing bucket centrifuge (Beckman coulter, UK) at 7500 rpm (6,600 x g) at 20°C for 15 minutes. The concentrated dispersion was then collected.

2.2.11 Preparation of Transferrin-bearing PEGylated TPGS dendrisomes

Transferrin-bearing PEGylated TPGS dendrisomes (DTPGSmdTf) were prepared by cross-linking transferrin (12 mg) with the PEGylated TPGS control dendrisomes previously prepared. This was done by cross-linking transferrin (12 mg) with the control dendrisomes. Modification of the transferrin was done with Traut's reagent. Transferrin (12 mg) was first dissolved in 1.2 mL sodium phosphate buffer containing sodium chloride (50 mM sodium phosphate buffer, 150 mM NaCl, pH 8.0) to make a 10 mg/mL solution. The Traut's reagent (106 μL of stock solution 2mg/mL in distilled water) was added to the transferrin solution (1.2 mL, 10mg/mL), to make it ten-fold molar excess of the molarity of transferrin. The reaction was then carried out for 1 h at 20^{o}C , under constant magnetic stirring (Hermanson 2013b).

Purification of the thiolated transferrin from unreacted Traut's reagent was then done through centrifugation in Vivaspin 6 centrifugal concentrator tubes (Sartorius® Göttingen, Germany) with molecular weight cut off of 5000 Daltons, at 9,500 rpm (10,500 x g) at 20°C for 15 minutes. The transferrin conjugation step was done immediately after purifying the thiolated transferrin to prevent the recyclization of the free thiol in the thiolated transferrin which could lead to a simultaneous decrease in thiol availability for linking with the maleimide group in the control dendrisomes. Transferrin conjugation (12 mg) with control dendrisomes (2 mL) was done by mixing over a magnetic stirrer for 2 h at 20^{o}C.

Purification of the transferrin-bearing (Tf-dendrisomes) and control PEGylated TPGS dendrisomes were then carried out using Vivaspin 6 centrifugal concentrator tubes

(Sartorius® Göttingen, Germany) with a molecular weight cut off of 100,000 Daltons in a swing bucket centrifuge (HermLe® Z323K Wehingen, Germany) at 7,500 rpm (6,600 x g) for 15 minutes. The concentrated dispersions were individually collected, made up to 4 mL with PBS pH 7.4 and stored in the store at 2-8°C (Figure 2.14).

2.2.12 Formulation of PEGylated TPGS dendrisomes encapsulating doxorubicin

Tf-bearing DTPGSmd and control DTPGSmd dendrisomes encapsulating doxorubicin (DTPGSmdDoxTf and control DTPGSmdDox) were also prepared. Formulation of DTPGSmd dendrisomes were formulated with TPGS (57 mg), Span 60® (65 mg), cholesterol (48 mg), cholesterol-PEG-maleimide5000 (10 mg), L-α-Phosphatidylethanolamine, dioleoyl (DOPE) (6 mg) and DAB-Am-16 (50 mg) at molar ratio (20:75:60:1:4:15). TPGS (57 mg) was added to 2 mL distilled water and allowed to dissolve for 5minutes. The resulting mixture was then probe sonicated (Sonics Vibracell™, Newton, CT) for 2 minutes. The dispersion formed was then added to the glass container containing Span 60® (65 mg), cholesterol (48 mg), cholesterol-PEG- maleimide5000 (10 mg), L-α-Phosphatidylethanolamine, dioleoyl (DOPE) (6 mg) and DAB-Am-16 (50 mg). The mixture was vortexed and heated with a magnetic stirrer for 1 h at 65 °C. Doxorubicin solution (300 µL) of concentration of 10 mg/mL was added to the mixture, which was then vortexed again. This was followed by probe sonication (Sonics Vibracell™, Newton, CT) for a total of 6 min, with 2 min interval between 2 min probe sonication sessions. The instrument was set at 75% of its maximal capacity. The formulation of Tf- bearing DTPGSmd dendrisomes encapsulating doxorubicin (DTPGSmdDoxTf) was done by first making

control DTPGSmdDox dendrisomes as described above. Conjugation of the control DTPGSmdDox dendrisomes with transferrin was carried out as earlier described.

2.2.12.1 Purification of PEGylated TPGS dendrisomes encapsulating doxorubicin

The removal of excess doxorubicin concurrently with the purification and concentration of the transferrin-bearing (Tf-dendrisomes) and control PEGylated TPGS dendrisomes encapsulating doxorubicin were then carried out using Vivaspin 6 centrifugal concentrator tubes (Sartorius® Göttingen, Germany) with a molecular weight cut off of 100,000 Daltons in a swing bucket centrifuge (HermLe® Z323K Wehingen, Germany) at 7,500 rpm (6,600 x g) for 15 minutes. The concentrated dispersions were individually collected, made up to 4 mL with PBS pH 7.4 and stored at store at 2-8°C. Experiments to assess the encapsulation efficiency of doxorubicin in the DTPGSmdDox dendrisomes were then carried out. The work flow schemes of the preparation of the DTPGSmd dendrisomes is shown on the following page (Figure 2.14).

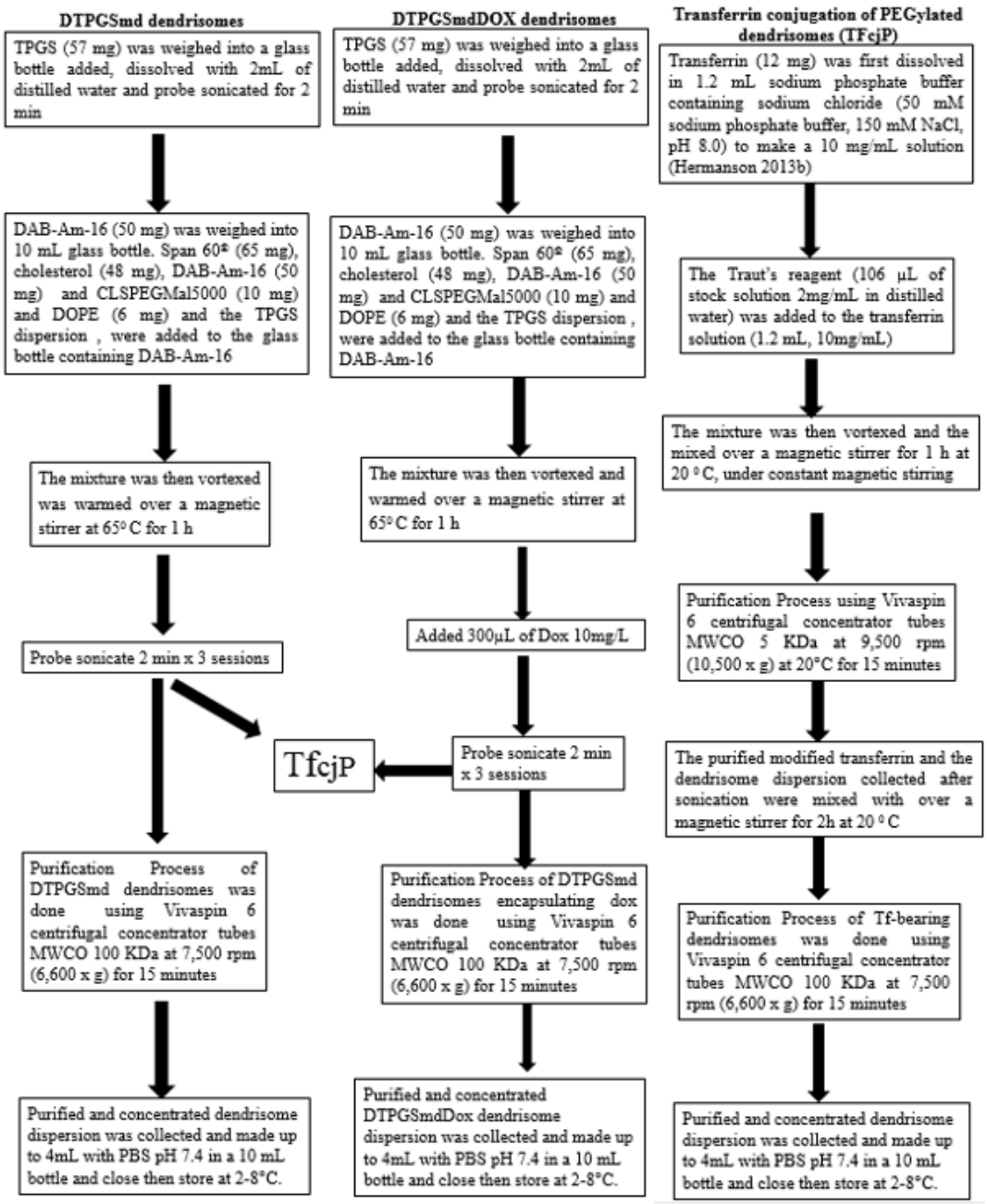

TfcjP: Transferrin conjugation process of PEGylated dendrisomes

Figure 2.14: Work Flow of Formulation of PEGylated TPGS (DTPGSmd) dendrisomes.

2.2.13 Quantification of doxorubicin in the dendrisomes

A standard calibration curve for doxorubicin for concentrations ranging from 10^{-4} to $14X10^{-4}$ mg/mL in distilled water. The quantity of doxorubicin entrapped in the dendrisomes was then measured by spectrofluorometry using the standard calibration curve for doxorubicin. The first method used for quantification of doxorubicin in the dendrisomes was done by disrupting first disrupting the dendrisomes with isopropanol. A 1:1000 dilution with the dendrisomes was done and the fluorescence measured at an excitation wavelength of 480 nm and an emission wavelength of 560 nm using a Cary eclipse spectrofluorometer (Varian® Palo Alto, California). Fluorescence measurements were done in quadruplicates. The fluorescence intensity measurements obtained were subsequently correlated with equation obtained from the doxorubicin standard calibration curve. The encapsulation efficiency of the dendrisomes was obtained by calculating the percentage of the amount doxorubicin encapsulated in the dendrisomes compared to the initial amount of doxorubicin added.

The second method used for the quantification of doxorubicin in the PEGylated dendrisomes was done using the supernatant obtained after centrifugation in the purification step, produced better results especially for the DTPGSmdDox dendrisomes. A 1:1000 dilution of supernatant with isopropanol was done and the fluorescence measured at an excitation wavelength of 480 nm and an emission wavelength of 560 nm using a Cary eclipse spectrofluorometer (Varian® Palo Alto, California). Fluorescence measurements were done in quadruplicates. The fluorescence intensity measurements obtained were subsequently correlated with equation obtained from the doxorubicin standard calibration curve. The encapsulation

efficiency of the dendrisomes was obtained by calculating the percentage of the amount doxorubicin encapsulated in the dendrisomes compared to the initial amount of doxorubicin added.

2.2.14 Quantification of Transferrin conjugated to the dendrisomes

The Lowry assay method as previously described (Dufès *et al*., 2000) was the method chosen to quantify the amount of transferrin conjugated to the dendrisomes. Sodium carbonate 2 % w/v solution (50 mL) was first prepared in sodium hydroxide 0.1 M. Sodium potassium tartrate 2 % w/v (1 mL) and cupric sulphate 1 % w/v (1 mL) were added to the sodium carbonate solution made to make up solution A. A transferrin standard solution (concentration ranging from 0 to 500 μg/mL) was prepared as well as a 100 μL of suspension (diluted 1:100 in PBS). Solution A (1 mL) was added to the individual transferrin standard solution samples as well as the 100 μL of 1:100 diluted suspension. An incubation period of 10 minutes was done at room temperature. Diluted Folin Ciocalteu's reagent (1:1 in distilled water) (100 μL) was then added to each sample, vortexed and incubated for another 30 minutes protected from light with aluminium film. The UV absorbance of each sample was determined at a wavelength of 750 nm (50 Bio UV-Visible Spectrophotometer), using PBS as zero reference. The measurements were carried out in quadruplicate. The amount of transferrin conjugated to dendrisome surface was calculated by correlation using the transferrin standard curve. The conjugation efficiency of transferrin to the dendrisomes was calculated as the percentage of transferrin conjugated to vesicles compared to the initial amount of transferrin added.

2.2.15 Measurements of the size and zeta potential of dendrisomes

Photon correlation spectroscopy and zeta potential measurements were done to confirm the presence of nano-sized dendrisomes and to determine if the dendrisomes carried any surface charges. Dendrisome dispersion (10 µL) was diluted in 990 µL of 5% glucose solution (1:100 dilution) to make up 1 mL of sample immediately before measuring its size and zeta potential, using the Malvern Zetasizer equilibrated at room temperature (25 ^{o}C). The size and zeta readings were taken in quadruplicates.

2.2.16 Observation of dendrisomes by Transmission electron microscopy

The Tf-bearing and control dendrisome structures were visualized with Transmission electron microscopy (TEM) to confirm their formation. Tf-bearing and control dendrisomes were diluted in a 1:10 dilution in 5 % glucose. A drop of each sample was applied to a pre-coated (carbon support film) copper grid. Excess liquid was blotted off each sample with filter paper prior to negative staining. Aqueous methylamine vanadate stain (1%) (NanoVan®) from Nanoprobes, (Yaphank, NY) 20 µL was applied and the mixture dried down immediately using filter paper. The carbon-coated 200-mesh copper grids were then glow-discharged. The structure of dendrisomes was visualized by transmission electron microscopy using a FEI Tecnai™ TF20 transmission electron microscope (Hillsboro, Oregon) operating at 200 kV fitted with a Multiscan CCD camera (Gatan MSC 794®) from (Gatan Pleasanton, CA) (Lemarié *et al*., 2013).

2.2.17 Plasmid DNA preparation

The plasmid DNA encoding β-galactosidase (pCMV β-Gal) and plasmid DNA encoding TNF- α used for this project were prepared and purified using QIAGEN Giga preparation kits. The *E. coli* bacteria encoding the required plasmid DNA was first incubated in L-both medium at 37^0C for 24 h. After which the culture medium was centrifuged, the supernatant discarded, and the pellets of the *E. coli* were removed. Harvesting and lysis of the bacteria was carried out in accordance with the laid-out instruction of the QIAGEN Giga preparation kits. Lysis of the harvested bacteria was done using a buffer containing sodium dodecyl sulfate (SDS) to release the entrapped plasmid DNA from the bacteria cells. The mixture was passed through a QIAfilter Cartridge that had a resin which trapped the bacteria lysed membranes. Plasmid DNA was collected and further purified and eluted using a QIAGEN tip 10000 and the required buffers. Precipitation of the eluted DNA was done by adding 70 mL room-temperature isopropanol. The mixture was centrifuged immediately at 11 000 rpm, 4ºC for 30 min. The translucent DNA pellets were washed with QIAGEN endotoxin-free room-temperature 70% ethanol and centrifuged at 11 000 rpm, 4 °C for 15 min. After centrifugation, the pellets were resuspended in glucose 5% solution and stored in the store at 2-8°C overnight (QIAGEN 2005).

2.2.18 Preparation of dendrisomplexes

Dendrisomplexes of various dendrisome: DNA ratios were prepared in PBS for the DNA condensation studies and TE for buffer for the Gel retardation studies. Formation of dendrisomplexes was done through manual mixing with a pipette and pipette and pipette tips immediately before the DNA condensation and Gel retardation experiments (Table 2.4 -Table 2.6). The plasmid encoding β- galactosidase (pCMV β gal) was the DNA utilized.

Table 2.4: DEN-SOL dendrisomes DNA complex formulation for DNA Condensation Studies

Dendrisome: DNA Ratio	**Dendrisome Portion of Dendrisomplex (0.5 mL)**		**DNA portion of dendrisomplex (0.5 mL)**
	dendrisome dispersion (µL)	**PBS pH 7.4 (µL)**	**DNA stock (10µg/mL) in PBS pH 7.4 (µL)**
10:1	100	400	500
5:1	50	450	500
2:1	20	480	500
1:1	10	490	500
0.5:1	5	495	500
DNA only	-	-	500

Table 2.5: DSOLm and DTPGSmd dendrisomes DNA complex formulation for DNA Condensation Studies

Dendrisome: DNA Ratio	**Dendrisome Portion of Dendrisomplex (0.5 mL)**		**DNA portion of dendrisomplex (0.5 mL)**
	dendrisome dispersion (µL)	**PBS pH 7.4 (µL)**	**DNA stock (10µg/mL) in PBS pH 7.4 (µL)**
10:1	200	300	500
5:1	100	400	500
2:1	40	460	500
1:1	20	480	500
0.5:1	10	490	500
DNA only	-	-	500

Table 2.6: DSOLm and DTPGSmd dendrisomes DNA complex formulation for Gel Retardation Assay

Dendrisome: DNA Ratio	Dendrisome Portion of Dendrisomplex (0.5 mL)		DNA portion of dendrisomplex (0.5 mL)
	dendrisome dispersion (µL)	TE buffer (µL)	DNA stock (20µg/mL) in PBS pH 7.4 (µL)
10:1	400	100	500
5:1	200	300	500
2:1	80	420	500
1:1	40	460	500
0.5:1	20	480	500
DNA only	-	-	500

2.2.19 Determination of complexation of DNA to dendrisomes

DNA condensation capabilities of dendrisomes to form dendrisome-DNA complexes (dendrisomplexes) were assessed using PicoGreen® assay. DNA plasmid encoding β-galactosidase was the plasmid of choice. The dendrisomplexes were formulated by adding dendrisomes in PBS buffer (made up to 0.5 mL) to DNA (0.5 mL of 10 µg/mL DNA) at different dendrisomes: DNA ratios 10:1, 5:1, 2:1, 1:1 and 0.5:1. PicoGreen® solution was freshly prepared by diluting PicoGreen® reagent 200-fold in Tris–EDTA (TE) buffer (10 mMTris, 1 mM EDTA, pH 7.5) on the day of the experiment. PicoGreen solution (1 mL) was then added to the complex (1 mL) formed and fluorescence of the samples was measured (Excitation wavelength 480 nm, emission wavelength 520 nm), using a Cary Eclipse Fluorescence spectrophotometer (Varian® Palo Alto, CA), over a 24-hour period. Samples with PicoGreen (1 mL) solution alone were used as a negative control, while samples of DNA only ((0.5 mL (10 µg/mL DNA) mixed with PBS (0.5 mL)) had PicoGreen (1 mL) added to them and were used

as a positive control for the experiment. If there was no complexation of DNA to dendrisomes, all double-stranded DNA would be able to interact with the PicoGreen® solution, leading to high fluorescence (Koppu *et al.*, 2010).

2.2.20 Gel Retardation assay

The DNA condensation ability of the dendrisome: DNA mixtures formed was examined using the agarose gel retardation assay. The DNA condensation ability of the dendrisomplexes was also assessed by agarose gel retardation assay. Dendrisomplexes were prepared at a final DNA concentration of 20 μg/mL, at different dendrisome: DNA ratios 10:1, 5:1, 2:1, 1:1, and 0.5:1 in TE buffer. After mixing with the loading buffer, the samples (10 μL) were loaded on a 1× Tris-Borate-EDTA (TBE) (89 mM Tris base, 89 mM boric acid, 2 mM Na_2-EDTA, pH 8.3) buffered 0.8% (w/v) agarose gel containing ethidium bromide (0.4 μg/mL), with 1× TBE as the running buffer. The DNA size marker was HyperLadder I. The gel was run at 50 V for 1 h and then photographed under UV light (Aldawsari *et al.*, 2011).

2.2.21 Determination of the drug release from the dendrisomes

The release of the drug from dendrisomes was measured using dialysis technique. Doxorubicin (300 μg) in dendrisome dispersion (made up to 2 mL with PBS pH7.4) was placed in a dialysis tubing membrane with a molecular weight cut-off of 3500 Da ThermoFisher Scientific (Paisley, UK). The dialysis tubing was then placed in 100 mL of pre-warmed PBS (37 ºC) with constant stirring at 37 ºC. Samples of 1 mL of the PBS containing the doxorubicin encapsulated dendrisome dispersions in dialysis tube

were taken in quadruplicates and replaced with the same volume of fresh PBS at intervals of 30 min, 45 min and 1 hour for the first six hours (2h, 3h, 4h, 5h, 6h), then every 2 h (8h, 10h, 12h) for 12 h then every 24 h for 10 days. The amount of doxorubicin released from the delivery system was quantified by spectrofluorimetry (excitation wavelength 480 nm, emission wavelength 560 nm), using a Cary Eclipse Fluorescence spectrophotometer (Varian Palo Alto, CA).

2.2.22 Differential scanning calorimetry DSC studies

The dendrisomes as well as the pure samples of the surfactants used in the formulation were analysed in the solid state using a DSC 822^{e} Metler Toledo Thermal Analysis DSC (Beaumont Leys, UK). The dendrisomes were air dried at 37^{o}C on aluminium studs. Individual sample weights of 4–7 mg was used for the DSC measurements. The dried samples were weighed individually into 40µL aluminium pans and then hermetically sealed. The experiment runs were started at an initial temperature of 10 ^{o}C, under nitrogen gas, with a scan rate of 5 ^{o}C/min to 150 ^{o}C. The results were evaluated using Star^{e} software (Gardikis *et al.*, 2006; Wilkhu *et al.*, 2014).

2.2.23 Shelf-life Stability studies

Shelf-life stability studies of the PEGylated dendrisomes were carried out at: 25°C for three months (Dick *et al.*, 2011; Ghanbarzadeh *et al.*, 2013). Photon correlation spectroscopy measurements were done. Dendrisome dispersion (10 µL) was diluted in 990 µL of 5% glucose solution (1:100 dilution) to make up 1 mL of sample immediately before measuring its size using the Malvern Zetasizer equilibrated at room temperature (25 ^{o}C). Size and PDI measurements were taken in triplicates.

2.2.23 Atomic Force Microscopy Observation of dendrisomes

DSOLm dendrisomes were visualized by atomic force microscopy (AFM) to assess shape. Following 10-fold dilution with glucose, 50 µL of the diluted dendrisome dispersion was placed on a mica surface and left to dry at 25 ºC. The scanning mode used was PeakForce Tapping® at room temperature, using a ScanAsyst-Air® probe (Bruker, Billerica, MA). Data were collected by a Dimension Fast Scan AFM (Bruker) equipped with an Icon scanner with nominal tip radius of 2 nm and nominal spring constant of k = 0.4 N/m. All data were analyzed using the NanoScope Analysis 1.5® software (Bruker), while height images were corrected by first-order flattening.

2.2.24 Statistical Analysis

The results obtained were expressed as means ± standard error of the mean. Statistical significance was determined by one-way analysis of variance (ANOVA) followed by the Tukey multiple comparison post-test (OriginPro 9® software). Differences were considered as significant when $P < 0.05$.

2.3 Results

2.3.1 Size and zeta potential measurements of dendrisomes

The Z-average size measurements demonstrated that the non-PEGylated dendrisomes formulated were between 410.2 ± 66.4 nm to 456.8 ±31.5 nm for control vesicles and 180.1 ± 1.1 nm to 205.1 ± 4.1 nm for dendrisomes encapsulating doxorubicin (Table 2.7). Polydispersity index (PDI) was found to be less than 0.6 for all formulations prepared. The zeta potential was observed to be close to zero for all samples: all the non-PEGylated formulations were neutral. The Z-average size measurements for the PEGylated dendrisomes formulated were between 142.3 ±1.59 nm to 313.44 ± 7.83 for empty DSOLm and DTPGSmd vesicles and 175.1 ± 1.00 nm to 266.06 ± 13.68 nm for DSOLmDox and DTPGSmdDox dendrisomes encapsulating doxorubicin. Polydispersity index (PDI) was found to be less than 0.5 for all the PEGylated formulations prepared. The zeta potential was observed to be 5.09 ± 3.20 to 14 ±0.79 (Table 2.7). Hence it is positively charged. However, the charge of the Tf-bearing dendrisomes was discovered to be less than 15 hence they are slightly positively charged which enables DNA complexation, but is not so high as to be taken up by the RES. This is desirable as this will ensure longer circulating times of the targeted dendrisomes and enhance higher accumulation of targeted dendrisomes within the cancer cells overexpressing transferrin.

Table 2.7: Size and zeta potential measurements for dendrisomes (n=12)

Dendrisome	Z-Ave d. nm ± SEM	PDI ±SEM	Zeta potential mV ± SEM
DEN-SOL	410.2 ± 66.4	0.527 ± 0.06	0.00 ± 4.19
DEN-SOL-DOX-C	205.1 ± 4.1	0.411 ± 0.00	0.10 ± 4.93
DEN-SOL- DOX-Tf	180.1 ± 1.1	0.312 ± 0.02	0.11 ± 5.04
DSOLm Control	142.3±1.59	0.306± 0.03	14±0.79
DSOLm Tf	162.7±7.12	0.378±0.05	13.7±0.77
DSOLmDox Control	181.3± 5.01	0.406±0.01	10.4±0.56
DSOLmDox Tf	175.1±1.00	0.487±0.01	8.19±0.78
DEN-TPGS1	456.8 ±31.5	0.507 ± 0.04	0.04 ± 4.80
DEN-TPGS2	238.8 ± 7.63	0.441±0.014	-0.58±30.7
DTPGSmd control	305.6±22.01	0.434± 0.01	6.17±3.42
DTPGSmdTf	313.44±7.83	0.234± 0.02	5.09± 3.20
DTPGSmdDOX Control	182.86± 8.91	0.406±0.04	11.77± 3.79
DTPGSmdDOXTf	266.06±13.68	0.356±0.04	5.95± 3.39
DEN-DHP	>1000	>1	37.77± 4.93

2.3.2 Transmission electron microscopy (TEM) observation of the dendrisomes

The TEM pictures showed that the dendrisomes were spherical in shape, with sizes in the nanometre range (Figures 2.15, 2.16 and 2.17).

A/

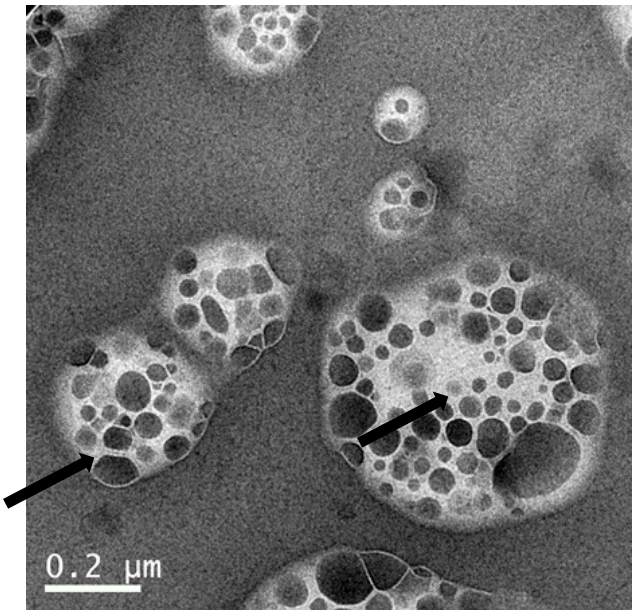

B/

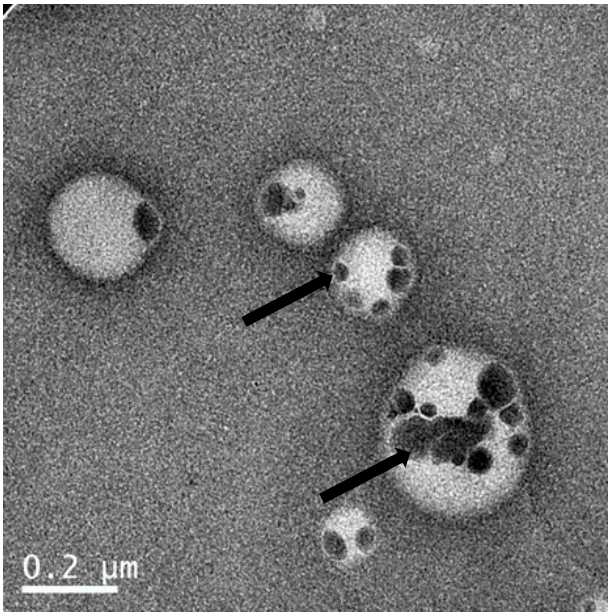

Figure 2.15: Transmission electron micrographs of Tf-bearing DEN-SOL (A) and control DEN-SOL (B) dendrisomes showing that spherical dendrisomes were successfully formed. (Bar: 0.2 µm).

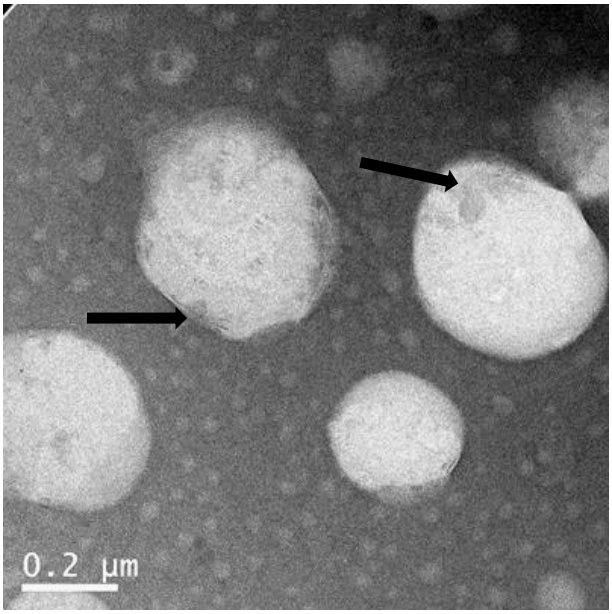

Figure 2.16: Transmission electron micrographs of control DEN-TPGS1 dendrisomes showing that spherical dendrisomes were successfully formed. (Bar: 0.2 µm).

A/

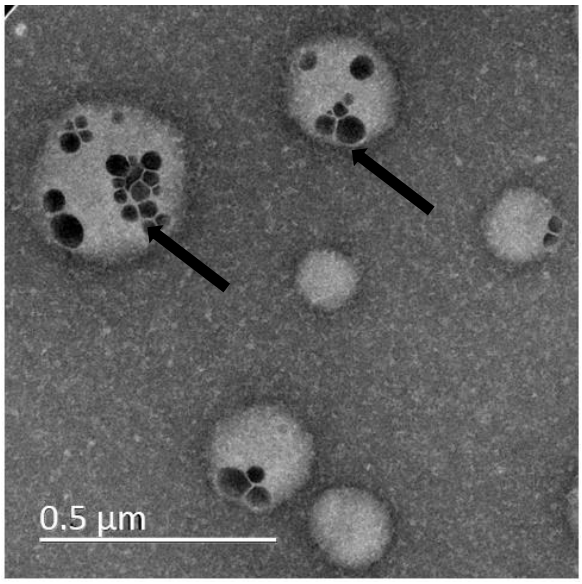

B/

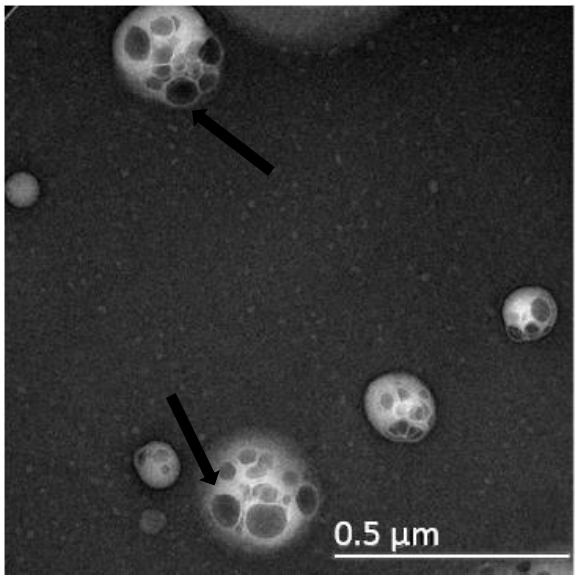

Figure 2.17: Transmission electron micrographs of Tf -bearing DSOLm (A) and DSOLm control (B) dendrisomes showing that spherical dendrisomes were successfully formed, with arrows specifying the location of the dendrimer on the surface. (Bar: 0.5µm).

2.3.3 Determination of complexation of DNA to dendrisomes

The PicoGreen® intercalation assay was carried out on Tf-bearing and control DEN-SOL dendrisomes, Tf-bearing and control DSOLm dendrisomes and Tf-bearing DTPGSmd dendrisomes using plasmid DNA encoding β-galactosidase (pCMV β-Gal). Plasmid DNA encoding β-galactosidase (pCMV β-Gal) is a plasmid used for experimental analysis to show condensation efficacy, transfection efficacy/ gene expression of delivery systems complexed with DNA by expressing the reporter protein β-galactosidase enzyme (Schatzlein and Zinselmeyer, 2005). The DNA condensation was observed to be immediate and it was found to be sustained over a 24-hour period with very little change (Figures 2.18, 2.19 and 2.20). The Tf -bearing and control DEN-SOL, Tf -bearing and control DSOLm and Tf-bearing DTPGSmd dendrisomes could condense more than 75 % of DNA at all dendrisome: DNA ratios.

The Tf –bearing and control DEN-SOL dendrisomes could condense more than 85% of DNA at all dendrisome: DNA ratios. The DNA condensation was observed to be immediate and it was found to be sustained over a 24-hour period with very little change. The highest percentage DNA condensation observed in DSOLmTf dendrisome: DNA ratio 10:1 at 88.3 % after 24 hours. The percentage DNA condensation after 24 hours for the control DSOLm dendrisome: DNA ratios were observed to be 86.9 %, 85.4 %, 83.4 %, 81.8%, and 81.5 % for DSOLmC: DNA ratios 10:1, 5:1, 2:1, 1:1, and 0.5:1 respectively. While for the other DSOLmTf: DNA ratios 5:1, 2:1, 1:1, and 0.5:1 had percentage DNA condensation at 88.2 %, 87.2%, 85.7 % and 84.8 %. There was no DNA condensation observed in the DNA only samples.

The DNA condensation for the DTPGSmdTf dendrisomes complexed with β-galactosidase was observed to be immediate and it was found to be sustained over a 24-hour period with very little change. The percentage DNA condensation in DTPGSmdTf dendrisomplexes after 24 hours was observed to be greater than 90% for all DTPGSmdTf dendrisome: DNA ratios with ratio 0.5:1 having the highest percentage at 95 %. The other DTPGSmdTf dendrisome: DNA ratios were observed to be 94.2 %, 94.4 %, 94.5 %, and 95 % for DTPGSmdTf: DNA ratios 10:1, 5:1, 2:1 and 1:1 respectively. There was no DNA condensation observed in the DNA only samples. This experiment showed that the dendrisomplexes formed are very stable over a 24-hour period which will ensure that they will be complexed long enough to be enable them to exert the required gene expression effect intracellularly.

A/

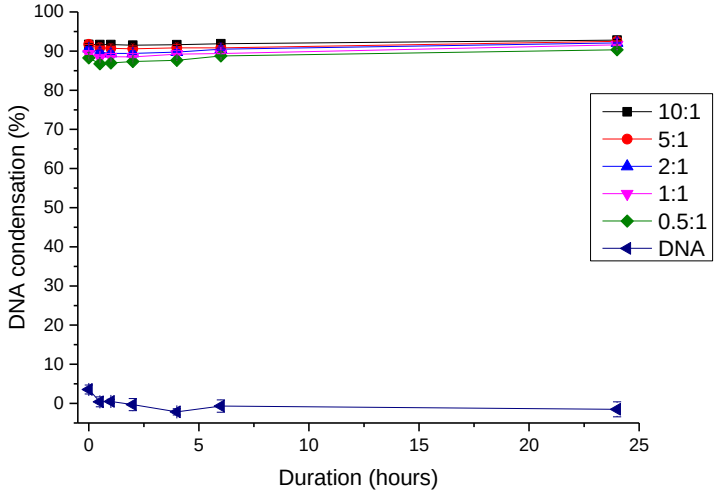

B/

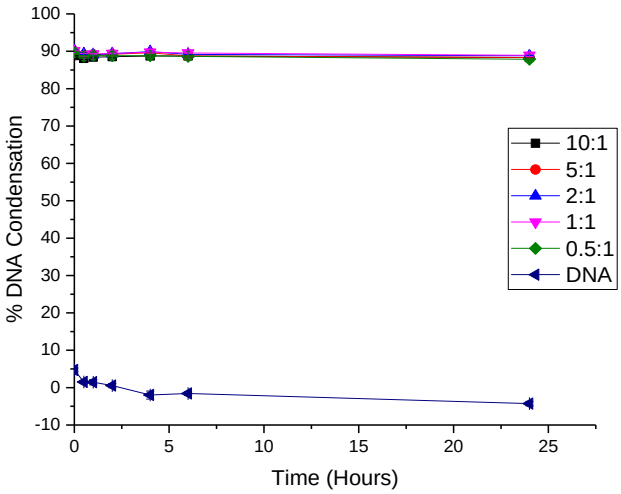

Figure 2.18: DNA condensation experiment of Tf-bearing DEN-SOL dendrisomes (A) and control DEN-SOL dendrisomes (B) complexed with plasmid DNA encoding β-galactosidase using PicoGreen® reagent at various durations and dendrisome: DNA weight ratios: Results are expressed as mean ± SEM (n= 4).

A/

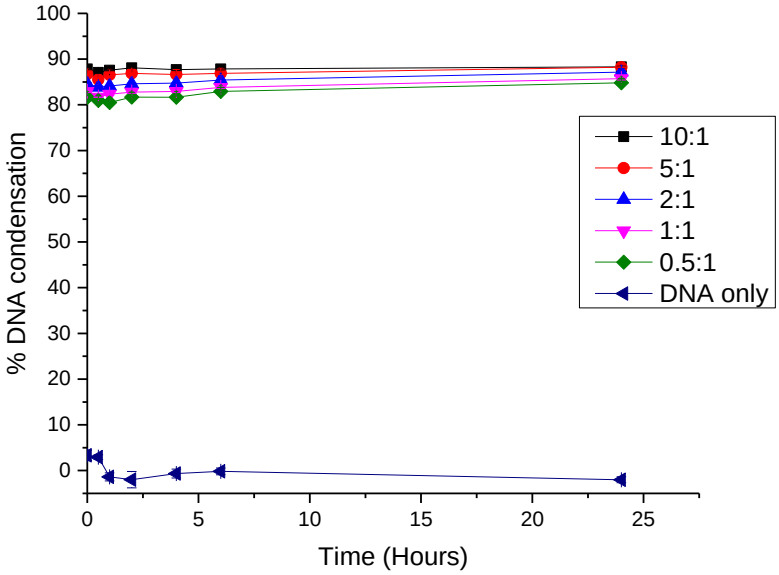

B/

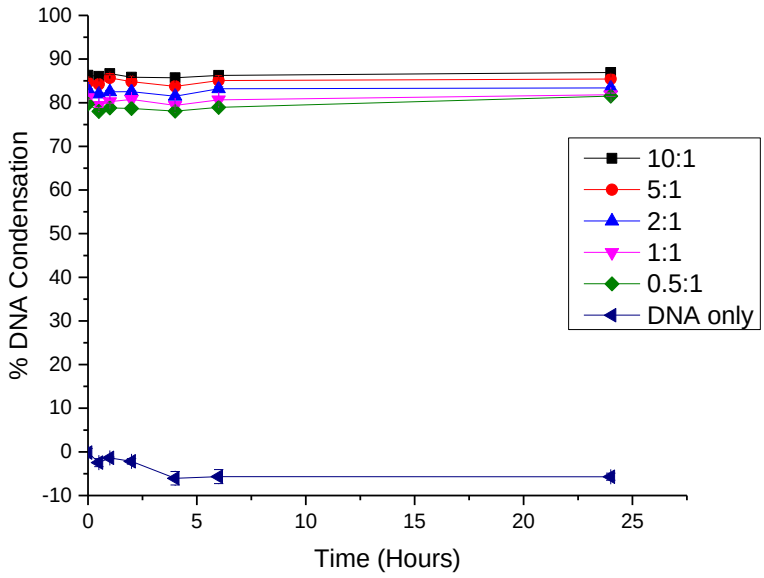

Figure 2.19: DNA condensation experiment of Tf-bearing DSOLm dendrisomes (A) and DSOLm control dendrisomes (B) complexed with plasmid DNA encoding β-galactosidase using PicoGreen® reagent at various durations and dendrisome: DNA weight ratios: Results are expressed as mean ± SEM (n= 4).

A/

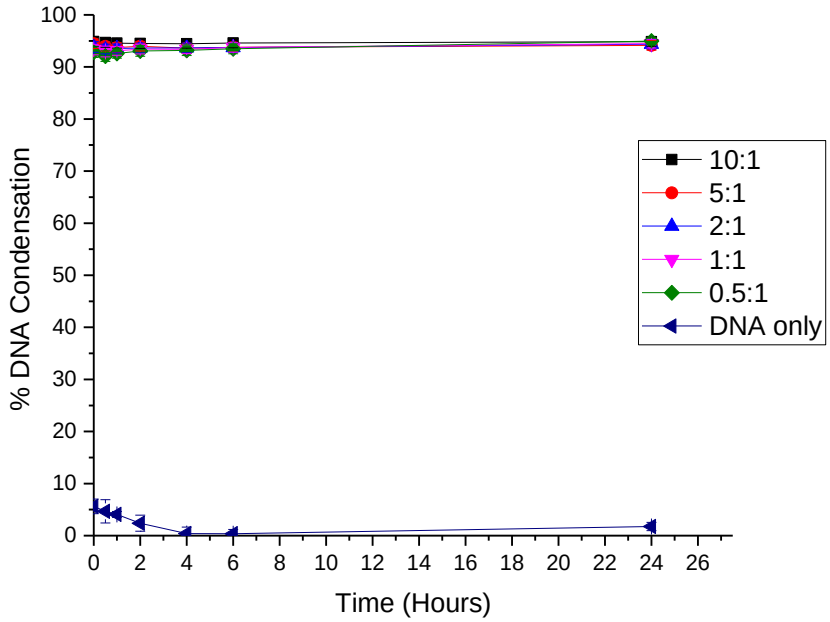

B/

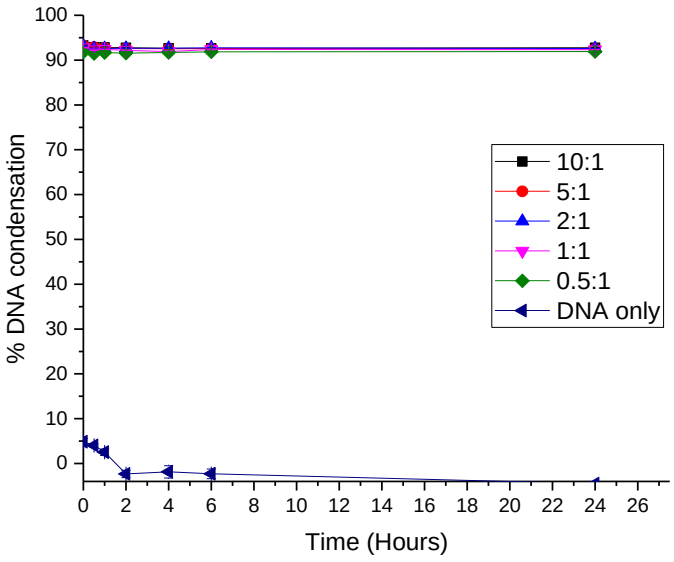

Figure 2.20: DNA condensation experiment of Tf-bearing DTPGSmd dendrisomes (A) and DTPGSmd control dendrisomes (B) complexed with plasmid DNA encoding β-galactosidase using PicoGreen® reagent at various durations and dendrisome: DNA weight ratios: Results are expressed as mean ± SEM (n= 4).

2.3.4 Gel Retardation assay

The Gel Retardation assay (Figure 2.21 and 2.22) gave visual confirmation that there was successful complexation of the plasmid DNA with the transferrin bearing dendrisomes. All the Dendrisomes: DNA ratios of 10:1, 5:1, 2:1, 1:1 and 0.5:1 showed little or no migration on the gel with the 10:1 dendrisomes: DNA ratio showing the highest complexation with the lowest migration. This could be attributed to the fact that they successfully condensed the DNA that they were complexed with, and hence there was little or no free DNA strands available to intercalate with ethidium bromide. However, the DNA only preparation showed the highest migration. This is attributed to the fact that since it was not complexed with the DSOLmTf dendrisomes or DTPGSmdTf dendrisomes hence it was not condensed. This made it available to readily available to be intercalated with the ethidium bromide gel layer because it maintained its negative charge and hence freely migrated.

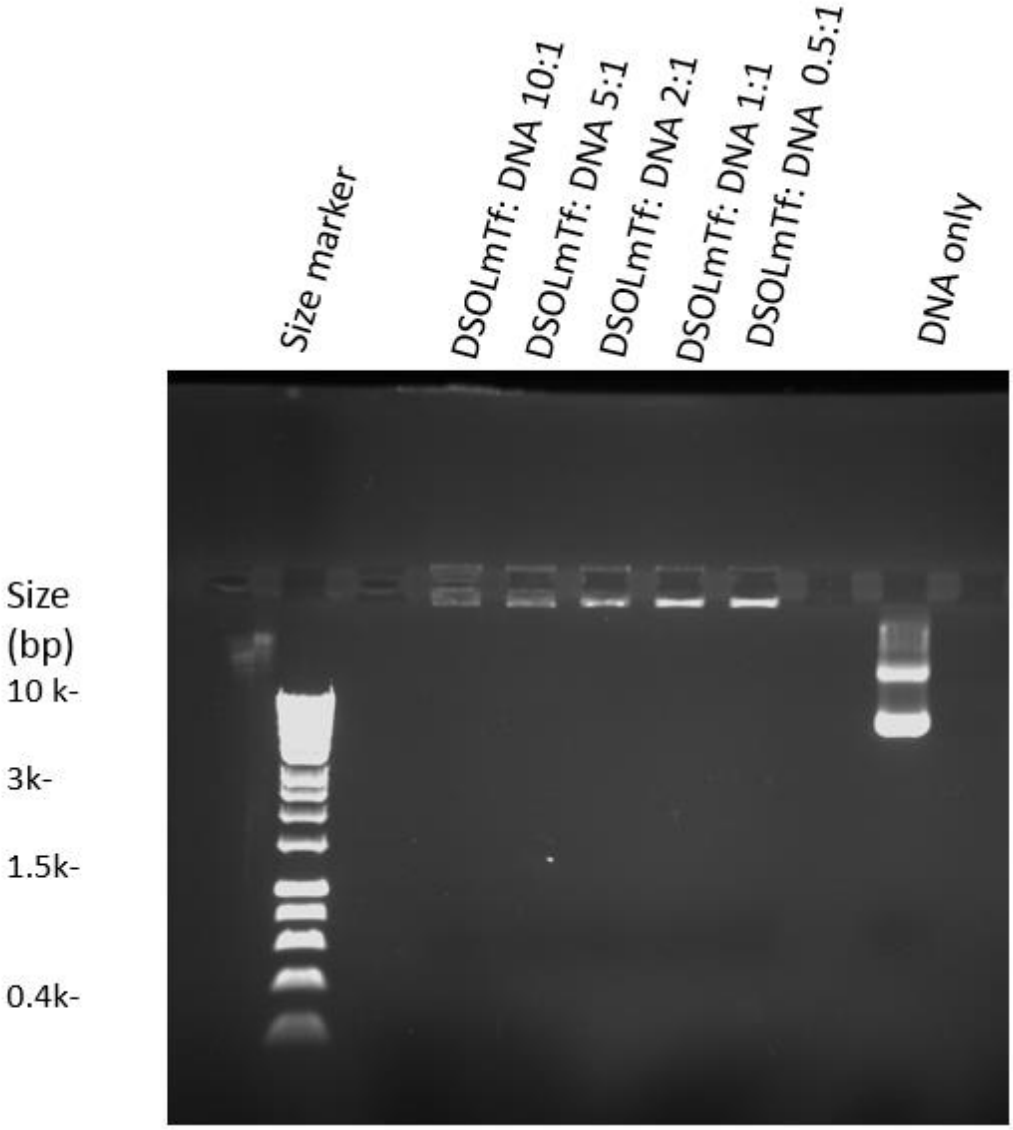

Figure 2.21: Gel Retardation assay of PEGylated Tf-bearing Solulan C24 dendrisomes complexed with DNA (DSOLmTf-DNA) at dendrisome: DNA weight ratios 10:1, 5:1, 2:1, 1:1, 0.5:1 and DNA only

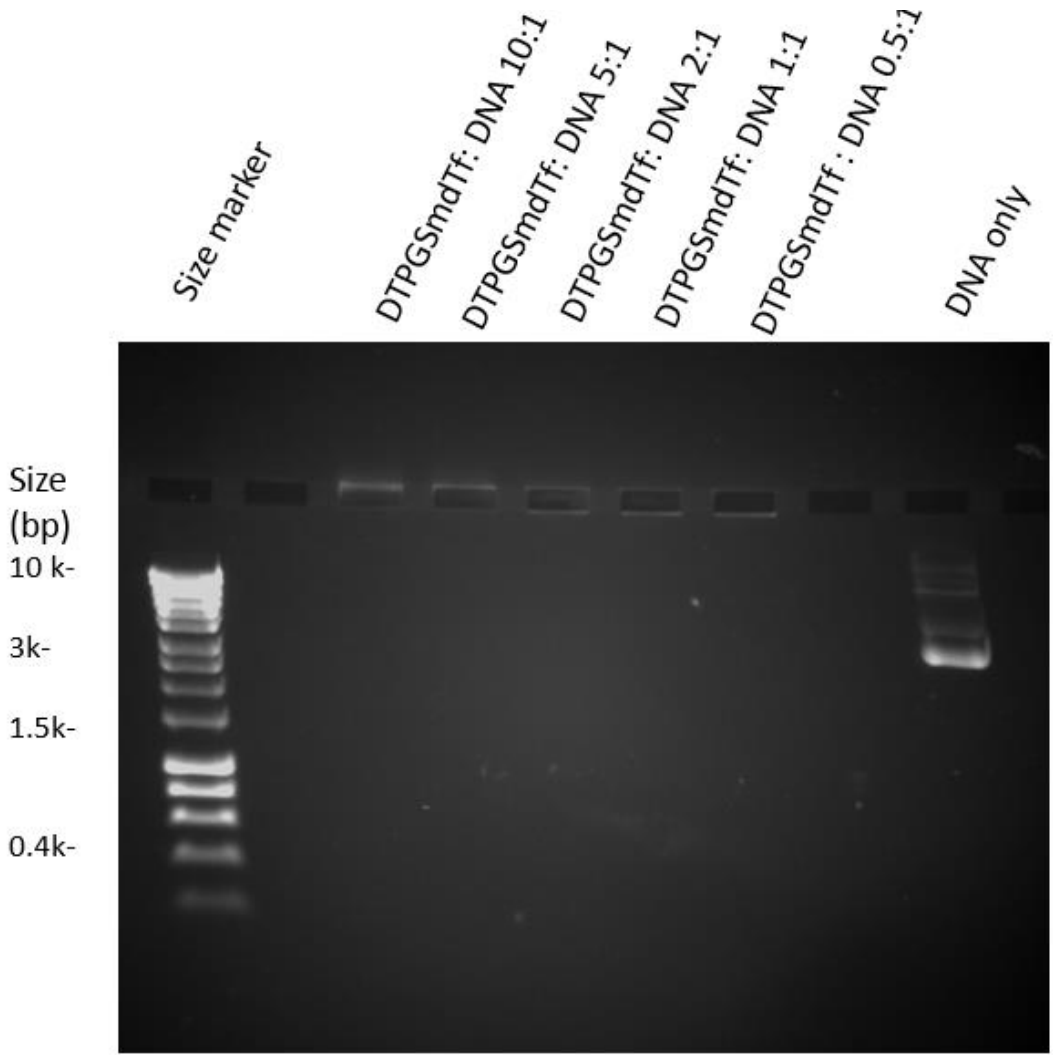

Figure 2.22: Gel Retardation assay of PEGylated Tf-bearing TPGS dendrisomes complexed with DNA (DTPGSmdTf-DNA) at dendrisome: DNA weight ratios 10:1, 5:1, 2:1, 1:1, 0.5:1 and DNA only.

2.3.5 Quantification of doxorubicin in the dendrisomes

A standard doxorubicin calibration curve was obtained (Figure 2.23). The Limit of Detection LOD was 1.45 µg/mL, and Limit of Quantification (LOQ) was 11.58 µg/mL. The quantity of doxorubicin encapsulated in the Tf-targeted and control DSOLm dendrisomes was quantified upon vesicle disruption with isopropanol. This was done through serial dilution to obtain a 1 in 1000 dilution. Fluorescence was measured in quadruplicates at excitation wavelength of 480 nm and emission wavelength of 560 nm. The amount of doxorubicin encapsulated in the dendrisomes was obtained using the equation obtained from the standard doxorubicin calibration curve (Equation 2.2). The encapsulation efficiency of the dendrisomes for doxorubicin was calculated as the percentage of doxorubicin encapsulated in dendrisomes compared to the theoretical amount of encapsulated doxorubicin (Arzani *et al.*, 2015) (Equation 2.3). The encapsulation efficiency for the Tf-bearing and control DEN-SOL dendrisomes encapsulating doxorubicin 93.11 ± 4.17 % when measured immediately after purification. The encapsulation efficiency of the DSOLmDox dendrisomes was found to be 97.95 ±0.3 %, while the encapsulation efficiency of the DTPGSmdDox dendrisomes was found to be 88%. This proved that dendrisomes have the capacity for high drug encapsulation.

Equation 2.2:

$$y = -0.26 + 11.13 * x$$

Where

y= fluorescence reading

x= concentration of doxorubicin in mg/mL

Equation 2.3:

$$\%EE = \frac{\text{Actual amount of drug entrapped in the dendrisomes}}{\text{Theortical amount of drug entrapped in the dendrisomes}} X\ 100\ \%$$

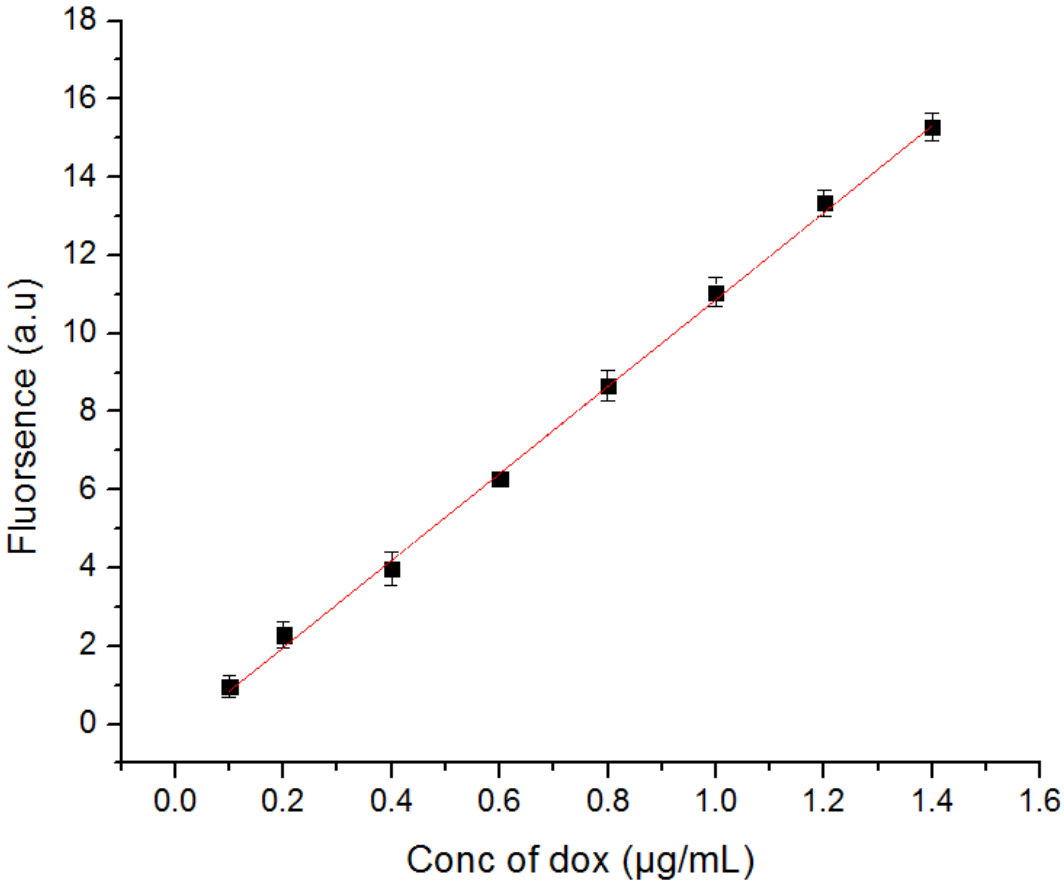

Figure 2.23: Standard Calibration Curve of doxorubicin for quantitative measurements of doxorubicin encapsulated in dendrisomes. Fluorescence intensity in arbitrary unit (a.u.) was obtained upon serial dilution of doxorubicin stock solution (10 mg/mL) in water. R^2 = 0.998 and Pearson's r=0.999. Results are expressed as mean ± SD (n=4).

2.3.6 Determination of the drug release from the dendrisomes

There was an initial burst release of doxorubicin within the first 24 hours in DEN-SOLDox dendrisomes. After which both Tf- bearing and control DEN-SOLDox dendrisomes could increase release of doxorubicin steadily for over the next 9 days with percentage cumulative doxorubicin release of 9.76 ± 0.004 % observed in the DEN-SOLDoxTf dendrisomes and 11.08 ± 0.006 % after 10 days. (Figure 2.24). Burst release of doxorubicin within the first 24 hours was also observed in DSOLmDox dendrisomes. After which both Tf- bearing and control DSOLmDox dendrisomes were able to increase release of doxorubicin steadily for another 24 hours. This release was sustained over the next 8 days with the highest percentage cumulative doxorubicin release observed in the DSOLmDoxTf dendrisomes at pH 6.5 14.6 %. Percentage cumulative drug release for DSOLmDoxC after 10 days at pH 5.5, 6.5 and pH 7.4 were 13.8 %, 12.5% and 13.6% respectively, while Percentage cumulative drug release for DSOLmDoxTf after 10 days at pH 5.5 and pH 7.4 were 10.3 % and 9.4% (Figure 2.25).

DTPGSmdDox dendrisomes doxorubicin release was observed to be slow and slight with the highest percentage cumulative release observed by the DTPGSmdDoxTf dendrisomes after 10 days as 5.2 % at pH 7.4. Percentage cumulative drug release for DTPGSmdDoxC after 10 days at pH 5.5, 6.5 and pH 7.4 were 3.9 %, 3.9 % and 4.5 respectively, while Percentage cumulative drug release for DTPGSmdDoxTf after 10 days at pH 5.5 and pH 6.5 were 4.0% and 4.5% respectively (Figure 2.26).

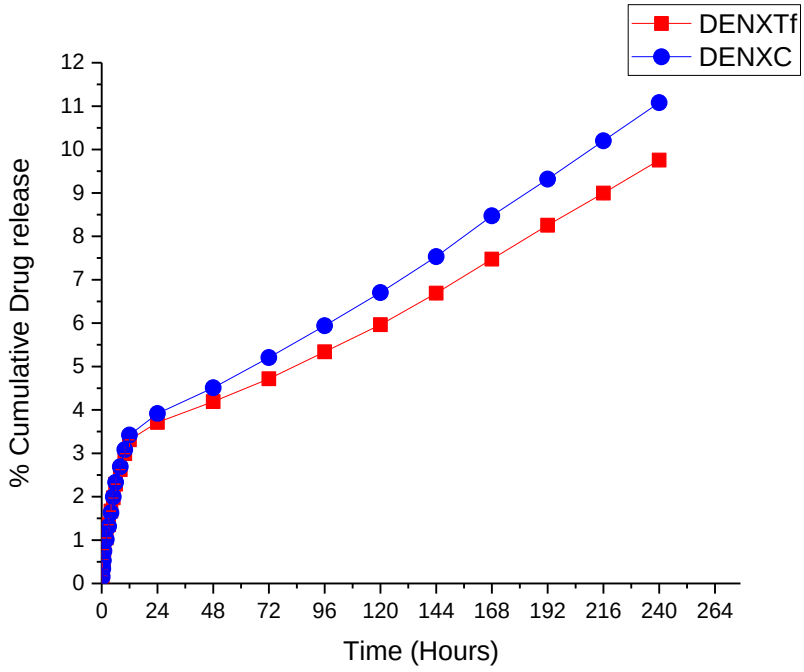

DENXTf: Transferrin-bearing DEN-SOL-DOX dendrisome
DENXC: DEN-SOLDOX control dendrisomes

Figure 2.24: Drug Release studies of doxorubicin from Tf- bearing DEN-SOL-DOX (DEN-SOL-DOX-Tf) and DEN-SOLDOX control dendrisomes in pH buffer 7.4 for 10 days at 37 ºC. Results are expressed as mean ± SEM. (n=4)

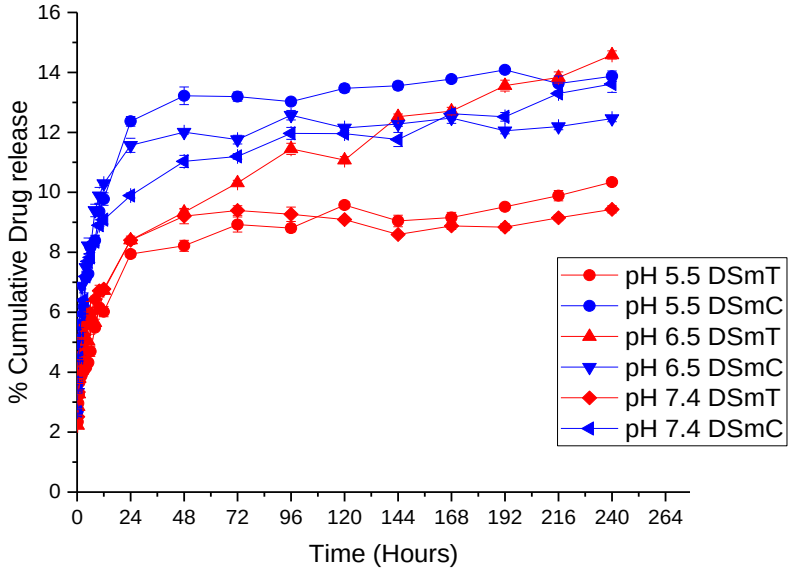

DSmT: transferrin-bearing DSOLmDox dendrisomes
DSmC: DSOLmDox control dendrisomes

Figure 2.25: Drug Release studies of doxorubicin from Tf- bearing DSOLmDox (DSOLmDoxTf) and DSOLmDox control dendrisomes in pH buffers 5.5, 6.5, and 7.4 for 10 days at 37 ºC. Results are expressed as mean ± SEM. (n=4)

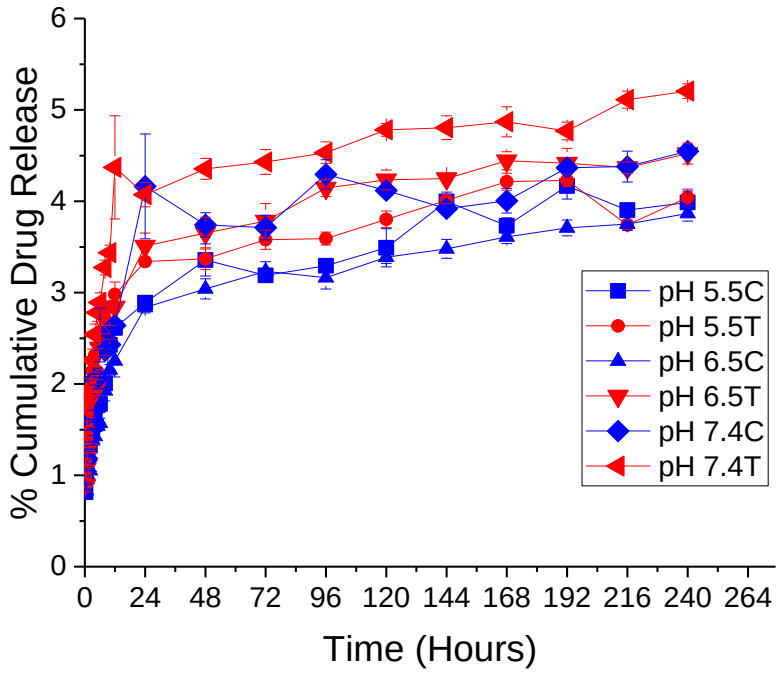

T: Transferrin-bearing DTPGSmdDox dendrisomes
C: DTPGSmdDox control dendrisomes

Figure 2.26: Drug Release studies of doxorubicin from Tf- bearing DTPGSmdDox (DTPGSmdDoxTf) and DSOLmDox control dendrisomes in pH buffers 5.5, 6.5, and 7.4 for 10 days at 37 ºC. Results are expressed as mean ± SEM. (n=4)

2.3.7 Quantification of Transferrin conjugated to the dendrisomes

A standard transferrin calibration curve was obtained (Figure 2.27). After the UV absorbance of each sample was determined at a wavelength of 750 nm using PBS as zero reference, the absorbance measurements carried out in quadruplicates were used to attempt to calculate the amount of transferrin conjugated to dendrisome surface This was calculated by correlation using the transferrin standard curve. The conjugation efficiency of transferrin to the dendrisomes was calculated as the percentage of transferrin conjugated to vesicles compared to the initial amount of transferrin added. It was observed that the values obtained for the transferrin dendrisomes showed decrease in absorbance on conjugation with transferrin. On further investigation it was obvious that other quantification could be tried in future studies (Knight and Chambers, 2003). Thus, the Lowry assay could not be used to quantify the exact conjugation efficiency of transferrin to the dendrisomes.

Equation 2.4:

$$y = 0.08 + 8.68.E\text{-}4*x$$

Where

y= absorbance reading

x= concentration of transferrin in μg/mL

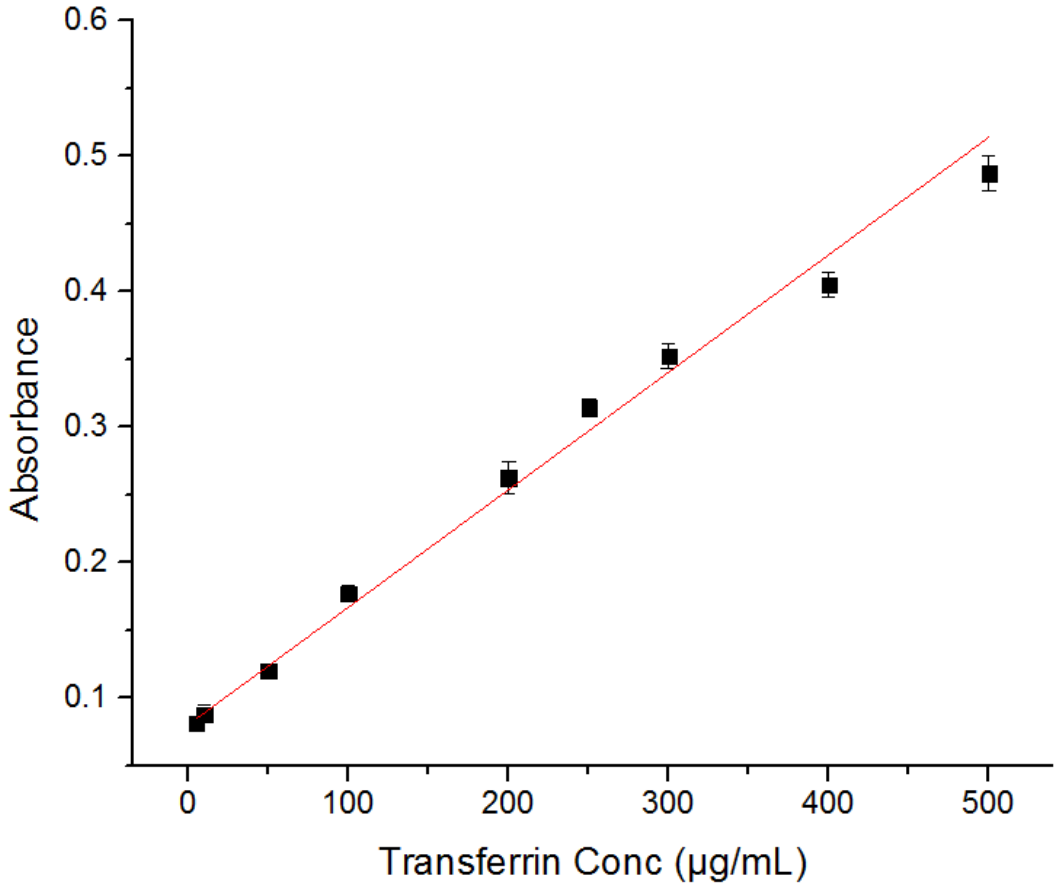

Figure 2.27: Standard Calibration Curve of transferrin for quantitative measurements of transferrin conjugated to dendrisomes. R^2 =0.991 and Pearson's r= 0.996. Results are expressed as mean ± SD (n= 4).

2.3.8 Differential scanning calorimetry (DSC) Studies

The DSC thermogram graphs showed sharp melting points for the pure compounds Solulan C24 and Span 60® at temperatures 31° C and 55° C and at times 4 min, 6 min and 9 min respectively. Both DSOLmC and DSOLmTf dendrisomes exhibited a small peak showing negative enthalpy at 38° C (5 min). However, the DSOLmC dendrisomes exhibited positive enthalpy at 115 ° C (21 min) while DSOLmTf dendrisomes showed negative enthalpy at 118 °C (22 min) (Figure 2.28). It was observed in DTPGSmd dendrisomes that even after 28 minutes of heating, no significant peak showing any form of melting or change in their structure was seen (Figure 2.29). This could be due to very strong electrostatic interactions between molecules. This experiment therefore demonstrates the formation of new delivery systems with different sets of electrostatic interactions.

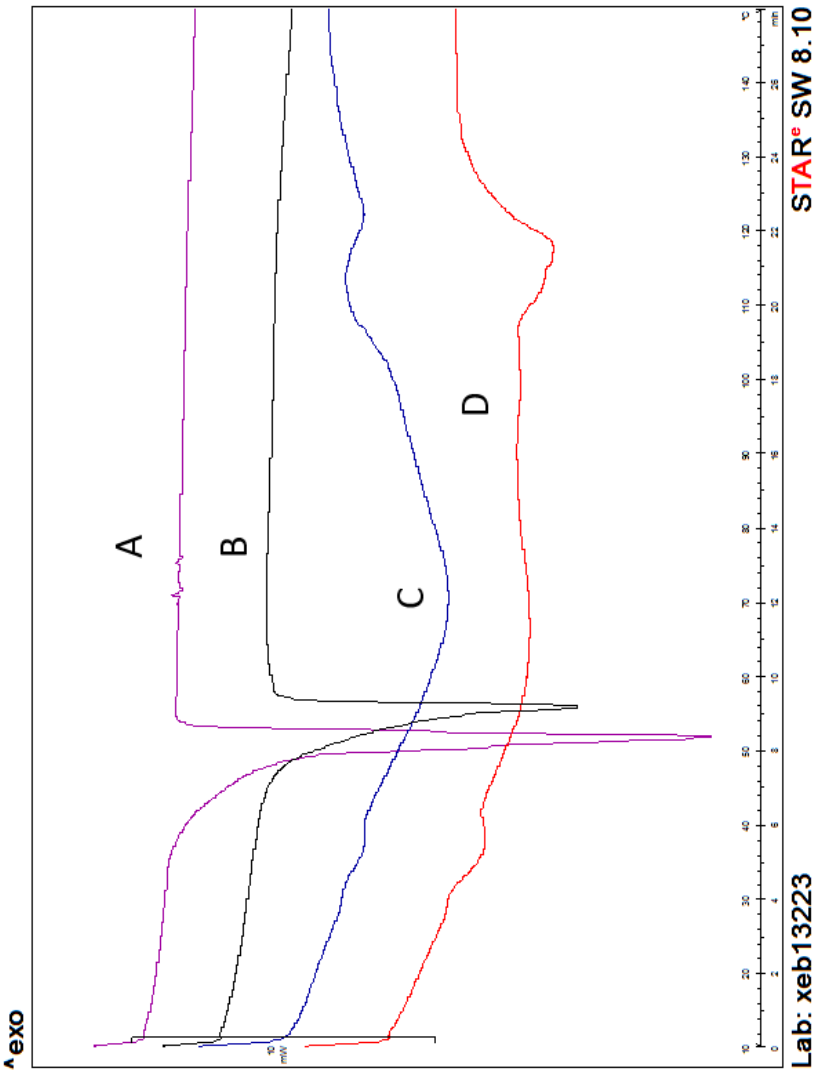

Figure 2.28: DSC thermograms of Solulan C24 powder (A), Span® 60 powder (B), DSOLmC (C) and DSOLmTf (D) in the region of 10–150 ºC at a scan rate of 5 ºC/min.

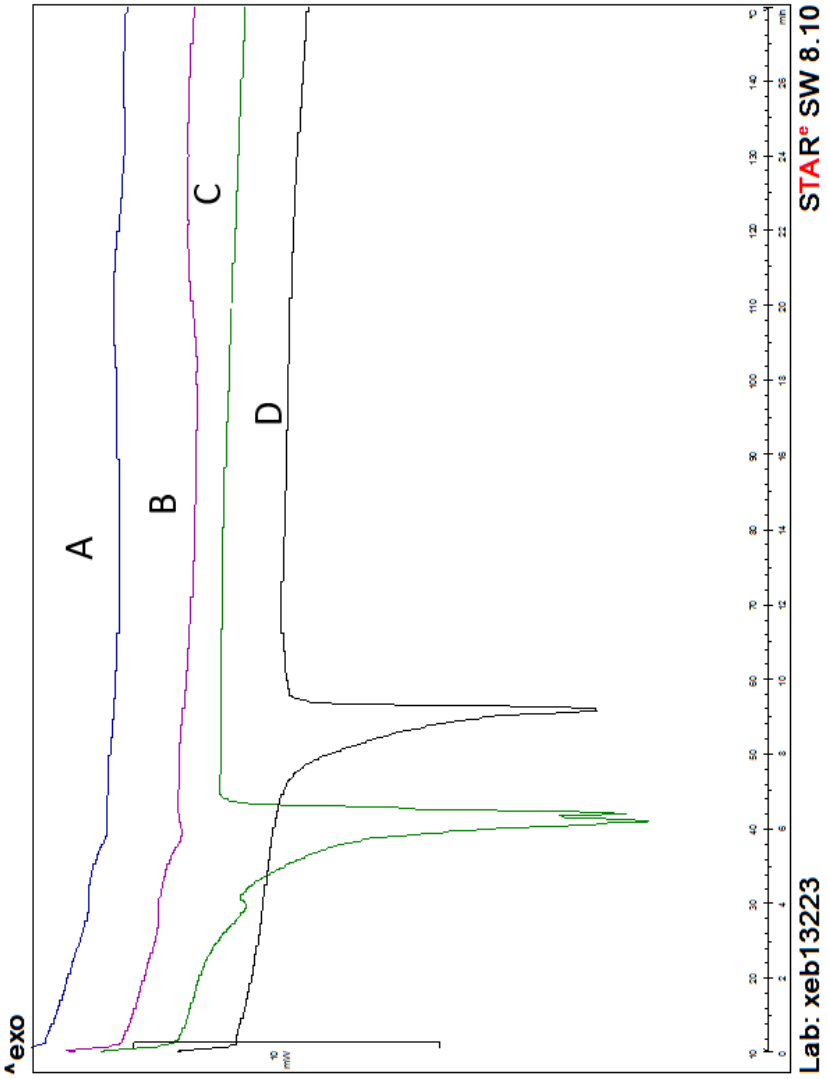

Figure 2.29: DSC thermograms of DTPGSmdC dendrisomes (A), DTPGSmdTf (B), TPGS powder (C) and Span® 60 powder (D) in the region of 10–150 ºC at a scan rate of 5 ºC/min.

2.3.9 Shelf-life Stability studies

Shelf-life stability studies at 25ºC was carried out over a period of 3 months. The DTPGSmd dendrisomes were removed from the study after 1 month due to physical instability. The DSOLm dendrisomes showed good stability for both the DSOLmTf and the DSOLmC dendrisomes for the size and PDI up to 3 months with statistically significant differences observed at 1 and 3 months between DSOLmTf and DSOLmC dendrisomes. It was observed that there was significant statistical difference for the size and PDI values of the DTPGSmd dendrisomes for size measurements at 3 months and for PDI measurements at 1 month (Figures 2.30-2.33). However, the size measurements for all the dendrisomes were less than 500 nm and the PDI measurements were all less than 0.5.

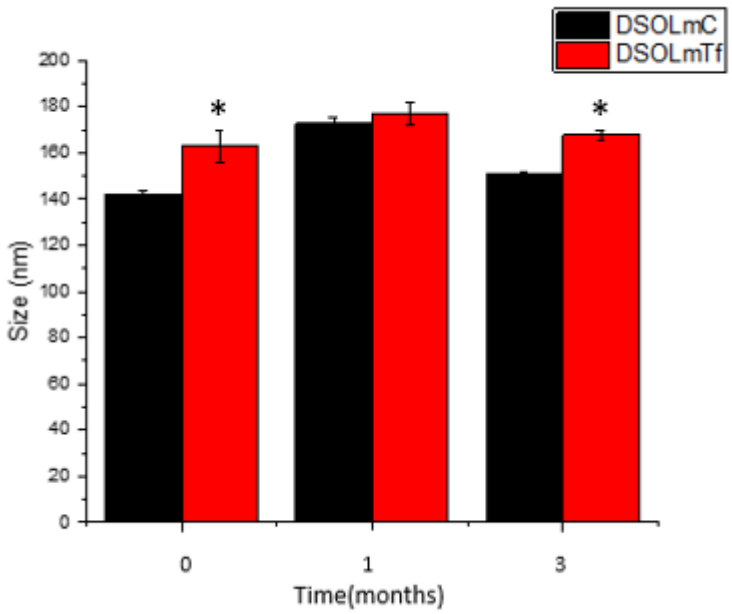

Figure 2.30: Size measurements for DSOLm dendrisomes for shelf-life stability studies (*: p<0.05: highest size measurement vs other treatments). Results are expressed as mean ± SEM (n=3).

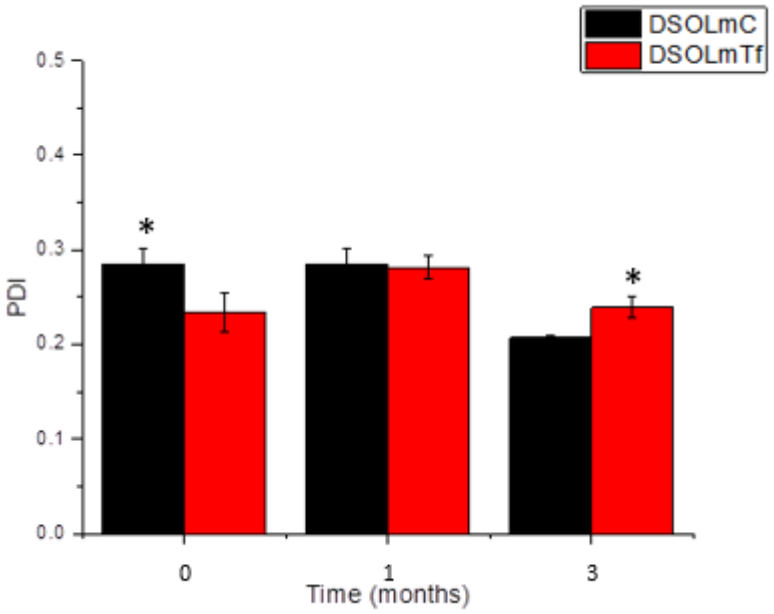

Figure 2.31: PDI measurements for DSOLm dendrisomes for shelf-life stability studies (*: p<0.05: highest PDI measurement vs other treatments). Results are expressed as mean ± SEM (n=3).

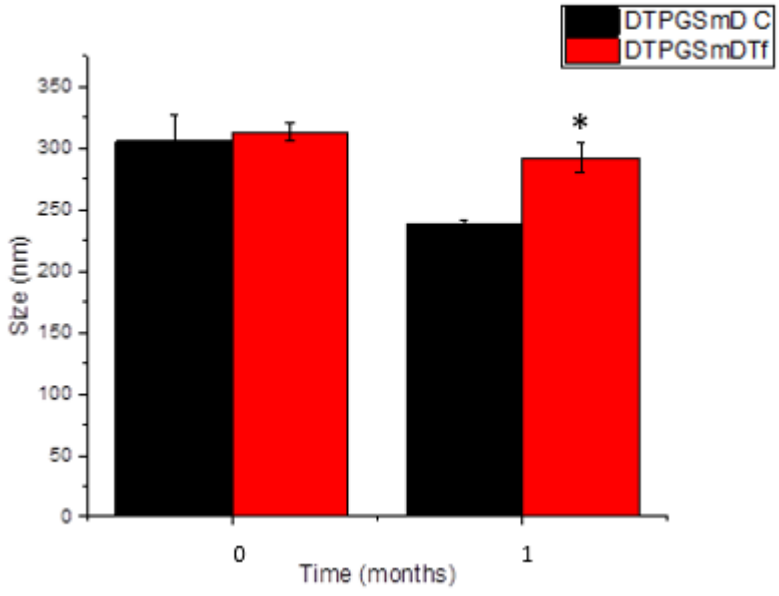

Figure 2.32: Size measurements for DTPGSmd for shelf-life stability studies (*: p<0.05: highest size measurements vs other treatments). Results are expressed as mean ± SEM (n=3).

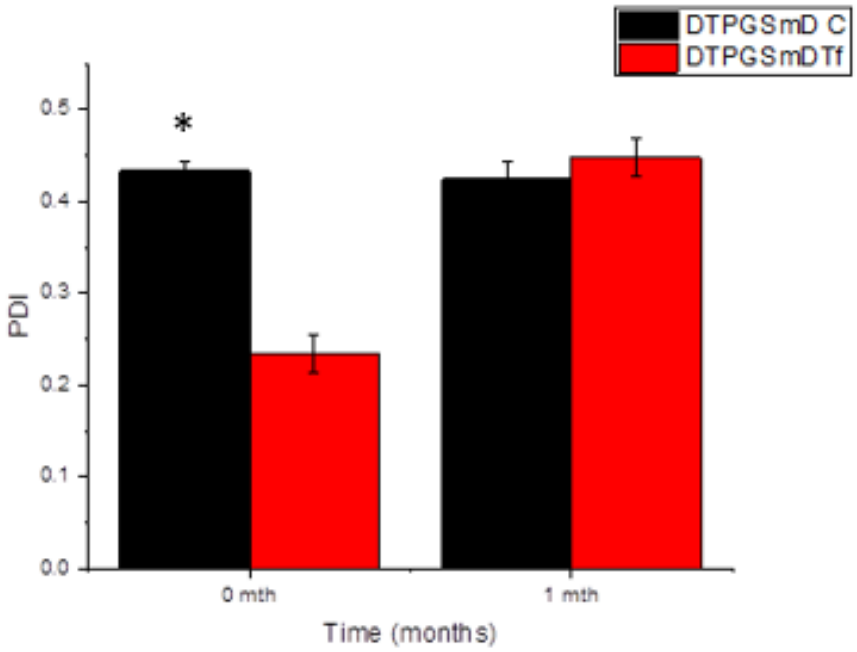

Figure 2.33: PDI measurements for DTPGSmd dendrisomes for shelf-life stability studies (*: p<0.05: highest PDI measurements vs other treatments). Results are expressed as mean ± SEM (n=3).

2.3.10 Atomic Force microscopy (AFM)

Atomic Force microscopy (AFM) pictures showed that the DSOLmTf, DSOLmC and DTPGSmdTf dendrisomes have a spherical structure in 3-dimensional images and are less than 200 nm in size (Figure 2.34 and 2.35).

A/

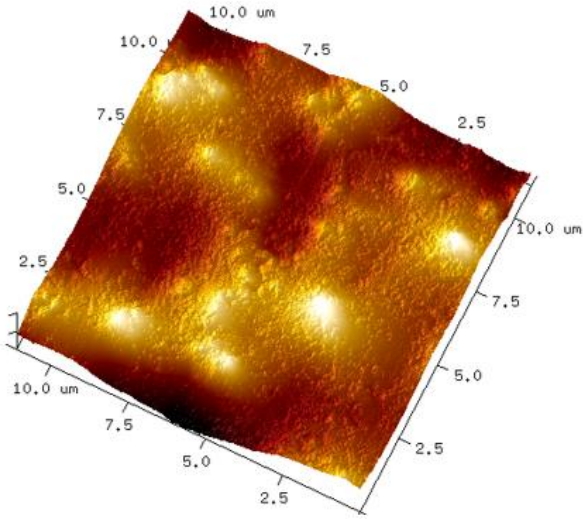

B/

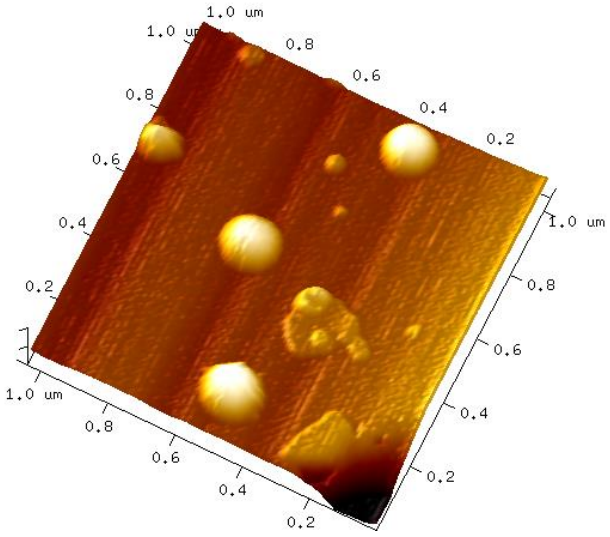

Figure 2.34: Atomic force microscopy (AFM) scans of DSOLmTf (A) and DSOLmC (B) dendrisomes showing the 3-dimensional spherical shape of dendrisomes.

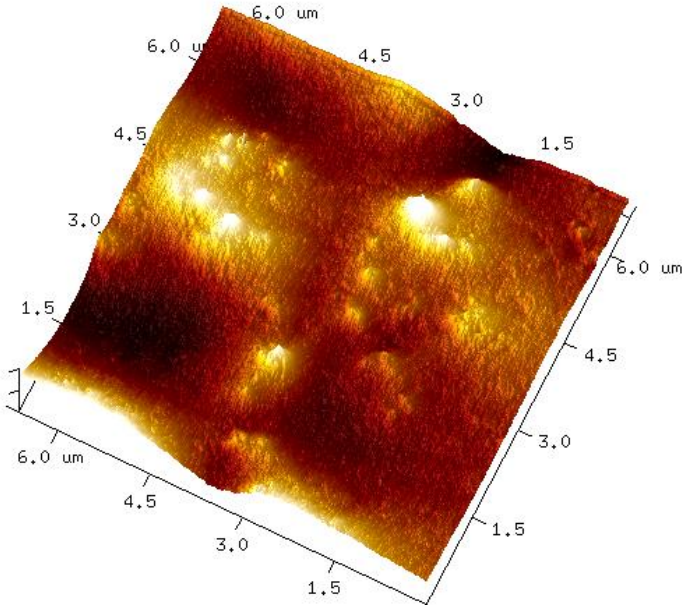

Figure 2.35: Atomic force microscopy (AFM) scans of DTPGSmdTf dendrisomes showing the 3-dimensional spherical shape of dendrisomes.

2.4 Discussion

The Z- average size of the dendrisomes formulated were found to be between 180.1 ± 1.1 nm to 456.8 ±31.5 nm for the non-PEGylated dendrisomes and 142.3 ±1.59 nm to 313.44±7.83 for the PEGylated dendrisomes. A size less than 500nm was to ensure that the dendrisomes could be taken up into the tumour vasculature either through passive targeting or active targeting. Probe sonication has been proved to cause reduction of particle size of niosomes (Sezgin-Bayindir and Yuksel 2012). It was on this basis that this method was used to formulate the dendrisomes formulated in this project. Purification of the dendrisomes was done to ensure that unreacted ingredients were removed. An example of the importance of the purification of dendrisomes was shown in a study that confirmed that free Solulan C24 solution caused increased toxicity on intestinal epithelial cells from man (Caco-2 cell monolayers) when compared to that of Solulan C24 incorporated in the bilayers of niosomes, which had cell viability of 100% when tested with MTT assay (Dimitrijevic *et al.,* 1997).

The zeta potential for the non-PEGylated dendrisomes were found to be neutral while zeta potential of the PEGylated DSOLm, DSOLmDox, DTPGSmd and DTPGSmdDox dendrisomes showed that the dendrisomes formulated were slightly positively charged with zeta potential values 5.09± 3.20 to 14±0.79. Though neutral charges were obtained by the non-PEGylated dendrisomes, DNA condensation studies demonstrated that they were still able to carry DNA successfully. The PDI studies showed that though the non-PEGylated dendrisomes had a slightly higher PDI than the PEGylated dendrisomes, all the dendrisome formulations had a PDI less than 0.6. This is desirable for ensuring enhanced intracellular uptake.

TEM confirmed that the lipid mix chosen was able to form vesicles with the DAB-Am-16 dendrimer, showing a spherical shape with black structures (Parimi *et al.*, 2008). A spherical shape would ease entry in passive targeting the porous tumour vasculature. The TEM also confirmed the size of the DSOLm dendrisomes as less than 200 nm. Formulation of DEN-DHP dendrisomes after many formulation attempts proved unsuccessful.

The DNA condensation studies carried out on the non-PEGylated DEN-SOL dendrisome formulations and the PEGylated DSOLm and DTPGSmd dendrisomplexes at the ratios tested showed steady fluorescence over the 24 h period of the experiment. This shows that the addition of a lipid blend to the DAB-Am-16 dendrimers to increase the stability worked. The DNA condensation studies for DSOLm and DTPGSmd dendrisomes showed that both formulations had percentage DNA condensation higher than 75% for all dendrisome: DNA complex ratios with all the DTPGSmdTf: DNA ratios having percentage DNA condensation higher than 90%. All the dendrisome: DNA complex ratios were stable at 24 h with little or no significant change in the percentage DNA condensation. As stability of DNA to ensure high therapeutic efficacy *in vivo*, these results point towards the possibility of this happening. Though the DEN-SOL dendrisomes demonstrated a neutral charge, they successfully condensed DNA. This result correlates with other studies by Sadeghizadeh *et al.,* where neutral charged nanocarriers have been demonstrated to have the capacity to condense DNA and successfully cause gene expression (Sadeghizadeh *et al.,* 2008). However, the mechanism of action was not mentioned, hence other bonding mechanisms like covalent bonding could be the cause. The DSOLm and DTPGSmd dendrisomes

(PEGylated dendrisomes) were found to be positively charged, thus it is being proposed that electrostatic binding is the mechanism action that enables these PEGylated dendrisomes successfully carry DNA successful condensation of DNA molecules which are negatively charged. The gel retardation assay carried out on the DSOLmTf dendrisomes gave visual confirmation that dendrisome and DNA complexation had successfully taken place. The gel retardation assay for the DTPGSmd dendrisomes will also be carried out soon.

The encapsulation efficiency studies carried out for the Tf-bearing and non- targeted DSOLm and DTPGSmd dendrisomes encapsulating doxorubicin showed that both formulations had a high entrapment efficiency. This proved that dendrisomes have the capacity to encapsulate drugs. However, the DSOLm dendrisomes had a higher entrapment efficiency than the DTPGSmd dendrisomes. Drug release studies also showed that the DSOLm dendrisomes had a higher initial percentage doxorubicin release than the DTPGSmd dendrisomes of the entrapped doxorubicin. This could be attributed to the fact that DSOLm dendrisomes are unilamellar structures and as such they have only one bi-lipid layer as compared to the proposed multiple bi-lipid layer of DTPGSmd dendrisomes. Hence drug entrapment into the dendrisome core will be easier and the release of the entrapped drug will also be easier. This could be attributed to the fact that the DSOLmDox dendrisomes are unilamellar vesicles which would have a larger core and a thinner lipid bilayer thereby enhancing entrapment of the doxorubicin in the dendrisomes. This was also seen to affect the percentage drug release of doxorubicin after 10 days, as it was observed that the percentage drug release of the doxorubicin from DSOLmDox dendrisomes was found to be higher than that of DTPGSmdDox at various pH.

Both formulations had a percentage doxorubicin release less than 50% at 10 days, however both formulations showed a sustained release up to day 10. The sustained release profile was desirable. The low percentage cumulative drug release for the dendrisomes was similar to that observed by the dendrisomes formulated by Al-Jamal *et al.,* who attributed that electrostatic forces could be the cause of this low drug release pattern (Al-Jamal *et al.,* 2005). Drug release studies at 37 ^{o}C and pH 7.4 by another group on amphiphilic triblock poly(2-ethyl-2-oxazoline)–PLA-g–PEI (PEOz–PLA-g–PEI) micelles encapsulating doxorubicin, showed a sustained drug release less than 10% over four days with no apparent initial burst release but with an increase in Dox release at 75 h which they stated could be correlated with degradation/erosion of the copolymer micelles (Gaspar *et al.*, 2014). Those hybrid micelles were used for the co-delivery of minicircle DNA and doxorubicin. Min *et al.*, and Gaspar *et al.,* stipulate that high retention and low drug release of the anti-tumor drugs in core of nanocarriers would help decrease off-target cytotoxic effects of the encapsulated drug, and hence increase direct anti-tumour effect inside the tumours, when such nanocarriers are administered *in vivo* (Min *et al.,* 2015 and Gaspar *et al.,* 2015). At day 10 DSOLmDox dendrisomes had the highest percentage cumulative doxorubicin release at 14.6% at pH 6.5. This is an indication that the drug could still be released *in vivo* over a prolonged period of time. This is desirable as this could lead to increased efficacy of the formulation *in vivo*.

The disappearance of the sharp melting point peaks in the DSC thermograms of the DSOLm and DTPGSmd dendrisomes was a confirmation that new compounds had been formulated with interactions that resulted in a different thermodynamic behaviour

from the pure constituents that they were formulated from. The DSC thermograms also showed that the combination of lipid blends with DAB-Am-16 dendrimer changed the thermotropic behaviour of the compound formed when compared with the lipid blends alone. The results obtained were similar to that obtained in previous research studies carried out on other dendrimer and lipid blend combinations (Gardikis *et al.,* 2006; Ionov *et al.,* 2011; Wrobel *et al.,* 2011). It was also observed in DTPGSmd dendrisomes that even after 28 minutes of heating, no significant peak showing any form of melting or change in their structure was seen. This could be due to very strong electrostatic interactions between molecules. In the DSOLmC dendrisomes, an endothermic reaction was observed, resulting in a positive peak at 115^{o} C (20 min) while DSOLmTf dendrisomes showed an exothermic reaction at 120^{o} C (22 min).

2.5 Conclusion

The aim of preparing and characterising novel targeted dendrisomes that had the capability to encapsulate anticancer drug doxorubicin, complex plasmid encoding β-galactosidase was achieved. The TEM micrographs and AFM scans confirmed that these novel dendrisomes are spherical in shape. Encapsulation efficiency and drug release studies demonstrated that these novel dendrisomes had high encapsulation efficiency with doxorubicin and a slow release rate respectively. DNA condensation and Gel retardation studies confirmed the capability of these novel dendrisomes to complex plasmid encoding β-galactosidase which was a major aim. DSC studies confirmed that new compounds had been formed. Shelf-life stability studies showed that the dendrisomes formulated with Solulan C24 were more stable than those formulated with TPGS dendrisomes. The foregoing results gave credence to the fact

that *in vitro* experiments could be proceeded to ascertain the capabilities of these novel dendrisomes in selected cancer cell lines.

CHAPTER 3: IN VITRO EVALUATION

3.1 Introduction

Cell culture refers to the process of cultivating and growing the cells of multicellular organisms (plants or animals) in specially formulated containers under a controlled environment of temperature and gas (Britanica.com 2017). Cell lines are immortalized cells that have the capacity to keep proliferating under controlled favourable conditions. They have the advantages of proving an unlimited supply of standardised biological material, are cost effective, easy to handle and do not require specialised ethical approval for handling (Kaur and Dufour, 2012). Cell culture is used as a preliminary step to justify the use of animals for testing new drug delivery systems. Cell culture helps in characterising novel compounds and provides information on the efficacy of these compounds (Nuffield Council on Bioethics, 2005). The three cancer cell lines used for this project were A431, B16F10-Luc-G5 and T98G.

A431 human epidermoid carcinoma (ATCC® CRL-1555™) is an adherent cell line established from solid tumours of the skin/epidermis of an 85-year-old female (Giard *et al.,* 1973). This cell line forms fast-growing subcutaneous tumours when inoculated in immunosuppressed mice and forms colonies in soft agar. A431 cells are known to show overexpression of transferrin receptors.

T98G human glioma cells (ATCC® CRL-1690™) are adherent cells that were derived from the human glioblastoma multiform tumour of a 61-year old Caucasian male (Bleeker *et al.,* 2012). Glioblastoma, also known as or astrocytoma WHO grade IV, is the most deadly brain primary brain cancer found in humans. Its poor prognosis is worse in the elderly (Bleeker *et al.,* 2012).

B16F10-Luc-G5 mouse melanoma is a luciferase expressing cell line that has been obtained from B16-F10-Luc-G5 mouse melanoma cells that have been modified to emit visible light. They also have the capability to produce measurable tumours that can be calipered after 10 days. These characteristics make them useful as *in vivo* tumour models in mice through bioluminescent imaging (Jenkins *et al.,* 2003; Caliper Life Sciences, 2008). Melanoma is a type of skin cancer that originates from the malignant alteration of melanocyte cells of the skin. It has been observed that A431, T 98G and cell line overexpresses transferrin receptors (Lemarié *et al.,* 2012). This attribute made these cell lines good candidates to demonstrate the gene effect of the novel targeted dendrisomes.

3.1.1 Cell Line Transfection

Transfection is a technique that comprises of the introduction of foreign nucleic acids into cells to cause a modification in the function of cells thereby leading to an alteration in the protein products that they produce. Transfection involves the investigation of genes and protein products made from expression. Transfection is used for investigating gene function and gene regulation in cells as well as protein function (Kim and Eberwine 2010).

Transfection also called gene expression as earlier mentioned, can be done through two main methodologies. The methodology chosen depends on the desired response that is wanted, and the nature/ characteristic of the genetic material being utilized. The first approach involves the conveyance of plasmid DNA or equivalent constructs, for the expression of the gene desired, with the use of a suitable promoter intracellularly.

These results demonstrated that there was an increase in the production of a specific cell protein intracellularly, thereby exerting required effect on the cell. The second methodology causes the reverse effect, it decreases the production of the target protein activity via the delivery of oligomeric genetic material like anti sense oligodeoxynucleotides or siRNA (short interfering RNA). This leads to the stoppage of harmful mRNA expression and/or production of harmful proteins. This method is also referred to as gene silencing (Dufès *et al.*, 2005; Shcharbin *et al.*, 2009; Shcharbin *et al.*, 2010). For this project, the first approach was the methodology used for gene delivery of plasmid DNA encoding β-galactosidase and DNA encoding TNF-α. This was because an increase in β-galactosidase activity and TNF-α activity respectively intracellularly was what was required for this project.

β-galactosidase was the assay used in ascertaining the transfection efficacy of the dendrisomes formulated in this project. β-galactosidase assay was an assay introduced by Jeffrey Miller in 1972 for the determination of the amount of β-gal expressed in a cell with the using the substrate o-nitrophenyl-β-D-galactoside (ONPG). Due to this discovery, the Miller units used in expressing the extent/degree of gene expression in cell samples were named after him (equation 2.5) (Miller, 1972 cited in Shcharbin, 2010).

Equation 2.5

$$1 \text{ Miller Unit} = 1000 \times \frac{Abs_{420} - (1.75\ X Abs_{550})}{t\ X\ v\ X\ Abs_{600}}$$

The β-galactosidase assay is based on the fact that on cellular uptake of ONPG into β-galactosidase transfected cells, the β-galactosidase enzyme causes cleavage of the ONPG molecules. The cleavage of the colourless substrate ONPG leads to the formation of the yellow chromophore o-nitrophenol (ONP) via hydrolysis that can be measured through spectrophotometry (Figure 3.1) (Griffith and Wolf, 2002).

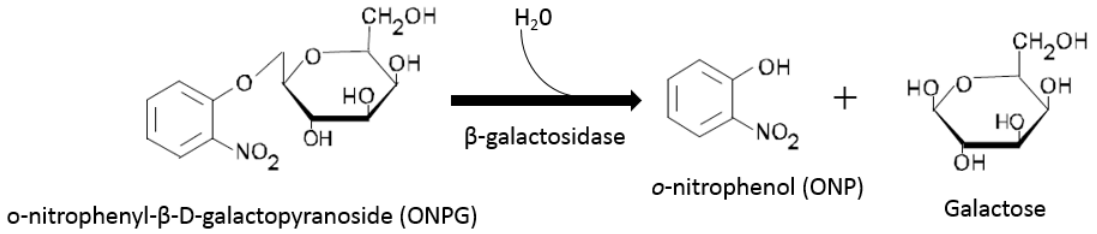

Figure 3.1: Schematic representation of the cleavage of O-nitrophenyl-beta-D-galactopyranoside (ONPG) by β-galactoside in transfection (Adapted from Held, 2007)

3.1.2 Anti-proliferative assay: MTT assay

One of the reasons that nano-carriers have been introduced in drug delivery as said earlier is to ensure safety of the normal cells without compromising the efficacy of the drug/ therapeutic gene when administered for cancer therapy. The 3-[4,5-dimethylthiazol-2-yl]-2,5 diphenyl tetrazolium bromide (MTT) assay is a quantitative, colorimetric, biological assay used to measure cell viability, cell survival and cytotoxicity, after treatment with drugs or toxins (Mosmann 1983; Sumantran 2011). This assay was introduced by Mosmann in 1983. MTT is a tetrazolium salt that is a yellow dye. The MTT assay is based on the principle that living cells have the capacity due to mitochondrial activities, to convert the reagent MTT to its insoluble form, dark blue/ purple formazan crystals. This conversion occurs only in living cells. When these

formazan crystals are dissolved with solvents like Dimethyl sulfoxide (DMSO), the absorbance/optical density can be measured using a spectrophotometric plate reader at a wavelength of 570nm (Mosmann, 1983; Aldawsari *et al.*, 2011). A high absorbance value is an indication of a large amount of cell proliferation/ viable cells. No colour change will be observed in the cells that are dead. The MTT assay is widely used in drug delivery studies due to its ease, rapidity and high sensitivity (Sumantran, 2011).

3.1.3 Confocal laser scanning microscopy (CLSM)

Confocal microscopy is a microscopic technique that gives high resolution, high contrast 3-dimensional images without the problem of artefacts seen in conventional microscopic techniques. Confocal microscopy was developed and patented by Marvin Minsky in 1955. The principle behind confocal microscopy was developed and patented by Marvin Minsky in 1955. This principle is based on using optical imaging to generate a virtual plane several micrometers thick, within specimens (Nwaneshiudu *et al.,* 2012). The contrast modes available in the confocal laser scanning microscope has made it a valuable tool in biology and the biomedical sciences, as well as in materials sciences (Claxton *et al.*, 2006).

A modern confocal laser scanning microscope consists of the laser system, electronic detectors, a computer, and a beam scanning unit. The 3-5 laser systems found in a confocal laser scanning microscope are controlled by high-speed acousto-optic tunable filters (AOTFs) which provide flexibility alongside precision in the regulation of the excitation wavelength and intensity of the laser beams. The confocal microscope has the several advantages over the conventional microscopes. It has the ability to capture

images that are thick greater than 2 µm, to eliminate or reduce background information (noise), it has the capacity to collect serial optical sections and control the depth of the field of view (Claxton *et al.,* 2006).

Confocal microscopy enhances the imaging of thick objects (up to 50 µm thick) by employing spatial filtering techniques that remove the out-of-focus light or glare in specimens whose thickness exceeds the immediate plane of focus, before the final image is formed. This leads to the production of images specimens that are very sharp and very detailed (Claxton *et al.,* 2006; Murray, 2011; Nwaneshiudu *et al.,* 2012). The use of fluorescence dyes also called fluorophores are used for labelling specimens which enable the viewing of specimens when using incident epifluorescent light. The confocal microscope generates images of the specimen by swiftly and serially scanning the area of focus in the X–Y plane using the appropriate lasers. This leads to the formation of several horizontal virtual-sectioned images. As scanning continues, signals from the detector are fed into a computer that collates all the "point images" of the sample and then serially builds up the image pixel by pixel leading to the production of the final image (Murray 2011; Nwaneshiudu *et al.,* 2012)

3.2 Aims and Objectives

The aim of chapter 3 is to investigate the effect of the dendrisomes successfully formulated in chapter 2 in cancer cell lines A431, T98G and B16F10-Luc-G5 *in vitro.* Investigation into the capabilities of the dendrisomes formulated for gene expression, qualitative analysis of cellular uptake as well as anti-proliferative activity studies was carried out.

3.3 Materials and Methods

Table 3.1 Materials and reagents

Materials/reagents	**Supplier/source**
Ampicillin	Sigma Aldrich (Poole, UK)
A431 human epidermoid carcinoma line	European Collection of Cell Cultures (Salisbury, UK).
B16-F10-Luc-G5 Bioware® mouse melanoma	Calliper Life Sciences (Hopkinton, MA)
Dulbecco's Modified Eagle Medium (DMEM) media	Invitrogen, ThermoFisher Scientific (Paisley, UK)
Dendrisomplexes	Formulated as described in Chapter 2
Transferrin bearing dendrisomplexes	Formulated as described in Chapter 2
Ethylenediaminetetraacetic acid (EDTA)	Sigma-Aldrich, (Poole, UK)
Expression plasmid encoding β-galactosidase (pCMVsport β-galactosidase)	Invitrogen, ThermoFisher Scientific (Paisley, UK)
Foetal bovine serum (FBS)	Invitrogen, ThermoFisher Scientific (Paisley, UK)
FluoroNunc® fluorescence 96-well Plates	Sigma-Aldrich (Poole, UK)
Isopropanol	Sigma-Aldrich (Poole, UK)
Label IT® Cy3 Nucleic Acid Labelling kit	Cambridge Biosciences, (Cambridge, UK)
o-nitrophenyl- β-D-galactosidase (ONPG)	Sigma-Aldrich, UK
pCMVsport β-Galactosidase	Invitrogen, ThermoFisher Scientific (Paisley, UK)
Passive Lysis Buffer (5x)	Promega, (Southampton, UK)
Penicillin-Streptomycin	Invitrogen, ThermoFisher Scientific (Paisley, UK)
Phosphate buffered saline tablet	Sigma-Aldrich, (Poole, UK)
Quanti-iT™ PicoGreen® dsDNA reagent	Invitrogen, ThermoFisher Scientific (Paisley, UK).
Roswell Park Memorial Institute (RPMI) 1640 medium	Invitrogen, ThermoFisher Scientific (Paisley, UK)
Dimethyl sulfoxide (DMSO)	Sigma-Aldrich, UK
T98G human glioma cell line	European Collection of Cell Cultures (Salisbury, UK).
Triton-X	Sigma-Aldrich (Poole, UK)
Trypsin	Invitrogen, ThermoFisher Scientific (Paisley, UK)
Tumour necrosis factor (TNF)α (pORF9-mTNFα)	InvivoGen, (San Diego, CA)

3.4 Cell Culture

A431 and T98G cells were grown as monolayers in DMEM while B16-F10-Luc-G5 cells were grown in RPMI-1640 medium supplemented with 10% (v/v) foetal bovine serum, 1% (v/v) L-glutamine and 0.5% (v/v) penicillin-streptomycin. The cells were cultured at 37 °C in a humid atmosphere of 5% CO_2 (Aldawsari *et al.,* 2011)

3.4.1 Preparation of dendrisomplexes

Dendrisomplexes of various dendrisome: DNA ratios were prepared in DMEM medium for A431 and T98G cells and RPMI medium for B16-F10-Luc-G5 cells for transfection studies, cellular uptake studies and anti-proliferative assay (MTT). Formation of dendrisomplexes was done through manual mixing with a pipette and pipette and pipette tips just prior to carrying out dendrisomplex characterization experiments (Table 3.2 and Table 3.3). The plasmid encoding β- galactosidase (pCMV β gal) was the DNA utilized while for the anti-proliferative assay the plasmid encoding TNF-α was the DNA utilized.

Table 3.2: DEN-SOL dendrisomes DNA complex formulation for Transfection Studies

Dendrisome: DNA Ratio	**Dendrisome Portion of Dendrisomplex (1 mL)**		**DNA portion of dendrisomplex (1 mL)**
	dendrisome dispersion (µL)	**Medium (µL)**	**DNA stock (10µg/mL) in medium (µL)**
10:1	200	800	1000
5:1	100	900	1000
2:1	40	960	1000
1:1	20	980	1000
0.5:1	10	990	1000
DNA only	-	-	1000

Table 3.3: DSOLm and DTPGSmd dendrisomes DNA complex formulation for Transfection Studies

Dendrisome: DNA Ratio	Dendrisome Portion of Dendrisomplex (1 mL)		DNA portion of dendrisomplex (1 mL)
	dendrisome dispersion (µL)	Medium (µL)	DNA stock (10µg/mL) in medium (µL)
10:1	400	600	1000
5:1	200	800	1000
2:1	80	920	1000
1:1	40	960	1000
0.5:1	20	980	1000
DNA only	-	-	1000

3.4.2 *In vitro* evaluation of gene expression in cancer cells following treatment with dendrisome- DNA complexes

The A431, B16-F10-Luc-G5 and T98G cells were seeded at 2.10^3 cells per well in 96-well plates in triplicates and incubated at 37 ^oC, 5% CO_2 for 72h prior to treatment. The seeded plates were incubated at 37 °C, 5% CO_2, for 72 hours. After the incubation period, treatment of the seeded plates was done using dendrisomplexes (0.1 mL)/well formed by dendrisomes complexed with plasmid encoding β- galactosidase (pCMV β gal) (1 µg DNA per well), using dendrisomes: DNA ratios 10:1, 5:1, 2:1, 1:1, 0.5:1 and DNA only (n=15). The plates were incubated at 37 °C, 5% CO_2, for another 72 hours.

Quantification of the expression of the β-galactosidase was done by ortho-nitrophenyl-β-D-galactopyranoside (ONPG) assay. The media was removed from the wells, followed by cell lysis by adding 50 µL 1X PLB Passive Lysis Buffer (PLB) solution to each well. Incubation was done for 20 min at 37 °C. ONPG 1.33 mg/mL in 2X Assay buffer (the assay buffer (2 mM magnesium chloride, 100 mM mercaptoethanol, 200mM sodium phosphate buffer, pH 7.3) solution was then added unto each well

containing the PLB (50µL/well) and the plates were protected from light and incubated for 2 h. The absorbance of the treated wells was read at 405 nm with a microplate reader (Thermo Lab Systems, Multiskan Ascent Cheshire, UK).

3.4.3 Cellular uptake Experiments

3.4.2.1 Cellular uptake of Cy3-labeled DNA complexed with dendrisomes using Fluorescence microscopy

Cancer cell lines A431, B16-F10-Luc-G5 and T98G cells were seeded at 10^5 cells/well in 6-well plates, 24 h prior treatment. The wells were then treated with Tf-bearing and control DEN-SOL dendrisomes complexed with Cy3-labeled DNA (2.5 µg DNA / well). Control slides were treated with naked DNA only. The plates were then incubated for 24 h. After incubation, the cells were washed with 3 mL PBS and then fixed in 2 mL methanol for 10 min. Imaging of cellular uptake of the Cy3-labeled DNA into the cancer cell lines was carried out using fluorescence microscopy. Staining of the cells was done using DAPI-stained Vectashield. The cells were then examined using an epifluorescence microscope with DAPI excitation at 405 nm, (bandwidth: 415-491nm) and Cy3 excitation at 543 nm (bandwidth: 550-620 nm).

3.4.2.2 Cellular uptake of Cy5-labeled DNA complexed with dendrisomes using Confocal Laser Scanning Microscopy

Cancer cell lines A431, B16-F10-Luc-G5 and T98G cells were seeded at 10^5 cells/well in 6-well plates, 24 h prior treatment. The wells were then treated with Tf-bearing and control dendrisomes complexed with Cy5-labeled DNA (2.5 µg DNA/ well). Control slides were treated with naked DNA only. The plates were then incubated for 4 h at 37^o C, 5% CO_2. After incubation, the cells were washed three times with 3 mL PBS

and then fixed in 2 mL methanol for 10 min. Imaging of cellular uptake of Cy5 labelled DNA into the cancer cells was carried out using laser scanning confocal microscopy (Leica Microsystems Wetzlar, Germany). Staining of the cells was done using DAPI-stained hard set Vectashield®. The cells were then examined using a Leica TCS SP5 Confocal laser scanning microscope with DAPI excitation at 405 nm, (bandwidth: 415-491nm), doxorubicin excitation at 488 nm (bandwidth: 488-600 nm) and for Cy5-labelled DNA excitation at 650nm (bandwidth: 633-690nm).

3.4.4 Anti-proliferative assay: MTT assay

A standard MTT [3-(4, 5-dimethylthiazol-2-yl)-2, 5-diphenyl-tetrazolium bromide] assay was carried out to evaluate the anti-proliferative activity of the dendrisome formulations. Anti-proliferative activity of the empty transferrin-bearing and non-transferrin-bearing dendrisomes, dendrisomes entrapping doxorubicin and dendrisomplexes complexed with plasmid DNA encoding TNFα were assessed in A431, B16F10-Luc-G5 and T98G cancer cell lines. The cells were seeded at 2×10^3 cells per well in 96-well plates in triplicates and incubated at 37^o C, 5% CO_2 for 72h prior to treatment. The seeded plates were then treated with transferrin-bearing and control dendrisomes not encapsulating doxorubicin, transferrin-bearing and control dendrisomes entrapping doxorubicin, and dendrisomplexes entrapping doxorubicin at final concentrations of $2.56.10^{-5}$ to 50 μg/mL of doxorubicin and $6.81.10^{-6}$ to 13.3 μg of plasmid DNA encoding TNFα for 72h at 37^o C, 5% CO_2. After the 72 h incubation, 50 μL of MTT stock solution (5 mg/mL) was then added to each well, protected from light, and followed by a 4 h incubation at 37^o C, 5% CO_2. The medium was then removed, and 200 μL of DMSO was added into each well. The plates were left for 10

min. Absorbance of the treated cells in the wells was then measured at 570 nm using a plate reader. Dose–response curves were fitted to percentage absorbance values to obtain IC_{50} values. Anti-proliferative activity of the formulations was assessed by measurement of the growth inhibitory concentration for 50% of the cell population (IC_{50}). This experiment was carried out in three independent experiments with n=5 for each concentration level in each experiment (Lemarié *et al.*, 2012).

3.4.5 Statistical analysis

The results obtained were expressed as means ± standard error of the mean. Statistical significance was determined by one-way analysis of variance (ANOVA) followed by the Tukey multiple comparison post-test (OriginPro 9® software). Differences were considered as significant when $P < 0.05$.

3.5 Results

3.5.1 *In vitro* Evaluation of gene expression in cancer cells following treatment with dendrisome- DNA complexes

In vitro experiments using treatments of Tf-bearing DEN-SOL dendrisomplexes at different dendrisomes/DNA ratios (10:1, 5:1, 2:1, 1:1 and 0.5:1) on the cancer cell lines A431, T98G and B16-F10-Luc-G5 and, showed that transfection occurred across all three cell lines. In A431 and T98G cells, maximum gene expression was observed at ratio 10:1 ($6.021.10^{-3} \pm 0.05.10^{-3}$ µg/mL in A431 and $4.269.10^{-3} \pm 0.238.10^{-3}$ µg/ml in T98G cells). In B16-F10 cells, however, maximum gene expression ($8.716.10^{-3} \pm 0.208.10^{-3}$ µg/mL) was found at a ratio of 0.5:1 (Figure 3.2).

In vitro experiments using treatments of Tf-bearing DSOLm dendrisomplexes at different dendrisomes/ DNA ratios (10:1, 5:1, 2:1, 1:1 and 0.5:1) on the cancer cell lines B16-F10-Luc-G5, A431 and T98G, showed that transfection occurred across all three cell lines. In A431 and T98G cells, maximum gene expression was observed at ratio 10:1 ($2.45 \pm 0.08.10^{-3}$ U/mL in A431, $3.19 \pm 0.11.10^{-3}$ U/ml in T98G cells $1.8 \pm 0.02.10^{-3}$ U/mL in B16F10-Luc-G5 cells) (Figure 3.3).

A

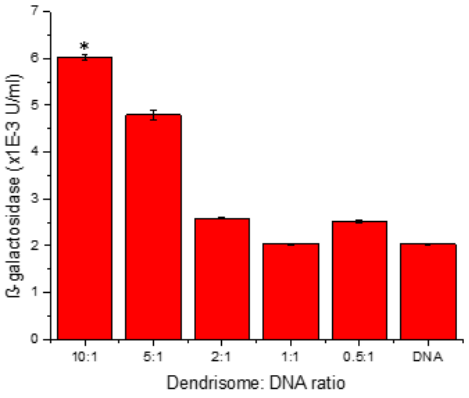

B

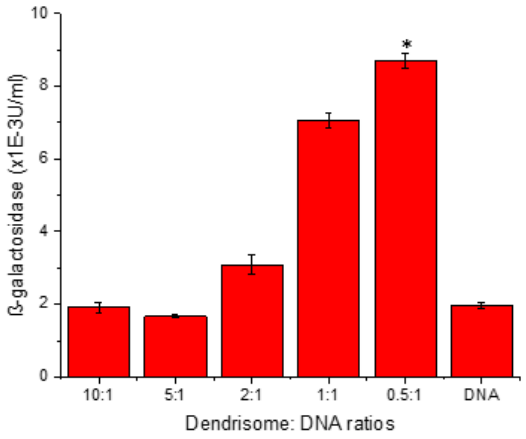

C

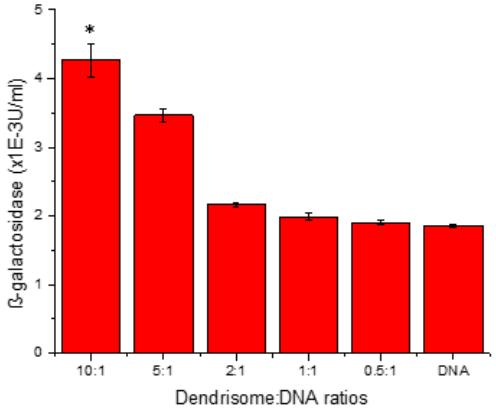

Figure 3.2: Transfection efficacy studies of A431 cells (A), B16F10-Luc-G5 cells (B) and T98G cells (C) treated with DEN-SOLTf dendrisomes complexed with DNA encoding β-galactosidase (DEN-SOLTf-DNA) at dendrisome: DNA ratios 10:1, 5:1, 2:1, 1:1, 0.5:1 and DNA only. Results are expressed as the mean ± SEM (n=15). (*: p<0.05: highest transfection vs other treatments)

A

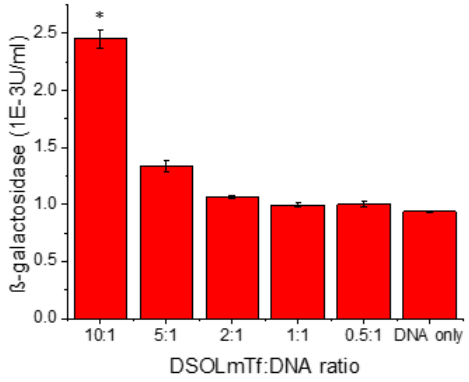

B

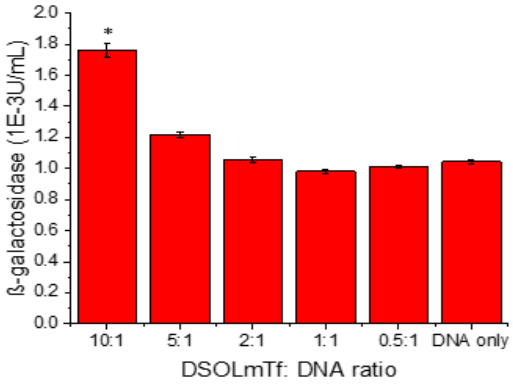

C

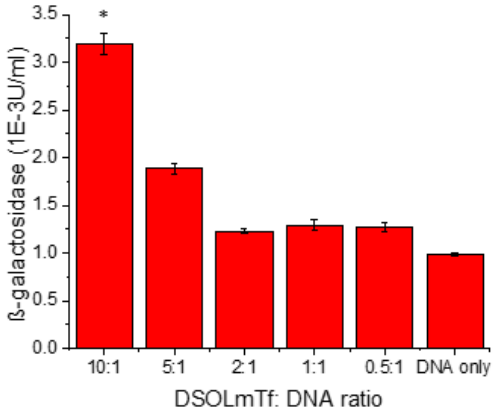

Figure 3.3: Transfection efficacy studies of A431 cells (A), B16F10-Luc-G5 cells (B) and T98G cells (C) treated with DSOLmTf complexed with DNA encoding β-galactosidase (DSOLmTf-DNA) at dendrisome: DNA weight ratios 10:1, 5:1, 2:1, 1:1, 0.5:1 and DNA only. Results are expressed as the mean ± SEM (n=15). (*: $p<0.05$: highest transfection vs other treatments).

Gene transfection *in vitro* experiments using treatments of Tf-bearing DTPGSmd dendrisomplexes at different dendrisomes/ DNA ratios (10:1, 5:1, 2:1, 1:1 and 0.5:1) were also carried out. Cancer cell lines B16-F10-Luc-G5, A431 and T98G, were experimented on and transfection was observed across all three cell lines (Figures 3.4). A431, B16F10-Luc-G5 and T98G cells showed maximum gene expression at ratio 5:1 (8.16±0.54 U/mL in A431, in B16F10-Luc-G5 cells 6.93±0.32 U/mL and 9.78±0.24 U/mL in T98G cells).

A

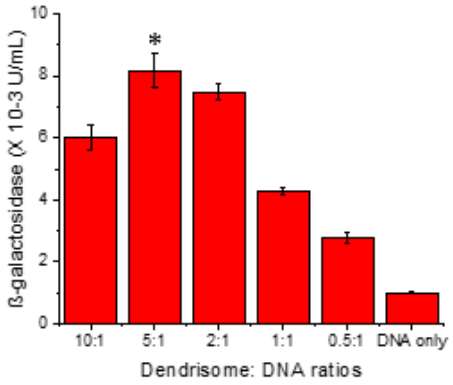

B

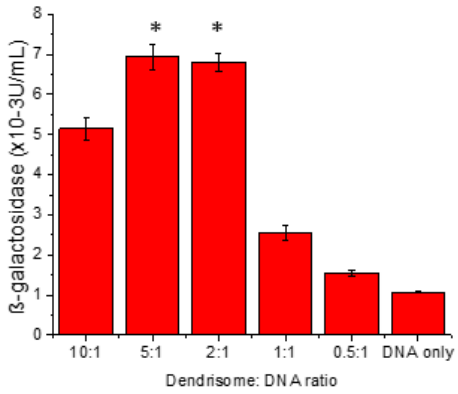

C

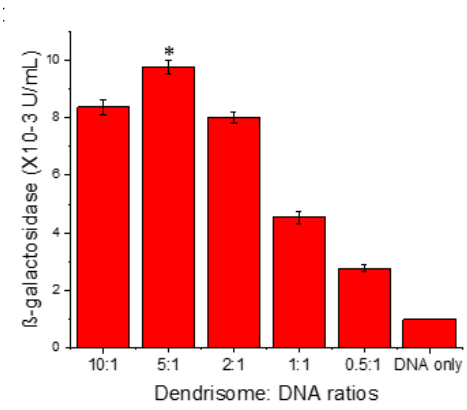

Figure 3.4: Transfection efficacy studies of A431 cells (A), B16F10-Luc-G5 cells (B) and T98G cells (C) treated with DTPGSmdTf dendrisomes complexed with DNA encoding β-galactosidase (DTPGSmdTf -DNA) at dendrisome: DNA weight ratios 10:1, 5:1, 2:1, 1:1, 0.5:1 and DNA only. Results are expressed as the mean ± SEM (n=15). (*: $p<0.05$: highest transfection vs other treatments).

3.5.2 Cellular uptake Experiments

3.5.2.1 Cellular uptake Experiments of Cy3-labeled DNA complexed with dendrisomes

Cellular uptake of Cy3-labeled DNA carried by Tf-bearing and control DEN-SOL dendrisomes was confirmed in the three cell lines by fluorescence microscopy. Cy3-labelled DNA was disseminated in the cytoplasm of the cells for the three cell lines. The DNA uptake appeared to be less pronounced in B16-F10 cell line (Figures 3.5 - 3.7).

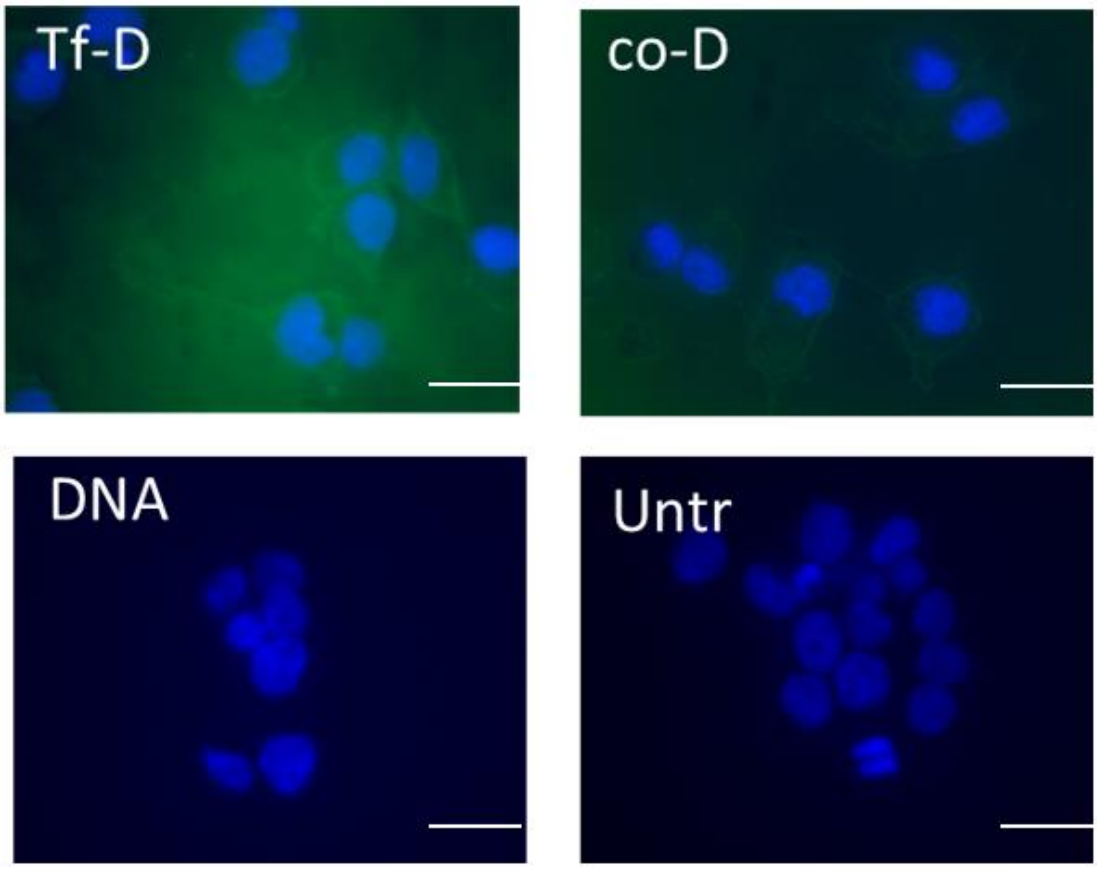

Figure 3.5: Epifluorescence microscopy imaging of the cellular uptake of Cy3-labelled DNA (2.5 µg DNA per well) either complexed with Tf-bearing DEN-SOL dendrisomes ("TF-D"), DEN-SOL control dendrisomes ("Co-D"), DNA only ("DNA") (Control: untreated cells) in A431 cell line (Blue: nuclei stained with DAPI (excitation: 405 nm, bandwidth: 415-491nm), green: Cy3-labelled DNA (excitation: 543 nm. bandwidth: 550-620 nm) (magnification: x 60) (Bar: 10 µm).

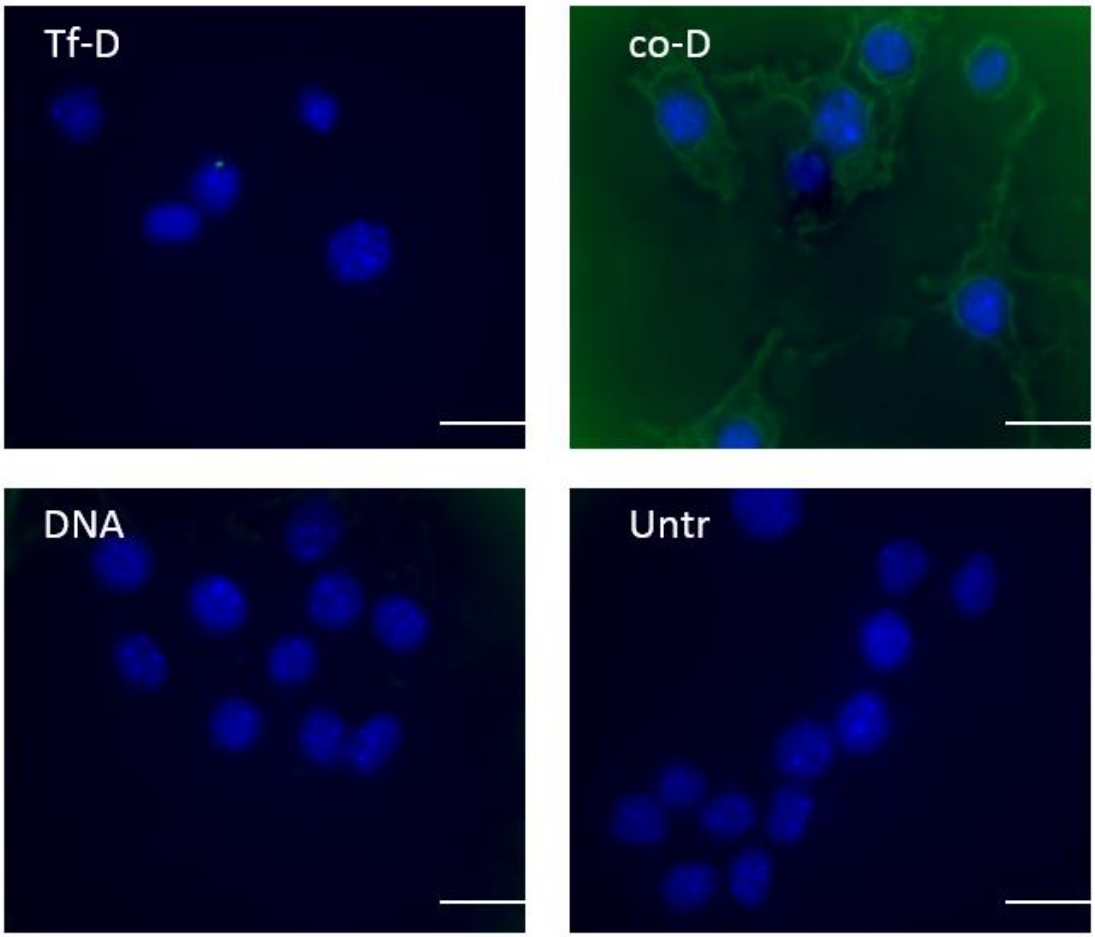

Figure 3.6: Epifluorescence microscopy imaging of the cellular uptake of Cy3-labelled DNA (2.5 µg DNA per well) either complexed with Tf-bearing DEN-SOL dendrisomes ("TF-D"), DEN-SOL control dendrisomes ("Co-D"), DNA only ("DNA") (Control: untreated cells) in B16-F10-Luc-G5 cell line (Blue: nuclei stained with DAPI (excitation: 405 nm, bandwidth: 415-491nm), green: Cy3-labelled DNA (excitation: 543 nm. bandwidth: 550-620 nm) (magnification: x 60) (Bar: 10 µm).

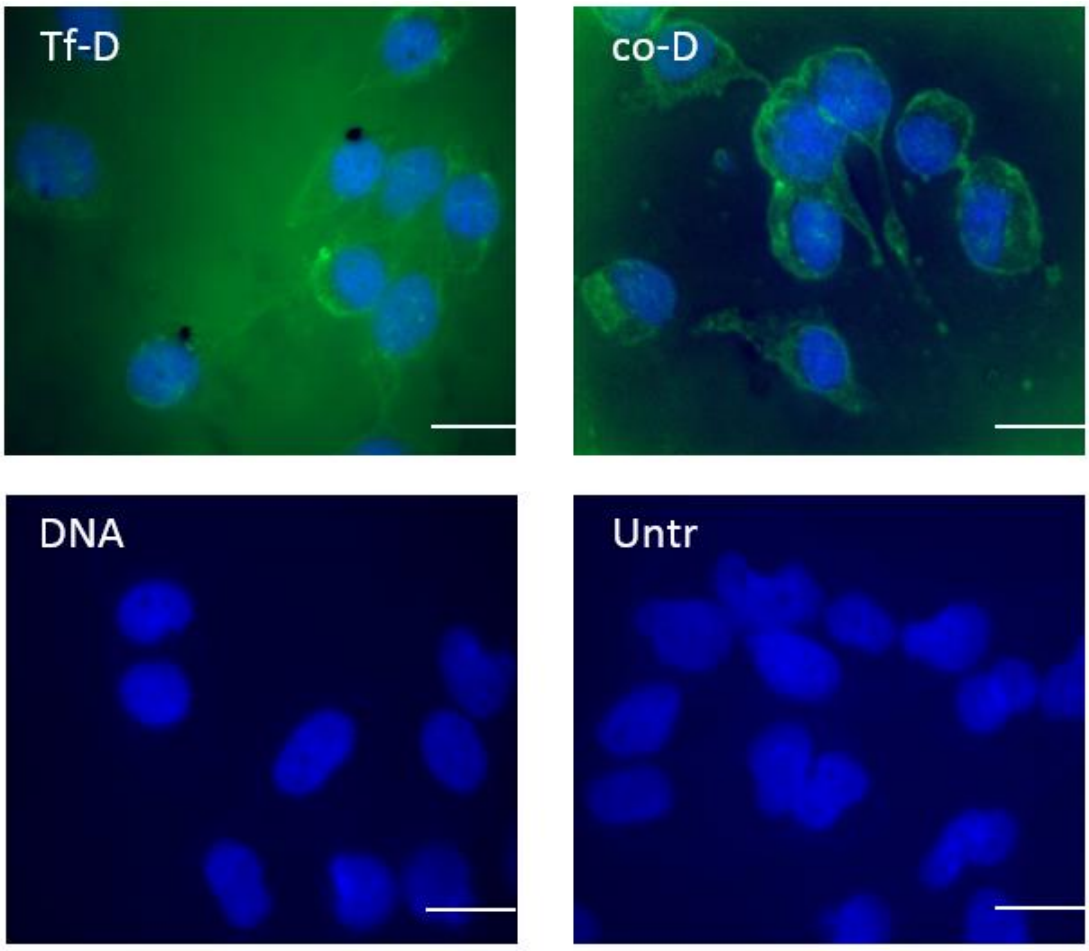

Figure 3.7: Epifluorescence microscopy imaging of the cellular uptake of Cy3-labelled DNA (2.5 µg DNA per well) either complexed with Tf-bearing DEN-SOL dendrisomes ("TF-D"), DEN-SOL control dendrisomes ("Co-D"), DNA only ("DNA") (Control: untreated cells) in T98G cell line (Blue: nuclei stained with DAPI (excitation: 405 nm, bandwidth: 415-491nm), green: Cy3-labelled DNA (excitation: 543 nm. bandwidth: 550-620 nm) (magnification: x 60) (Bar: 10 µm).

3.5.2.1 Cellular uptake of Cy5-labeled DNA complexed with dendrisomes using Confocal Laser Scanning Microscopy

Cellular uptake of DSOLmDox and DTPGSmdDoxC dendrisomes was carried out using treatments of Cy5-labelled DNA complexed with dendrisomes on cancer cell lines A431, B16F10-Luc-G5 and T98G (Figure 3.8-3.13). The images obtained gave a visual confirmation that cellular uptake of DNA carried by the dendrisomes had taken place for all three cancer cell lines. It was also observed that there was no cellular uptake following treatment with DNA only, doxorubicin only and, as expected, there was no visible fluorescence in untreated cells. Higher cellular uptake was obtained following treatment with transferrin-bearing dendrisomes complexed DNA. The DTPGSmdTf dendrisomes showed the highest cellular uptake. This result correlated with what was observed in the transfection studies.

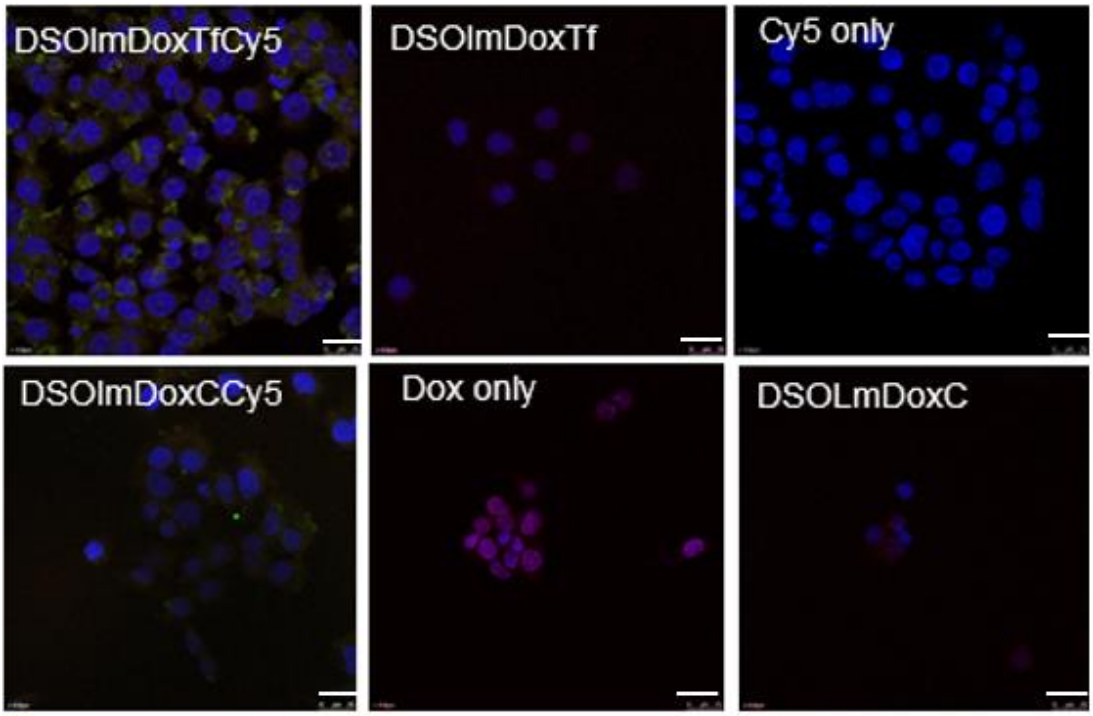

Figure 3.8: Confocal microscopy imaging of the cellular uptake of Cy5-labelled DNA (2.5 µg DNA per well) either complexed with Tf-bearing DSOLmDox dendrisomes ("DSOLmDoxTf"), control dendrisomes ("DSOLmDoxC"), DNA only ("Cy5"), Control: untreated cells in A431 cell line Blue: nuclei stained with DAPI (excitation: 405 nm, bandwidth: 415-491nm), Alexa Fluor 488 for doxorubicin excitation at 488nm (bandwidth 450 -550 nm), green: Cy5-labelled DNA excitation at 650nm (bandwidth 633-690nm) (magnification: x 63 oil) (Bar: 10 µm).

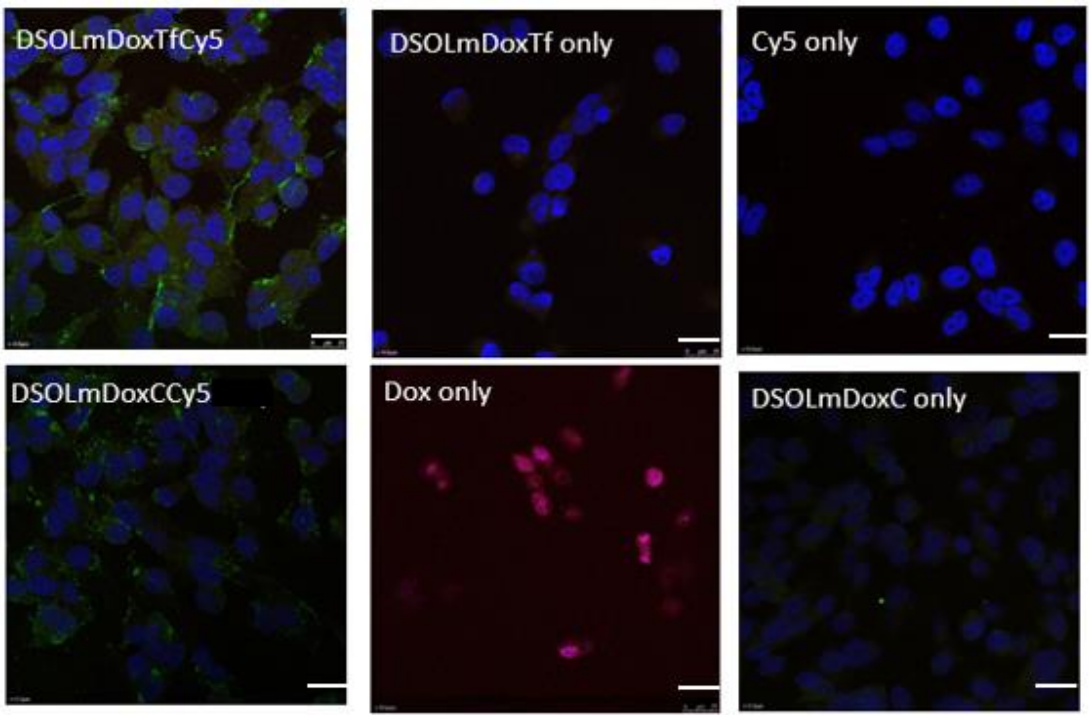

Figure 3.9: Confocal microscopy imaging of the cellular uptake of Cy5-labelled DNA (2.5 µg DNA per well) either complexed with Tf-bearing DSOLmDox dendrisomes ("DSOLmDoxTf"), control dendrisomes ("DSOLmDoxC"), DNA only ("Cy5"), Control: untreated cells in B16F10-Luc-G5 cell line Blue: nuclei stained with DAPI (excitation: 405 nm, bandwidth: 415-491nm), Alexa Fluor 488 for doxorubicin excitation at 488nm (bandwidth 450 -550 nm), green: Cy5-labelled DNA excitation at 650nm (bandwidth 633-690nm) (magnification: x 63 oil) (Bar: 25 µm).

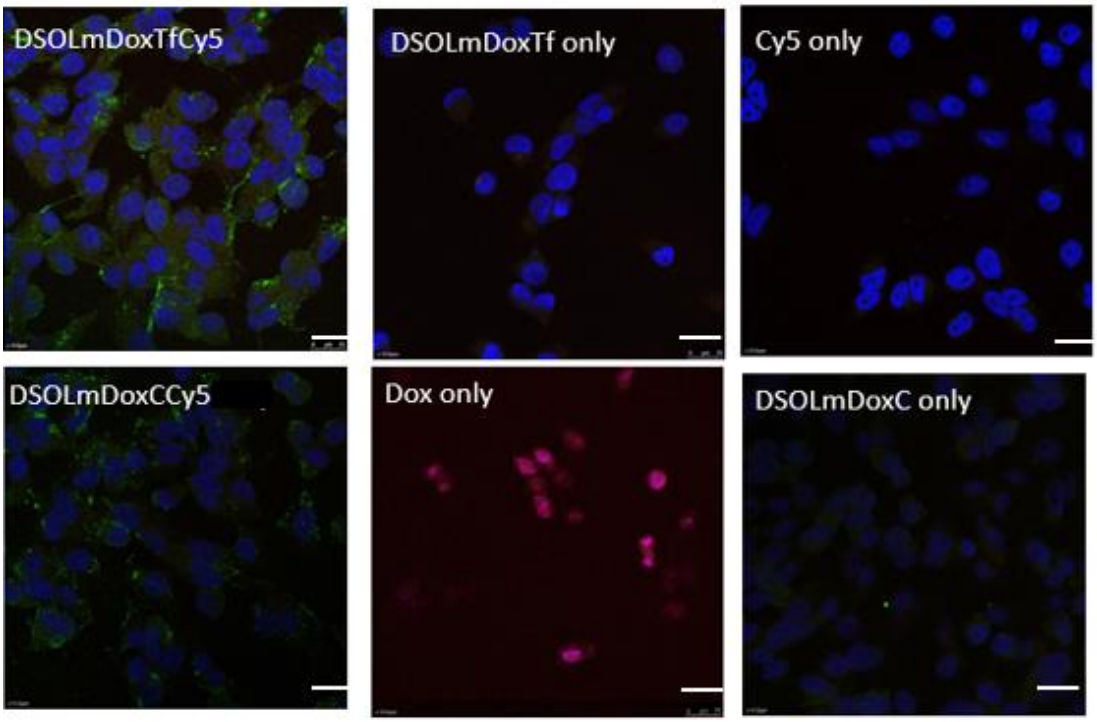

Figure 3.10: Confocal microscopy imaging of the cellular uptake of Cy5-labelled DNA (2.5 µg DNA per well) either complexed with Tf-bearing DSOLmDox dendrisomes ("DSOLmDoxTf"), control dendrisomes ("DSOLmDoxC"), DNA only ("Cy5"), Control: untreated cells in T98G cell line Blue: nuclei stained with DAPI (excitation: 405 nm, bandwidth: 415-491nm), Alexa Fluor 488 for doxorubicin excitation at 488nm (bandwidth 450 -550 nm), green: Cy5-labelled DNA excitation at 650nm (bandwidth 633-690nm) (magnification: x 63 oil) (Bar: 25 µm).

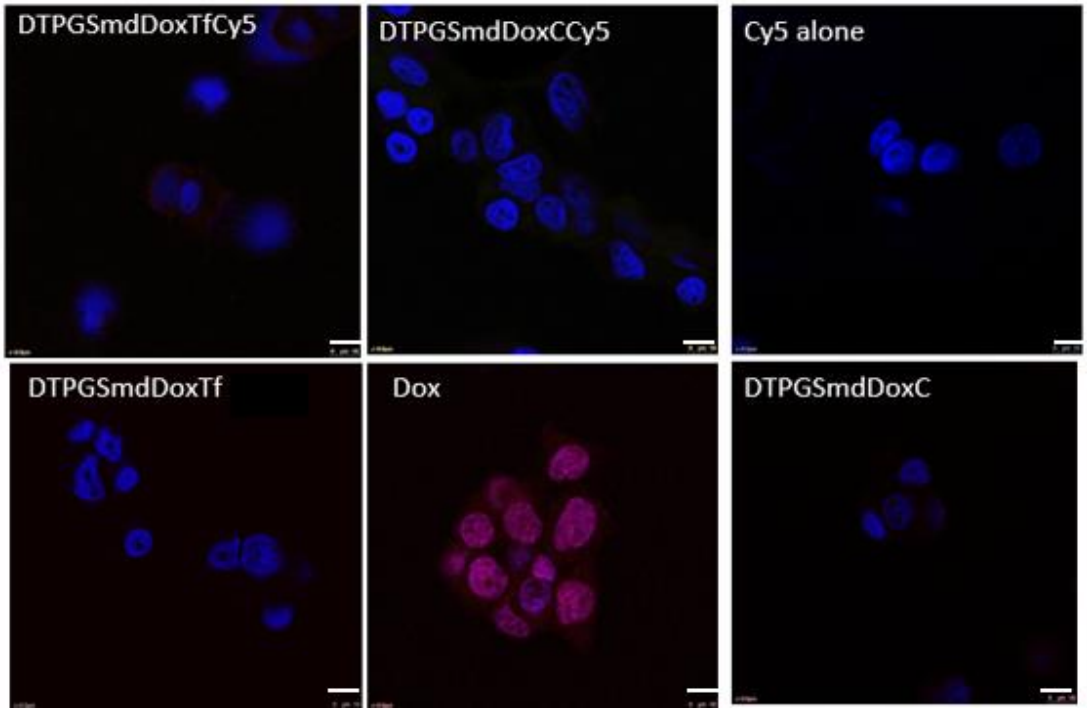

Figure 3.11: Confocal microscopy imaging of the cellular uptake of Cy5-labelled DNA (2.5 µg DNA per well) either complexed with Tf-bearing DTPGSmdDox dendrisomes ("DTPGSmdDoxTf"), control dendrisomes ("DTPGSmdDoxC"), DNA only ("Cy5"), Control: untreated cells in A431 cell line Blue: nuclei stained with DAPI (excitation: 405 nm, bandwidth: 415-491nm), Alexa Fluor 488 for doxorubicin excitation at 488nm (bandwidth 450 -550 nm), green: Cy5-labelled DNA excitation at 650nm (bandwidth 633-690nm) (magnification: x 63 oil) (Bar: 25 µm)

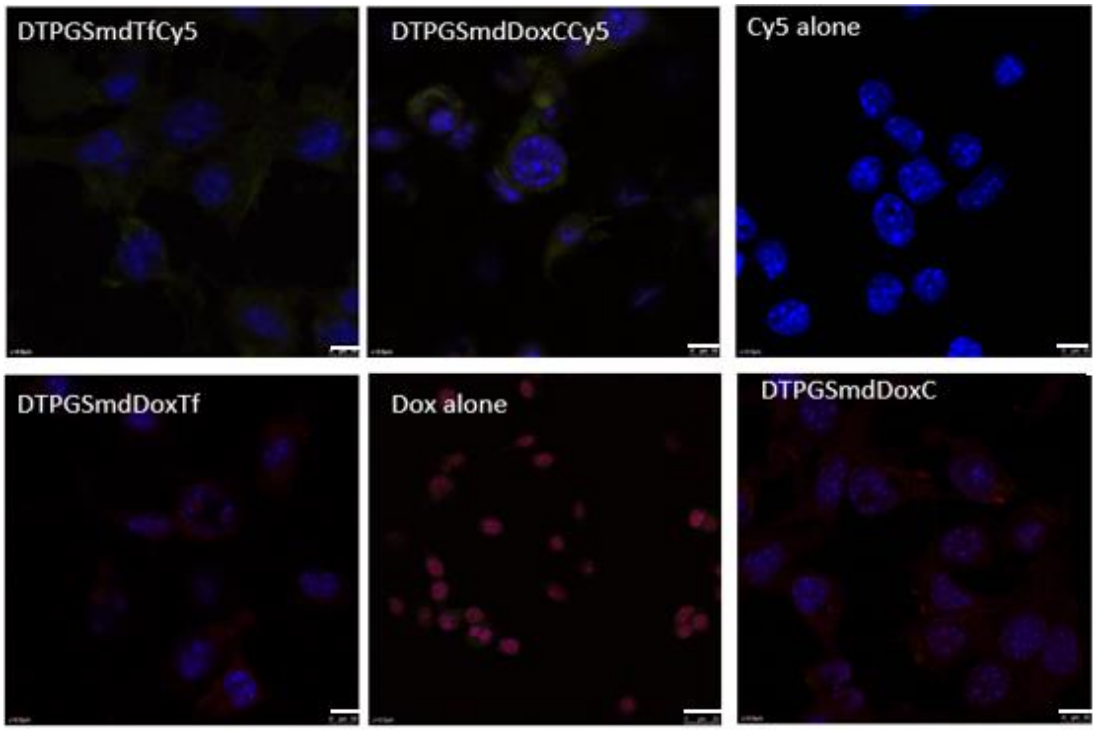

Figure 3.12: Confocal microscopy imaging of the cellular uptake of Cy5-labelled DNA (2.5 µg DNA per well) either complexed with Tf-bearing DTPGSmdDox dendrisomes ("DTPGSmdDoxTf"), control dendrisomes ("DTPGSmdDoxC"), DNA only ("Cy5"), Control: untreated cells in B16F10-Luc-G5 cell line Blue: nuclei stained with DAPI (excitation: 405 nm, bandwidth: 415-491nm), Alexa Fluor 488 for doxorubicin excitation at 488nm (bandwidth 450 -550 nm), green: Cy5-labelled DNA excitation at 650nm (bandwidth 633-690nm) (magnification: x 63 oil) (Bar: 25 µm).

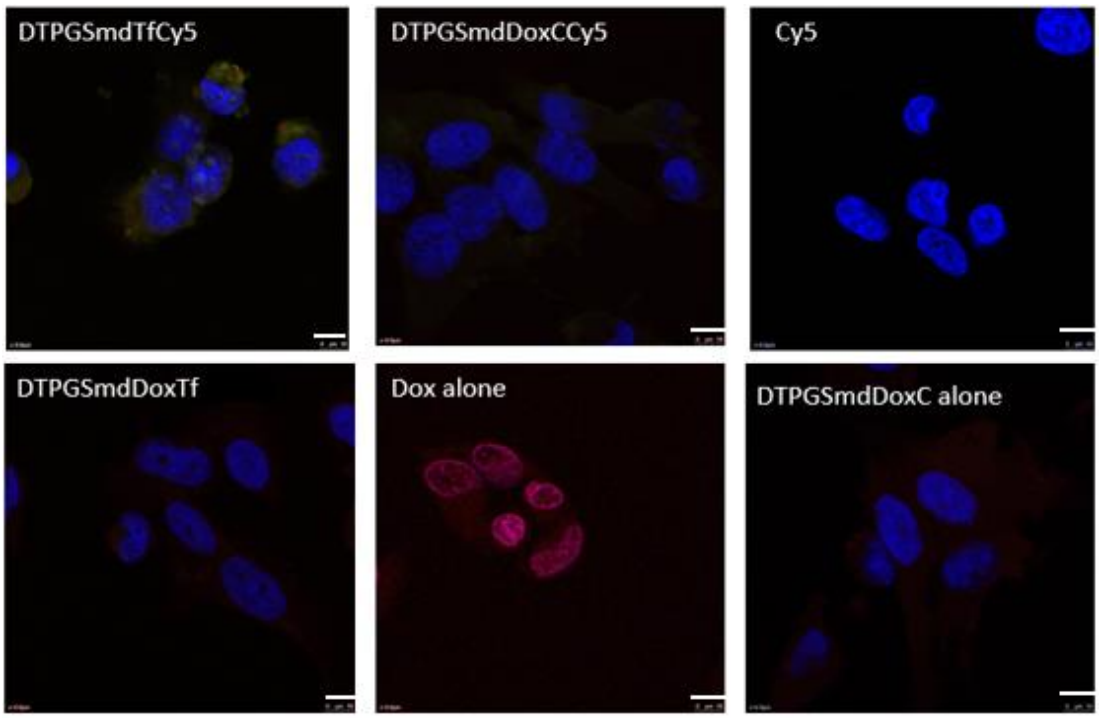

Figure 3.13: Confocal microscopy imaging of the cellular uptake of Cy5-labelled DNA (2.5 µg DNA per well) either complexed with Tf-bearing DTPGSmdDox dendrisomes ("DTPGSmdDoxTf"), control dendrisomes ("DTPGSmdDoxC"), DNA only ("Cy5"), Control: untreated cells in T98G cell line Blue: nuclei stained with DAPI (excitation: 405 nm, bandwidth: 415-491nm), Alexa Fluor 488 for doxorubicin excitation at 488nm (bandwidth 450 -550 nm), green: Cy5-labelled DNA excitation at 650nm (bandwidth 633-690nm) (magnification: x 63 oil) (Bar: 25 µm).

3.5.3 Anti-proliferative assay

The anti-proliferative assay was carried out using DSOLmDoxTf, DSOLmDoxC, DSOLmTf, DSOLmC, DTPGSmdDoxTf, DTPGSmdDoxC, DTPGSmdTf, DTPGSmdC alone or complexed with DNA encoding TNF α, Doxorubicin only and DNA encoding TNF- α only on cancer lines A431, B16F10-Luc-G5 and T98G. In A431 cancer cells, no significant difference was observed following treatment with transferrin-bearing and non-transferrin bearing DSOLm dendrisomes and dendrisomplexes. However, a 2-fold higher anti-proliferative effect was observed when the transferrin bearing doxorubicin encapsulated DTPGSmd dendrisomplexes were compared with the non-transferrin bearing doxorubicin encapsulated DTPGSmd dendrisomplexes in A431 cancer cells. It was observed that DNA only caused no cytotoxicity. Empty dendrisomes complexed with TNF-α and in dendrisomes entrapping doxorubicin only, cytotoxicity was observed with IC_{50} values ranging from 0.02±0.17 - 0.5 ± 0.24 µg / mL for DNA encoding TNF α concentrations and IC_{50} values ranging from 0.15±0.11 - 0.55±0.18 µg/mL for doxorubicin concentrations following treatment of A431 cells. Treatment with doxorubicin only on A431 cells showed cytotoxicity with an IC_{50} of 0.11±0.05 µg/mL (Table 3.4).

B16F10-Luc-G5 cells treated with the above-mentioned treatments showed cytotoxicity of IC_{50} values ranging from 0.07±0.06 - 0.57±0.04 µg/ mL for DNA encoding TNF α concentration and IC_{50} values ranging from 0.26±0.22 - 2.17±0.16 µg/mL for doxorubicin concentrations. Treatment with doxorubicin only and TNFα only on B16F10-Luc-G5 cells showed cytotoxicity with an IC_{50} of 0.37±0.04 µg/mL and no significant cytotoxicity respectively. In the

B16F10-Luc-G5 cells, synergism was observed in the cells treated with the concentration of the IC_{50} of doxorubicin and TNF-α of DSOLmDoxTfTNF-α dendrisomplexes (transferrin bearing) showing at least a 3-fold higher anti-proliferative effect when compared to the DSOLmDoxCTNF-α dendrisomplexes (non-transferrin bearing) (Table 3.5).

The anti-proliferative assay carried out with the treatments on T98G cells showed cytotoxicity of IC_{50} values ranging from 0.05±0.0 - 0.18±0.33 µg/ mL for DNA encoding TNF α concentration and IC_{50} values ranging from 0.05±0.11 - 0.38±7.2 µg/mL for doxorubicin concentrations. Treatment with doxorubicin only and TNFα only on T98G cells showed cytotoxicity with an IC_{50} of 1.93±7.4 µg/mL and no significant cytotoxicity respectively. The T98G cells demonstrated no significant difference in the anti-proliferative activity of DSOLmDoxTfTNF-α dendrisomplexes (transferrin bearing) when compared to the DSOLmDoxCTNF-α dendrisomplexes (non-transferrin bearing) or in the. DTPGSmdDoxTfTNF-α dendrisomplexes when compared to the DTPGSmdDoxCTNF-α in the IC_{50} concentrations of doxorubicin and TNF-α (Table 3.6).

Table 3.4: Cytotoxicity studies of DNA encoding TNF-α complexed with DSOLm and DTPGSmd dendrisomes, DNA encoding TNF-α alone, doxorubicin in free solution in A431 cells, expressed as IC_{50} values (n=15). (μg/mL) IC_{50} (mean ± S.E.M.)

Formulation	**Tf-dendrisomes**		**Control dendrisomes**		**TNF-α or Dox alone**
	TNF-α	**Dox**	**TNF-α**	**Dox**	
DSOLmDoxTNFα	0.14±0.04	0.55±0.18	0.12±0.03	0.46±0.11	n/a
DSOLmTNFα	0.14±0.02	n/a	0.15±0.02	n/a	n/a
DSOLmDox	n/a	0.39±0.37	n/a	0.48±0.09	n/a
DTPGSmdDoxTNFα	0.02±0.17	0.15±0.11	0.5 ± 0.24	0.33±0.13	n/a
DTPGSmdTNFα	0.1±0.07	n/a	0.13± 0.11	n/a	n/a
DTPGSmdDox	n/a	0.37±7.02	n/a	0.27±0.17	n/a
Dox alone	n/a	n/a	n/a	n/a	0.11±0.05
TNFα alone	n/a	n/a	n/a	n/a	> 50

n/a: Not applicable

Table 3.5: Cytotoxicity studies of DNA encoding TNF-α complexed with DSOLm and DTPGSmd dendrisomes, DNA encoding TNF-α alone, doxorubicin in free solution in B16F10-Luc-G5 Cells expressed as IC_{50} (µg/mL) (mean ± S.E.M.), values (n=15).

Formulation	**Tf-dendrisomes**		**Control dendrisomes**		**TNF-α or Dox alone**
	TNF-α	**Dox**	**TNF-α**	**Dox**	
DSOLmDoxTNFα	0.13±0.02	0.47±0.09	0.57±0.04	2.17±0.16	n/a
DSOLmTNFα	0.16±0.04	n/a	0.13±0.03	n/a	n/a
DSOLmDox	n/a	0.48±0.4	n/a	0.7±0.09	n/a
DTPGSmdDoxTNFα	0.07±0.06	0.26±0.22	0.09±0.04	0.34±0.17	n/a
DTPGSmdTNFα	0.1±0.07	n/a	0.27±0.27	n/a	n/a
DTPGSmdDox	n/a	0.39±1.76	n/a	0.39±2.42	n/a
Dox alone	n/a	n/a	n/a	n/a	0.37±0.04
TNFα alone	n/a	n/a	n/a	n/a	>50

n/a: Not applicable

Table 3.6: Cytotoxicity studies of DNA encoding TNF-α complexed with DSOLm and DTPGSmd dendrisomes, DNA encoding TNF-α alone, doxorubicin in free solution in T98G cells, expressed as IC_{50} values (n=15) IC_{50} (µg/mL) (mean ± S.E.M.)

Formulation	**Tf-dendrisomes**		**Control dendrisomes**		**TNF-α or Dox alone**
	TNF-α	**Dox**	**TNF-α**	**Dox**	
DSOLmDoxTNFα	0.1±1.93	0.38±7.2	0.07±0.02	0.26±0.09	n/a
DSOLmTNFα	0.05±0.0	n/a	0.04±0.0	n/a	n/a
DSOLmDox	n/a	0.37±3.9	n/a	0.27±0.05	n/a
DTPGSmdDoxTNFα	0.13±0.31	0.2±0.2	0.15	0.1±0.06	n/a
DTPGSmdTNFα	0.18±0.33	n/a	0.15±0.09	n/a	n/a
DTPGSmdDox	n/a	0.05±0.11	n/a	0.09±0.06	n/a
Dox alone	n/a	n/a	n/a	n/a	1.93±7.4
TNFα alone	n/a	n/a	n/a	n/a	>50

n/a: Not applicable

3.6 Discussion

Transfection studies with Transferrin bearing dendriplexes have previously demonstrated that transferrin conjugation to nanocarriers led to an increase in transfection when compared with DNA alone (Al Robaian *et al.,* 2014). The DEN-SOL dendrisomplexes at the highest transfection ratio demonstrated a 3-fold, 4-fold and 2-fold higher transfection compared to DNA only treated cells in A431, B16F10-Luc-G5 cells and T98G cells respectively. The DSOLm dendrisomplexes at the highest transfection ratio demonstrated a 2.5-fold, 1.7-fold and 3-fold higher transfection compared to DNA only treated cells in A431, B16F10-Luc-G5 cells and T98G cells respectively. These results corresponded to the results obtained by Al Robaian *et al.,* (Al Robaian *et al.,* 2014). The non-PEGylated Solulan C24 (DEN-SOL) dendrisome formulations, achieved the best transfection results at the dendrisome: DNA ratio 10:1 ratio in A431 and T98G cells. However, the highest transfection in the DEN-SOL dendrisomplex B16F10-Luc-G5 cells treated cells was the 0.5:1 ratio. PEGylated Solulan C24 (DSOLm) dendrisomplexes achieved the best transfection results at the dendrisome: DNA ratio 10:1 ratio in A431 and T98G cells. while the DSOLm dendrisomplex treated B16F10-Luc-G5 cells demonstrated the highest transfection at 10:1 ratio. These results correlated with the transfection results obtained by Koppu *et al.,* where non-viral transfections in A431 and T98G cells demonstrated that the dendrimer: DNA ratio 10:1 gave the best transfection results (Koppu *et al.,* 2010).

The inclusion of DOPE in the DTPGSmd dendrisomes was to increase transfection efficacy. The DTPGSmd dendrisomplexes at the highest transfection ratio of 5:1 across all three cell lines demonstrated an 8-fold, 6.5-fold and 9-fold higher

transfection compared to DNA only treated cells in A431, B16F10-Luc-G5 cells and T98G cells respectively. The results of the transfection showed that this inclusion showed a significant difference in the transfection results between the DSOLm dendrisomes and the DTPGSmd dendrisomes with the DTPGSmdTf dendrisomes showing transfection values at least three times higher than what was observed in the DSOLmTf dendrisomes across all three cell lines. Farhood *et al.,* demonstrated that cationic liposomes incorporated with DOPE had a higher transfection efficacy than the formulations that did not contain DOPE in a reporter gene assay (Farhood *et al.,*1994). This result confirmed the capability of DOPE to increase transfection efficacy as was shown in the results obtained in another study done on hybrid Peptide Dendrimer/Lipid nanocarriers formulated (Kwok *et al.,* 2013), their studies showed that the DOPE lipid/peptide dendrimer/DNA complexes that they formulated synergistically improved the transfection efficiency when compared with the transfection efficacy when compared to dendrimer/DNA complexes alone that they also formulated.

The DEN-SOL dendrisomes showed a larger transfection when compared to the DSOLm dendrisomes. However, the inclusion of Chol-PEG-maleimide (a PEGylated lipid) in the DSOLm formulation to increase circulation time and evade the reticuloendothelial system RES system (Bose *et al.,* 2018), which should lead to increased gene expression and therapeutic efficacy *in vivo*, studies on the DSOLm dendrisomes were continued since successful gene expression was achieved across all three cell lines as well.

As earlier mentioned, the DEN-SOL dendrisomes showed a larger transfection when compared to the DSOLm dendrisomes. As the main difference between these two Solulan C24 formulations is the PEGylation of the DSOLm dendrisomes, however PEGylation may or may not be the cause. This is because some researchers argue that PEGylation does not cause a decrease in transfection while others say that it does. *In vivo* studies in BALB/c female mice (Simonsen) tumor cells of the J6456 lymphoma demonstrated that PEGylated doxorubicin liposomal formulations caused a 25-fold increase in the concentration of anticancer agents in tumors with a concomitant reduction of RES toxicity when compared to other treatments (Gabizon *et al.,*1988). DSPE-PEG (2000) folate was added to a formulation of lipid–polymer hybrid nanoparticles (LPNPs) to increase cellular uptake and increase their therapeutic activity *in vitro* and *in vivo*. This resulted in increased their therapeutic activity *in vitro* and *in vivo* as will be discussed later (Zhang *et al.,* 2015). Based on the foregoing non-PEGylated Solulan C24 (DEN-SOL) dendrisomes were the dendrisomes containing Solulan C24 chosen for cellular uptake experiments alone, while DSOLm dendrisomes (PEGylated Solulan C24 dendrisomes) were the dendrisomes containing Solulan C24, chosen for the confocal cellular uptake experiments and anti-proliferative assays.

The images obtained from the cellular uptake studies confirmed that cellular uptake of DNA successfully occurred in DEN-SOL, DSOLm and DTPGSmd dendrisomes. Cy3-labeled plasmid DNA encoding β-galactosidase was the florescent label initially chosen to investigate the cellular uptake activity across the three cell lines so that the activity could be compared with previous cellular uptake studies of DAB-Am-16 dendriplexes. The transferrin bearing DEN-SOL dendriplexes demonstrated that

increased cellular uptake of the Cy3-labeled plasmid DNA encoding β-galactosidase in the A431 and T98G cell lines when compared to non-transferrin bearing DEN-SOL dendrisomplexes. However, the non-transferrin bearing DEN-SOL dendrisomplexes demonstrated a higher cellular uptake in the B16F10-Luc-G5 than the transferrin bearing DEN-SOL dendrisomplexes. No cellular uptake was observed in the DNA alone treatment and the untreated cells. The A431 and T98G demonstrated that these results were similar to the cellular uptake of DAB-Am-16 dendriplexes in A431 and T98G cells as observed by in a previous study (Koppu *et al.*,2010).

Cy5-labeled plasmid DNA encoding β-galactosidase was the florescent label chosen to investigate the cellular uptake activity in the PEGylated dendrisomes across the three cell lines so that cellular uptake of doxorubicin the activity and DNA could be concurrently evaluated. This is because there is an overlap in the excitation and emission spectrum of doxorubicin and Cy3 with excitation and emission wavelength at (488 nm excitation, 570 nm emission) and (554 nm excitation, 568 nm emission) respectively (Mohan and Rapoport, 2010; Thermofisher.com 2018). DSOLm dendrisomplexes showed successful concurrent cellular uptake of doxorubicin and DNA across all three lines with the transferrin bearing, doxorubicin encapsulated dendrisomplexes exhibiting the highest cellular uptake across all three cell lines. This results thus demonstrated that the aim of concurrently delivering the model drug doxorubicin and DNA intracellularly was achieved.

Higher DNA uptake was observed in DTPGSmd dendrisomplexes in the B16F10 and T98G cells. This corresponded with the results obtained from the transfection studies.

However, the cellular uptake of the doxorubicin entrapped in the dendrisomes into the cancer cell lines was observed to be higher in the DSOLmDox dendrisomplexes than in the DTPGSmdDox dendrisomplexes. This could be attributed to the higher percentage cumulative drug release observed in the DSOLmDox dendrisomes than that observed in the DTPGSmdDox dendrisomes. These results demonstrated that these novel dendrisomes increased cellular uptake of DNA *in vitro.*

The anti-proliferative assay of the various treatments including the DSOLm dendrisomes on cancer cells A431, B16F10-Luc-G5 and T98G showed that there was a difference between IC_{50} cytotoxicity values with all the dendrisome treatments when compared with DNA encoding TNF-α treatment alone. A study by Zhang *et al.,* showed that Folate-modified/ targeted lipid–polymer hybrid nanoparticles loaded with paclitaxel (PTX-loaded FLPNPs) led to a higher reduction in cell viability than non-folate-modified/ targeted PTX-loaded LPNPs though their anti-proliferative effect was still lower than the free drug Taxol® (Zhang *et al.,*2015). However, it was observed that there was no significant difference in the values between the Tf-bearing and non-Tf dendrisomplex treatments for A431 cells treated with DSOLmDoxTfTNF-α. This corresponds to what has been observed in some papers suggesting that this difference would be visible *in vivo* (Han *et al.,* 2011; He *et al.* 2015). On the contrary however, there was a 2-fold higher anti-proliferative effect in the A431 cells treated with dendrisomplex DTPGSmdDoxTfTNF-α when compared with. This was the result that demonstrated that targeting with transferrin made in difference in with both formulations but in different cell lines and no difference in T98G cells.

In the B16F10-Luc-G5 cells, synergism was observed in the cells treated with the concentration of the IC_{50} of doxorubicin and TNF-α of DSOLmDoxTfTNF-α dendrisomplexes (transferrin bearing) showing at least a 3-fold higher anti-proliferative effect when compared to the DSOLmDoxCTNF-α dendrisomplexes (non-transferrin bearing). This study correlated with studies by Lasek *et al.,* that demonstrated that the treatment combination of TNF-α with Actinomycin D in MmB 16 melanoma cells resulted in synergistic anti-proliferative effects (Lasek et al., 1996)

However, when B16F10-Luc-G5 cells were treated with DTPGSmdDoxTfTNF-α dendrisomplexes DTPGSmdDoxCTNF-α no significant difference was observed in the IC_{50} concentrations of doxorubicin and TNF-α.

The T98G cells demonstrated no significant difference in the anti-proliferative activity of DSOLmDoxTfTNF-α dendrisomplexes (transferrin bearing) when compared to the DSOLmDoxCTNF-α dendrisomplexes (non-transferrin bearing) or in the. DTPGSmdDoxTfTNF-α dendrisomplexes when compared to the DTPGSmdDoxCTNF-α in the IC_{50} concentrations of doxorubicin and TNF-α. However as earlier mentioned the DSOLmDoxTfTNF-α dendrisomplexes, DSOLmDoxCTNF-α dendrisomplexes, DTPGSmdDoxTfTNF-α dendrisomplexes and DTPGSmdDoxCTNF-α demonstrated a significant difference between IC_{50} cytotoxicity values when compared with TNF-α alone.

3.7 Conclusion

The *in vitro* results proved that the novel dendrisomes formed successfully caused gene expression across three cancer cell lines A431, B16F10-Luc-G5 and T98G via transfection experiments. It also proved that there was concurrent delivery of fluorescent labeled Cy5 plasmid DNA encoding β-galactosidase via cellular uptake experiments. Anti-proliferative MTT assay showed synergism occurred in the anti-proliferative assay with B16F0-Luc-G5 cells and DSOLmDoxTfTNF-α dendrisomplexes (transferrin bearing, doxorubicin encapsulated DSOLm dendrisomes complexed to plasmid encoding TNF-α).

Synergism was observed in the cellular uptake experiment and the anti-proliferative assay with B16F0-Luc-G5 cells and DSOLmDoxTfTNF-α dendrisomplexes (transferrin bearing, doxorubicin encapsulated DSOLm dendrisomes complexed to plasmid encoding TNF-α). An additive effect was observed in A431 cells between the DTPGSmdDoxTNF-α dendrisomplexes (transferrin bearing, doxorubicin encapsulated DTPGSmd dendrisomes complexed to plasmid encoding TNF-α) when compared to DTPGSmdDoxCTNF-α (non-transferrin bearing doxorubicin encapsulated DTPGSmd dendrisomes complexed to plasmid encoding TNF-α). However, no significant difference was observed on the anti-proliferative activity between the DSOLm doxorubicin encapsulated dendrisomplexes (DSOLmDoxTfTNF-α and DSOLmDoxCTNF-α) in A431 cells. The T98G cells showed no significant difference in the anti-proliferative activity between the DSOLm doxorubicin encapsulated dendrisomplexes and the DTPGSmd doxorubicin encapsulated dendrisomplexes.

Based on the synergism observed in the cellular uptake experiment and the anti-proliferative assay with B16F0-Luc-G5 cells and DSOLmDoxTfTNF-α dendrisomplexes (transferrin bearing), *in vivo* experiments were proceeded to ascertain the capabilities of these novel targeted dendrisomes *in vivo* with B16F10-Luc-G5 as the cell line of choice.

CHAPTER 4: IN VIVO EVALUATION

4.1 Introduction

Despite the vast array of *in vitro* models currently available in cancer research, the use of animals in cancer research for *in vivo* experiments currently does not have an alternative model that would give translational data on new compounds that can be directly translated to their efficacy in human subjects such as safe, efficacious therapeutic doses in a living multicellular biological system (Dey *et al.,* 2010). The use of animals for testing dates back as far as the time of Greek physician-scientists like Aristotle, (384 – 322 BC) and Erasistratus, (304 – 258 BC), who carried out experiments on live animals. Erasistratus discovered the fact that the trachea was the tube for supplying air to the lungs and that the lungs were the organs through which gas exchange/ purification took place in the body while carrying out experiments on pigs. Over time other individuals carried out more animal testing which resulted in more discoveries (Hajar 2011; Baer *et al.,* 2015).

There has been and there still is a lot of debate currently on going regarding the use of animals for testing. There are groups that are against the use of animals for research. This argument led to the onset of the 3Rs campaign. The 3Rs campaign has been promoting the following themes (1) the replacement of animals with non-living models; (2) reduction in the use of animals; and (3) refinement of animal use practices. However, despite the 3Rs, animal testing is still necessitated to ensure that novel compounds are safe for use in humans. The practise of testing novel compounds on animals became imperative in the twentieth century with the problems that arose due to the adverse effects from novel compounds not initially tested on animals, on the human patients that took them. The first recorded reports came from the incidences

that occurred with a drug called sulfanilamide in 1937. A pharmaceutical company in the USA made the formulation sulfanilamide using diethylene glycol (DEG) as a solvent, and called the preparation 'Elixir Sulfanilamide' and sold it without animal testing. At the time unknown to the chief pharmacist and chemist of the company that the excipient DEG was poisonous to humans. The preparation led to mass poisoning causing the deaths of more than a hundred people. Due to the public uproar that resulted from this occurrence and other similar events that arose, the 1938 Federal Food, Drug, and Cosmetic Act was passed into law which then required safety testing of new drugs and compounds on animals before they could be marketed to humans (Hajar 2011; Batchelor *et al.*, 2014).

4.2 Animal studies using mice

In the pharmaceutical industry, non-animal *in vitro* techniques such as cell culture are first used to test and characterise novel compounds or drug delivery systems to identify compounds that show the potential of achieving the set-out objective such as killing cancer cells, reducing high blood pressure or reducing high blood sugar. Ethically, animal studies are carried out after these *in vitro* tests have been carried out to validate the pharmacological activity, absorption, duration of action and delivery to the target sites of these novel compounds. The results determine whether the lead (successful) compounds have the potential for subsequent testing in human trials, and therefore the qualities to become candidates for medicines (Nuffield Council on Bioethics, 2005).

Current advancements made in cancer therapy could only have been achieved due to the use of animals in *in vivo* experiments for understanding the characteristics,

underlying mechanisms and behaviour of cancer cells. Cancer is considered as a life-threatening disease; hence various tumour models have been formed and have become essential in testing the efficacy of novel anti-cancer compounds. The exposure of animals especially mice (which make up 95 % of the animals used in *in vivo* experiments) to various cancer cells is considered a source of concern to the groups of individuals that consider this process as cruelty to animals. However based on past experience as earlier stated novel compounds especially anticancer drugs do no not have any other *in vitro* models that can provide relevant data that could ascertain their efficacy alongside their safety as found *in vivo* experiments (Workman *et al.,* 2010; Dey *et al.,* 2010).

There are various *in vivo* tumour models currently being used in cancer research and they are divided into two broad groups. In the first group, the tumour cells are introduced into the host via transplantation of cancer cells into the host while in the second group, the tumour cells are induced in the host organism through various mechanisms such as chemical induction with chemicals like Azoxymethane (Hirose *et al.,* 2004; Workman *et al.,* 2010) and radiation induction using Ultraviolet light (Ahsan *et al.,* 2005; Workman *et al.,* 2010). The choice of tumour model used depends on the purpose and type of data that is desired (Workman *et al.,* 2010). The tumour model chosen for this project was a xenograft model based on the first type of tumour models. It involved the subcutaneous injection of the cancer cells via the tail of balb/ c mice. Balb/c mice a strain of albino mice was chosen for this project because they are immunodeficient, tumour-prone and the most commonly used mice strain for *in vivo* cancer research models (Labome.com 2016). They have also been known to show

responses to disease states and treatments in a manner similar to humans (Budhu *et al.*, 2014).

4.3 Quantification of β-galactosidase activity *in vivo*

The development of new non-viral transfection agents requires the use of reporter genes to measure their gene expression capabilities. The β-galactosidase (β-gal) reporter gene obtained from the LacZ gene of *Escherichia coli*, is currently the most commonly used reporter gene for evaluating gene expression in non-viral gene delivery agents. When expressed, it produces the enzyme β-galactosidase *in vitro* and *in vivo* which causes cleavage of a substrates that are susceptible to β-galactosidase enzyme. This principle was utilized in carrying out *in vitro* transfection experiments in the previous chapter using colorimetric substrate o-nitrophenyl-b-D-galactopyranoside (ONPG) (Serebriiskii and Golemis 2000; Gong *et al.*, 2009).

The use of reporter genes assays *in vivo* in the past had the challenge of not adequately quantifying the amount of gene expression achieved in various organs by novel delivery systems. This led to Zinselmeyer *et al* developing a bio distribution assay that was based on the premise, that the cleavage of the substrate 9H-{1,3-dichloro-9,9-dimethylacridin-2-one-7-yl} β-D-galactopyranoside (DDAO-G) by β-galactosidase led to the production fluorescent product, 7-hydroxy-9H- {1,3-dichloro-9,9-dimethylacridin-2-one (DDAO) *in vivo.* It was discovered that the DDAO produced caused shifts in the fluorescence generated towards longer wavelengths; far red. The fluorescence shift caused was found to be quantifiable using Spectrofluorimetry. The

quantity of fluorescence produced was found to be directly proportional to the amount of gene expression that had occurred (Zinselmeyer *et al.*, 2003).

4.4 Aims and objectives

The previous chapter investigated into the capabilities of the dendrisomes formulated for gene expression, anti-proliferative activity as well as qualitative analysis of cellular uptake *in vitro*. The *in vitro* results obtained showed that the dendrisomes formulated had good potential for favourable outcomes *in vivo*.

This current chapter investigated the evaluation of gene expression *in vivo* using fluorescent probe 9H-(1,3-Dichloro-9,9-Dimethylacridin-2-One-7-yl) β-D-Galactopyranoside (DDAO-Galactoside) to detect β-galactosidase activity. *In vivo* experiments on the therapeutic efficacy effect of the dendrisomes formulated when concurrently encapsulating anticancer drug doxorubicin, complexed with therapeutic plasmid DNA encoding TNF –α, in B16F10-Luc-G5 cancer cell line were also carried out.

4.5 Materials and Methods

Table 4.1 Materials and reagents

Materials	Supplier
A431 human epidermoid carcinoma	The European Collection of Cell Cultures (Salisbury, UK)
B16-F10-Luc-G5 Bioware® mouse melanoma	Calliper Life Sciences (Hopkinton, MA)
DDAO-Galactoside (9H-(1,3-Dichloro-9,9-Dimethylacridin-2-One-7-yl) β-D-Galactopyranoside)	Invitrogen, ThermoFisher Scientific (Paisley, UK)
Dimethyl sulfoxide (DMSO)	Sigma-Aldrich, (Poole, UK)
D-glucose	Sigma-Aldrich, (Poole, UK)
DNA encoding TNF-α	Prepared as earlier described in Chapter 2
DSOLm dendrisomes	Prepared as earlier described in Chapter 2
Dulbecco's Modified Eagle Medium (DMEM)	Invitrogen, ThermoFisher Scientific (Paisley, UK)
L-Glutamine	Invitrogen, ThermoFisher Scientific (Paisley, UK)
Maltose	Sigma-Aldrich, (Poole, UK)
Passive Lysis Buffer (5x)	Promega, (Southampton, UK)
Penicillin-Streptomycin	Invitrogen, ThermoFisher Scientific (Paisley, UK)
Phenylmethylsulfonyl fluoride (PMSF)	Sigma-Aldrich, (Poole, UK)
Protease Inhibitor Cocktail (PIC)	Sigma-Aldrich, (Poole, UK)
Roswell Park Memorial Institute (RPMI)1640 medium	Invitrogen, ThermoFisher Scientific (Paisley, UK)
Trypsin	Invitrogen, ThermoFisher Scientific (Paisley, UK)

4.5.1 Cell Culture

Cancer cell line B16-F10-luc-G5 were grown as monolayers in RPMI-1640 medium for intravenous injection into the selected animals. The RPMI-1640 growth medium was supplemented with 10 % v/v foetal calf serum, 1 % v/v L-glutamine and 0.5 % v/v penicillin-streptomycin. The cells were incubated in an incubator at 37 ^{0}C in a humid atmosphere of 5 % CO_2.

4.5.2 Animals

The *in vivo* experiments were carried out using immunocompromised female albino Balb/c mice of initial average weight 20g. These mice were housed in groups of five at 19 ^{o}C to 23 ^{o}C with a 12 h light to dark cycle. They were fed a conventional diet (Rat and Mouse Standard Expanded, B&K Universal, Grimston, United Kingdom) with mains water *ad libitum*. Experimental work was carried out in accordance with UK Home Office regulations and approved by the local ethics committee.

4.5.3 Quantification of β-galactosidase activity *in vivo* following treatment with dendrisome- DNA complexes

Female immunodeficient albino Balb/ c mice (n=5, initial mean weight 20 g) bearing subcutaneously implanted B16F10-Luc-G5 tumours were used in this study. Tumours were palpable (typical diameter 5 mm) 6 days after subcutaneous implantation of B16F10-Luc-G5 cancer cells in exponential growth (10^6 cells/ flank). Mice were treated with a single injection of carrying β-galactosidase expression plasmid (25 μg of DNA) and/ or doxorubicin (8 μg) via tail vein injection. Mice were sacrificed 24 h after injection. Their tumours were removed, immediately frozen in liquid nitrogen and analysed for their β-galactosidase levels. A homogenization / Passive lysis buffer

mix was prepared. Passive lysis buffer mix (25 mL) was prepared as follow: protease inhibitor cocktail (500 µL), PMSF 50 mM in methanol (PMSF: 50 mmole/L: 87.1 mg PMSF in 10 mL methanol) (1000 µL), PLB 5X (5 mL) and distilled water (18.5 mL).

Tumours in homogenization/lysis buffer were homogenized using a tissue homogenizer (PowerGen 125, Fischer Scientific), and the resultant tissue homogenates were incubated on ice. Quantification of β-galactosidase enzymatic activity were performed by measurement of β-galactosidase enzymatic cleavage of its substrate 9H-(1, 3-dichloro-9, 9-dimethylacridin-2-one-7-yl) β-D-galactopyranoside (DDAO-Galactoside) to 7-hydroxy-9H-(1, 3-dichloro-9, 9-dimethylacridin-2-one) (DDAO) product.

A DDAO-Galactoside Reaction Master Mix was prepared for each tissue homogenate, as follows: (For 1 sample: 15 µL DDAO gal in DMSO 5 mg/mL, 20 µl PMSF, 100 µl maltose in PBS: 20 g for 100 mL, 15 µl protease inhibitor cocktail, 150 µl PBS). To 100 µl tissue homogenates, 300 µl of DDAO-Galactoside reaction master mix was added and the mixture incubated at 37^{o} C, with occasional mixing for the appropriate incubation time optimized for each organ. A volume of 200 µl of the incubated reaction mixture was then transferred into another container and incubated in a heating block at 90 ^{o}C for 2 minutes. The heated incubation was performed to stop the enzymatic cleavage of β-galactosidase on the DDAO-galactoside substrate and precipitate a large proportion of proteins. To extract the DDAO compound, 800 µl isopropanol were added to dissolve the DDAO and the mixture incubated for 20 minutes at 4^{o} C. Subsequently, the mixtures were centrifuged (10 minutes at 13 000 rpm). 500 µl of the

supernatant were mixed with 500 µl of 80% (v/v) water-isopropanol mixture and measured in a fluorescence spectrophotometer (Varian Cary Eclipse Fluorescence spectrophotometer, excitation wavelength 630nm, emission wavelength 650 nm, excitation and emission slit 5 nm). A standard curve for each organ was also done using a concentrated Master Mix.

For 1 sample: DDAO-Galactoside (15 µL), PMSF (20 µL), maltose in PBS (100 µL), protease inhibitor cocktail (15 µL) and PBS (50 µL).

Each sample was prepared with 100 µL of β-gal solution + 100 µL of Organ mesh + 200 µL of Concentrated Master mix. The fluorescence units were used to calculate the β-galactosidase activity based on a linear regression ($f(x) = a + b.x$) fitted to a β-galactosidase standard curve. The concentration of β-galactosidase in the tumours was determined by using the following equations (Equations 4.1), given by a β-galactosidase standard curve:

Concentration of β-galactosidase in 100 µL sample C1 (in mU):

Equation 4.1

C1 = (Fluorescence-intercept)/slope

Concentration of β-galactosidase per tumour C2 (in mU):

Equation 4.2

C2 = C1 x (amount of PLB buffer per tumour + weight))/0.1

4.5.4 Therapeutic efficacy of DSOLm dendrisomes

Tumours were palpable (typical diameter 5 mm) 6 days after subcutaneous implantation of B16-F10-luc-G5 cancer cells in exponential growth (10^6 cells per flank). DNA encoding TNF- α complexed with DSOLmDoxTf and DSOLmDoxC dendrisomes, DSOLmDoxTf alone, TNF- α complexed with DSOLmTf dendrisomes, free DNA encoding TNF-α or free doxorubicin was administered by intravenous tail vein injections (25 μg of DNA encoding TNF-α and 8 μg doxorubicin per injection). Free doxorubicin was prepared in distilled water at 10 mg/mL. Injections of the treatments were done every 2 days for the duration of the experiment. Animals were weighed daily, and tumour volume was determined by calliper measurements calculated as follows:

Equation 4.3

$$\text{Tumour volume} = d^3 \times \pi/6$$

Where d: tumour diameter measured using callipers

Results were expressed as relative tumour volume:

Equation 4.4

$$\text{Rel. Vol}_{tx} = \text{Vol}_{tx} / \text{Vol}_{t0}$$

Where Rel. Vol_{tx}: relative tumour volume; Vol_{tx}: tumour volume on the day of treatment; Vol_{t0}: initial tumour volume on the first day of experiment.

(If the tumour is not spherical the ellipsoidal formula can be used to calculate tumour volume as follows:

Equation 4.5

Tumor volume = $1/2(\text{length} \times \text{width}^2)$

Tumour response was classified analogous to Response Evaluation Criteria in Solid Tumours (RECIST) guidelines (Eisenhauer *et al.*, 2009). Progressive disease is defined as an increase in relative tumour volume of higher than 1.2-fold, stable disease as a relative volume between 0.7 and 1.2 of starting volume, partial response as measurable tumour with a reduction of more than 30 % (0 to 0.7-fold) and complete response as the absence of any tumour.

4.5.5 Statistical analysis

The results obtained were expressed as means ± standard error of the mean. Statistical significance was determined by one-way analysis of variance (ANOVA) followed by the Tukey multiple comparison post-test (OriginPro 9® software). Differences were considered as significant when $P < 0.05$.

4.6 Results

4.6.1 Quantification of β-galactosidase activity in the tumours following treatment with dendrisome- DNA complexes

Intravenous administration of the transferrin bearing, doxorubicin encapsulated dendrisomplexes (DSOLmDoxTfDNA), led to a significant increase of gene expression in the tumours, with a β-galactosidase amount at least 3-fold higher β-galactosidase expression than that obtained after treatment with non-transferrin bearing doxorubicin encapsulated dendrisomplexes (DSOLmDoxCDNA) and minute or no gene expression observed in the DNA alone, dox alone and untreated tumours. The gene expression levels for the various treatments used were found to be: 197.82 ± 55.21mU β-galactosidase for DSOLmDoxTfDNA, 55.18±49.13 mU β-galactosidase for DSOLmDoxCDNA, -30.70 ± 32.26 β-galactosidase for DNA alone, -79.92 ± 21.46 β-galactosidase for dox alone and -35.50±18.41 mU β-galactosidase for untreated tumours (Figure 4.1).

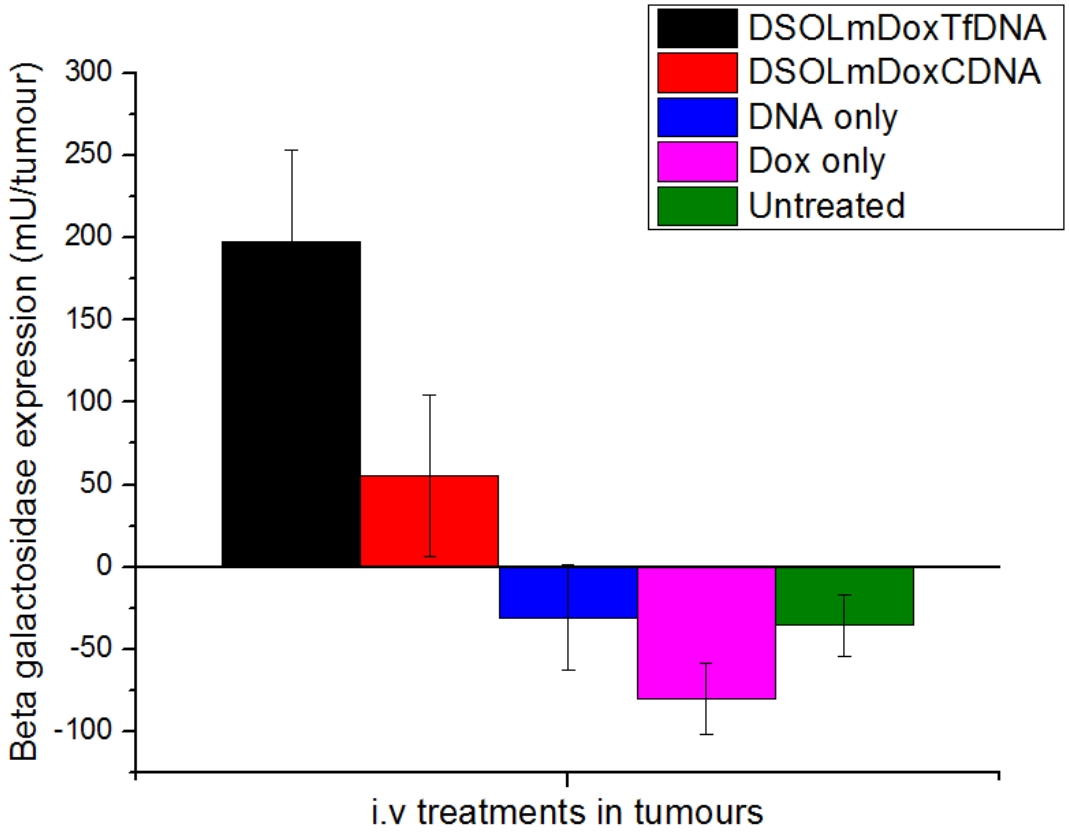

Figure 4.1: Quantification of gene expression 24h after a single intravenous administration of DSOLmDoxTf dendrisomes complexed with DNA encoding TNF-α (DSOLmDoxTfDNA) (8 µg of doxorubicin and 25 µg DNA administered), DSOLmDoxC dendrisomes complexed with DNA encoding TNF-α (DSOLmDoxCDNA) (8 µg of doxorubicin and 25 µg DNA administered) plasmid DNA encoding TNF-α (25 µg DNA administered), Doxorubicin only (8 µg of doxorubicin administered). Results were expressed as milliunits β- galactosidase per tumour (n=5). *: P <0.05: highest gene expression treatment vs. other treatments for each tumour.

4.5.2 Therapeutic Efficacy of DSOLm Dendrisomes

The therapeutic efficacy of DSOLm dendrisomes was investigated *in vivo* in B16F10-Luc-G5 xenograft models after the anti-proliferative studies showed that this drug delivery system demonstrated great potential *in vitro*. It was observed that after eight days of treatment, that the best results were obtained on the tumours in the mice treated with DNA encoding TNF-α complexed with DSOLmDoxTf dendrisomes (transferrin bearing, doxorubicin encapsulated dendrisomplexes). There was partial tumour regression in 10% of the mice, in 10% of the mice the tumour was stable hence not growing, while the remaining 80% of tumours were progressing for the DNA encoding TNF-α complexed with DSOLmDoxTf dendrisome treatment. The DNA encoding TNF-α complexed with DSOLmDoxC (non-transferrin bearing, doxorubicin encapsulated dendrisomplexes) treatment and the doxorubicin alone treatment had 10% of the tumours being stable. The other treatments namely DSOLmTf dendrisomes complexed with DNA encoding TNF-α (DTfp), DNA encoding TNF-α alone (DNA (p)) and untreated (untr), 100% tumour progression in all the mice treated with them was observed, thus leading to the mice treated with them being removed from the study. Relative tumour growth was observed to be lowest in the DNA encoding TNF-α complexed with DSOLmDoxTf dendrisomes and the DNA encoding TNF-α complexed with DSOLmTf dendrisomes. The relative animal weight percentage was constant throughout the experiment with no significant difference observed across the groups (Figures 4.2 and 4.3).

A/

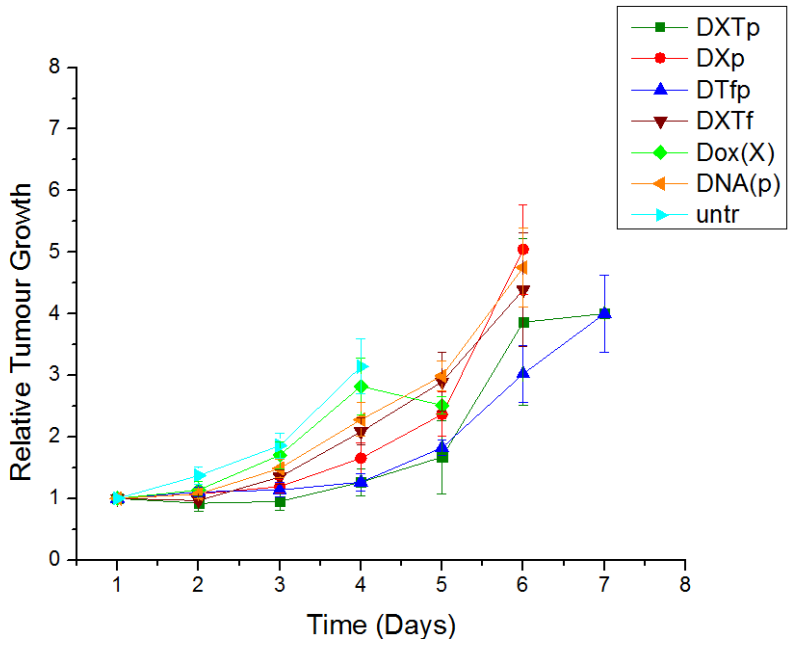

B/

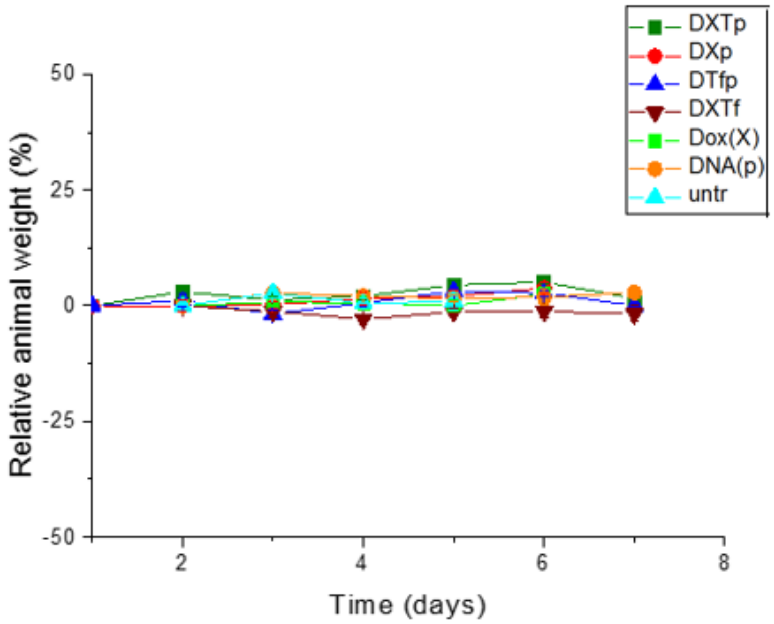

Figure 4.2: Antitumour studies in a mouse B16F10-Luc-G5 xenograft after intravenous administration of DSOLmDoxTf dendrisomes complexed with DNA encoding TNF-α (DXTfp), DSOLmDoxC dendrisomes complexed with DNA encoding TNF-α (DXp), DSOLmTf dendrisomes complexed with DNA encoding TNF-α (DTfp), DSOLmDoxTf (DXTf), doxorubicin (X), DNA encoding TNF-α (DNA(p)) and untreated (untr). (B) Variations of the animal body weight throughout treatment regime. Results are expressed as the mean ± SEM (n=5).

A/

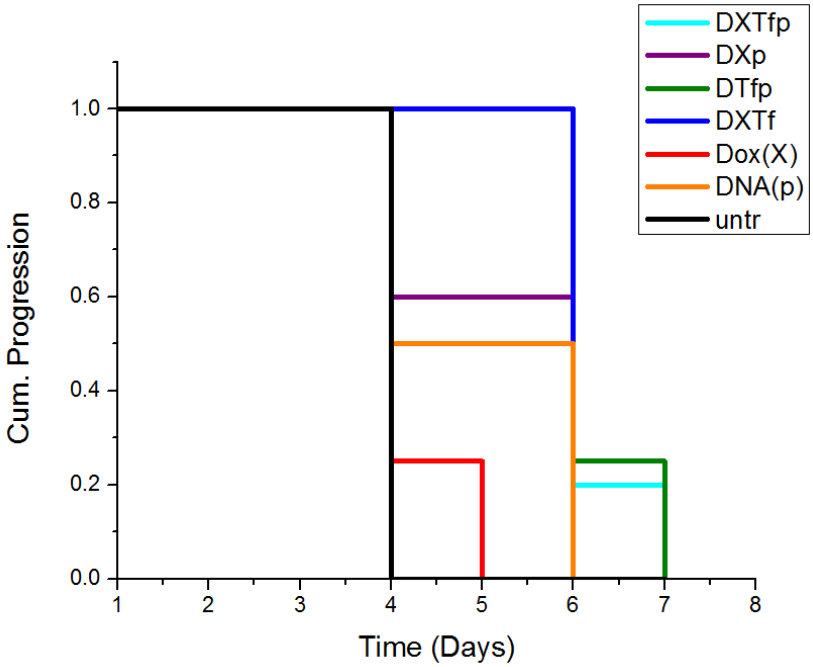

B/

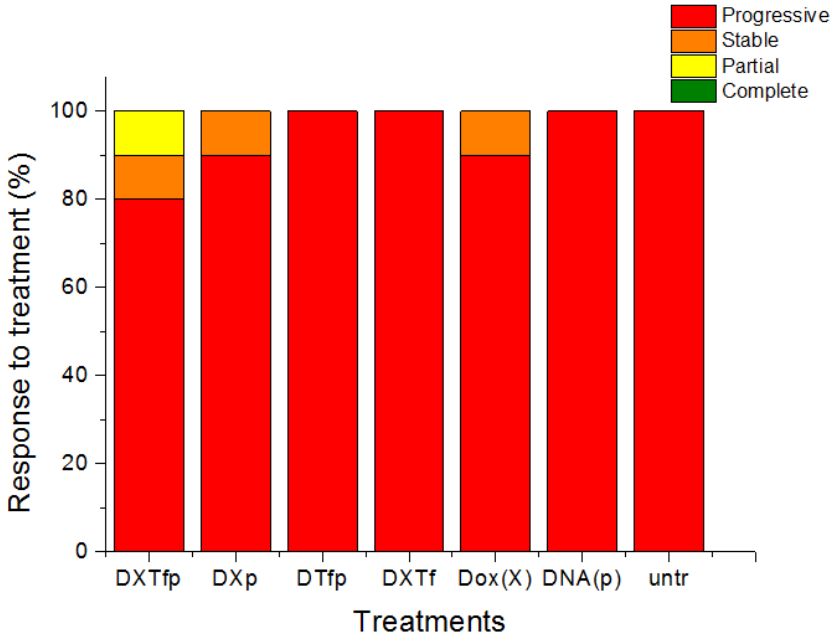

Figure 4.3: Antitumour studies in a mouse B16F10-Luc-G5 xenograft after intravenous administration of DSOLmDoxTf dendrisomes complexed with DNA encoding TNF-α (DXTfp), DSOLmDoxC dendrisomes complexed with DNA encoding TNF-α (DXp), DSOLmTf dendrisomes complexed with DNA encoding TNF-α (DTfp), DSOLmDoxTf (DXTfp), doxorubicin (X), DNA encoding TNF-α (DNA(p)) and untreated (untr). (A) Timescale to disease progression where animals were removed from the study once their tumour reached 12 mm diameter. (B) Overall tumour response to treatments was stratified according to the change in tumour volume.

4.7 Discussion

The *in vivo* evaluation of gene expression in tumours following treatment with dendrisome- DNA complexes demonstrated that there was a significant uptake in the tumours that were treated with DSOLmDoxTf dendrisomes complexed with plasmid encoding β-galactosidase (DSOLmDoxTfDNA) as compared to the tumours treated with DSOLmDoxC dendrisomes complexed with plasmid encoding β-galactosidase (DSOLmDoxCDNA). The results showed that there was showed that β-galactosidase expression was found to be at least 3-fold higher β-galactosidase expression in the transplanted B16F10-Luc-G5 tumours treated with 197.82 ± 55.21mU β-galactosidase expression for DSOLmDoxTfDNA, as compared to that obtained after treatment with DSOLmDoxC dendrisomes complexed with plasmid encoding β-galactosidase (DSOLmDoxCDNA) at 55.18±49.13 mU β-galactosidase expression, while no β-galactosidase expression was detected in the tumours treated with doxorubicin alone, DNA alone and the untreated. These results correlated with what was observed in the cellular uptake and anti-proliferative assay experiments in which B16F10-Luc-G5 cells treated with transferrin bearing, doxorubicin encapsulated dendrisomes complexed with Cy5 labeled plasmid DNA β-galactosidase showed concurrent higher cellular uptake of doxorubicin and Cy5 labeled plasmid DNA β-galactosidase. These results also correlated with the 3-fold higher antiproliferative effect of transferrin bearing, doxorubicin encapsulated dendrisomes complexed with plasmid encoding DNA TNF-α when compared with non-transferrin bearing, doxorubicin encapsulated dendrisomes complexed with plasmid encoding DNA TNF-α in B16F10-Luc-G5 cells. This demonstrated that the transferrin targeted doxorubicin encapsulated dendrisomes complexed with DNA, results in a significant increase in gene expression *in vivo* in

B16F10-Luc-G5 tumour bearing mice when compared with non-targeted, non-transferrin bearing doxorubicin encapsulated dendrisomes complexed with DNA or DNA alone.

This assay has been successfully used in determining gene expression in another published research work. Thus, giving credence to the above results. *In vivo* quantification of β-galactosidase expression studies by Hibah *et al.,* showed that on intravenous administration of β-galactosidase complexed with PEI modified with arginine (Arg), Lysine (Lys) and Leucine (Leu): PEI-Arg, PEI-Lys and PEI-Leu non-viral drug delivery systems respectively, showed that β-galactosidase expression was found to be at least 3-fold higher in the transplanted A431 tumours than that obtained after treatment with unmodified PEI polyplexes. The β-galactosidase amount was observed to be (18.2 ± 1.2, 20.4 ± 3.7, 19.2 ± 3.1mU for PEI-Arg, PEI-Lys and PEI-Leu polyplexes) β-galactosidase per tumour respectively, as compared to 6 ± 1.8 mU β-galactosidase per tumour for the PEI polyplex (Aldawsari, *et al.* 2011).

The antitumour activity of the DSOLm dendrisomes showed that the Tf-bearing DSOLmDox dendrisomes complexed with DNA encoding TNF –α showed a slightly improved therapeutic efficacy when compared with Dox alone or therapeutic DNA alone with 10% of the tumours showing partial tumour regression and 10% being stable, though 80 % of the tumours were still growing. The targeted co-delivery of DNA encoding TNF-α with doxorubicin with Tf-bearing DSOLmDox dendrisomes showed a slightly additive effect. The slight therapeutic response and not complete tumour regression could be attributed to several factors such as: whether the dose of

DNA encoding TNF-α (25 μg) and doxorubicin (8 μg) used was sufficient to cause a therapeutic effect, the transfection efficiency into B16F10-Luc-G5 cells at the dose used, as the transfection efficiency is a crucial factor in ensuring a therapeutic response, the type of cell line; as transfection studies showed that there was a variation in the amount of gene expression observed across the three cancer cell lines used, or the low drug release profile of doxorubicin from the formulation. However, the results obtained show that with optimisation, the Tf-bearing DSOLmDox dendrisomes complexed with TNF –α could produce the desired degree of antitumour activity in B16F10-Luc-G5 cells.

Lasek *et al.*,1996 investigated the effect of the combination of TNF-α and Actinomycin D in various cancer cell lines. Their studies showed that this combination produced synergistic cytotoxic effects against MmB16 melanoma, Lewis lung (LL/2) and L1 sarcoma cells but not against L1210 leukemia cells. An *in vivo* model of localized therapy in which tumor-bearing mice were treated with the combination of TNF-α and Actinomycin D, a correlation with between the *in vivo* and *in vitro* results was observed in mice treated on the MmB I6 melanoma, LL/2 carcinoma and LI sarcoma tumours. Delay of tumor growth and the induction of complete tumor regression was observed in some cases. However, a contrary result was obtained in the mice bearing L1210 leukemia cells. This study demonstrates clearly that types of cancer cell lines used in an *in vivo* study could lead to very diverse results (Lasek *et al.*,1996).

In an *in vivo* study carried out by Lemarié *et al.,* B16F10-Luc-G5 tumours were intravenously treated with Tf- bearing DAB-Am-16 complexed with p DNA encoding p 73 (50 µg). At the last day of treatment, 10 % of the B16F10-Luc-G5 tumours had complete tumour regression while 10% had a partial response (Lemarié *et al.*, 2012). Another study by Al Robaian *et al.,* observed tumor suppression in 60 % of PC-3 and 50% of DU145 prostate cancer cells treated with Tf- bearing DAB-Am-16 complexed with p DNA encoding TNF-α (50 µg) (Al Robaian *et al.,* 2014). Lim *et al.,* also carried out an investigation using intravenous administration of lactoferrin- and lactoferricin-bearing DAB-Am-16 dendriplexes encoding TNFα (50 µg of DNA). Their studies demonstrated that lactoferrin- and lactoferricin-bearing DAB-Am-16 dendriplexes encoding TNFα led to the complete tumour regression of 60% of A431 tumors and up to 50% of B16-F10 tumors in female immunodeficient BALB/c mice over one month (Lim *et al.,* 2015). Based on the foregoing, it could be said the amount of therapeutic DNA used, could be deduced as the cause for total tumour regression not being observed. Based on previous studies utilizing therapeutic plasmid DNA, 50 µg of therapeutic plasmid is the dose usually used to elicit a therapeutic response. It can be argued that tumour regression could have been achieved had a higher dose been used (Lemarié *et al.,* 2012; Al Robaian *et al.,* 2014).

However, some research projects have demonstrated that the non-translation of successful *in vitro* results into a therapeutic advantage *in vivo* could be due to unknown/unclear reasons. A study by Dufès *et al.,* showed that though transferrin (Tf) conjugation using DMSI to doxorubicin loaded palmitoylated glycol chitosan (GCP) vesicles led to improved cellular uptake and increased cytotoxicity for Tf targeted

when compared to GCP Dox vesicles alone, the *in vitro* benefit of targeted Tf vesicles did not translate into a therapeutic advantage *in vivo* (Dufès *et al.*, 2004). The conclusion of that research work was the suggestion that improvement of the *in vivo* activity of the transferrin (Tf) conjugated doxorubicin loaded palmitoylated glycol chitosan (GCP) vesicles delivery systems by using a higher dose, reducing the size of the vesicles and improving the transferrin targeting conjugation process of the (GCP) vesicles.

Another research work by Jones *et al.,* in a randomised phase II trial investigated the rate of response to BCNU alone as well as in combination with TNF in patients with advanced melanoma. The randomised phase II trial demonstrated that the rate of response to anticancer drug Carmustine (BCNU) alone was 20% [95% confidence interval (CI), 2%-38%], and that it was not improved by the addition of TNF (response rate, 10.5%; 95%CI, 1.3%-33%). There was also no difference in survival between the combination therapy and monotherapy even though data from the animal studies carried out in a murine melanoma model and in human melanoma xenografts suggested that there was a positive interaction between BCNU and rhTNFα, resulting in a greater cytotoxic effect on tumours than that produced by either drug alone (Jones *et al.*, 1990; Jones *et al.*,1992). Thus, the challenge of not seeing the translation of positive results from one level/phase of investigation of therapeutic efficacy to another at times can be plagued with unsuccessful outcomes for no clear-cut reasons.

4.8 Conclusion

The results from the quantification of β-galactosidase *in vivo* studies showed that the novel transferrin bearing doxorubicin encapsulated dendrisomes when complexed with DNA showed a 3-fold higher gene expression when compared with non-transferrin bearing doxorubicin encapsulated dendrisomes when complexed with DNA observed. This novel transferrin bearing doxorubicin encapsulated dendrisomes when complexed with therapeutic DNA, showed some therapeutic efficacy *in vivo* leading to partial tumour regression in 10% of the tumours and 10% of the tumours being stable and not progressing. However, complete tumour regression with the dose combination of doxorubicin and plasmid DNA encoding TNF-α used was not achieved. A slight additive effect was what was observed. A research study by van der Veen *et al.,* 2000 demonstrated that when doxorubicin in combination with TNF-α was used in isolated limb perfusion (ILP), the addition of TNF-α caused a synergistic anti-tumour effect, thereby resulting in tumour regression in 54% and 100% of the BN175-fibrosarcoma and the ROS-1 osteosarcoma bearing rats respectively. Their study also showed that combination of doxorubicin with TNF-α treatments was required to achieve optimal tumour regression response in BN175-fibrosarcoma and the ROS-1 osteosarcoma tumours bearing rats (van der Veen *et al.,* 2000). These results could be obtained because of localised treatment via isolated limb perfusion ILP; which is a procedure that may be used to deliver anticancer drugs directly to an arm or leg (Cancer.gov, 2018). However, this procedure is limited in cases of metastasized tumours hence the need for drug delivery carriers that can be targeted passively or actively to metastasized tumours (Giles and Coventry, 2013). Based on the foregoing, further investigation should be carried out to achieve the desired outcomes with these

novel dendrisome structures as they have shown to have the capability to target and deliver therapeutic agents to metastasized tumours from the quantification of β-galactosidase activity *in vivo* and the therapeutic efficacy studies.

CHAPTER 5: CONCLUSION AND FUTURE WORKS

5.1 Conclusion

The formulation of a novel dendrisome hybrid nanocarrier delivery system was based on the fact that non-viral delivery systems with the capability of being efficacious as well as safe for gene therapy are still being widely investigated. Several types of for dendrisomes formulations were attempted using Solulan C24 (DEN-SOL), PEGylated Solulan C24 dendrisomes (DSOLmTf, DSOLmC, DSOLmDoxTf, DSOLmDoxC), TPGS (DEN-TPGS1, DEN-TPGS2) PEGylated TPGS dendrisomes (DTPGSmdTf, DTPGSmdC, DTPGSmdDoxTf, DTPGSmdDoxC) and dihexadecyl phosphate (DEN-DHP).

The preparation and characterisation chapter demonstrated that the formation of transferrin-bearing and control dendrisomes was successfully achieved. This was confirmed with TEM microscopy showing the dendrisome morphology as spherical structures. A spherical shape would enhance entry in passive targeting the porous tumour vasculature. The TEM also confirmed the size of the dendrisomes as less than 500 nm. The images obtained from TEM microscopy verified that the Span 60®, Solulan, cholesterol and lipid mix chosen was able to form dendrisomes with the DAB-Am-16 dendrimer, showing a spherical shape with black structures which based on an a research work done showed the position of the dendrimer on the lipid bilayer (Parimi, Barnes, and Prestidge 2008). Akesson *et al.,* proposed that PAMAM G6 dendrimer formed dendrisomes with lipid vesicles through lipid removal from the vesicle, and translocation of the dendrimers on the vesicle wall (Akesson *et al.,* 2010). Initial dendrisome formulations were lysine-derived amphiphilic dendron aggregates with cholesterol (Al-Jamal *et al.,* 2003; Al-Jamal *et al.,* 2005a and b; Florence *et al.,*

2005). A recent research work showed that the co-assembly of amphiphilic dendrimers with palmitoyloleoylphosphocholine (POPC) could form hybrid nanocarriers (Hinman *et al.,* 2016). Thus, the successful use of DAB-Am-16 generation 3.0 dendrimers to formulate dendrisomes with non-ionic surfactants is worth further investigation.

Size measurements of the PEGylated dendrisomes DSOLm and DTPGSmd gave values that were less than 200nm. This was similar to what was obtained on the TEM. The use of Vivaspin 6 centrifugal concentrator tubes as the preferred method of preparation produced better results in terms of size and a reduction in the amount of agglomerates. The zeta potential measurements showed that the PEGylated dendrisomes were slightly positively charged which enabled successful DNA complexation. This was less than the zeta potential measurements observed in previous studies (Al-Jamal *et al.,* 2005).

Size and zeta measurements of the DEN-SOL and DEN-TPGS dendrisomes gave sizes of 274 to 586 nm that were quite comparable to what has been obtained by other research work done on dendrisomes formulated from lipid-modification of cationic polylysine based dendron by self-assembly of vesicle sizes 310 to 560 nm. The TEM pictures confirmed that the DEN-SOL and DEN-TPGS dendrisomes formulated were spherical shaped nanostructures that were smaller than what was observed in the nano zetasizer. This could be explained to be due to the presence of large particles or aggregates in the formulation. This scenario was similar to what was also observed in dendrisomes formed with the lipid-modified cationic dendrons with Z-average sizes of 311 ± 8 nm, but a smaller vesicle size of < 100 nm obtained via TEM.

The DEN-SOL and DEN-TPGS dendrisomes formulated in this study were neutral while the dendrisomes formulated with lipid-modified cationic dendrons had positive surface charges zeta-potential higher than +50 mV (Al-Jamal *et al.,* 2005). But studies carried out by Sadeghizadeh *et al.,* (2008) demonstrated that neutrally charged dendrosomes entities were able to successfully condense DNA. This correlated with the neutral DEN-SOL and DEN-TPGS (non-PEGylated) dendrisomes formulated in this project (Sadeghizadeh *et al.,* 2008). The DSOLm and DTPGSmd dendrisomes (PEGylated dendrisomes) were found to be positively charged, thus it is being proposed that electrostatic binding is the mechanism action that enables these PEGylated dendrisomes successfully carry DNA successful condensation of DNA molecules which are negatively charged.

The gel retardation assay carried out on the Tf-bearing PEGylated DSOLm and DTPGSmd dendrisomes gave visual confirmation that dendrisome and DNA complexation had successfully taken place. The DNA condensation studies using PicoGreen® intercalation assays carried out on the dendrisomplexes at the ratios tested demonstrated steady fluorescence over the 24 h period of the experiment. A study carried out by Santander-Ortega *et al.,* showed that though therapeutic efficiency was high using DAB-Am16 dendriplexes complexed with plasmid encoding TNFα leading to a regression of 100% of the tumours after ten days, the issue of stability of the dendriplexes was a challenge. Hence, treatments had to be made immediately before injecting the animals to ensure the desired therapeutic response was achieved (cited in Santander-Ortega *et al.*, 2014). This was one of the reasons that this project combined the advantage of the high transfection capability of DAB-Am-16 dendrimer in

expressing therapeutic plasmids and the high stability characteristic of non-ionic surfactants in the formulation of the hybrid dendrisomes. The PicoGreen® assay carried out in this project proved that this hypothesis worked. Complexation of the dendrisomes formulated in this project gave immediate DNA condensation efficiency higher than 75% for all Dendrisome: DNA ratios with ratio 10:1 giving the highest results for both DSOLm and DTPGSmd dendrisomes. Not only was high percentage DNA condensation efficiency immediate, it remained stable over 24 hours with no significant change, for all the dendrisome: DNA ratios for the three formulations DSOLm, DTPGSmd and DEN-SOL dendrisomes. There was no decrease in fluorescence over time in any of the DEN-SOL, DSOLm or DTPGSmd dendrisome: DNA ratios. This is the first report confirming that dendrisomes have the capability to complex DNA. Electrostatic binding is being proposed as a probable mechanism action that enables these dendrisomes successfully carry DNA.

The encapsulation efficiency for the dendrisome formulations that were successfully used for encapsulating doxorubicin were above 80 %. The DEN-SOL, DSOLm, and DTPGSmd dendrisomes encapsulating doxorubicin had 93.11 ± 4.17 %, 97.95 ±0.3 % and 88 % encapsulation efficiency respectively, when measured immediately after purification. This proved that dendrisomes have the capacity for high drug encapsulation. Drug release studies showed that the DEN-SOL and the DSOLm dendrisomes had the capacity to release the encapsulated doxorubicin. The DTPGSmd dendrisomes had a cumulative release of less than 5% which could be attributed to the formation of a complex with the DTPGSmd dendrisomes that did not allow a good release of doxorubicin from them.

The main challenge as mentioned earlier on with the use of doxorubicin in cancer therapy is its dose dependent cardiotoxicity amongst other dose related side effects. As has been reported in several papers this could be attributed to the drug release pattern of free doxorubicin. Doxorubicin has been shown to have a high initial burst followed by a very high percentage cumulative drug release of 100% after just one hour (Han *et al.,* 2011; He *et al.,* 2015). The slow but sustained drug release characteristics observed in the dendrisome formulations made in this project as well as the multifunctional nanocarriers formulated in the other projects mentioned including Al-Jamal *et al.,* demonstrate that continuous administration and high doses required for free doxorubicin with its inherent toxicity issues can be done away with.

Synthetic lipids or non-ionic surfactants as earlier said have the advantage of high stability, easy production and storage and low cost of production as compared to phospholipids when used in drug delivery. Nevertheless, their use in gene delivery has been quite a challenge due to low complexation and transfection capabilities. However, a study on the delivery of pCMS-EGFP plasmid using niosomes based on cationic lipids showed high transfection but very harmful effects *in vitro*. Hence it was suggested that more investigation had to be carried out to ensure efficacy and safety could be achieved (Ojeda *et al.,* 2015). To solve the challenge of transfection, the DAB-Am16 dendrimer with proven high transfection efficiency was incorporated in the dendrisome formulations for this project. The gel retardation assay results showed that the dendrisomplexes showed little or no migration on the as compared to the free DNA for all the dendrisome: DNA complex ratios as seen in chapter 3. The transfection studies also showed good transfection when compared with free DNA as

seen in chapter 3. These results proved that the hypothesis of including a high complexation and transfection efficient dendrimer worked. Dendrisomes have been postulated to be able to carry and DNA. However, no studies have demonstrated the capacity of dendrisomes to carry DNA and drug until now.

Liposomes complexed with PEG (LPPC) were used in a previous study to encapsulate curcumin. This led to enhancement of its cytotoxicity up to 20-fold. Xenograft B16F10-Luc-G5 cells treated with curcumin/LPPC *in vivo*, led to the inhibition of about 60 – 90% of tumour growth. It achieved this by various mechanisms one of which was by initiating cell cycle arrest at G2/M phase, thereby quickly leading to apoptosis. This was an indication that this PEGylation of nano-vesicles could be lead to an increment in therapeutic efficacy even in multi-drug resistant cancers thus supporting the argument that PEGylation of nano-vesicles could lead to the exertion a higher therapeutic effect of anticancer drugs (Lin *et al.*, 2012). The *in vivo* studies showed that there was an additive improvement in the case of the PEGylated Solulan C24 dendrisomes (DSOLm) *in vivo* when compared with all the other treatments used for the *in vivo* study.

Ultracentrifugation in glass tubes was the initial method chosen for purification of the dendrisomes. Sizeable pellets were seen after 1 h of ultracentrifugation of the non-targeted control dendrisomes. However, it was discovered that no discernible pellets of dendrisomes could be seen even after 2 h of ultracentrifugation for the transferrin targeted dendrisomes. Hence the use Sephadex column and dialysis membrane was chosen which successfully purified both the non-targeted control dendrisomes and the

transferrin targeted dendrisomes for the DEN-SOL formulations. After further investigation, it was discovered that the dendrisomes could be retrieved using the Vivaspin® 6 centrifugal concentrators which was which was less laborious and much less time consuming. Hence it was the Vivaspin® 6 centrifugal concentrators that was used for the PEGylated dendrisomes which could account for the slightly higher encapsulation efficiency observed.

The capability of Tf-bearing DEN-SOL dendrisomes to successfully cause transfection in *in vitro* studies was shown using three cancer cell lines A431 human epidermoid and T98G glioma cells and B16-F10-Luc-G5 melanoma. The high transfection values obtained confirmed the opinion formed by studies done by Kwok *et al.,* (2013) that hybrid system of lipids and polymers tend to yield higher transfection values due to a synergistic effect. His team discovered that the addition of lipid combination DOTMA/ DOPE to a novel cationic three-generational peptide dendrimer DNA complexes, enhanced transfection in HeLa cells transfected with a luciferase-expressing plasmid by at least 30-fold when compared to the novel cationic three-generational peptide dendrimer DNA complexes without a lipid component (Kwok *et al.*, 2013). Preclinical studies of PEGylated nano-liposomes (Doxil)® demonstrated that intravenous administration of Doxil® led to prolonged drug circulation time and avoidance of the RES (Barenholz 2012). Gabizon *et al.,* in human studies reported that PEGylated doxorubicin liposomal formulation (Doxil®), demonstrated 4- to 16-fold enhancement of drug levels in cancer patients with malignant effusions as compared to the non-PEGylated doxorubicin liposomal formulation. A research work done by Perry *et al.,* they reported that PEGylation of hydrogel PRINT nanoparticles resulted in at least a

17-fold increase in circulation half-life and a 136-fold decrease in clearance in comparison to non-PEGylated hydrogel PRINT nanoparticles (Perry *et al.*, 2012). Based on the fact that research has confirmed that PEGylation of nanocarriers leads to an increase in circulation *in vivo* thereby leading to an increase in therapeutic efficacy, the DSOLm dendrisomes were the dendrisomes continued with for confocal microscopy and anti-proliferative assay.

The pictures obtained from fluorescence and confocal microscopy confirmed that cellular uptake of DNA and doxorubicin did occur. This finding correlated with previous studies made, confirming that dendrimer-based vesicles have the ability to internalize DNA *in vitro* (Florence *et al.*, 2005).

The anti-proliferative assay demonstrated that the transferrin bearing, doxorubicin encapsulating DSOLm dendrisomplexes demonstrated synergistic antiproliferative activity in B16F10-Luc-G5 cells with a 3-fold higher anti-proliferative activity than non-transferrin bearing, doxorubicin encapsulating DSOLm dendrisomplexes. Thus, confirming the hypothesis that targeting a nanocarrier bearing therapeutic agents with transferrin leads to an increase in anti-proliferative activity. This correlates with other antiproliferative studies carried out, such as transferrin targeted DAB-Am-16 that were complexed with TNF-α, led to significantly increased anti-proliferative effect *in vitro* with 5.1-fold increase in PC-3 cells, 1.7-fold increase in DU145 cells and by more than 100-fold increase in LNCaP cells when compared with non-transferrin conjugated dendriplexes (Al Robaian *et al.*,2014). While in another study by Lemarié *et al.*, demonstrated that epigallocatechin-3-gallate (EGCG) encapsulated in Tf-bearing

vesicles significantly improved the *in vitro* therapeutic efficacy by 1.9-fold for A431 cells; 2.7-fold for B16-F10 cells; and 4-fold for T98G cells when compared with control non-Tf bearing vesicles (Lemarié et al. 2013). These studies thus confirm that transferrin targeting leads to improved anti-proliferative activity *in vitro* at different degrees. The results of the anti-proliferative assay resulted in DSOLm doxorubicin encapsulated dendrisomplexes to be the formulation chosen for *in vivo* studies.

The quantification of β-galactose activity exhibited that transferrin bearing DSOLm doxorubicin encapsulated dendrisomplexes showed significant gene expression when intravenously injected into in female albino immunodeficient BALB/c mice bearing B16F10-Luc-G5 tumours after 24 h of treatment. Therapeutic efficacy studies showed slight therapeutic efficacy with an additive effect was observed in the tumours extracted from female albino immunodeficient BALB/c mice bearing B16F10-Luc-G5 tumours that had been intravenously injected with DSOLm doxorubicin encapsulated dendrisomplexes. Thus, suggesting that with optimisation of the DSOLm dendrisome formulation, complete tumour regression could be achieved.

In this project, we hypothesized that a novel nano-sized dendrisome gene delivery system could be formulated with the capability to encapsulate a drug and concurrently complex plasmid DNA. It was proposed that a transferrin-bearing dendrisome would be prepared and characterized for its ability to encapsulate a model drug and characterize its ability to carry a plasmid DNA on its periphery. The results obtained from chapter 2 have demonstrated that the hypothetical nano size drug delivery system

called dendrisome based on dendrimer and lipid constituents, was successfully formulated. Secondly, this project so far has shown that dendrisomes have the capability to encapsulate and release encapsulated drugs using model anticancer drug doxorubicin as seen in chapter 2. Thirdly experiments done thus far have proven that dendrisomes are able to form dendrisomplexes with non-therapeutic DNA namely β galactosidase as also seen in chapter 2. Fourthly successful transfection, cellular uptake experiments, anti-proliferative assays with dendrisomplexes has been achieved using cancer cell lines B16-F10-Luc-G5 melanoma, A431 human epidermoid and T98G glioma as shown in chapter 3 of this thesis. *In vivo* studies have demonstrated that the co-delivery of plasmid DNA and doxorubicin with Tf-bearing DSOLmDox dendrisomes gave an additive effect when compared with other treatments. Hence the formulation of an efficacious nano size non-viral dendrisome drug delivery system that has the capacity to encapsulate and release a drug, as well as concurrently complex plasmid DNA and successfully cause significant gene expression and some therapeutic activity *in vivo* been successfully formulated.

5.2 Future Works

The results obtained from all the investigations carried out demonstrated that dendrisomes are nanocarriers with high potential for gene delivery, as well as for co-delivery with anticancer drugs for cancer therapy. Though the *in vivo* studies of the DSOLmDoxTf dendrisomes complexed to DNA encoding TNF-α showed only a slight improvement in the area of antitumour activity, with optimisation of these delivery systems, the desired therapeutic effect of complete tumour regression could be achieved. This can be achieved through various means. Investigation into the anti-proliferative and antitumour activity of dendrisomes in other cancer cell lines could be carried out. Another possible approach would be to utilize other targeting ligands such as peptides, folic acid (Vaitilingam *et al.,* 2012; Chen *et al.,* 2013), glucose (Dufès *et al.,* 2000). The use of other targeting moieties could lead to improved therapeutic efficacy *in vivo*. Different combinations of the of the drug and therapeutic DNA other than those chosen for the *in vivo* experiment could also be considered using a high-throughput screening (HTS) cytotoxicity assay (Meng *et al.,* 2013). This could assist in obtaining the best drug and therapeutic DNA combination that would yield the desired results.

The use of other therapeutic DNA for complexing with the dendrisome formulations could also be investigated. Examples of other therapeutic plasmid DNA that could be considered are plasmid DNA encoding p73 (Lemarié *et al.,* 2012), plasmid DNA encoding Human tumor necrosis factor α-related apoptosis-inducing ligand (TRAIL) (Al Robaian *et al.,* 2014; Wang *et al.,* 2015) and plasmid DNA encoding interleukin-

12 (IL-12) (Cha and Daud 2012; Al Robaian *et al.,* 2014). Optimization of this delivery system could also involve investigating the use of other cytotoxic agents such as camptothecin (Ma *et al.,* 2015; Martins *et al.,* 2012) or paclitaxel (Liu *et al.,* 2015; Zhang *et al.,* 2015). Other options for optimizing these novel dendrisome formulations could be to modify the formulation to cause a modification in the size, charge or drug release characteristics of the dendrisome formulations.

On optimisation of these delivery systems, formulation of these dendrisome formulations using other methods such as microfluidics with the nanoassemblr could be considered as microfluidics method would enable scale up. Niosomes have been successfully formulated using a NanoAssemblr™ Benchtop™ (Precision Nano-Systems Inc., Vancouver, Canada) (Obeid *et al.,* 2016). This apparatus uses the principle of microfluidics to formulate the vesicles through hydrodynamic flow leading to nanoprecipitation. The NanoAssemblr™ Benchtop™ has the advantage of being able to produce a large volume of vesicles per run under very controlled conditions: temperature and flow rate. Lipid nanoparticles formulated using microfluidics when complexed with siRNA were able to successfully attain 50% target gene silencing in hepatocytes when administered at a dose level of 10 µg/kg siRNA in mice (Belliveau *et al.,* 2012). Although, this method has the disadvantage of utilizing organic solvents to dissolve the lipid phase. Thus, investigation into the effect of the use of organic solvent in the formulation process on the translocation of the dendrimer unto the lipid bilayer may also be explored.

APPENDIX

APPENDIX 1 CONFERENCE ABSTRACT

Controlled Release Society Annual Meeting and Exposition Boston, USA 2017

Synthesis and evaluation of novel targeted hybrid nanocarriers as DNA and drug co-delivery systems for cancer therapy

Joan Onyebuchi Erebor[1], Sukrut Somani[1], Margaret Mullin[2], Rothwelle Tate[1] and Christine Dufès[1], (1) University of Strathclyde, Glasgow, United Kingdom, (2) University of Glasgow, Glasgow, United Kingdom

Abstract Text:

Introduction: Cancer therapeutic agents have the challenge of non-selective uptake in both normal cells and cancer cells thus leading to a reduced efficacy and adverse effects. The main aim of this study was to synthesize and evaluate novel transferrin-bearing hybrid nanocarriers in order to achieve more selective and efficacious co-delivery of therapeutic DNA encoding TNF-α and anticancer drug doxorubicin. Transferrin receptors are overexpressed on most cancer cells and, can therefore be used as target sites for selective receptor-mediated tumour targeting.

Methods: The hybrid nanocarriers were formulated with a combination of a lipid blend incorporating non-ionic surfactants and a dendrimer via heating and probe sonication. Doxorubicin was encapsulated in the hybrid nanocarriers through probe sonication. Conjugation of transferrin to the hybrid nanocarriers was done via bi-functional cross-linking. Characterization of the hybrid nanocarriers was then carried out through techniques including TEM, size and zeta potential measurements, DNA condensation assays, transfection, confocal microscopy and anti-proliferative assay.

Results: Spherical hybrid nanocarriers were successfully formulated, as demonstrated by TEM. They were in the nanometer range (less than 200 nm) and positively charged. DNA condensation and doxorubicin encapsulation efficiency were respectively above 75% and 95% and demonstrated the ability of the hybrid nanocarriers to carry both DNA and drug. DNA encoding β-galactosidase was successfully expressed in A431, B16 F10-Luc and T98G cancer cells. Anti-proliferative efficacy was improved following treatment with hybrid nanocarriers co-delivering DNA encoding TNF-α and doxorubicin, compared to that observed with doxorubicin alone or DNA encoding TNF-α alone.

Conclusion: Novel targeted hybrid nanocarriers were shown to have the capacity to co-deliver a therapeutic plasmid DNA and anticancer drug doxorubicin to cancer cells, thus leading to increased antiproliferative effect in cancer cell lines overexpressing transferrin.

NOVEL TARGETED HYBRID NANOCARRIERS AS DNA AND DRUG CO-DELIVERY SYSTEMS FOR CANCER THERAPY

Joan Erebor[1], Sukrut Somani[1], Margaret Mullin[2], Rothwelle Tate[1], Christine Dufès[1]

[1] University of Strathclyde Glasgow, G1 1XQ, United Kingdom. [2] Electron Microscopy Facility School of Life Sciences MVLS, University of Glasgow, G12 8QQ, United Kingdom.

Background: Cancer therapeutic agents currently have the challenge of non-selective uptake in both cancer cells and normal cells, thus leading to reduced efficacy. This has prompted the formulation of nanocarriers that can selectively target cancer cells and hence achieve the desired therapeutic outcome at safe doses. The aim of this study was to synthesize, characterize and evaluate the targeting and therapeutic efficacy of novel transferrin-bearing hybrid nanocarriers for the co-delivery of therapeutic DNA encoding TNF-α and anticancer drug doxorubicin to cancer cells. Transferrin was used as a tumour targeting ligand in this study as its receptors are overexpressed on most cancer cells.

Methods: The hybrid nanocarriers were formulated with a combination of a lipid blend incorporating non-ionic surfactants and a dendrimer via heating and probe sonication. Doxorubicin was encapsulated in the hybrid nanocarriers through probe sonication. Conjugation of transferrin to the hybrid nanocarriers was done via bi-functional cross-linking. Characterization of the hybrid nanocarriers was then carried out by TEM, size and zeta potential measurements, DNA condensation assay, transfection, confocal microscopy and anti-proliferative assay.

Results: Spherical hybrid nanocarriers were successfully formulated, as demonstrated by TEM. They were in the nanometer range (less than 200 nm) and positively charged. DNA condensation and doxorubicin encapsulation efficiency were above 75% and 95% respectively. They demonstrated the ability of the hybrid nanocarriers to carry both DNA and drug. DNA encoding β-galactosidase was successfully expressed in A431, B16 F10-Luc and T98G cancer cells. Anti-proliferative efficacy was improved following treatment with hybrid nanocarriers co-delivering DNA encoding TNF-α and doxorubicin, compared to that observed with doxorubicin alone or DNA encoding TNF-α alone.

Conclusions: Novel targeted hybrid nanocarriers were shown to have the capacity to co-deliver a therapeutic plasmid DNA and anticancer drug doxorubicin to cancer cells, thus leading to increased antiproliferative effect in cancer cell lines overexpressing transferrin.

REFERENCES

Acevedo-Morantes, C., Acevedo-Morantes, M., Suleiman-Rosado, D., and Ramírez-Vick, J. (2013). Evaluation of the cytotoxic effect of camptothecin solid lipid nanoparticles on MCF7 cells. Drug Delivery, 20(8), 338–348.

Ahsan, H., Aziz, M. H., Ahmad N (2005). Ultraviolet B exposure activates Stat3 signaling via phosphorylation at tyrosine ^{705} in skin of SKH1 hairless mouse: a target for the management of skin cancer? Biochemical and Biophysical Research Communications 333: 241–246.

Akesson, A., Bendtsen, K. M., Beherens, M. A, Pedersen, J. S., Alfredsson, V., and Cárdenas Gómez, M. (2010). The effect of PAMAM G6 dendrimers on the structure of lipid vesicles. Physical Chemistry Chemical Physics: PCCP, 12(38), 12267–12272.

Al Robaian, M., Chiam, K. Y., Blatchford, D. R., and Dufès, C. (2014). Therapeutic efficacy of intravenously administered transferrin-conjugated dendriplexes on prostate carcinomas. Nanomedicine (London, England), 9(4), 421–34.

Aldawsari, H., Edrada-Ebel, R., Blatchford, D. R., Tate, R. J., Tetley, L., and Dufès, C. (2011). Enhanced gene expression in tumors after intravenous administration of arginine-, lysine- and leucine-bearing polypropylenimine polyplex. Biomaterials, 32(25), 5889–99.

Al-Jamal, K. T., Sakthivel, T., and Florence, A. T. (2005b). Dendrisomes: vesicular structures derived from a cationic lipidic dendron. Journal of Pharmaceutical Sciences, 94(1), 102–113.

Al-Jamal K.T., Sakthivel T., and Florence A.T., (2003). Dendrisomes: cationic lipidic dendron vesicular assemblies. International Journal of Pharmaceutics, (254) 33-36

Al-Jamal, K.T., Ramaswamy C., and Florence A.T., (2005a). Supramolecular structures from dendrons and dendrimers. Advanced Drug Delivery Reviews, (57) 2238-2270.

Allen, T. M., and Cullis, P. R. (2013). Liposomal drug delivery systems: From concept to clinical applications. Advanced Drug Delivery Reviews, 65(1), 36–48.

Alves, C., and Cunha, C. (2012). Electrophoretic Mobility Shift Assay: Analyzing Protein – Nucleic Acid Interactions. Gel Electrophoresis-Advanced Techniques, 205–228.

Almeida, C., and Barry, S. (2010). Cancer: Basic Science and Clinical Aspects. (Wiley-Blackwell, Ed.) (First). West Sussex: Wiley-Blackwell (pp 1-50).

American Cancer Society (2014). Cancer Facts and Figures. Cancer Facts and Figures. http://www.cancer.org/acs/groups/content/@research/documents/webcontent/acspc-042151.pdf

Arzani, G., Haeri, A., Daeihamed, M., Bakhtiari-Kaboutaraki, H., and Dadashzadeh, S. (2015). Niosomal carriers enhance oral bioavailability of carvedilol: effects of bile salt-enriched vesicles and carrier surface charge. International Journal of Nanomedicine, 10(1), 4797–813.

Auda, S. H., Fathalla, D., Fetih, G., El-Badry, M., and Shakeel, F. (2016). Niosomes as transdermal drug delivery system for celecoxib: in vitro and in vivo studies. Polymer Bulletin, 73(5), 1229–1245.

Bayindir, Z., and Yuksel, N. (2010). Characterization of niosomes prepared with various nonionic surfactants for paclitaxel oral delivery. Journal of Pharmaceutical Sciences, 99(4), 2049–2060.

Barenholz, Y. (2012). Doxil ® - The first FDA-approved nano-drug: Lessons learned. Journal of Controlled Release, 160(2), 117–134.

Béduneau, A., Saulnier, P., Hindré, F., Clavreul, A., Leroux, J. C., and Benoit, J. P. (2007). Design of targeted lipid nanocapsules by conjugation of whole antibodies and antibody Fab' fragments. Biomaterials, 28(33), 4978–4990.

Bei, D., Meng, J., and Youan, B. (2010). Engineering nanomedicines for improved melanoma therapy progress and promises. Nanomedicine (London, England), 5 (9) 1385–1399.

Bertrand, N., Wu, J., Xua, X., Kamaly, N., and Farokhzad, O. C (2014). Cancer Nanotechnology: The impact of passive and active targeting in the era of modern cancer biology. Advanced Drug Delivery Reviews. 66: 2–25.

Birnboim H.C., and Doly J (1979). A rapid alkaline extraction procedure for screening recombinant plasmid DNA. Nucleic acids Research, 7 (6) 1513-1523.

Bleeker, F. E., Molenaar, R. J., and Leenstra, S. (2012). Recent advances in the molecular understanding of glioblastoma. Journal of Neuro-Oncology, 108(1), 11–27.

Bodley, A., Liu, L. F., Israel, M., Seshadri, R., Koseki, Y., Giuliani, F. C., Kirschenbaum, S., Silber, R., Potmesil, M. (1989). DNA topoisomerase II-mediated interaction of doxorubicin and daunorubicin congeners with DNA. Cancer Research, 49 (21), 5969–5978.

Bose, R. J., Lee, S.-H., and Park, H. (2016). Lipid-based surface engineering of PLGA nanoparticles for drug and gene delivery applications. Biomaterials Research, 20: 34.

Brar, S. K., and Verma, M. (2011). Measurement of nanoparticles by light-scattering techniques. TrAC - Trends in Analytical Chemistry, 30 (1), 4–17.

Budd, G. T., Green, S., Baker, L. H., Hersh, E. P., Weick, J. K., and Osborne, C. K. (1991). A Southwest Oncology Group Phase II Trial of recombinant tumor necrosis factor in metastatic breast cancer. Cancer. 68(8):1694-1695.

Budhu, S., Wolchok, J., and Merghoub, T. (2014). The importance of animal models in tumor immunity and immunotherapy. Current Opinion in Genetics and Development, 24, 46–51.

Çağdaş, M., Sezer, A. D., and Bucak, S. (2014). Liposomes as Potential Drug Carrier Systems for Drug Delivery. In A. D. Sezer (Ed.), Nanotechnology and Nanomaterials » "Application of Nanotechnology in Drug Delivery" (pp. 1–50).

Caliper Life Sciences. (2008). Bioware Cell Line B16-F10-Luc-G5. Hopkinton: Caliper Life Sciences.

Cancer Research UK. (2014). Cancer Incidence in the UK in 2011: Cancer Statistics report.

Cancer Research UK. (2015). All cancers combined: Cancer Statistics Key Facts.

Cancer.gov (2018). Isolated limb perfusion. https://www.cancer.gov/publications/dictionaries/cancer-terms/def/isolated-limb-perfusion acessed 280218

Caramelo-Nunes C., Gabriel, M. F., Almeida, P., Marcos J.C., and Tomaz C, T. (2012). Purification of plasmid DNA from clarified and non-clarified *Escherichia coli* lysates by berenil pseudo-affinity chromatography. Journal of Chromatography B 904 81– 87.

Cha, E., and Daud, A. (2012). Plasmid IL-12 electroporation in melanoma Human Vaccine Immunotherapy. 8(11), 1734–1738

Chai, M., and Niu, Y. (2001). Structure and conformation of DAB dendrimers in solution via multidimensional NMR techniques. Journal of the American Chemical Society. 266(7), 4670–4678.

Chamberlain, M. C. (2012). Neurotoxicity of intra-CSF liposomal cytarabine (DepoCyt) administered for the treatment of leptomeningeal metastases: a retrospective case series. Journal of Neuro-Oncology, 109(1), 143–148.

Chang, H.-I., and Yeh, M.-K. (2012). Clinical development of liposome-based drugs: formulation, characterization, and therapeutic efficacy. International Journal of Nanomedicine, 7, 49–60.

Chaplot, S. P., and Rupenthal, I. D. (2014). Dendrimers for gene delivery--a potential approach for ocular therapy? The Journal of Pharmacy and Pharmacology, 66(4), 542–56.

Chen, C., Ke, J., Zhou, X. E., Yi, W., Brunzelle, J. S., Li, J., Yong, E., Xu, H E., Melcher, K. (2013). Structural basis for molecular recognition of folic acid by folate receptors. Nature, 500(7463), 486–9.

Chen, N., Wu, C., Chung, C., Hwu, Y., Cheng, S., Mou, C., and Lo, L (2012). Probing the dynamics of doxorubicin-DNA intercalation during the initial activation of apoptosis by fluorescence lifetime imaging microscopy (FLIM). PloS One, 7(9), e44947.

Cheng, Y., Samia, A. C., Meyers, J. D., Panagopoulos, I., Fei, B., and Burda, C. (2008). Highly efficient drug delivery with gold nanoparticle vectors for *in vivo* photodynamic therapy of cancer. Journal of the American Chemical Society, 130(32), 10643–10647.

Dahm, R. (2005). Friedrich Miescher and the discovery of DNA. Developmental Biology, 278 (2), 274–288.

de Brabander-van den Berg, E.M.M., and Meijer, E.W., (1993). Poly (propy1ene imine) Dendrimers: Large-Scale Synthesis by Hetereogeneously Catalyzed Hydrogenations Angewandte Chemie International Edition in English 32 (9), 1308-1311.

Dey, N., De, P., Smith, B. R., and Leyland-Jones, B (2010). Of mice and men: the evolution of animal welfare guidelines for cancer research. British Journal of Cancer 102 (11) 1553 – 1554.

Dhaliwal A (2013) DNA Extraction and Purification Mater Methods 3:191.

Dimitrijevic, D., Lamandin, C., Uchegbu, I. F., Shaw, A J., and Florence, A T. (1997). The effect of monomers and of micellar and vesicular forms of non-ionic surfactants (Solulan C24 and Solulan 16) on Caco-2 cell monolayers. The Journal of Pharmacy and Pharmacology, 49: 611–616.

Dimitrijevic, D., Shaw, A. J., and Florence, A. T. (2000). Effects of some non-ionic surfactants on transepithelial permeability in Caco-2 cells. The Journal of Pharmacy and Pharmacology, 52 (2), 157–162.

Dintaman, J., and Silverman, J. (1999). Inhibition of P-Glycoprotein by D-α Tocopheryl Polyethylene Glycol 1000 Succinate (TPGS). Pharmaceutical Research, 16 (10), 1550–1556.

Dobrovolskaia, M. A, and McNeil, S. E. (2007). Immunological properties of engineered nanomaterials. Nature Nanotechnology, 2 (8), 469–78.

Janssen (2015) Doxil.com https://www.doxil.com/hcp/mechanism-of-action accessed 250816

Dragan, A. I., Casas-Finet, J. R., Bishop, E. S., Strouse, R. J., Schenerman, M. A., and Geddes, C. D. (2010). Characterization of PicoGreen® interaction with dsDNA and the origin of its fluorescence enhancement upon binding. Biophysical Journal, 99 (9), 3010–3019.

Driscoll, M. D., Rentergent, J., and Hay, S. (2014). A quantitative fluorescence-based steady-state assay of DNA polymerase. FEBS Journal, 281: 2042–2050.

Dufès, C., Muller, J. M., Couet, W., Olivier, J. C., Uchegbu, I. F., and Schätzlein, A. G. (2004). Anticancer Drug Delivery with Transferrin Targeted Polymeric Chitosan Vesicles. Pharmaceutical Research, 21 (1), 101–107.

Dufès, C., Robaian, M. Al, and Somani, S. (2013). Transferrin and the transferrin receptor for the targeted delivery of therapeutic agents to the brain and cancer cells. Therapeutic Delivery, 4 (5), 629–40.

Dufès, C., Schätzlein, A. G., Tetley, L., Gray, A. I., Watson, D. G., Olivier, J. C., Couet, W., and Uchegbu, I. F. (2000). Niosomes and polymeric chitosan based vesicles bearing transferrin and glucose ligands for drug targeting. Pharmaceutical Research, 17(10), 1250–1258.

Dufès, C., Uchegbu, I. F., and Schätzlein, A. G. (2005). Dendrimers in gene delivery. Advanced Drug Delivery Reviews, 57(15), 2177–202.

Duncan, R., and Izzo, L. (2005). Dendrimer biocompatibility and toxicity. Advanced Drug Delivery Reviews, 57(15), 2215–37.

Dutta T., Garg M., Jain N.K. (2008). Poly (propyleneimine) dendrimer and dendrosome mediated genetic immunization against hepatitis B Vaccine, 26 (27-28) 3389-3394.

El-Aneed, A. (2004). An overview of current delivery systems in cancer gene therapy. Journal of Controlled Release, 94(1), 1–14.

Encyclopædia Britannica.com (2016). Cholesterol Chemical Compound https://www.britannica.com/science/cholesterol acessed 05/07/16

Etheridge, M. L., Campbell, S. A., Erdman, A. G., Haynes, C. L., Wolf, S. M., and McCullough, J. (2013). The big picture on nanomedicine: the state of investigational and approved nanomedicine products. Nanomedicine: Nanotechnology, Biology, and Medicine, 9(1), 1–14.

Fanciullino, R., Ciccolini, J., and Milano, G. (2013). Challenges, expectations and limits for nanoparticles-based therapeutics in cancer: A focus on nano-albumin-bound drugs. Critical Reviews in Oncology/Hematology, 88(3), 504–513.

Fang J, Nakamura H and Maeda H (2011). The EPR effect: Unique features of tumor blood vessels for drug delivery, factors involved, and limitations and augmentation of the effect. Advanced Drug Delivery Reviews, 63: 136–151.

Farhood, H., Serbina, N., and Huang, L. (1995). The role of dioleoyl phosphatidylethanolamine in cationic liposome mediated gene transfer. Biochimica et Biophysica Acta, 1235: 289-295

Feldman E. R., Creagan, E. T., Schaid, D. J., and Ahmann, D. L. (1992). Phase II Trial of Recombinant Tumor Necrosis Factor in Disseminated Malignant Melanoma. American Journal of Clinical Oncology, 15(3):256-259.

Florence, A. T., Ramaswamy, C., Ruenraroengsak, P., Rubeiro, S., and Singh, B. (2005). Dendrimers as Carriers in Drug and Gene Delivery. Drug Delivery, (5), 11–12.

Fraley, R., Subramani, S., Berg, P., and Papahadjopoulos, D. (1980). Introduction of liposome-encapsulated SV40 DNA into cells. Journal of Biological Chemistry, 255(21), 10431–10435.

Frank, D., Tyagi, C., Tomar, L., Choonara, Y. E., du Toit, L. C., Kumar, P., Penny, C., Pillay, V. (2014). Overview of the role of nanotechnological innovations in the detection and treatment of solid tumors. International Journal of Nanomedicine, 9, 589–613.

Fu, J. Y., Blatchford, D. R., Tetley, L., and Dufès, C. (2009). Tumor regression after systemic administration of tocotrienol entrapped in tumor-targeted vesicles. Journal of Controlled Release, 140(2), 95–9.

Fu, J. Y., and Dufès, C. (2014). Anti-Cancer Efficacy of Intravenously Administered Tumor-Targeted Vesicles Entrapping Tocotrienol, Pharmaceutical Nanotechnology, 2 (3) 1–9.

Gao, X., Cui, Y., Levenson, R., Chung, L., and Nie, S. (2004). *In vivo* cancer targeting and imaging with semiconductor quantum dots. Nature Biotechnology, 22, 969–976.

Gabizon, A., and Papahadjopoulos, D. (1988). Liposome formulations with prolonged circulation time in blood and enhanced uptake by tumors. Proceedings of the National Academy of Sciences, 85:6949–6953.

Gabizon, A., Catane, R., Uziely, B., Kaufman, B., Safra, T., Cohen, R., Martin, F., Huang, A., and Barenholz, Y. (1994). Prolonged circulating time and enhanced accumulation in malignant exudates of doxorubicin encapsulated in polyethylene-glycol coated liposomes. Cancer Research, 54: 987–992.

Gabizon, A., Shmeeda, H., and Barenholz, Y. (2003). Pharmacokinetics of PEGylated liposomal Doxorubicin: review of animal and human studies. Clinical Pharmacokinetics, 42(5), 419–436.

Gardikis, K., Hatziantoniou, S., Viras, K., Wagner, M., and Demetzos, C. (2006). A DSC and Raman spectroscopy study on the effect of PAMAM dendrimer on DPPC model lipid membranes. International Journal of Pharmaceutics, 318, 118–123.

Gaspar, V. M., Gonçalves, C., De Melo-Diogo, D., Costa, E. C., Queiroz, J. A., Pichon, C., Sousa, F., and Correia, I. J. (2014). Poly(2-ethyl-2-oxazoline)-PLA-g-PEI amphiphilic triblock micelles for co-delivery of minicircle DNA and chemotherapeutics. Journal of Controlled Release, 189, 90–104.

Gaspar, V. M., Moreira, A. F., Costa, E. C., Queiroz, J. a., Sousa, F., Pichon, C., & Correia, I. J. (2015). Gas-generating TPGS-PLGA microspheres loaded with nanoparticles (NIMPS) for co-delivery of minicircle DNA and anti-tumoral drugs. Colloids and Surfaces B: Biointerfaces, 134, 287–294.

Gentekos, D. T., Dupuis, L. N., and Fors, B. P. (2016). Beyond Dispersity: Deterministic Control of Polymer Molecular Weight Distribution. Journal of the American Chemical Society, 138(6), 1848–1851.

Gerstein, M. B., Bruce, C., Rozowsky, J. S., Zheng, D., Du, J., Korbel, J. O., Emanuelsson, O., Zhengdong Z. D., Weissman, S., Snyder, M. (2007). What is a gene, post-ENCODE? History and updated definition. Genome Research, 17, 669–681.

Giard, D. J., Aaronson, S. A, Todaro, G. J., Arnstein, P., Kersey, J. H., Dosik, H., and Parks, W. P. (1973). *In vitro* cultivation of human tumors: establishment of cell lines derived from a series of solid tumors. Journal of the National Cancer Institute, 51(5), 1417–1423.

Gilbert, R., Hess, M., Jenkins, A. D., Jones, R., Kratochvíl, P., and Stepto, R. F. T. (2009). Dispersity in polymer science (IUPAC Recommendations 2009). Pure and Applied Chemistry, 81(2), 351–353.

Giles, M. H. and Coventry, B. J. (2013). Isolated limb infusion chemotherapy for melanoma: an overview of early experience at the Adelaide Melanoma Unit. Cancer Management and Research, 5: 243–249.

Ginn, S. L., Alexander, I. E., Edelstein, M. L., Abedi M. R., Wixon J. (2013). Gene therapy clinical trials worldwide to 2012 – an update. The Journal of Gene Medicine, 15: 65–77.

Gregorc, V., Santoro, A., Bennicelli, E., Punt, C. J., Citterio, G., Timmer-Bonte, J. N., Caligaris Cappio, F., Lambiase, A., Bordignon, C., and van Herpen C.M. (2009). Phase Ib study of NGR-hTNF, a selective vascular targeting agent, administered at low doses in combination with doxorubicin to patients with advanced solid tumours. British Journal of Cancer, 101, 219 – 224.

Hajar, R. (2011). Animal Testing and Medicine. Heart Views: The Official Journal of the Gulf Heart Association, 12(1), 42.

Han, L., Huang, R., Li, J., Liu, S., Huang, S., and Jiang, C. (2011). "Plasmid pORF-hTRAIL and Doxorubicin Co-Delivery Targeting to Tumor Using Peptide-Conjugated Polyamidoamine Dendrimer." Biomaterials 32 (4).

Han, X., Li, Z., Sun, J., Luo, C., Li, L., Liu, Y., Du, Y., Qiu, S., Ai, X., Wu, C., Lian, H., He, Z. (2015). Stealth CD44-targeted hyaluronic acid supramolecular nanoassemblies for doxorubicin delivery: Probing the effect of uncovalent pegylation degree on cellular uptake and blood long circulation. Journal of Controlled Release, 197, 29–40.

Han, Y., Zhang, Y., Li, D., and Chen, Y. (2014). Transferrin-modified nanostructured lipid carriers as multifunctional nanomedicine for codelivery of DNA and doxorubicin. Journal of Nanomedicine, 9, 4107–4116.

Hanahan, D., and Weinberg, R. A. (2011). Hallmarks of cancer: the next generation. Cell, 144(5), 646–74.

Hanahan, D., and Weinberg, R. A. (2000). The Hallmarks of Cancer Review University of California at San Francisco. Cell, 100, 57–70.

Hajar, R. (2011). Animal Testing and Medicine. Heart Views: The Official Journal of the Gulf Heart Association, 12(1), 42.

He, X., Alves, C.S., Oliveira, N., Rodrigues, J., Zhu, J., Bányaic, I., Tomás, H., and Shi, X. (2015). "RGD Peptide-Modified Multifunctional Dendrimer Platform for Drug Encapsulation and Targeted Inhibition of Cancer Cells." Colloids and Surfaces B: Biointerfaces (125) 82-89.

Heimans, J. (1962). Hugo de Vries and the gene concept. American Naturalist (96) 93–104.

Heim, M. E., Siegmund, R., Illiger, H. J., Klee, M., Rieche, K., Berdel, W. E and Edler, L (1990). Tumor necrosis factor in advanced colorectal cancer: a phase II study. A trial of the phase I/II study group of the Association for Medical Oncology of the German Cancer Society. Onkologie. 13(6):444-7.

Held, P (2007). Kinetic Analysis of β-Galactosidase Activity using the PowerWave™ HT and Gen5™ Data Analysis Software Basic enzyme kinetic determinations. https://www.biotek.com/resources/docs/B-Gal_Michaelis-Menten_App_Note.pdf acessed 11/12/2016

Hermanson, G. T., (2013). Functional Targets. In J. Audet and M. Preap (Eds.), Bioconjugate Techniques (Third edition), Oxford. Chapter 2 (pp. 127–168).

Hermanson, G. T. (2013). The Reactions of Bioconjugation. In J. Audet and M. Preap (Eds.), Bioconjugate Techniques (Third edition), Oxford. Chapter 3 (pp. 229–258).

Hinman, S. S., Ruiz, C. J., Cao, Y., Ma, M.C., Tang, J., Laurini, E., Posocco, P., Giorgio, S., Pricl, S., Peng, L., and Cheng Q (2017). Mix and Match: Coassembly of Amphiphilic Dendrimers and Phospholipids Creates Robust, Modular, and Controllable Interfaces. ACS Applied Materials and Interfaces, 9, 1029−1035.

Hirose, Y., Hata, K., Kuno, T., Yoshida, K., Sakata, K., Yamada, Y., Tanaka, T., Reddy, BS., Mori H (2004) Enhancement of development of azoxymethane-induced colonic premalignant lesions in C57BL/KsJ-*db/db* mice. Carcinogenesis 25: 821 –825.

Huang, R., Qu, Y., Ke, W., Zhu, J., Pei, Y., Jiang, C (2007) Efficient gene delivery targeted to the brain using a transferrin-conjugated polyethyleneglycol-modified polyamidoamine dendrimer. The FASEB Journal 21 (4), 1117-1125.

Ibraheem, D., Elaissari, A., and Fessi, H. (2014). Gene therapy and DNA delivery systems. International Journal of Pharmaceutics, 459(1-2), 70–83.

Intmedpress.com (https://www.intmedpress.com/journals/avcc/article.cfm?id=1684andpid=92andsType=AVCC accessed on 090816)

Interchim (2017). DMA, DMP, DMS Homobifunctional imidoester cross-linkers http://www.interchim.fr/ft/0/06633A.pdf acessed 110217

Ionov, M., Gardikis, K., Wróbel, D., Hatziantoniou, S., Mourelatou, H., Majoral, J., Klajnert, B., Bryszewska, M., and Demetzos.C (2011). "Interaction of Cationic Phosphorus Dendrimers (CPD) with Charged and Neutral Lipid Membranes." Colloids and Surfaces B: Biointerfaces, 82 (1), 8-12.

Jain, K. (2008). Drug Delivery Systems - An Overview. (Jain, K., Ed.) Methods in Molecular Biology Humana Press. Totowa, NJ, (pp 1-50)

Jain, K., Kesharwani, P., Gupta, U., and Jain, N. K. (2010). Dendrimer toxicity: Let's meet the challenge. International Journal of Pharmaceutics, 394(1-2), 122–142.

Jenkins, D. E., Oei, Y., Hornig, Y. S., Yu, S. F., Dusich, J., Purchio, T., and Contag, P. R. (2003). Bioluminescent imaging (BLI) to improve and refine traditional murine models of tumor growth and metastasis. Clinical and Experimental Metastasis, 20(8), 733–744.

Jin, L., Zeng, X., Liu, M., Deng, Y., and He, N. (2014). Current progress in gene delivery technology based on chemical methods and nano-carriers. Theranostics, 4(3), 240–55.

Jones, A.L., Millar, J. L., Millar, B. C., Powell, B., Selby, P., Winkley, A., Lakhani, S., Gore, M. E and McElwain, T. J (1990). Enhanced anti-tumour activity of carmustine (BCNU) with tumour necrosis factor *in vitro* and *in vivo*. British Journal of Cancer 62:776.

Jones, A.L., O'Brien, M. E., Lorentzos, A., Viner, C., Hanrahan, A., Moore, J., Millar, J. L and Gore, M. E (1992). A randomised phase II study of carmustine alone or in combination with tumour necrosis factor in patients with advanced melanoma. Cancer Chemotherapy and Pharmacology, 30 (1), 73-76.

Johannsen, W. 1909. Elemente der exakten Erblichkeitslehre, Jena. Cited by Nils Roll-Hansen (2014). The holist tradition in twentieth century genetics. Wilhelm Johannsen's genotype concept. The Journal of Physiology, 592 (11), 2431–2438.

Joy, D. C., Brian, S. B., and Ford, J. (2016). Transmission electron microscope: Instrument. Encyclopædia Britannica.com https://www.britannica.com/technology/transmission-electron-microscope acessed 050716

Junyaprasert, V. B., Singhsa, P., and Jintapattanakit, A. (2013). Influence of chemical penetration enhancers on skin permeability of ellagic acid-loaded niosomes. Asian Journal of Pharmaceutical Sciences, 8(2), 110–117.

Kamboj, S., Saini, V., Magon, N., Bala, S., and Jhawat, V. (2013). Vesicular drug delivery systems: A novel approach for drug targeting. International Journal of Drug Delivery, 5: 121–130.

Kane, M. A., Elwood, P. C., Portillo, R. M., Antony, A. C., Najfeld, V., Finley, A., Waxman, X., Kolhouse, J. F (1988). Influence on immunoreactive folate-binding proteins of extracellular folate concentration in cultured human cells. Journal of Clinical Investigation, 81 (5), 1398–1406.

Kaur, G., and Dufour, J. M (2012) Cell lines: Valuable tools or useless artifacts. Spermatogenesis 2 (1), 1-5.

Kemeny, N., Childs, B., Larchian, W., Rosado, K., Kelsen, D (1990). A phase II trial of recombinant tumor necrosis factor in patients with advanced colorectal carcinoma. Cancer, 66 (4):659-63.

Kesharwani, P., Jain, K., and Jain, N (2014). Dendrimer as nanocarrier for drug delivery. Progress in Polymer Science, (39), 268–307.

Khalil, I.A., Kogure, K., Akita, H., and Harashima, H., (2006). Uptake Pathways and Subsequent Intracellular Trafficking in Nonviral Gene Delivery
Pharmacological Reviews 58:32–45.

Kim, H. P., Gerhard, B., Harasym, T. O., Mayer, L. D., and Hogge, D. E., (2011). Liposomal encapsulation of a synergistic molar ratio of cytarabine and daunorubicin enhances selective toxicity for acute myeloid leukemia progenitors as compared to analogous normal hematopoietic cells. Experimental Hematology, 39 (7), 741–750.

Kim, T. K., and Eberwine, J. H., (2010). Mammalian cell transfection: the present and the future. Analytical and Bioanalytical Chemistry, 397 (8), 3173–8.

Knight, M. I., and Chambers, P. J. (2003). Problems associated with determining protein concentration Problems associated with determining protein concentration: A comparison of techniques for protein estimations. Molecular Biotechnology, 23(1), 19-28.

Koppu, S., Oh, Y. J., Edrada-Ebel, R., Blatchford, D. R., Tetley, L., Tate, R. J., and Dufès, C. (2010). Tumor regression after systemic administration of a novel tumor-targeted gene delivery system carrying a therapeutic plasmid DNA. Journal of Controlled Release, 143(2), 215-221.

Kraft, J. C., Freeling, J. P., Wang, Z., and Ho, R. J. Y. (2014). Emerging research and clinical development trends of liposome and lipid nanoparticle drug delivery systems. Journal of Pharmaceutical Sciences, 103(1), 29–52.

Kulve, H. Te. (2010). Anticipating Market Introduction of Nanotechnology-Enabled Drug Delivery Systems. In A. D. Sezer (Ed.), Application of Nanotechnology in Drug Delivery (pp. 501–524).

Kumar, G. P., and Rajeshwarrao, P. (2011). Nonionic surfactant vesicular systems for effective drug delivery—an overview. Acta Pharmaceutica Sinica B, 1(4), 208–219.

Kumbhar, D., Wavikar, P., and Vavia, P. (2013). Niosomal gel of lornoxicam for topical delivery: in vitro assessment and pharmacodynamic activity. AAPS PharmSciTech, 14(3), 1072–82.

Kwok, A., Eggimann, G. a, Reymond, J., Darbre, T., and Hollfelder, F. (2013). Peptide Dendrimer / Lipid Hybrid Systems are Efficient DNA Transfection Generations Reagents: Relationships Highlight the Role of Charge Distribution Across Dendrimer, 44, 4668–4682.

Lahoti, T., Patel, D., Thekkemadom, V., Beckett, R., and Ray, S. (2012). Doxorubicin-induced *in vivo* nephrotoxicity involves oxidative stress-mediated multiple pro- and anti-apoptotic signaling pathways. Current Neurovascular Research, 9(4), 282–295.

Labome.com (2016). https://www.labome.com/method/Laboratory-Mice-and-Rats.html

Lakowicz, J. R. (2011). Principles of fluorescence spectroscopy Joseph R. Lakowicz, editor. Principles of fluorescence spectroscopy, Springer, New York, USA, 3rd edn, 2006. (Third). New York: Springer pg 1-28.

Lane, D., Prentki, P., and Chandler, M. (1992). Use of gel retardation to analyze protein-nucleic acid interactions. Microbiological Reviews, 56(4), 509–528.

Laouini, A., Jaafar-Maalej, C., Limayem-Blouza, I., Sfar, S., Charcosset, C., and Fessi, H. (2012). Preparation, Characterization and Applications of Liposomes: State of the Art. Journal of Colloid Science and Biotechnology, 1(2), 147–168.

Lasek, W., Giermasz, A., Kuc, K., Wankowicz, A., Wojciech, F., Golab, J., Zadgozdzon, R., Stoklosa, T., and Jakobisiak, M (1996). Potentiation of The Anti-Tumor Effect of Actinomycin D by Tumor Necrosis Factor α In Mice: Correlation Between *in vitro* and *in vivo* Results. International Journal of Cancer 66,374-379.

Lemarié, F., Croft, D. R., Tate, R. J., Ryan, K. M., and Dufès, C. (2012). Tumor regression following intravenous administration of a tumor-targeted p73 gene delivery system. Biomaterials, 33(9), 2701–9.

Lemarié, F., Chang, C. W., Blatchford, D. R., Amor, R., Norris, G., Tetley, L., McConnell, G., and Dufès, C. (2013). Antitumor activity of the tea polyphenol epigallocatechin-3-gallate encapsulated in targeted vesicles after intravenous administration. Nanomedicine, 8(2), 181–192.

Li, J., Wang, Y., Liang, R., An, X., Wang, K., Shen, G., Tu, Y., Zhu, J., Tao, J. (2015). Recent advances in targeted nanoparticles drug delivery to melanoma. Nanomedicine: Nanotechnology, Biology, and Medicine, 11(3), 769–794.

Li, K., Wen, S., Larson, A. C., Shen, M., Zhang, Z., Chen, Q., Shi, X., Zhang, G. (2013). Multifunctional dendrimer-based nanoparticles for *in vivo* MR/CT dual-modal molecular imaging of breast cancer. International Journal of Nanomedicine, 8, 2589–600.

Lim, L. Y., Koh, P. Y., Somani, S., Robaian, M. Al., Karim, R., Yean, Y. L., Mitchell, J., Tate, R. J., Edrada-Ebel, R., Blatchford, D. R., Mullin, M and Dufès, C. (2015). Tumor regression following intravenous administration of lactoferrin- and lactoferricin-bearing dendriplexes. Nanomedicine: Nanotechnology, Biology and Medicine, 11(6), 1–10.

Lin, Y. L., Liu, Y. K., Tsai, N. M., Hsieh, J. H., Chen, C. H., Lin, C. M., and Liao, K. W. (2012). A Lipo-PEG-PEI complex for encapsulating curcumin that enhances its antitumor effects on curcumin-sensitive and curcumin-resistance cells. Nanomedicine: Nanotechnology, Biology, and Medicine, 8(3), 318–327.

Liu, C., Liu, F., Feng, L., Li, M., Zhang, J., and Zhang, N. (2013). The targeted co-delivery of DNA and doxorubicin to tumor cells via multifunctional PEI-PEG based nanoparticles. Biomaterials, 34 (10), 2547–2564.

Liu, Y., Ng, Y., Toh, M. R., Chiu, G. N. C (2015). Lipid-dendrimer hybrid nanosystem as a novel delivery system for paclitaxel to treat ovarian cancer. Journal of Controlled Release, 220: 438–446.

Lodish H, Berk A, Zipursky SL, Matsudaira, P., Baltimore, D., and Darnell, J., Molecular Cell Biology. 4th edition. New York: W. H. Freeman; 2000. Section 7.1, DNA Cloning with Plasmid Vectors. Available from: https://www.ncbi.nlm.nih.gov/books/NBK21498/ accessed 061216

Lundstrom, K. (2003). Latest development in viral vectors for gene therapy. Trends in Biotechnology, 21(3), 117–122.

Ma, M., Shang, W., Xing, P., Li, S., Chu, X., Hao, A., Liu, G and Zhang., Y (2015). A supramolecular vesicle of camptothecin for its water dispersion and controllable releasing. Carbohydrate Research, 402: 208–214.

Ma, Q., Han, Y., Chen, C., Cao, Y., Wang, S., Shen, W., Zhang, H., Li, Y., van Dongen, M. A., He, B., Yu, M., Xu, L., Holl, M. M. B., Liu, G., Zhang, Q., and Qi, R. (2015). Oral Absorption Enhancement of Probucol by PEGylated G5 PAMAM Dendrimer Modified Nanoliposomes. Molecular Pharmaceutics, 12, 665−674.

Maderspacher, F. (2004). Rags before the riches: Friedrich Miescher and the discovery of DNA. Current Biology: CB, 14(15), R608.

Maeda, H., Nakamura H and Fang J (2013). The EPR effect for macromolecular drug delivery to solid tumors: Improvement of tumor uptake, lowering of systemic toxicity, and distinct tumor imaging *in vivo*. Advanced Drug Delivery Reviews 65: 71–79.

Mahale N. B., Thakkar P.D., Mali R.G., Walunj D.R and Chaudhari S.R. (2012). Niosomes: Novel sustained release nonionic stable vesicular systems — An overview. Advances in Colloid and Interface Science 183–184: 46–54.

Maherani, B., Arab-Tehrany, E., Mozafari, M., Gaiani, C., and Linder, M. (2011). Liposomes: A Review of Manufacturing Techniques and Targeting Strategies. Current Nanoscience, 7(3), 436–452.

Malik, N., Wiwattanapatapee, R., Klopsch, R., Lorenz, K., Frey, H., Weener, J. W., Meijer, E. W., Paulus, W., Duncan, R. (2000). Dendrimers: Relationship between structure and biocompatibility *in vitro*, and preliminary studies on the biodistribution of ^{125}I-labelled polyamidoamine dendrimers *in vivo*. Journal of Controlled Release, 65, 133–148.

Malvern, I. (2011). Inform White Paper Dynamic Light Scattering. Malvern Guides, 1–6.

Marianecci, C., Di Marzio, L., Rinaldi, F., Celia, C., Paolino, D., Alhaique, F., Esposito, S., Carafa, M. (2014). Niosomes from 80s to present: The state of the art. Advances in Colloid and Interface Science, 205, 187–206.

Marianecci, C., Rinaldi, F., Di Marzio, L., Mastriota, M., Pieretti, S., Celia, C., Paolino, D., Iannone, M., Fresta, M., Carafa, M. (2014). Ammonium glycyrrhizinate-loaded niosomes as a potential nanotherapeutic system for anti-inflammatory activity in murine models. International Journal of Nanomedicine, 9, 635–51.

Martins, S., Tho, I., Reimold, I., Fricker, G., Souto, E., Ferreira, D and Brandl, M., Brain delivery of camptothecin by means of solid lipid nanoparticles: Formulation design, *in vitro* and *in vivo* studies. International Journal of Pharmaceutics, 439: 49–62.

McNeil-Watson, F., Tscharnuter, W., and Miller, J. (1998). A new instrument for the measurement of very small electrophoretic mobilities using phase analysis light scattering (PALS). Colloids and Surfaces A: Physicochemical and Engineering Aspects, 140(1-3), 53–57.

Meany, H. J., Seibel, N. L., Sun, J., Finklestein, J. Z., Sato, J., Kelleher, J., Sondel, P and Reaman G (2008). Phase II trial of recombinant tumor necrosis factor-alpha in combination with dactinomycin in children with recurrent Wilms tumor. Journal of Immunotherapy 31(7):679-83.

Meng, H., Mai, W. X., Zhang, H., Xue, M., Xia, T., Lin, S., Wang, X., Zhao, Y., Ji, Z., Zink, J. I and Nel, A. E. (2013). Codelivery of an Optimal Drug/siRNA Combination Using Mesoporous Silica Nanoparticles to Overcome Drug Resistance in Breast Cancer *in vitro* and *in vivo*. ACS Nano, 7(2), 994–1005.

Merck Index (2001). An Encyclopaedia of Chemicals, Drugs, and Biologicals. 13th Edition, Whitehouse Station, NJ: Merck and Co., Inc., O'Neil, M.J. (ed.) p. 381

Michler, G. (2008). "Overview of Techniques Chapter 1." In Electron Microscopy of Polymers, edited by Prof. Harald Pasch. Heidelberg: Springer-Verlag Berlin Heidelberg (pp 7-12).

Miller, J. F., Schatzel, K., and Vincent, B. (1991). The Determination of Very Small Electrophoretic Mobilities In Polar and Nonpolar Colloidal Dispersions Using Phase-Analysis Light-Scattering. Journal of Colloid Interface Science., 143(2), 532–554.

Miller, J.H., Experiments in Molecular Genetics, 1972 Cold Spring Harbor, N.Y. (cited in Shcharbin *et al.,* 2010)

Min, K. H., Min, H. S., Lee, H. J., Park, D. J., Yhee, J. Y., Kim, K., Kwon, I. C., Jeong, S.Y., Silvestre, O.F., Chen, X., Hwang, Y.-S. Kim, E.-C., and Lee, S. C. (2015). PH-controlled gas-generating mineralized nanoparticles: A theranostic agent for ultrasound imaging and therapy of cancers. ACS Nano, 9(1), 134–145.

Minton, A. P. (2016). Recent applications of light scattering measurement in the biological and biopharmaceutical sciences. Analytical Biochemistry, 501: 4–22.

Mohan, P., and Rapoport N., (2010). Doxorubicin as a molecular nanotheranostic agent: effect of doxorubicin encapsulation in micelles or nanoemulsions on the ultrasound-mediated intracellular delivery and nuclear trafficking. Molecular Pharmaceutics, 7(6): 1959–1973.

Moghassemi, S., and Hadjizadeh, A. (2014). Nano-niosomes as nanoscale drug delivery systems: An illustrated review. Journal of Controlled Release, 185: 22–36.

Moorthi, C., Manavalan, R., and Kathiresan, K. (2011). Nanotherapeutics to overcome conventional cancer chemotherapy limitations. Journal of Pharmacy and Pharmaceutical Sciences, 14(1), 67–77.

Mosmann, T. (1983). Rapid colorimetric assay for cellular growth and survival: Application to proliferation and cytotoxicity assays. Journal of Immunological Methods, 65(1-2), 55–63.

Nakamura, H., and Maeda, H. (2013). Cancer Chemotherapy. In Fundamentals of Pharmaceutical Nanoscience. Chapter 15 (pp. 401–426).

NANOCS.net (2016). http://www.nanocs.net/PEG/Lipid-PEGs/Cholesterol-PEG-Maleimide/Cholesterol-PEG-maleimide-5k.htm accessed 250816

Nichols, J., and Bae, Y. (2013). Nanotechnology for Cancer Treatment: Possibilities and Limitations. In Y. Bae, R. Mrsny, and K. Park (Eds.), Cancer Targeted Drug Delivery: An Elusive Dream (pp. 37–56). New York: Springer.

Niven, R., Pearlman, R., Wedeking, T., Mackeigan, J., Noker, P., Simpson-Herren, L., and Smith, J. G. (1998). Biodistribution of radiolabeled lipid-DNA complexes and DNA in mice. Journal of Pharmaceutical Sciences, 87(11), 1292–1299.

Nuffield Council on Bioethics, (2005). The Use of Animals for Research in the Pharmaceutical Industry. In The Ethics of Research Involving Animals. Chapter 8 (pp 133–51).

Nuffield Council on Bioethics, (2005). Replacements. In The Ethics of Research Involving Animals. Chapter 11 (pp193-194).

Nwaneshiudu, A., Kuschal, C., Sakamoto, F. H., Anderson, R. R., Schwarzenberger, K., and Young, R. C. (2012). Introduction to confocal microscopy. The Journal of Investigative Dermatology, 132, e3.

Ojeda, E., Puras, G., Agirre, M., Zárate, J., Grijalvo, S., Pons, R., Eritja, R., Martinez-Navarrete, G., Soto-Sanchez, C., Fernández, E., Pedraz, J. L. (2015). Niosomes based on synthetic cationic lipids for gene delivery: the influence of polar head-groups on the transfection efficiency in HEK-293, ARPE-19 and MSC-DEN-TPGS cells. Organic Biomolecular Chemistry, 13(4), 1068–1081.

Paecharoenchai, O., Niyomtham, N., Leksantikul, L., Ngawhirunpat, T., Rojanarata, T., Yingyongnarongkul, B., and Opanasopit, P. (2014). Nonionic Surfactant Vesicles Composed of Novel Spermine-Derivative Cationic Lipids as an Effective Gene Carrier *In vitro*. AAPS PharmSciTech, 15(3), 722–730.

Paolino, D., Sinha, P., Fresta, M., and Ferrari, M. (2006). Drug Delivery Systems. Encyclopedia of Medical Devices and Instrumentation. (J. Webster, Ed.). Wiley online library.

Parimi, S., Barnes, T. J., and Prestidge C. A. (2008). PAMAM Dendrimer Interactions with Supported Lipid Bilayers: A Kinetic and Mechanistic Investigation Langmuir, 24, 13532-13539.

Park, T. G., Jeong, J. H., and Kim, S. W. (2006). Current status of polymeric gene delivery systems. Advanced Drug Delivery Reviews, 58(4), 467–86.

Perrie, Y. and Rades, T. (2012). Site-directed drug targeting. In FASTtrack Pharmaceutics: Drug Delivery and Targeting Pharmaceutical Press second edition Chapter 7 (pp.154 -156).

Perry, J. L, Reuter, K. G., Kai, M. P., Herlihy, K. P., Jones, S. W., Luft, J. C., Napier, M., Bear, J. E., and DeSimone, J. M., (2012). PEGylated PRINT nanoparticles: the impact of PEG density on protein binding, macrophage association, biodistribution, and pharmacokinetics. Nano Letters, 12(10), 5304-5310.

Peer, D., Karp, J. M., Hong, S., Farokhzad, O. C., Margalit, R., and Langer, R. (2007). Nanocarriers as an emerging platform for cancer therapy. Nature Nanotechnology, 2(12), 751–60.

Persidis, A. (1999). Cancer multidrug resistance. Nature Biotechnology, 17, 94–95.

Plapied, L., Duhem, N., des Rieux, A., and Préat, V. (2011). Fate of polymeric nanocarriers for oral drug delivery. Current Opinion in Colloid and Interface Science, 16(3), 228–237.

Pmcisochem (2008) Vitamin E TPGS NF* and Food Grade https://pmcisochem.fr/sites/default/files/documents/ISOCHEM%20TPGS%202015%2008.pdf acessed 250218

Pray, L. (2008) Discovery of DNA structure and function: Watson and Crick. Nature Education 1(1):100

Puras, G., Mashal, M., Zárate, J., Agirre, M., Ojeda, E., Grijalvo, S., Eritja, R., Diaz-Tahoces, A., Martínez Navarrete, G., Avilés-Trigueros, M., Fernández, E., Pedraz, J. L. (2014). A novel cationic niosome formulation for gene delivery to the retina. Journal of Controlled Release, 174, 27–36.

Qi, R., Gao, Y., Tang, Y., He, R.-R., Liu, T.-L., He, Y., Sun, S., Li, B., Li, Y., Liu, G. (2009). PEG-conjugated PAMAM dendrimers mediate efficient intramuscular gene expression. The American Association of Pharmaceutical Scientists Journal, 11(3), 395–405.

QIAGEN (2005). EndoFree® Plasmid Purification Handbook pp 22-35.

Ratko, T. A, Cummings, J. P., Blebea, J., and Matuszewski, K. A. (2003). Clinical gene therapy for nonmalignant disease. The American Journal of Medicine, 115(7), 560–569.

Ritwiset, A., Krongsuk, S., and Johns, J. R. (2016). Molecular structure and dynamical properties of niosome bilayers with and without cholesterol incorporation: A molecular dynamics simulation study. Applied Surface Science, 380, 23–31.

Robbins, P. D., and Ghivizzani, S. C. (1998). Viral vectors for gene therapy. Pharmacology and Therapeutics, 80(1), 35–47.

Roberts, N. J., Zhou, S., Diaz, L. A Jr. and Holdhoff, M (2011). Systemic use of tumor necrosis factor alpha as an anticancer agent. Oncotarget, 2 (10): 739 - 751.

Rogošić, M., Mencer, H. J., and Gomzi, Z. (1996). Polydispersity index and molecular weight distributions of polymers. European Polymer Journal, 32(11), 1337–1344.

Roll-Hansen, N. (2014). The holist tradition in twentieth century genetics. Wilhelm Johannsen's genotype concept. The Journal of Physiology, 592(Pt 11), 2431–8.

Ruddon, R. (2007). Cancer Biology. (R. Ruddon, Ed.) (Fourth). New York: Oxford University Press Inc. (pp 1-59).

Ruponen, M., Honkakoski, P., Rönkkö S., Pelkonenb, J., Tammi, M., and Urtti, A. (2003). Extracellular and intracellular barriers in non-viral gene delivery. Journal of Controlled Release, 93(2), 213–217.

Sadeghizadeh, M., Ranjbar, B., Damaghi, M., Khaki, L., Sarbolouki, M. N., Najafi, F., Parsaee, S., Ziaee, A.-A., Massumi, M., Lubitz, W., Kudela, P., Paukner, S. and Karami, A. (2008), Dendrosomes as novel gene porters-III. Journal of Chemical Technology and Biotechnology. 83: 912–920.

Sankhyan, A., and Pawar, P. (2012). Recent Trends in Niosome as Vesicular Drug Delivery System. Journal of Applied Pharmaceutical Science, 02(06), 20–32.

Sankhyan, A., and Pawar, P. K. (2013). Metformin loaded non-ionic surfactant vesicles: optimization of formulation, effect of process variables and characterization. Daru: Journal of Faculty of Pharmacy, 21(1), 7.

Santander-Ortega, M., de la Fuente, M., Lozano, M., Tsui, M., Bolton, K., Uchegbu, I., and Schätzlein, A. (2014). Optimisation of synthetic vector systems for cancer gene therapy - the role of the excess of cationic dendrimer under physiological conditions. Current Topics in Medicinal Chemistry, 14 (9), 1172–1181.

Sauer, M., Hofkens, J., and Enderlein, J. (2011). Basic Principles of Fluorescence Spectroscopy. Handbook of Fluorescence Spectroscopy and Imaging: From Single Molecules to Ensembles, 1–30.

Schatzlein AG, Zinselmeyer BH, Elouzi A, Dufès C, Chim YT, Roberts CJ, Davies MC, Munro A, Gray AI, Uchegbu IF. (2005). Preferential liver gene expression with polypropylenimine dendrimers. Journal of Controlled Release, 101(1-3), 247–58.

Scott, V., Clark, A. R., and Docherty, K. (1994). The Gel Retardation Assay.pdf. Methods in Molecular Biology, 31, 339–347.

Sella, A., Aggarwal, B. B., Kilbourn, R. G., Bui, C. A., Zukiwski, A. A., and Logothetis, C. J (1995). Phase I study of tumor necrosis factor plus actinomycin D in patients with androgen-independent prostate cancer. Cancer Biotherapy and Radiopharmaceuticals, 10 (3), 225-35.

Semenza, G. (2003). Fifty years ago - DNA: The double helix. FEBS Letters, 544(1-3), 1–3.

Sezgin-Bayindir, Z., and Yuksel, N. (2012). Investigation of Formulation Variables and Excipient Interaction on the Production of Niosomes. AAPS PharmSciTech, 13(3), 826–835.

Sharma, A., and Sharma, U. (1997). Liposomes in drug delivery: progress and limitations. International Journal of Pharmaceutics, 154, 123–140.

Shcharbin, D. G., Klajnert, B., and Bryszewska, M. (2009). Dendrimers in gene transfection. Biochemistry. Biokhimiia, 74(10), 1070–1079.

Shcharbin, D., Pedziwiatr, E., Blasiak, J., and Bryszewska, M. (2010). How to study dendriplexes II: Transfection and cytotoxicity. Journal of Controlled Release, 141(2), 110–127.

Sigma-Aldrich (2016). DAB-Am-16, Polypropylenimine hexadecaamine Dendrimer, Generation 3.0.
http://www.sigmaaldrich.com/catalog/product/aldrich/469076?lang=en&region=GB
acessed 120616

Sigma-Aldrich (2016). Dihexadecyl phosphate https://www.sigmaaldrich.com/catalog/product/sigma/d2631?lang=en&region=US acessed 250216

Singh, Y., Omidian, H., and Sinko, P. (2011). Drug delivery and targeting. In P. Sinko and Y. Singh (Eds.), Martin's Physical Pharmacy and Pharmaceutical Sciences (sixth, pp. 594–645). Baltimore: Wolters Kluwer/Lippincott Williams and Wilkins.

Singh, R., Kats, L., Blättler, W. A., and Lambert, J. M. (1996). Formation of N-substituted 2-iminothiolanes when amino groups in proteins and peptides are modified by 2-iminothiolane. Analytical Biochemistry, 236(236), 114–125.

Skotland, T., Iversen, T.-G., and Sandvig, K. (2014). Development of nanoparticles for clinical use. Nanomedicine (London, England), 9(9), 1295–9.

Slingerland, M., Guchelaar, H. J., and Gelderblom, H. (2012). Liposomal drug formulations in cancer therapy: 15 years along the road. Drug Discovery Today, 17(3-4), 160–166.

Somani, S., Blatchford, D. R., Millington, O., Stevenson, M. L., and Dufès, C. (2014). Transferrin-bearing polypropylenimine dendrimer for targeted gene delivery to the brain. Journal of Controlled Release, 188, 78–86.

Stone N. R., Bicanic T., Salim R., and Hope W (2016). Liposomal Amphotericin B (AmBisome®): A review of the pharmacokinetics, pharmacodynamics, clinical experience and future directions. Drugs 76 (4): 485–500.

Sun, B., Yu, X., Yin, Y., Liu, X., Wu, Y., Chen, Y., Zhang, X., Jiang, C., and Kong W. (2013). Large-scale purification of pharmaceutical-grade plasmid DNA using tangential flow filtration and multi-step chromatography Journal of Bioscience and Bioengineering 116 (3), 281-286.

Sun, X., and Zhang, N. (2010). Cationic Polymer Optimization for Efficient Gene Delivery. Mini-Reviews in Medicinal Chemistry, 10 (2), 108–125

Svenson, S. (2009). Dendrimers as versatile platform in drug delivery applications. European Journal of Pharmaceutics and Biopharmaceutics, 71 (3), 445–62.

Szwed, M., Kania, K. D., and Jozwiak, Z. (2014). Relationship between therapeutic efficacy of doxorubicin-transferrin conjugate and expression of P-glycoprotein in chronic erythromyeloblastoid leukemia cells sensitive and resistant to doxorubicin. Cellular Oncology (Dordrecht), 1–8.

Tang, Y., Li, Y. B., Wang, B., Lin, R. Y., Van Dongen, M., Zurcher, D. M., Gu, X., Banaszak Holl, M. M., Liu, G., Qi, R. (2012). Efficient in vitro siRNA delivery and intramuscular gene silencing using PEG-modified PAMAM dendrimers. Molecular Pharmaceutics, 9(6), 1812–1821.

Tasset, C., and Roland, M. (1992). Comparison of the in vivo antifungal activity of amphotericin B-Synperonic A50 with fungizone, International Journal of Pharmaceutics, 81(1992) R5-R9.

Tewey, K., Rowe, T., Yang, L., Halligan, B., and Liu, L. (1984). Adriamycin-Induced DNA Damage Mediated by. Science, 226 (4673), 466–8.

Thermofisher.com (2016). Cy3 dye https://www.thermofisher.com/uk/en/home/life-science/cell-analysis/fluorophores/cy3-dye.html accessed 050216

Tomalia, D., Baker, J. R., Dewald, J., Hall, M., Kallos, G., Martin, S., Roeck, J., Ryder, J., Smith, P. (1986). Dendritic Macromolecules: Synthesis of Starburst Dendrimers. Macromolecules, 19(9), 2466–2468.

Torchilin, V. P. (2010). Passive and Active Drug Targeting: Drug Delivery to Tumors as an Example. In M. Schäfer-Korting (Ed.), Drug Delivery (pp. 3–53). Springer Berlin Heidelberg.

Uchegbu, I. F., and Florence, A. T. (1995). Non-Ionic Surfactant Vesicles (Niosomes): Physical and Pharmaceutical Chemistry. Advances in Colloid and Interface Science, 58, 1–55.

Uchegbu, I. F., and Schatzlein, A. G. (2006). Vesicles prepared from Synthetic Amphiphiles- Polymeric vesicles and niosomes. In Nanoparticulates as Drug Carriers Edited by Torchilin V. P. Imperial College Press, London. Chapter 6 (p 112).

Uchegbu, I. F., and Siew, A. (2013). Nanomedicines and nanodiagnostics come of age. Journal of Pharmaceutical Sciences, 102(2), 305–310.

Uchegbu, I. F., and Vyas, S. P. (1998). Non-ionic surfactant based vesicles (niosomes) in drug delivery. International Journal of Pharmaceutics, 172(1-2), 33–70.

Uchegbu, I., Turton, J., Double, J., and Florence, A. (1994). Drug distribution and a pulmonary adverse effect of intraperitoneally administered doxorubicin niosomes in the mouse. Biopharmaceutics and Drug Disposition, 15(8), 691–707.

Vaitilingam, B., Chelvam, V., Kularatne, S. A., Poh, S., Ayala-Lopez, W., and Low, P. S. (2012). A Folate Receptor -α- Specific Ligand That Targets Cancer Tissue and Not Sites of Inflammation. Journal of Nuclear Medicine, 53, 1127–1134.

van der Veen A.H., de Wilt J.H.W., Eggermont, A.M.M., van Tiel, ST., Seynhaeve A.L.B., and ten Hagen T.L.M (2000). TNF-α augments intratumoural concentrations of doxorubicin in TNF-α-based isolated limb perfusion in rat sarcoma models and enhances anti-tumour effects. British Journal of Cancer 82 (4) 973–980.

Wagner, A., and Vorauer-Uhl, K. (2011). Liposome technology for industrial purposes. Journal of Drug Delivery, 1–9.

Wain, H. M., Bruford, E. A., Lovering, R. C., Lush, M. J., Wright, M. W., and Povey, S. (2002). Guidelines for Human Gene Nomenclature. Genomics, 79 (4), 464–470.

Walter, M. V., and Malkoch, M. (2012). Simplifying the synthesis of dendrimers: accelerated approaches. Chemical Society Reviews, 41(13), 4593.

Wang, G., Yu, B., Wu, Y., Huang, B., Yuan, Y., and Liu, C. S. (2013). Controlled preparation and antitumor efficacy of vitamin e TPGS-functionalized PLGA nanoparticles for delivery of paclitaxel. International Journal of Pharmaceutics, 446, 24–33.

Wang, D., Zhong, L., Nahid, M., and Gao, G. (2014). The potential of adeno-associated viral vectors for gene delivery to muscle tissue. Expert Opinion on Drug Delivery, 11(3), 345–364.

Wang, K., Kievit, F. M., Jeon, M., Silber, J. R., Ellenbogen, R.G., and Zhang, M (2015). Nanoparticle-mediated target delivery of TRAIL as gene therapy for glioblastoma. Advanced Healthcare Materials, 4(17), 2719–2726.

Wempe, M. F., Wright, C., Little, J. L., Lightner, J. W., Large, S. E., Caflisch, G. B., Buchanan, C. M., Rice, P. J., Wacher, V. J., Ruble, K. M., and Edgar, K. J. (2009). Inhibiting efflux with novel non-ionic surfactants: Rational design based on vitamin E TPGS. International Journal of Pharmaceutics, 370(1-2), 93–102.

Whitehead, R. P., Fleming, T., Macdonald, J. S., Goodman, P. J., Neefe, J., Braun, T. J., Swinnen, L.J, Hersh, E. M. (1990). A phase II trial of recombinant tumor necrosis factor in patients with metastatic colorectal adenocarcinoma: A Southwest Oncology Group study. Journal of Biological Response Modifiers, 9(6), 588-591.

Wilkhu, J. S., Ouyang, D., Kirchmeier, M. J., Anderson, D. E., and Perrie, Y. (2014). Investigating the role of cholesterol in the formation of non-ionic surfactant based bilayer vesicles: Thermal analysis and molecular dynamics. International Journal of Pharmaceutics, 461(1-2), 331–341.

Wirth, T., Parker, N., and Ylä-Herttuala, S. (2013). History of gene therapy. Gene, 525(2), 162–169.

Wolpert, L. (1984). DNA and Its Message. The Lancet, 2(8407), 853–856.

Wrobel, D., Ionov, M., Gardikis, K., Demetzos, C., Majoral, J., Palecz, B., Klajnert, B., and Bryszewska. M., (2011). “Interactions of Phosphorus-Containing Dendrimers with Liposomes.” Biochimica et Biophysica Acta (BBA) - Molecular and Cell Biology of Lipids 1811 (3), 221–226.

Workman, P., Aboagye, EO., Balkwill, F., Balmain, A., Bruder, G., Chaplin, DJ., Double, JA., Everitt, J., Farningham, DAH., Glennie, MJ., Kelland, LR., Robinson, V., Stratford, IJ., Tozer, GM., Watson, S., Wedge, SR., SA Eccles (2010). Guidelines for the welfare and use of animals in cancer research British Journal of Cancer 102, 1555 – 1577.

Xu, J., Zhao, Q., Jin, Y., and Qiu, L. (2014). High loading of hydrophilic/hydrophobic doxorubicin into polyphosphazene polymersome for breast cancer therapy. Nanomedicine: Nanotechnology, Biology, and Medicine, 10(2), 349–58.

Yang, F., Kemp, C. J., and Henikoff, S. (2013). Doxorubicin enhances nucleosome turnover around promoters. Current Biology, 23(9), 782–787.

Yang, F., Teves, S. S., Kemp, C. J., and Henikoff, S. (2014). Doxorubicin, DNA torsion, and chromatin dynamics. Biochimica et Biophysica Acta - Reviews on Cancer, 1845(1), 84–89.

Yamamoto, M., Oshiro, S., Tsugu, H., Hirakawa, K., Ikeda, K., Soma, G., Fukushima, T. (2002). Treatment of recurrent malignant supratentorial astrocytomas with carboplatin and etoposide combined with recombinant mutant human tumor necrosis factor-alpha. Anticancer Research, 22(4), 2447-2453.

Yhee, J., Son, S., Son, S., Joo, M., and Kwon, I. (2013). The EPR Effect in Cancer. In Y. Bae, R. Mrsny, and K. Park (Eds.), Cancer Targeted Drug Delivery: An Elusive Dream, New York: Springer, pp. 621–632.

Yin, H., Liao, L., and Fang J. (2014). Enhanced Permeability and Retention (EPR) Effect Based Tumor Targeting: The Concept, Application and Prospect. JSM Clinical Oncology and Research 2(1), 1010.

Ylä-Herttuala, S. (2012). Endgame: Glybera Finally Recommended for Approval as the First Gene Therapy Drug in the European Union. Molecular Therapy, 20(10), 1831–1832.

Yu, M. K., Park, J., and Jon, S. (2012). Targeting strategies for multifunctional nanoparticles in cancer imaging and therapy. Theranostics, 2(1), 3–44.

Zhang, S., Liu, X., Bawa-Khalfe, T., Lu, L.-S., Lyu, Y. L., Liu, L. F., and Yeh, E. T. H. (2012). Identification of the molecular basis of doxorubicin-induced cardiotoxicity. Nature Medicine, 18(11), 1639- 1642.

Zhang, L., Zhu, D., Dong, X., Sun, H., Song, C., Wang, C., and Kong, D. (2015). Folate-modified lipid – polymer hybrid nanoparticles for targeted paclitaxel delivery. International Journal of Nanomedicine, 10: 2101–2114.

Zinselmeyer, B., Mackay, S., Schatzlein, A., and Uchegbu, I. (2002). The lower-generation polypropylenimine dendrimers are effective gene-transfer agents. Pharm Res, 19(7), 960–967.

Zinselmeyer, B. H., Beggbie, N., Uchegbu, I. F., and Schatzlein AG. Quantification of β-galactosidase activity after non-viral transfection *in vivo* (2003). Journal of Controlled Release 91; 201–208

American Cancer Society https://www.cancer.org/cancer/multiple-myeloma/about/what-is-multiple-myeloma.html (accessed 22/04/17)

https://www.britannica.com/science/Brownian-motion accessed 05/07/16

(http://www.nanosoftpolymers.com/product/cholesterol-peg-maleimide/ accessed 14/04/16).

https://www.genome.gov/25520880/deoxyribonucleic-acid-dna-fact-sheet/ accessed 260716

http://www.mibioresearch.com/imaging/bioluminescence-imaging/ accessed 241116

https://www.britannica.com/science/cell-culture accessed 300517